DOCTOR OF PHILOSOPHY

Cell cycle-dependent regulation of the human RNA cap methyltransferase (RNMT)

Aregger, Michael

Award date:
2013

DOCTOR OF PHILOSOPHY

Cell cycle-dependent regulation of the human RNA cap methyltransferase (RNMT)

Michael Aregger

2013

University of Dundee

Cell cycle-dependent regulation of the human RNA cap methyltransferase (RNMT)

Michael Aregger

A thesis submitted for the degree of
Doctor of Philosophy

14th of November 2013

Abstract

The N-7 methylguanosine cap structure is conserved from yeast to man. It is essential for cell proliferation as it influences several steps in eukaryotic gene expression including transcription, pre-mRNA processing, RNA export and translation. The N-7 methylguanosine cap is added co-transcriptionally to RNA pol II transcripts. In mammals, two enzymes catalyse the synthesis of the N7-methylguanosince cap. RNGTT adds an inverted guanosine group to the first transcribed nucleotide and RNMT methylates the guanosine cap at the N7-position.

RNMT consists of a catalytic domain and an N-terminal domain that is absent in lower eukaryotes. Experiments presented in this thesis revealed that the N-terminus mediates RNMT recruitment to transcription start sites. Furthermore, it was found that the RNMT N-terminal domain is phosphorylated at Threonine-77 (T77) by CDK1/Cyclin B in a cell cycle-dependent manner during G2/M-phase.

RNMT T77 phosphorylation activates cap methyltransferase activity *in vitro*. Furthermore, it negatively regulates the interaction of RNMT with KPNA2 (Importin-α), which was found to inhibit RNMT activity *in vitro*. RNMT T77 phosphorylation is required for normal cell proliferation suggesting an important biological function. Initial experiments indicated that RNMT T77 phosphorylation functions to regulate gene expression in a gene-specific manner. Future work is focused on establishing an experimental system to perform a genome-wide study in order to elucidate which transcripts are affected by RNMT T77 phosphorylation.

To summarise, this study for the first time revealed that the RNA cap methyltransferase activity is regulated in a cell-cycle dependent manner.

Table of Contents

List of Illustrations

Figures

Tables

Acknowledgment

I would like to thank my PhD supervisor Victoria Cowling for giving me the opportunity to work in her laboratory. Her scientific support and guidance was essential for the success of this PhD. The collaborative atmosphere at the College of Life Sciences greatly facilitated the work of this PhD and I appreciate all the help I received from other labs in CLS. I am very grateful for the financial support of Cancer Research UK that provided a PhD stipend and offered training opportunities throughout my PhD. Furthermore, other funding bodies such as the Biochemical Society, the RNA society, EMBO/EMBL and RNA UK provided money allowing me to attend several conferences which offered me the opportunity to present my work and to expand my scientific knowledge.

A special thank to Nicola and Dhaval for their help throughout the writing process of this thesis but also for their great company outside the lab. I also would like to mention all other lab members, Sianadh, Laura, Anna, Christine and Becky who are a great group of people with whom I enjoyed working. Thanks to my PhD committee members Doreen Cantrell and Andrew Hopkins for their advice and comments and to Andrew Sharrocks and John Brown for spending the time to examine my thesis.

An enormous thanks goes to Thomas for his critical comments and analysis of my work in the lab but also during writing. I am extremely grateful for his scientific support and even more, his company and friendship outside the lab. Efharisto poli!

Last but not least, I would like to thank my family that greatly supported and motivated me during good but also difficult times throughout my PhD. I highly appreciate their love, support and understanding. Danke vöu mou för alles!

Declarations

I hereby declare that the following thesis is based on the results of investigations conducted by myself, and that this thesis is of my own composition. Work other than my own is clearly indicated in the text by reference to the researchers or their publications. This dissertation has not in whole, or in part, been previously presented for a higher degree.

Michael Aregger

I certify that Michael Aregger has spent the equivalent of a least nine terms in research work in the College of Life Sciences, University of Dundee, and that he has fulfilled the conditions of the relevant Ordinance and Regulations of the University of Dundee and is qualified to submit the accompanying thesis in application for the degree of Doctor of Philosophy.

Dr. Victoria H. Cowling

Abbreviations

2D: two-dimensional

4E-BP: eIF4 binding protein

ATP: adenosine triphosphate

bp: base pairs

c: centi

CBC: cap-binding complex

CDK: cyclin-dependent kinase

ChIP: chromatin immunoprecipitation

Ci: currie

cpm: counts per minute

CTD: carboxyl-terminal domain

DAPI: 4',6-diamidino-2-phenylindole

DNA: deoxyribonucleic acid

DRB: 5,6-dichloro-1-β-D-ribofuranosylbenzimidazole

DSIF: DRB-sensitive induced elongation factor

DSTT: Division of Signal Transduction Therapy, University of Dundee

eIF: eukaryotic initiation factor

Fg: flag-tag

g: gram

GDP: guanosine diphosphate

GFP: green fluorescent protein

GMP: guanosine monophosphate

GST: glutathione S-transferase

GTP: guanosine triphosphate

HA: hemagglutinin

HEK-293: human embryonic kidney 293 cells

IBB domain: Importin-β binding domain

IMEC: immortalised mammary epithelial cells

IP: immunoprecipitation

IRES: internal ribosome entry site

kDa: kilo Dalton

KPNA2: Importin-α

l: litre

LC-MS/MS: liquid chromatography coupled to high-resolution tandem mass spectrometry

m: metre

m: milli

M: molar

m7G: N7-methylguanosine

MAPK: mitogen-activated protein kinase

Met-rRNA$_i^{Met}$: initiator methionyl tRNA

miRNA: micro RNA

mRNA: messenger RNA

mTOR: mammalian target of rapamycin

mTORC1: mTOR complex 1

N-terminal: amino-terminal

n: nano

NELF: negative elongation factor

NLS: nuclear localisation signal

NMD: nonsense mediated decay

nt: nucleotides

PABP: poly(A) binding protein

PCR: polymerase chain reaction

poly(A): polyadenylate

pTEFb: positive transcription elongation factors

RAM: RNMT-activating mini protein

RNA pol II: RNA polymerase II

RNA: ribonucleic acid

RNGTT: RNA guanylyltransferase and triphosphatase

RNMT: RNA guanine-7 methyltransferase

rpm: rounds per minute

rRNA: ribosomal RNA

RT-PCR: real time polymerase chain reaction

S79: Serine-79

S79A: Serine-79 mutated to Alanine

SAH: S-adenosyl homocysteine

SAM: S-adenosyl methionine

SDS-PAGE: sodium dodecyl sulfate polyacrylamide gel electrophoresis

SILAC: stable isotope labelling by amino acids in cell culture

siRNA: small interfering RNA

snRNA: small nuclear RNA

snRNP: small ribonucleoprotein particle

T77: Threonine-77

T77A: Threonine-77 mutated to Alanine

T77D: Threonine-77 mutated to Asparagine

TFII: transcription factor II

TLC: thin layer chromatography

TOP: terminal oligopyrimidine

tRNA: transfer RNA

TSS: transcription start site

U: unit

UTR: untranslated region

V: volt

v/v: volume to volume

Vhr: volt hour

w/v: weight to volume

x g: gravitational force

μ: micro

Amino acid code

Amino acid	One letter symbol
Alanine	A
Arginine	R
Asparagine	N
Aspartate	D
Cysteine	C
Glutamate	E
Glutamine	Q
Glycine	G
Histidine	H
Isoleucine	I
Leucine	L
Lysine	K
Methionine	M
Phenylalanine	F
Proline	P
Serine	S
Threonine	T
Tryptophan	W
Tyrosine	Y
Valine	V
any amino acid	x

Nucleotide code

Nucleotide	One letter code
Adenine	A
Cytosine	C
Guanine	G
Thymine	T
Uracil	U

Chapter 1:

Introduction

1.1 Introduction to eukaryotic gene expression

The principles of gene expression are conserved from bacteria to humans and have been described as the central dogma of molecular biology by Francis Crick (Crick, 1970, 1958). This includes the general transfer of genetic information from DNA to RNA to protein. Despite the general conservation of the mechanics of gene expression, its regulation is very diverse between species and the pattern of gene expression varies even between different cell types of the same organism. In metazoans, hundreds of different cell types contain the same genetic information, but still exhibit different functions and respond to physiological and environmental signals in different ways. Thus, the tight and differential control of gene regulation is required for overall functioning of an organism (Orphanides, 2002).

In eukaryotic cells, RNA processing is an important step in the expression of genes that can affect the fate of an RNA molecule or even alter the coding capacity of a particular gene. The addition of a N7-methylguanosine cap to RNA polymerase II transcripts is the first of several RNA processing steps and this thesis aims to investigate the regulation of N7-methylguanosine cap formation in human cells. Before presenting the literature describing the formation and function of the N7-methylguanosine cap, the basic processes of eukaryotic gene expression are going to be illustrated in the next subchapter.

1.1.1 RNA Pol II transcription and CTD phosphorylation

Gene expression starts with the transcription of genetic information from a DNA segment into RNA. Protein-coding messenger (m)RNA and some non-coding RNAs such as micro (mi)RNA and small nuclear (sn)RNA are transcribed by the multisubunit enzyme RNA polymerase II (RNA pol II). Initiation of RNA pol II transcription involves a range of different general transcription factors. TFIID recognises the TATA-box in the core promoter and TFIIB binds to the TFIID-promoter complex, thus allowing the recruitment of the TFIIF/RNA pol II complex. The pre-initiation complex is completed by binding of TFIIE and TFIIH and it is stabilised by TFIIA (Orphanides et al., 1996). In addition to these basal transcription factors, the transcription initiation complex may also include further regulators such as the mediator complex and/or gene-specific transcription factors which activate or repress transcription in response to metabolic or environmental signals (Sikorski and Buratowski, 2009).

RNA pol II is recruited to promoters in an unphosphorylated state (Lu et al., 1991). However, after the formation of the pre-initiation complex the amino acids of the carboxyl-terminal domain (CTD) of the largest subunit of RNA pol II become sequentially phosphorylated. The CTD is unique to RNA pol II and it consists of tandem heptad repeats with a consensus sequence of $Tyrosine_1$-$Serine_2$-$Proline_3$-$Threonine_4$-$Serine_5$-$Proline_6$-$Serine_7$. The length of the heptad repeats depends on the complexity of the organisms with yeast possessing 26 and vertebrates possessing 52 repeats (Chapman et al., 2008; Liu et al., 2010). The CTD serves as a scaffold or landing platform for several proteins involved in transcription, messenger (m)RNA maturation and chromatin modification (Hsin and Manley, 2012). Binding of these proteins to the CTD is dynamically regulated by the phosphorylation of Serine-5 and Serine-2 but also Serine-7, Threonine-4 and Tyrosine-1 (Heidemann et al., 2013). The TFIIH subunit CDK7/Cyclin H/MAT1 phosphorylates the CTD at Serine-5 during transcription initiation (Feaver et al., 1991; Lu et al., 1992; Trigon et al., 1998), which has been shown to

correlate with increased promoter clearance and dissociation of the mediator complex from RNA pol II (Max et al., 2007). Furthermore, Serine-5 phosphorylation serves to recruit the RNA capping machinery as described in detail below.

Chromatin immunoprecipitation (ChIP) followed by sequencing demonstrated that shortly after transcription initiation RNA pol II globally pauses at promoter proximal sites in metazoan cells (Guenther et al., 2007; Kim et al., 2005; Rahl et al., 2010). This pausing is observed at most protein-encoding genes including those that are thought to be transcriptionally inactive, which suggests that transcription is regulated at the elongation step rather than at initiation. Promoter-proximal pausing, which occurs 20 - 60 base pairs (bp) after the transcription start site (TSS), is caused by two factors: 5,6-dichloro-1-β-D-ribofuranosylbenzimidazole (DRB) sensitive induced elongation factor (DSIF) and negative elongation factor (NELF). DSIF consists of the two subunits Spt4 and Spt5 whereas NELF is composed of five polypeptides named NELF A-E. DRB treatment was previously shown to inhibit transcription elongation (Chodosh et al., 1989) and DSIF and NELF were found to mediate sensitivity to DRB-mediated transcription inhibition (Wada et al., 1998; Yamaguchi et al., 1999). Binding of DSIF and NELF to RNA pol II was demonstrated to cooperatively cause pausing of RNA pol II and accumulation of short 20 - 50 bp transcripts (Wada et al., 1998; Yamaguchi et al., 1999). This repression of transcription elongation is reversed by pTEFb-mediated phosphorylation of RNA pol II (Yamaguchi et al., 1999). The pTEFb complex contains the kinase CDK9/Cyclin T, which phosphorylates the RNA pol II CTD at Serine-2 and also phosphorylates Spt5 (Marshall et al., 1996; Yamada et al., 2006). This causes the dissociation of NELF from RNA pol II and allows productive transcription elongation.

In addition to TFIIH and pTEFb, other kinases also phosphorylate the RNA pol II CTD during the transcription cycle. These include the mediator subunit CDK8/Cyclin C, which phosphorylates Serine-5 during transcription initiation (Galbraith et al., 2010), or CDK12, which is responsible for Serine-2 phosphorylation on elongating RNA pol II

(Bartkowiak et al., 2010; Blazek et al., 2011). Furthermore, CDK13 was also found to phosphorylate RNA pol II CTD Serine-2 *in vitro* (Bartkowiak et al., 2010). Together these kinases create a general CTD phosphorylation pattern with high Serine-5 and Serine-7 phosphorylation during transcription initiation and Serine-2, Threonine-4 and Tyrosine-1 phosphorylation during transcription elongation (Heidemann et al., 2013). Furthermore, recent studies have indicated that the CTD is also modified by other post-translational modifications including methylation and glycosylation (Heidemann et al., 2013). Overall, these modifications generate a complex and dynamic CTD code that regulates transcription and other nuclear processes as described further below.

1.1.2 mRNA processing and export

Eukaryotic pre-mRNA must be extensively processed before being exported to the cytoplasm where translation occurs. The CTD of RNA pol II serves to recruit several processing factors in a timely manner, thus coordinating the processing events. mRNA processing includes capping, splicing and polyadenylation, and these processing steps are crucial for gene expression since they determine the fate of the transcripts (Hocine et al., 2010).

The first processing event that occurs is the addition of an N7-methylguanosine cap to the 5' end of nascent RNA pol II transcripts. The mechanics and function of N7-methylguanosine cap formation are described in separate subchapters (subchapters 1.2 and 1.5).

The removal of non-coding intronic sequences from pre-mRNA and subsequent rejoining of exons is called splicing. Splicing is catalysed by the spliceosome, a large complex consisting of the small nuclear RNAs snRNA U1, U2, U4, U5 and U6 as well as a large number of proteins (Hoskins and Moore, 2012). The selection of splicing sites is a highly complex process which not only depends on cis-elements in the RNA, but also on trans-acting regulatory factors that enhance or repress recruitment of the

splicing machinery to splice sites. Splicing predominantly occurs co-transcriptionally and several splicing factors interact with the phosphorylated CTD of RNA pol II (Braunschweig et al., 2013). In metazoans, splicing is often differentially regulated during development and in various tissues leading to alternative inclusion of exons, a process called alternative splicing (Braunschweig et al., 2013). Alternative splicing allows production of different protein isoforms from a single gene and with 95 % of human multi-exon genes being alternatively spliced, this highly abundant process creates an enormous diversity in gene expression (Pan et al., 2008; Wang et al., 2008).

The final mRNA processing event is the formation of a polyadenylate (poly(A)) tail at the 3' end. This process is a two-step reaction that involves the endonucleolytic cleavage of the pre-mRNA followed by the synthesis of a poly(A) tail onto the 3' end of the upstream cleavage product (Hocine et al., 2010). Several polyadenylation factors interact with the Serine-2 phosphorylated CTD of RNA pol II and bind to the conserved poly(A) signal on the RNA (Hsin and Manley, 2012). After cleavage of the RNA 10 - 35 nucleotides downstream of the poly(A) signal the poly(A) polymerase (PAP) adds an adenosine tail of 200 - 250 residues. The poly(A) tail influences many aspects of mRNA metabolism such as transcription termination, mRNA stability, mRNA export and translation (Weill et al., 2012). As with splicing, transcripts can be alternatively polyadenylated and this contributes to gene expression by producing alternative protein isoforms or by altering stability or localisation of the mRNA (Di Giammartino et al., 2011).

After the pre-mRNA is processed into mature mRNA, it is exported via the nuclear pore complex into the cytoplasm. While many shorter RNAs such as micro (mi)RNAs and transfer (t)RNAs directly associate with export receptors, large RNAs such as mRNAs or ribosomal (r)RNAs assemble with RNA binding proteins into complexes that are then recognised by the RNA export machinery (Köhler and Hurt, 2007). Several proteins deposited during mRNA processing mediate the contact with the heterodimeric

mRNA export receptor TAP/p15. Among these proteins are the members of the exon-junction complex, the TREX complex and also the cap-binding complex, the latter of which will be further discussed below (Hocine et al., 2010; Köhler and Hurt, 2007).

1.1.3 Translation initiation

Efficient translation of most mRNAs is dependent on the N7-methylguanosine cap, which is recognised by the eIF4F complex consisting of eIF4E, eIF4G and eIF4A. eIF4E binds the N7-methylguanosine cap and interacts with the scaffolding protein eIF4G, which has binding sites for the RNA helicase eIF4A and eIF3. eIF3 recruits the 43S pre-initiation complex consisting of the 40S ribosomal subunit, the initiator methionyl tRNA (Met-$tRNA_i^{Met}$) and several translation initiation factors. After recruitment to the mRNA this translation pre-initiation complex scans for the AUG start codon that would base pair with Met-$tRNA_i^{Met}$. After removal of certain translation factors, the 60S ribosomal subunit joins to form the 80S initiation complex, which subsequently starts with the synthesis of the polypeptide (Jackson et al., 2010; Sonenberg and Hinnebusch, 2009).

Although most mRNAs use the scanning mechanism described above, a subset of mRNAs can initiate translation in a cap-independent manner via secondary structures within their 5' untranslated region (UTR) called internal ribosomal entry sites (IRES). It is thought that low levels of IRES-mediated translation may occur for mRNAs with highly structured 5' UTRs under normal growth conditions, however efficient IRES-mediated translation is supported when cap-dependent translational initiation is compromised during mitosis or following various stress conditions such as viral infections, apoptosis, heatshock or hypoxia (Komar and Hatzoglou, 2011; Spriggs et al., 2010). IRES-mediated translation initiation is cap-independent since the 43S initiation complex is directly recruited to structured RNA elements in proximity of the start codon. IRESs have been discovered and extensively studied in viruses, in which

certain IRESs can directly recruit the 43S initiation complex whereas others depend on translation initiation factors such as eIF4G, eIF4A and eIF3 (Balvay et al., 2009). Cellular IRESs generally require IRES-trans-acting-factors (ITAFs) to attain a structure that is competent to recruit the ribosomal subunits. However, little is currently known about the mechanics underlying cellular IRES function and it can be assumed that several different mechanisms exist since the structures of cellular IRES are very diverse (Komar and Hatzoglou, 2011).

1.1.4 Protein post-translational modifications

Once synthesised, the function of many polypeptides is regulated by post-translational modifications (PTMs). PTMs are highly diverse with well over 200 different PTMs identified by mass spectrometry. Some PTMs are chemical modifications including protein phosphorylation, acetylation, methylation and glycosylation. However, proteins are not only modified by the addition of small chemical moieties but can also be targeted for the attachment of small modifier proteins such as ubiquitin, small-ubiquitin-like modifier (SUMO) or other ubiquitin-like proteins. PTMs can alter protein functions in a dynamic manner by changing catalytic activity, subcellular localisation, stability or the interactions with other proteins. Some PTMs, such as glycosylation, are stable modifications required for protein maturation and folding. Others are reversible, dynamic modifications that can be added in response to intracellular or extracellular stimuli via the action of signalling pathways (Deribe et al., 2010).

Protein phosphorylation is a ubiquitous PTM used in many signal transduction pathways (Cohen, 2002; Deribe et al., 2010). Signalling pathways can be activated by nutrients, growth factors, hormones, cell cycle progression, stress and other signals, and serve to transduce or amplify intracellular or extracellular stimuli in order to control a cellular response. The addition of phosphate groups to protein substrates is catalysed by protein kinases of which there are more than 518 in the human genome

(Manning et al., 2002; Martin et al., 2009). Most eukaryotic protein kinases are structurally similar and possess a conserved catalytic domain that contains an adenosyl triphosphate (ATP) binding pocket. Kinases phosphorylate proteins by binding to ATP and the protein substrate and catalysing the transfer of the ATP γ-phosphate to the hydroxyl group of Serine, Threonine or Tyrosine residues in the protein substrate (Endicott et al., 2012; Ubersax and Ferrell, 2007). Although kinases share a common catalytic fold, they differ in charge and hydrophobicity of the surface residues. Therefore, kinases bind to specific protein substrates and for specific kinases consensus sequences can be determined around the phosphorylation site (Endicott et al., 2012; Ubersax and Ferrell, 2007). The action of kinases can be opposed by protein phosphatases that remove phosphate groups from protein substrates.

1.1.5 Nuclear protein import

Following synthesis in the cytoplasm, many polypeptides require translocation into the nucleus in order to reach their sites of function. Proteins greater than 40 kDa depend on active transport across the nuclear envelope through the nuclear pore complex. Karyopherins such as importins and exportins mediate nuclear trafficking of proteins by directly recognising specific nuclear localisation signals (NLSs) or nuclear export signals. Classical NLSs consist of one or two clusters of basic amino acids, which are recognised by Importin-α (Dingwall et al., 1982; Kalderon et al., 1984). Importin-α itself consists of three structural units: a central NLS-binding domain, an N-terminal Importin-β binding (IBB) domain and a C-terminal domain of unknown function. The central NLS-binding domain consists of a tandem series of 10 Armadillo repeats that generate a bent molecule which binds to classical NLSs (Conti and Kuriyan, 2000; Conti et al., 1998; Fontes et al., 2000). The IBB domain mediates the interaction with Importin-β but, via a cluster of positively charged amino acids resembling a NLS, also competes with cargos for binding to the NLS-binding site of Importin-α when

dissociated from Importin-β (Kobe, 1999). Importin-β consists of 19 - 20 helical HEAT repeats that are arranged into a ring-like structure which binds the Importin-α IBB domain (Cingolani et al., 1999).

Once Importin-α is bound to the NLS-containing cargo and to Importin-β, the complex is transported to the nucleus through interactions between Importin-β and the nuclear pore complex. Binding of Importin-β by nuclear Ran-GTP induces a conformational change that results in dissociation of Importin-α from Importin-β (Goldfarb et al., 2004; Stewart, 2007). Once free from Importin-β, the IBB domain of Importin-α competes for binding to the NLS binding site and together with interactions of nucleoporins with Importin-α causes the release of the cargo from of Importin-α (Gilchrist et al., 2002; Matsuura and Stewart, 2005; Matsuura et al., 2003). Finally, Importin-β bound to Ran-GTP and Importin-α bound to the nuclear export factor CAS and Ran-GTP are transported back to the cytoplasm. There, RanGAP stimulates GTP hydrolysis that releases Ran from Importin-β and CAS and thus freeing the Importins (Stewart, 2007).

In addition to the Importin-α/β system recognising classical NLSs there are several other nuclear transport pathways recognising non-classical NLSs. Non-classical NLS, such as the PY-NLS, have diverse amino acid sequences that are directly recognised by different Importin-β family members (Xu et al., 2010). Since Importin-β directly binds non-classical NLSs there is no requirement for Importin-α adaptors in these nuclear import pathways.

1.2 Formation of the N7-methylguanosine cap

1.2.1 The N7-methylguanosine cap structure

The N7-methylguanosine cap was first identified in viral RNA (Furuichi and Miura, 1975; Furuichi et al., 1975a) and subsequently also described in HeLa mRNA (Furuichi et al., 1975b). It consists of an inverted guanosine group that is linked via a 5' to 5' triphosphate bridge to the first transcribed nucleotide and is methylated at the N7 position (Figure 1.1a). The N7-methylguanosine cap is found on all eukaryotic RNA pol II transcripts and on eukaryotic viral RNA but it is absent in bacteria and archea (Shuman, 2001).

The N7-methylguanosine cap structure described above is called Cap0. In addition, further methylated cap structures have been identified in HeLa cells with methylation at the 2'-O ribose position of the first and second transcribed nucleotides termed Cap1 and Cap2 respectively (Figure 1.1b) (Furuichi et al., 1975b). Cap1 and Cap2 structures are only found in higher eukaryotes, including insects and vertebrates, and are absent in yeast (Furuichi and Shatkin, 2000). The enzymes catalysing 2'-O ribose methylation, hMTr1 and hMTr2, have been only recently identified and the exact functions of the Cap1 and Cap2 structures are still to be determined (Bélanger et al., 2010; Werner et al., 2011).

An alternate methyl cap structure has been described for small nuclear RNAs (snRNAs) that carry methylations on the positions 2,2,7 of the terminal guanosine resulting in a trimethylguanosine cap (Reddy et al., 1992). snRNAs are transcribed by RNA pol II and thus are initially capped with a N7-methylguanosine. However, following their assembly into small ribonucleoproteins (snRNPs) in the cytoplasm the cap becomes further methylated leading to a trimethyl guanosine cap, which is required for the nuclear import of snRNPs (Shaw et al., 2008).

a)

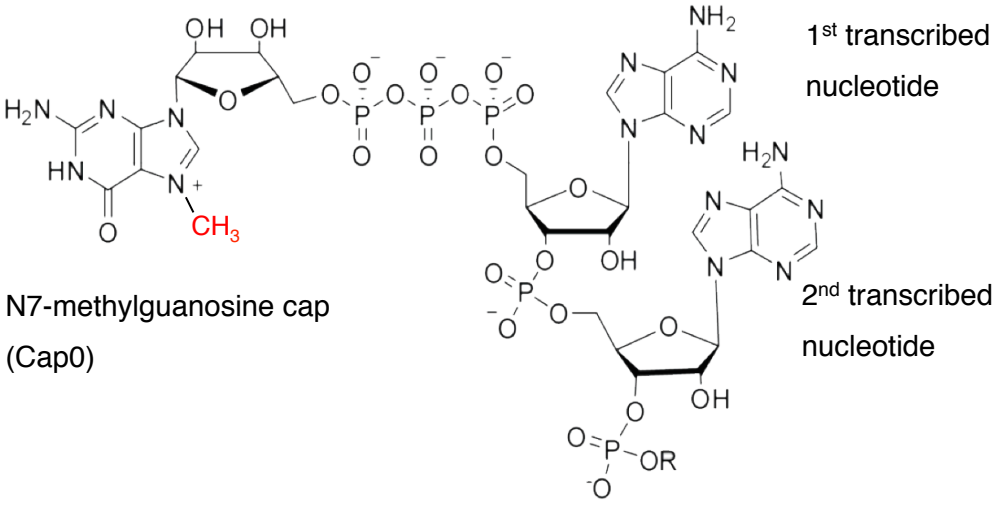

b)

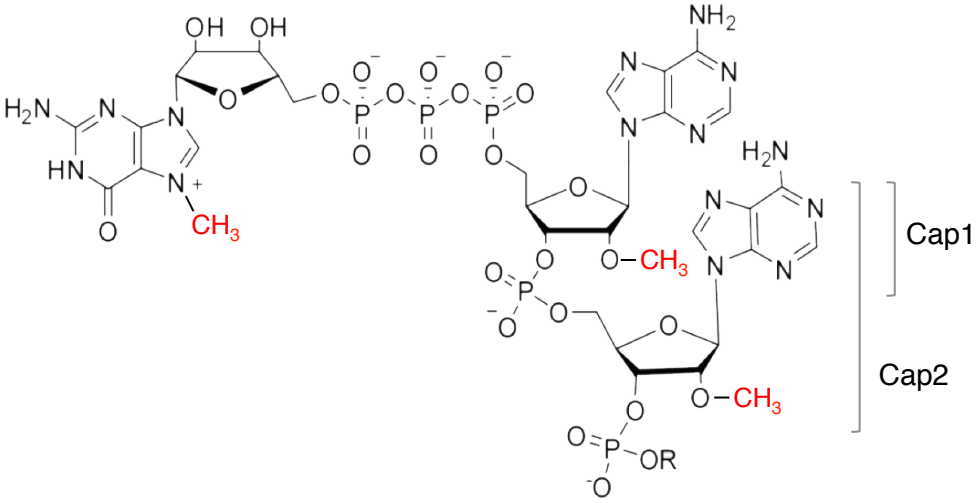

Figure 1.1 The structure of the N7-methylguoanosine cap (Cap0), Cap1 and Cap2.

a) The N7-methylguaonsine cap (Cap0) consists of a inverted guanosine group that is linked via a triphosphate bridge to the first transcribed nucleotide and is methylated at the N7-position. The Cap0 structure is conserved from yeast to man.

b) In higher eukaryotes, Cap1 or Cap2 structures have been identified. In addition to the methylation at the N7 guanosine position, the Cap1 structure is methylated at the 2'-O ribose of the first transcribed nucleotide and the Cap2 structure is further methylated at the 2'-O ribose of the second transcribed nucleotide.

The work presented in this thesis focuses on the N7-methylguanosine cap (Cap0) and thus the rest of the introduction describes the function of the N7-methylguaosine cap structure.

1.2.2 Enzymology of N7-methylguaonosine cap synthesis

The synthesis of the N7-methylguanosine cap requires a series of three enzymatic activities. First, an RNA triphosphatase removes the γ-phosphate from the triphosphate end of RNA pol II transcripts, yielding in a diphosphorylated 5' end (pppN → ppN). Following this, a guanylyltransferase catalyses the addition of a guanosine monophosphate (GMP) to the diphosphate end of the RNA producing the guanosine cap (ppN → GpppN). Finally, the guanosine cap is methylated at the N7-position by an RNA guanine-7 methyltransferase completing the formation of the N7-methylguanosine cap (GpppN → m7GpppN) (Figure 1.2) (Furuichi and Shatkin, 2000). The cap methyltransferase does not methylate free GTP but is only active towards guanosine triphosphate linked to an RNA molecule (Cowling lab, unpublished observations). While the guanylylation reaction is reversible, the triphosphatase and methyltransferase reactions are not (Shatkin, 1976).

N7-methylguaonosine cap formation occurs in all eukaryotes, including eukaryotic viruses. Initial insights into cap synthesis were obtained from studying viral systems. However, for the purpose of this thesis this introduction focuses and eukaryotic cell systems.

In the budding yeast *Saccharomyces cervisiae,* the three enzymatic activities required for N7-methylguaonosine cap synthesis reside within three separate polypeptides (Mao et al., 1995; Shibagaki et al., 1992; Tsukamoto et al., 1997) and the same is true for the fission yeast *Schizosaccharomyces pombe* (Pei et al., 2001; Saha et al., 1999; Shuman et al., 1994). The triphosphatases Cet1p and Pct1, the

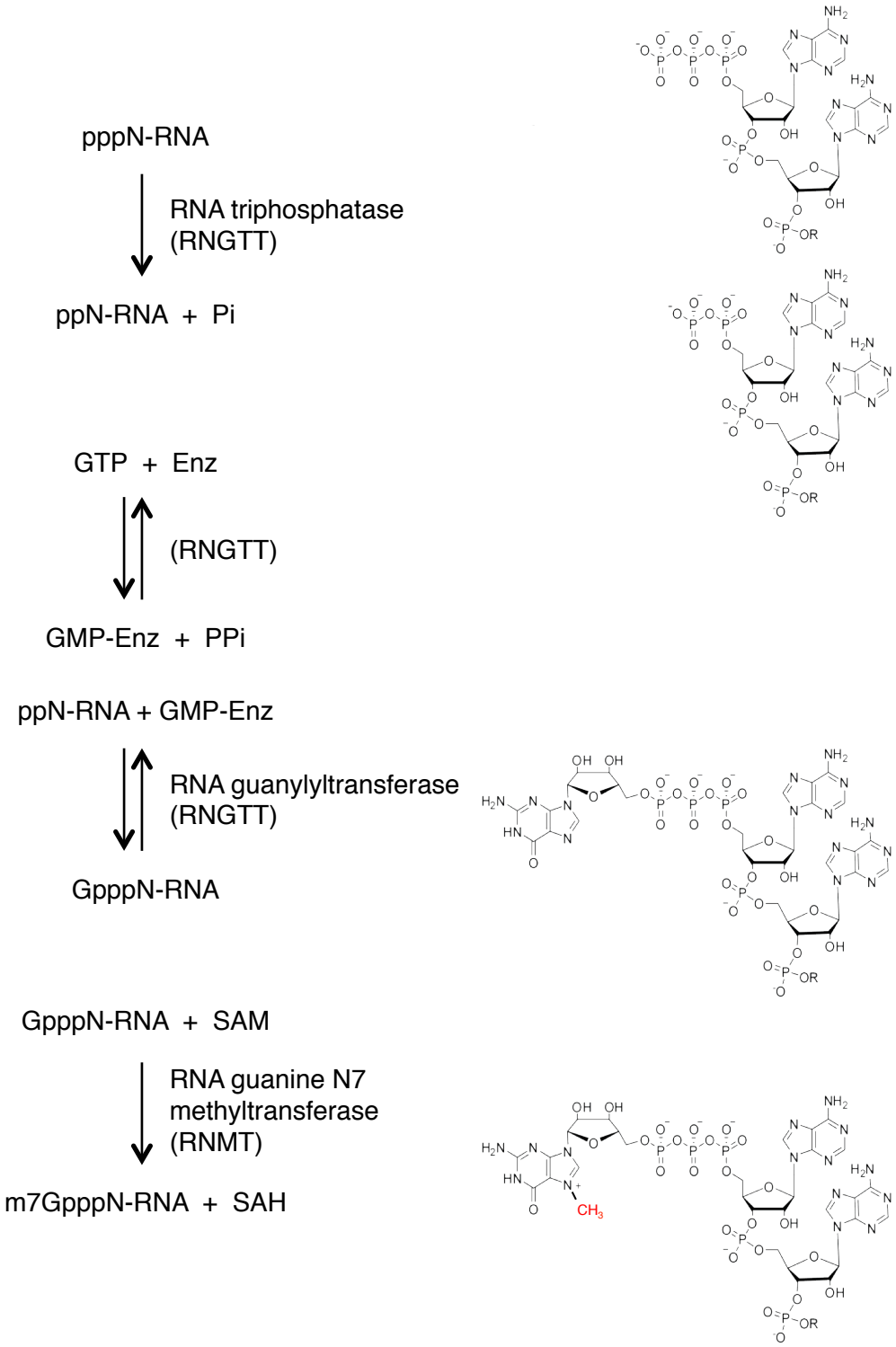

Figure 1.2 Reactions that are required for N7-methylguanosine cap synthesis. The synthesis of the N7-methylguanosine cap is described in the main text. This figure lists the enzymatic reactions on the left and graphically illustrates the reaction products on the right. The activities responsible for the reaction catalysis are indicated next to the arrows. The name of the actual mammalian enzyme is indicated in brackets.

guanylyltransferases Ceg1p and Pce1p and the RNA guanine-7 methyltransferases Abd1p and Pcm1p in *S. cervisae* and *S. pombe* respectively, are all essential for cell viability in yeast.

In contrast to yeast, metazoans possess a two-component system in which the triphosphatase and guanylyltransferase activities are combined into a single protein, whereas the RNA guanine-7 methyltransferase exists as a separate polypeptide. In mammals the bifunctional capping enzyme is called RNA guanylyltransferase and triphosphatase (RNGTT) (Pillutla et al., 1998a; Yamada-Okabe et al., 1998; Yue et al., 1997) and the methyltransferase is termed RNA guanine-7 methyltransferase (RNMT) (Pillutla et al., 1998a, 1998b; Saha et al., 1999; Tsukamoto et al., 1998). The capping machinery is functionally conserved from single-cell to multicellular organisms. Yeast deletion mutants can be rescued by their mammalian orthologues and the yeast capping system can be completely replaced by the mammalian enzymes (Saha et al., 1999; Yamada-Okabe et al., 1998; Yue et al., 1997). As in yeast, the human capping enzymes are essential for cell viability (Chu and Shatkin, 2008; Shafer et al., 2005) demonstrating the importance of the N7-methylguanosine cap and indicating that no other triphosphate, guanylyltransferase or methyltransferase can compensate for the loss of RNGTT and RNMT in cells.

In mammalian cells RNMT was demonstrated to exist in a complex with a 14 kDa protein termed RNMT activating miniprotein (RAM) (Gonatopoulos-Pournatzis et al., 2011). RAM was described as an obligate component of the mammalian cap methyltransferase complex and is required for normal cap methylation and gene expression. The RAM N-terminus interacts with the catalytic domain of RNMT and increases cap methyltransferase activity up to five-fold. In addition to the RNMT-interaction domain, RAM contains an RNA-binding domain and enhances RNA recruitment to RNMT. However, the RNA-binding domain is not required for RNMT activation suggesting that binding of RAM to RNMT induces a conformational change

that leads to increased cap methyltransferase activity (Gonatopoulos-Pournatzis et al., 2011).

1.2.3 The mechanics of N7-methylguanosine cap formation

Structural data on the yeast and mammalian capping machinery has revealed the mechanics of capping in further detail. In metazoans, the bifunctional capping enzyme RNGTT consist of a N-terminal triphosphatase domain (1-210) and a C-terminal guanylyltransferase domain (211-597) (Ho et al., 1998; Yamada-Okabe et al., 1998; Yue et al., 1997). The first step of N7-methylguanosine cap formation is the removal of the terminal phosphate group of the pre-mRNA by an RNA triphosphatase. Sequence and crystal structure analysis demonstrated that the RNA triphosphatase is not conserved amongst eukaryotes (Changela et al., 2001; Lima et al., 1999). The crystal structure of the mouse RNA triphosphatase domain revealed that it functions in a metal-independent way, whereby a cysteine phosphatase motif HCxxxxxR(S/T) (x is any amino acid) forms a phospho-enzyme intermediate during ATP hydrolysis (Changela et al., 2001). The active site pocket of the RNA triphosphatase domain can accommodate a triphosphate group but is too deep to allow diphosphate or monophosphate groups to assess the active site, thus providing substrate specificity towards the triphosphate 5' ends of pre-mRNA.

The second step in the capping process is the addition of an inverted guanosine group to the 5' end of the diphosphate RNA. The crystal structures of the guanylyltransferase from several organisms, including the human RNGTT 229-567 domain, revealed that the active sites are structurally related in eukaryotes (Chu et al., 2011; Fabrega et al., 2003; Gu et al., 2010; Håkansson and Wigley, 1998; Håkansson et al., 1997). Insights into the mechanism of the guanylylation reaction were obtained from crystal structures of viral and fungal enzymes. The addition the guanosine cap occurs in two steps. Firstly, the GTP covalently binds to a Lysine within the

guanylyltransferase active site forming an enzyme-GMP intermediate. GTP-binding causes a conformational change, which after release of the pyrophosphate exposes the RNA binding site and subsequently allows GMP transfer onto the diphosphate RNA (Fabrega et al., 2003; Håkansson and Wigley, 1998; Håkansson et al., 1997).

The final step in N7-methylguaonsine cap synthesis is the methylation of the guanosine cap by the RNA guanine-7 methyltransferase. The crystal structure of the cap methyltransferase Ecm1 of the microsporidian parasite *Encephalitozoon cuniculi* has been solved alone and in complex with the methyl donor S-adenosyl-methionine (SAM), the methylation biproduct S-adenosyl-homocysteine (SAH) or with a cap analogue (m7GpppG) (Fabrega et al., 2004). Furthermore, the crystal structure of the catalytic domain of the human RNMT (165-476) in complex with SAH or with the methyltransferase inhibitor sinefungin has been deposited online by The Structural Gene Consortium (Wu et al., 2007; Zeng et al., 2008). These crystal structures demonstrate that the active site is conserved amongst eukaryotes and contains two separate ligand-binding pockets for the SAM methyl donor and the guanosine cap methyl acceptor. Moreover, the crystal structure of Ecm1 revealed that the cap methyltransferase does not directly bind the methyl donor or acceptor suggesting that the enzyme optimally orients the substrates to facilitate methyl transfer (Fabrega et al., 2004).

1.2.4 N7-methylguanosine cap formation occurs predominantly co-transcriptionally

The formation of the N7-methylguanosine cap is the first pre-mRNA processing step and several studies demonstrated that this is a co-transcriptional event. *In vivo* labelling experiments with [^{3}H] methyl-L-methionine and [^{32}P] PO_4 in Chinese hamster ovary cells demonstrated that transcripts shorter than 750 nucleotides (nt) carry a methylated cap structure (Salditt-Georgieff et al., 1980). Nuclear run-on reactions performed on

purified engaged polymerases at heat shock induced genes from *Drosophila melanogaster* nuclear extracts demonstrated that RNA as short as 20 - 30 nt was guanosine capped (Rasmussen and Lis, 1993).

In vitro transcription experiments with HeLa nuclear extracts demonstrated that transcripts as short as 17 nt are not capped but those of 79 nt in length do carry a cap structure (Coppola et al., 1983). Another study found 15 nt long transcripts to be uncapped but 25 nt or longer transcripts were found to be capped (Moteki and Price, 2002). Furthermore, pulse chase experiments revealed that capping occurs on transcripts of 25 - 35 nt in length and methylation of the cap follows when the transcripts reach a size of 35 nt (Moteki and Price, 2002). Two other independent studies found that *in vitro* transcribed RNA associated with the transcription complex as short as 22 - 24 nt in length can be efficiently capped *in vitro* (Chiu et al., 2002; Mandal et al., 2004).

The suggestion that N7-methylguanosine cap formation is coupled to transcription came from two studies showing that both *in vitro* capping and methylation reactions of free RNA are much slower than that of RNA associated in transcription complexes (Jove and Manley, 1984; Moteki and Price, 2002). It was also observed that the inhibitory by-product of the methylation reaction, S-adenosylmethionine (SAH), inhibits *in vitro* transcription.

All the above studies collectively demonstrate that N7-methylguanosine cap formation occurs very early during transcription, probably as soon as the transcript is long enough to reach the end of the exit channel of RNA pol II. The model of co-transcriptional N7-methylguanosine cap formation is supported by reports studying the association of the capping machinery with chromatin and RNA pol II. Chromatin immunoprecipitation (ChIP) experiments in both yeast and human cells demonstrated that the capping enzymes accumulate at TSS (Glover-Cutter et al., 2008; Guiguen et al., 2007; Komarnitsky et al., 2000; Schroeder et al., 2000). However in contrast to

yeast, in human cells both RNGTT and RNMT were also crosslinked throughout the gene body and downstream of the poly(A) sites of the genes studied (Glover-Cutter et al., 2008). Furthermore, the capping machinery was found to be associated with the TSS at inactive gene promoters that are occupied by paused RNA pol II.

ChIP experiments in yeast revealed that the recruitment of all three capping enzymes is dependent on the Serine-5 phosphorylated CTD of RNA pol II (Komarnitsky et al., 2000; Schroeder et al., 2000). Moreover, direct interactions of RNA pol II with capping enzymes have also been reported. Yeast guanylyltransferase and cap methyltransferase were shown to bind the phosphorylated CTD of RNA pol II, whereby the triphosphatase is recruited via binding to the guanylyltransferase (Cho et al., 1997, 1998; McCracken et al., 1997). Furthermore, it was demonstrated that the CTD is required for efficient capping of RNA pol II transcripts (McCracken et al., 1997). A direct interaction of the mammalian RNGTT with phosphorylated CTD was also reported by several studies (Ho and Shuman, 1999; Ho et al., 1998; Yue et al., 1997) and the crystal structure of mouse RNGTT in complex with Serine-5 phosphorylated CTD of RNA pol II has been solved (Ghosh et al., 2011). Moreover, the Serine-5 phosphorylated CTD of RNA pol II is not only required for the recruitment of RNGTT to TSS but also stimulates guanylyltransferase activity of RNGTT (Ho and Shuman, 1999). Unlike in yeast, a direct interaction of the mammalian cap methyltransferase RNMT has not been reported despite exploiting yeast-two hybrid screens, immunoprecipitation studies, affinity purification experiments and SILAC analysis (Shatkin and Manley, 2000) (Cowling lab, unpublished data). However, a direct interaction of RNMT with RNGTT was observed with recombinant protein and a trimeric complex was detected when recombinant RNMT, RNGTT and cellular RNA pol II were incubated together *in vitro* (Pillutla et al., 1998b). Nonetheless, the exact mechanism of how mammalian RNMT is recruited to TSS *in vivo* remains to be determined.

The eukaryotic capping machinery mainly functions in the nucleus and immunofluorescence analysis of RNGTT and RNMT confirmed predominant nuclear localisation for both enzymes (Gonatopoulos-Pournatzis et al., 2011; Otsuka et al., 2009; Wen and Shatkin, 2000). However, besides co-transcriptional addition of the N7-methylguanosine cap, a subset of transcripts has been identified as a target for cytoplasmic capping. The initial indication for cytoplasmic capping originates from a study that observed the accumulation of truncated β-Globin mRNA harbouring premature termination stop codons (Lim and Maquat, 1992). The truncated mRNAs lacked parts of their 5' ends but were found to have a N7-methylguanosine cap-like structure. A cytoplasmic cap methyltransferase activity was also detected in *Xenopus laevis* oocytes (Gillian-Daniel et al., 1998). Furthermore, an enzyme identical to RNGTT in complex with an unidentified kinase was identified at low levels in the cytoplasmic fraction of human cell lines (Otsuka et al., 2009). Although a cap methyltransferase was not detected in the complex, low levels of RNMT were observed in cytoplasmic cell extracts by western blot. This cytoplasmic capping complex was demonstrated to be able to phosphorylate the 5' end of monophosphorylated RNAs and catalyse the addition of a GMP to the RNA 5' terminus. Furthermore, cytoplasmic capping was found to enhance the survival of cells following stress. More recently, a report described a subset of mRNAs that depend on cytoplasmic capping for maintenance of their transcript levels and translational activity (Mukherjee et al., 2012). These cytoplasmic capping targets are enriched for transcripts coding for proteins associated with nucleotide binding, protein and RNA localisation, and the mitotic cell cycle. Furthermore, enrichment for micro RNA sites and AU-rich elements was detected in the 3' UTR of these transcripts. However, the exact mechanism of how transcripts are recognised for cytoplasmic capping and its biological relevance remain unclear.

1.3 Regulation of N7-methylguoanosine cap formation in mammalian cells

1.3.1 Co-transcriptional activation of the capping enzyme

The guanylylation reaction catalysed by RNGTT occurs via an enzyme-GMP intermediate. Binding of the Serine-5 phosphorylated CTD of RNA pol II to the guanylyltransferase domain of RNGTT stimulates the formation of the enzyme-GMP intermediate and subsequently capping of RNA (Ho and Shuman, 1999; Wen and Shatkin, 1999). The extent of this activation was found to be directly proportional to the length of the CTD polypeptide ranging between 1.5 – 5.4-fold stimulation for 4 - 42 CTD heptad repeats. Experiments with differentially phosphorylated peptides demonstrated that this stimulatory effect only occurs with Serine-5 phosphorylated CTD but not Serine-2 phosphorylated CTD, despite the latter's ability to bind RNGTT (Ho and Shuman, 1999). Furthermore, RNGTT is activated by the interaction with the DSIF subunit Spt5, which was observed to stimulate enzyme-GMP complex formation by two-fold (Wen and Shatkin, 1999). Although Spt5 binds to both the triphosphatase and the guanylytransferase domain, only the latter is regulated by this interaction. The stimulatory effects of the Serine-5 phosphorylated CTD and Spt5 on RNGTT catalytic activity are not cumulative, and thus it is unclear whether RNGTT can bind to both proteins simultaneously. However, the requirement of RNA pol II and Spt5 for maximal RNGTT activity further supports the model of co-transcriptional capping.

1.3.2 Stimulation of the cap methyltransferase activity by the interaction with Importin-α

A direct interaction of RNMT with components of the transcription apparatus has not been reported but the Importin-α family member KPNA2 was identified as an RNMT binding protein in a yeast-two-hybrid screen (Wen and Shatkin, 2000). Importin-α functions in nuclear protein import by binding the NLS of a polypeptide and interacting with Importin-β, which mediates the translocation across the nuclear envelope. The interaction of RNMT with KPNA2 was confirmed by co-immunoprecipitations in HeLa cells, along with pull-down experiments with recombinant RNMT and *in vitro* translated ^{35}S-labelled KPNA2. Truncation mutants were used to map the binding domains, which revealed that RNMT 96-144 and KPNA2 455-496 are essential for the interaction between the two proteins. RNA band shift assays demonstrated that RNMT specifically binds to RNA containing a 5' GpppG but not to m7GpppG, whereby KPNA2 increases RNA recruitment to RNMT. Furthermore, full length KPNA2 was found to stimulate RNMT catalytic activity by up to 10-fold, whereas KPNA2 1-455, which did not bind to RNMT, did not alter RNMT activity. Incubation with Importin-β did not abolish the interaction between KPNA2 and RNMT, but it did inhibit the stimulatory effect of KPNA2 on RNA recruitment and RNMT activity. This was further supported by the observation that Ran-GTP, but not Ran-GDP, could reverse this inhibitory effect of Importin-β. The biological significance of a regulation of RNMT catalytic activity by KPNA2 remains unclear and it is unknown whether it occurs *in vivo*.

1.3.3 Accumulation of incompletely capped mRNAs under stress and normal growth conditions

The N7-methylguanosine cap is added by the sequential activities of a triphosphatase, a guanylyltransferase and a methyltransferase. It has long been thought that a complete N7-methylguanosine cap is constitutively added to the 5'

termini of all freshly synthesised RNA pol II transcribed RNA. However, recent evidence suggests that this may not be the case. The Myc transcription factor was found to upregulate cap methylation of specific mRNAs in a transcription-independent manner in mammalian cells (Cole and Cowling, 2009; Cowling and Cole, 2007a). Moreover, amino acid or glucose starvation of yeast cells leads to accumulation of mRNAs lacking the methylated cap structure, which were found not to bind to an anti-trimethylguanosine antibody column (Jiao et al., 2010). Furthermore, incompletely capped mRNAs were also detected under normal growth conditions both in yeast and mammalian cells. Unlike the canonical yeast decapping enzyme Dcp2 that targets methylated m7GpppN-capped RNA, the yeast decapping enzymes Rai1p and Dxo1p preferentially target unmethylated GpppN-capped RNA and thus form a quality control mechanism for mRNA 5' ends (Chang et al., 2012; Jiao et al., 2010). In yeast Rai1p Dxo1p deletion strains total mRNA levels were found to be increased due to an accumulation of incompletely capped mRNAs (Chang et al., 2012). These incompletely capped RNA species failed to bind to an anti-trimethylguanosine antibody column but were resistant to exoribonucleolytic degradation by Xrn1, which targets monophosphorylated RNA, indicating that they either carry an unmethylated cap structure or a triphosphate group at their 5' termini.

When the mammalian homolog of the yeast decapping enzymes Rai1 and Dxo1, termed DXO, was depleted with siRNAs from HEK-293 cells, the levels of mature, spliced mRNA only increased modestly (Jiao et al., 2013). A more dramatic increase was observed in the levels of intron-containing pre-mRNA. Further analysis using an anti-trimethylguanosine antibody column demonstrated an increase of RNA lacking a methylated cap structure relative to total pre-mRNA in DXO-depleted cells. These results suggest that incompletely capped pre-mRNA is produced in human cells, however these RNA species are not efficiently processed into mature mRNA but instead are degraded by DXO.

1.3.4 Stimulation of N7-methylguanosine cap formation by regulators of cell proliferation

There is an accumulation of evidence suggesting that the addition of the N7-methylguanosine cap is not a constitutive but a regulated process. The detection of incompletely capped transcripts demonstrates that N7-methylguanosine cap formation does not always occur to completion. Moreover, the observation that RNAs lacking the methylated guanosine cap accumulate under nutritional stress suggests that growth factors can regulate N7-methylguanosine cap formation. Indeed, the transcription factors Myc and E2F1 were found to upregulate N7-methylguanosine cap formation of specific transcripts (Cole and Cowling, 2009; Cowling and Cole, 2007a).

The proto-oncogenes Myc and E2F1 are upregulated in response to growth factors and are essential for cell proliferation and cell growth (Iaquinta and Lees, 2007; Meyer and Penn, 2008). The Myc family of transcription factors, consisting of N-Myc, c-Myc and L-Myc, are weak transcription factors which typically upregulate transcript levels by two-fold. A recent study suggested that rather than being an on/off specifier of transcription, c-Myc acts as a universal amplifier of expressed genes (Nie et al., 2012). Initially, it was reported that N-Myc increases translation of its target genes in a post-transcriptional manner without elevating their mRNA levels (Cowling and Cole, 2007a). Further experiments revealed that this is achieved by increased expression of the kinases CDK7 and CDK9. ChIP experiments demonstrated that N-Myc also increases recruitment of TFIIH to transcription initiation sites, thus leading to increased phosphorylation of the CTD of RNA pol II. This is thought to be required for the recruitment of the capping machinery and immunoprecipitation experiments with an anti-trimethylguanosine antibody indeed showed elevated N7-methylguanosine cap levels upon N-Myc-expression. c-Myc and E2F1 were also found to increase cap methylation of their target genes and for most genes investigated this increase was more than the increase in total mRNA level (Cole and Cowling, 2009). Moreover,

elevated RNA pol II CTD phosphorylation was shown to be required for E2F1-dependent upregulation of N7-methylguanosine cap levels, as treatment with the kinase inhibitor DRB was found to abolish this stimulation effect (Figure 1.3) (Aregger and Cowling, 2012).

In addition to increasing Serine-5 phosphorylation of the RNA pol II CTD and presumably promoting recruitment of the capping machinery to transcription initiation sites, c-Myc also increases the expression of S-adenosyl homocysteine hydrolase (SAHH), which removes the inhibitory bi-product of the methylation reaction (Fernandez-Sanchez et al., 2009). Experiments with cells depleted of SAHH demonstrated that the upregulation of SAHH is required for c-Myc-induced mRNA cap methylation, protein synthesis, cell proliferation and cell transformation. Furthermore, treatment with tubercidin at a concentration that inhibits cap methylation but not transcription confirmed that increased cap methylation is required for Myc-induced cell proliferation and protein synthesis (Figure 1.3).

1.3.5 RNMT overexpression promotes cap methylation of specific transcripts

Exogenous Myc expression does not result in increased RNMT protein levels or RNMT catalytic activity (Cowling, 2010). However, overexpression of RNMT leads to increased cell transformation allowing human mammary epithelial cells to grow in an anchorage-independent manner. Moreover, RNMT overexpression was found to increase Cyclin D1 protein expression by specifically elevating N7-methyguanosine cap levels on Cyclin D1 mRNA, while total Cyclin D1 mRNA levels did not change.

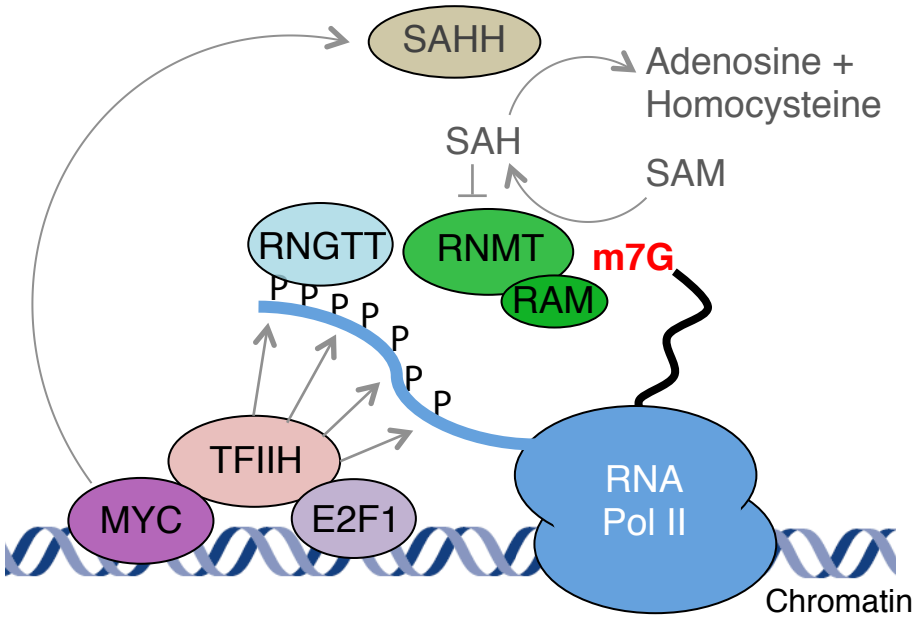

Figure 1.3 Upregulation of N7-methylguanosine cap synthesis by Myc and E2F1.

Formation of the N7-methylguanosine (m7G) cap occurs predominantly co-transcriptionally and the recruitment of the the capping machinery is dependent on Serine-5 phosphorylated (P) RNA pol II CTD. Myc and E2F1 upregulate the m7G cap levels of specific target transcripts by increasing recruitment of TFIIH, which is responsible for Serine-5 phosphorylation of the CTD. Furthermore, Myc increases the expression of SAHH, an enzyme that removes the inhibitory byproduct of the methylation reaction, SAH, and thus Myc can promote the formation of m7G in a second manner.

The discovery of incompletely capped mRNAs, together with the observation that N7-methylguanosine cap levels of specific mRNAs are upregulated in response to RNMT, Myc or E2F1 overexpression, suggests that there is a distinct cellular pool of mRNA lacking a methylated cap structure. It therefore is possible that induction of N7-methylguanosine cap formation is used to rapidly and specifically activate the expression of certain genes.

1.4 Cap-binding proteins

The N7-methylguanosine (m7G) cap functions in several aspects of gene expression including transcription, pre-mRNA processing, RNA export and translation. Cap-binding proteins that specifically recognise the methylated cap structure mediate many of these functions. The Cap-binding complex (CBC), eukaryotic initiation factor 4E (eIF4E) and the poly(A) deadenylase (PARN) have been demonstrated to interact with the m7G cap. These cap-binding proteins will be briefly described below and their cap-mediated function will be explained in the subchapter 1.5. In addition to the above mentioned cap-binding proteins, other polypeptides have also been reported to bind the m7G cap, including the poly(A) binding protein C (PABPC), the RNA-binding protein Pumillo2 (Pum2) and the exon junction complex component Y14, but the binding specificity for the methylated cap structure or the biological function for these interactions *in vivo* remain unclear (Cao et al., 2010; Chuang et al., 2013; Khanna and Kiledjian, 2004).

1.4.1 The cap-binding complex (CBC)

The cap-binding complex (CBC) consists of Cbp20 and Cbp80, 20 and 80 kDa in size respectively, and was first purified from HeLa cells using m7Gppp-sepharose (Izaurralde et al., 1994, 1995a). Crosslinking of RNA to the CBC in the presence of cap analogues demonstrated that CBC specifically binds to m7Gppp-RNA and not to other methylated cap structures (Izaurralde et al., 1994). The two components of the complex bind to RNA synergistically since neither of the subunits alone binds RNA efficiently (Izaurralde et al., 1994, 1995a; Kataoka et al., 1995). The crystal structure and mutational analysis of CBC revealed that the N7-methylguanosine-binding pocket resides solely in Cbp20, whereas Cbp80 stabilises structural changes required for binding to the methylated cap (Calero et al., 2002; Mazza et al., 2001, 2002).

CBC is predominantly nuclear, however it is also thought to function in the cytoplasm (Izaurralde et al., 1995b). In yeast, CBC is not essential for cell viability but is required for cell growth (Abovich et al., 1994; Das et al., 2000; Fortes et al., 1999; Uemura and Jigami, 1992) and in mammalian cells depletion of CBC by siRNAs also results in reduced cell proliferation (Narita et al., 2007; Pabis et al., 2013). The essential role of CBC in gene expression will later be described in detail (subchapter 1.5).

mTOR is a kinase that acts in the PI3K signal transduction pathway and integrates nutrient, growth factor, energy and stress signals to regulate cell growth and proliferation (Zoncu et al., 2011). CBC can be regulated by the mTOR pathway: orthophosphate labelling experiments demonstrated that Cbp80 is phosphorylated upon stimulation by growth factors and this phosphorylation is blocked by Rapamycin, an inhibitor of mTOR complex 1 (mTORC1) (Wilson et al., 2000). Cpb80 was found to be phosphorylated *in vitro* by S6 kinase, an mTORC1 target, which was found to elevate the cap-binding affinity of CBC (Wilson et al., 2000).

1.4.2 The eukaryotic initiation factor 4E (eIF4E)

Soon after its identification, the m7G cap was revealed to be essential for translation and thus it was tested whether translation initiation factors bind to it. A 24 kDa protein, that was later named eIF4E, was identified to specifically bind to the methylated cap structure and was purified from both human and yeast cells (Altmann et al., 1985, 1987; Sonenberg et al., 1978, 1979). eIF4E has been co-crystallised with a cap analogue and biophysical studies confirmed a specific association with the methylated cap structure (Marcotrigiano et al., 1997; Niedzwiecka et al., 2002). eIF4G, a scaffold polypeptide, interacts with eIF4E and stimulates its cap binding affinity by an allosteric activation mechanism (Gross et al., 2003; Haghighat and Sonenberg, 1997).

The translation initiation complex, termed eIF4F, consists of eIF4E, eIF4G and the RNA helicase eIF4A. The eIF4F complex recruits the 43S initiation complex containing the small ribosomal subunit to the mRNA (Sonenberg and Hinnebusch, 2009). Thus the binding of the eIF4F complex is essential for initiation of translation of most mRNAs.

Overexpression of eIF4E causes tumorigenic transformation of fibroblasts and promotes tumour formation in mice (Lazaris-Karatzas et al., 1990; Ruggero et al., 2004). In mammalian cells eIF4E is phosphorylated at Serine-209 by the mitogen-activated protein kinases Mnk1 and Mnk2 (Waskiewicz et al., 1997). Mnk1 has been shown to be recruited via its interaction with eIF4G (Pyronnet et al., 2001). Phosphorylation of eIF4E increases its affinity for the cap (Minich et al., 1994). Furthermore, eIF4E-promoted tumour formation in mice was found to be dependent on Serine-209 phosphorylation (Wendel et al., 2007).

eIF4E function is negatively regulated via eIF4E-binding proteins (4E-BPs). 4E-BP1, 2 and 3 comprise a family of low molecular weight proteins that bind to eIF4E and inhibit translation (Pause et al., 1994; Poulin et al., 1998). 4E-BPs compete with eIF4G for binding to eIF4E and thus inhibit cap-dependent translation by blocking eIF4F complex assembly (Haghighat et al., 1995; Mader et al., 1995; Marcotrigiano et al.,

1999). 4E-BPs are hyperphosphorylated by mTORC1, which abolishes their interaction with eIF4E and increases cap-dependent translation (Beretta et al., 1996; Brunn et al., 1997). In cells eIF4E and 4E-BPs are under homeostatic control, whereby overexpression of eIF4E induces dephosphorylation of 4E-BPs which in turn inhibits eIF4E activity (Khaleghpour et al., 1999). Furthermore, knockdown of eIF4E results in degradation of hyperphosphorylated 4E-BPs leading to only a minor decrease in translation (Yanagiya et al., 2012). Nevertheless, aberrant mTOR signalling can still lead to tumour formation via increasing eIF4E-mediated cap-dependent translation (Zoncu et al., 2011).

1.4.3 PARN

Deadenylation is the first step in mRNA decay and is catalysed by the poly(A)-specific ribonuclease (PARN) (Garneau et al., 2007). PARN was found to interact with m7G capped RNA and this interaction could be abolished by the cap analogue m7GpppG, but not GpppG, suggesting that the interaction is specific (Dehlin et al., 2000; Gao et al., 2000). Furthermore, experiments performed with HeLa cell extracts and *Xenopous laevis* oocytes demonstrated that capped RNA is deadenylated more efficiently than uncapped RNA and the m7GpppG analogue abolishes this deadenylation *in vitro* (Dehlin et al., 2000; Gao et al., 2000; Martinez et al., 2000). Recently, the crystal structure of PARN in complex with m7GpppG was solved and mutational analysis demonstrated that the residues involved in cap binding are essential for cap-stimulated deadenylation activity (Wu et al., 2009).

1.5 Functions of the N7-methylguanosine cap in gene expression

The m7G cap is conserved in eukaryotes and is essential for cell viability from yeast to man. Functions of the m7G cap in eukaryotic gene expression are diverse and some of them are species-specific. The m7G cap is involved in RNA stability, transcription, splicing, 3' end processing, RNA export, translation and miRNA biogenesis, where most of its functions are mediated via the cap-binding proteins described above. This subchapter aims to give an overview about the effects of the 5' cap on gene expression.

1.5.1 The N7-methylguanosine cap stabilises RNA

One of the first observed functions of the m7G cap is its ability to increase RNA stability. Injection of capped or uncapped RNA into *X. laevis* oocytes demonstrated that RNA with a m7GpppG or GpppG structure at its 5' end is more stable than uncapped RNA (Furuichi et al., 1977; Green et al., 1983). Furthermore, the same result was obtained when capped RNA or RNA treated with tobacco acid phosphatase (TAP), which removes the cap structure by hydrolysing the pyrophosphate bond, was incubated in wheat germ extracts (Furuichi et al., 1977; Shimotohno et al., 1977).

ApppG capped RNA is as stable as m7GpppG capped RNA indicating that the cap could act as blocking structure preventing exoribonucleolytic degradation (Inoue et al., 1989). This was confirmed by a study where capped but not uncapped RNA was protected from an exoribonuclease purified from HeLa nuclear extracts (Murthy et al., 1991). Furthermore, incubation with m7GpppG cap analogues, which compete for binding to cap-binding proteins, did not destabilise the capped transcripts. This

suggests that the cap structure on its own is sufficient to protect capped RNA from exoribonucleolytic attack and cap-binding proteins are not required for this effect.

Another report found that m7GpppG capped transcripts are more stable than GpppG capped transcripts when electroporated into mouse cells, suggesting that the addition of the methyl group to the cap further prevents degradation (Grudzien et al., 2006). Cap-binding proteins such as CBC and eIF4E specifically bind to the m7G cap and thus can increase RNA stability by competing with decapping enzymes (Jiao et al., 2013; Schwartz and Parker, 2000). Furthermore, eIF4E and CBC can also protect the m7GpppG-RNA from deadenylation. PARN was found to bind and deadenylate m7G capped RNA more efficiently than uncapped RNA (Dehlin et al., 2000; Gao et al., 2000; Martinez et al., 2000). The addition of eIF4E to this reaction inhibited deadenylation suggesting that eIF4E competes with PARN for binding to the m7G cap. Furthermore, CBC directly interacts with PARN and this interaction was found to inhibit PARN deadenylation activity (Balatsos et al., 2006). The guanylyltransferase activity of the capping enzyme is reversible whereas cap methylation is not (Shatkin, 1976). Therefore, another explanation for increased stability of m7GpppG capped RNA is that methylation prevents the reversibility of the capping reaction and thus stops formation of uncapped RNA, which can be rapidly degraded.

The influence of the m7G cap on endogenous transcripts was studied in the yeast *S. cerevisiae* using temperature-sensitive mutants of the guanylyltransferase Ceg1p. Mutation of Ceg1p reduced total transcript levels of various genes as detected by northern blotting (Fresco and Buratowski, 1996; Schwer and Shuman, 1996; Schwer et al., 1998). This phenotype was rescued in a Ceg1p Xrn1p double mutant lacking both the guanylyltransferase and the 5’ to 3’ exoribonuclease XRN1 indicating that uncapped transcripts are normally degraded by XRN1 (Schwer et al., 1998).

Mutation of the *S. cerevisiae* cap methyltransferase Abd1p also reduced transcript levels but the reduction was gene-specific and not as strong as in the Ceg1p mutant

(Schwer et al., 2000). Interestingly, the loss of mRNA levels in Abd1p mutated cells was partially rescued in mutants lacking the decapping enzyme Rai1p, which preferentially targets unmethylated GpppG-RNA for degradation (Jiao et al., 2010). This further confirms that the observed increase in stability of m7G capped RNA compared to unmethlyated guanosine capped RNA is due to its resistance to the decapping reaction.

1.5.2 The role of the N7-methylguanosine cap in transcription

ChIP experiments in yeast and mammalian cells demonstrated that CBC is localised at the 5' ends of genes and within gene bodies (Glover-Cutter et al., 2008; Lahudkar et al., 2011; Listerman et al., 2006; Narita et al., 2007; Zenklusen et al., 2002). The CBC subunits Cbp20 and Cbp80 alone do not localise to chromatin but are recruited as a complex only (Lahudkar et al., 2011; Wong et al., 2007). Moreover, inhibition of cap methylation by deletion of the yeast cap methyltransferase Abd1p results in a reduced ChIP signal for CBC (Wong et al., 2007). These experiments suggest that CBC recruitment to chromatin is dependent on the m7G cap and that CBC binds to RNA co-transcriptionally.

In addition to this, there is also evidence that once recruited, CBC can also regulate transcription. In *S. cervisiae*, CBC interacts with the transcription factor Mot1p, which in a gene-specific way activates or represses formation of the transcription pre-initation complex (Lahudkar et al., 2011). Furthermore, CBC was reported to bind to the yeast homologues of the mammalian pTEFb kinase CDK9 and to CDK12, which are responsible for RNA pol II CTD Serine-2 phosphorylation (Hossain et al., 2013). Consistent with this, depletion of CBC decreased recruitment of these CDK complexes to expressed genes, which in turn lead to reduced transcription due to a reduction in Serine-2 phosphorylation levels (Hossain et al., 2013; Lidschreiber et al., 2013).

It is not clear whether CBC interacts with the mammalian homologue of Mot1p but studies in human cells showed that CBC also binds to pTEFb (Lenasi et al., 2011). pTEFb phosphorylates the RNA pol II CTD at Serine-2 and the Spt5 subunit of DSIF, which abolishes NELF/DSIF-mediated promoter proximal pausing of RNA pol II and thus promotes transcription elongation. Depletion of CBC resulted in reduced pTEFb recruitment to promoters, a reduction in Serine-2 phosphorylation and accumulation of RNA pol II within gene bodies. Thus CBC can promote transcription elongation in both yeast and mammalian cells.

In addition to CBC-mediated effects, the mammalian capping enzyme, RNGTT, was found to promote transcription elongation *in vitro* (Mandal et al., 2004). The addition of RNGTT to paused transcription complexes was found to overcome NELF-mediated repression of transcription. This effect is independent of RNGTT catalytic activity and may be mediated by the interaction of RNGTT with Spt5 (Wen and Shatkin, 1999).

An interaction of Spt5 with the capping enzymes was also detected in yeast and was found to be essential for the recruitment of the capping machinery to chromatin (Lidschreiber et al., 2013; Lindstrom et al., 2003; Pei and Shuman, 2002). Furthermore, in *S. pombe* the RNA triphosphatase and cap methyltransferase were found to bind to CDK9 and deletion of the cap methyltransferase resulted in decreased Serine-2 phosphorylation and promoter-proximal stalling of RNA pol II (Guiguen et al., 2007; Pei et al., 2003; St Amour et al., 2012). In addition, the *S. cerevisiae* cap methyltransferase was found to act independently of its catalytic activity as a gene-specific transcription factor required for RNA pol II recruitment and promoter clearance (Schroeder et al., 2004).

All the above demonstrates, that the capping machinery as well as the m7G cap via CBC promote transcription elongation and therefore the capping process may act as a quality checkpoint avoiding transcription elongation of uncapped RNA.

1.5.3 CBC is required for efficient pre-mRNA splicing

Pre-mRNA often contains non-coding intronic sequences that are removed co-transcriptionally by splicing. The effect of the m7G cap on pre-mRNA splicing has been extensively studied. In initial experiments, splicing was assessed by incubating *in vitro* transcribed capped and uncapped RNA with HeLa nuclear extracts (Edery and Sonenberg, 1985; Izaurralde et al., 1994; Konarska et al., 1984; Ohno et al., 1987; Patzelt et al., 1987). These experiments revealed that the m7G cap is required for splicing. Interestingly, for RNA containing two introns, only the splicing of the 5' proximal intron was found to be dependent on the cap structure (Ohno et al., 1987).

RNA carrying a methylguanosine (m7GpppG) and guanosine (GpppG) cap were both efficiently spliced when incubated with HeLa cell extracts (Edery and Sonenberg, 1985; Ohno et al., 1987). However, when S-adenosyl homocysteine (SAH) was added to inhibit the methylation of GpppG-RNA, splicing of the guanosine capped RNA was inhibited suggesting that a methylated cap structure is required for splicing (Ohno et al., 1987). Furthermore, the cap analogues m7Gppp and m7GpppG inhibit splicing more strongly than the GpppG analogue suggesting that the effect of the cap on splicing is dependent on a methylguanosine cap binding protein (Edery and Sonenberg, 1985; Izaurralde et al., 1994; Konarska et al., 1984; Ohno et al., 1987; Patzelt et al., 1987). Indeed, depletion of CBC from nuclear cell extracts strongly inhibited splicing (Izaurralde et al., 1994; Lewis et al., 1996).

Microinjection of RNA into *Xenopus laevis* oocytes confirmed that splicing of the 5' proximal intron is dependent on the cap structure (Inoue et al., 1989). Furthermore, co-injection of antibodies against Cbp80 into *X. laeavis* oocytes reduced splicing demonstrating the requirement of CBC for splicing *in vivo* (Izaurralde et al., 1995a). The m7G cap and CBC were also found to enhance splicing in *S. cerevisiae* (Colot et al., 1996; Fresco and Buratowski, 1996; Lewis et al., 1996; Schwer and Shuman, 1996;

Schwer et al., 2000). Furthermore, splicing in *Arabidopsis thaliana* was also observed to be dependent on CBC (Laubinger et al., 2008).

A recent study investigated the role of CBC in splicing in mammalian cells and identified a direct interaction of CBC with the spliceosomal small nuclear ribonucleoprotein particles U4/U6•U5 tri-snRNP (Pabis et al., 2013). This interaction was shown to be required for recruitment and assembly of the spliceosome. Furthermore, studies investigating the splicing of endogenous transcripts revealed that the m7G cap and CBC not only enhance splicing of the 5' proximal intron, but also promote removal of downstream introns (Jiao et al., 2013; Pabis et al., 2013). However, only selected transcripts were investigated in this study and further experiments are required to determine whether this is a gene-specific or a global effect.

Finally, along with constitutive splicing, CBC has also been reported to influence alternative splicing in both humans and plants (Lenasi et al., 2011; Raczynska et al., 2010). It was demonstrated that CBC is required for the recruitment of the alternative splicing factor SRSF1 (Lenasi et al., 2011).

1.5.4 CBC and pre-mRNA 3' end processing

Following transcription termination the 3' end of the newly synthesised pre-mRNA is cleaved and a poly(A) tail is attached. The m7G cap has been reported to influence this 3' end processing event. Incubation of *in vitro* transcribed RNA with HeLa nuclear extracts or injection of RNA into *X. laevis* oocytes demonstrated that the m7G cap promotes RNA cleavage at the poly(A) site (Cooke and Alwine, 1996; Georgiev et al., 1984; Gilmartin et al., 1988). A requirement for the m7G cap for 3' end cleavage was also observed in HeLa cells where m7G-capped transcripts were found to be more efficiently cleaved at the poly(A) site than uncapped transcripts (McCracken et al., 1997). The addition of the cap analogue m7GpppG inhibits 3' end cleavage suggesting an involvement of a m7G cap-binding protein in this process (Cooke and Alwine, 1996).

Depletion of CBC from HeLa nuclear extracts was found to reduce mRNA 3' end cleavage, which could be rescued by the addition of recombinant CBC, confirming that CBC is required for proper mRNA 3' end processing in mammalian cells (Flaherty et al., 1997).

Contrary to this, in yeast the m7G cap does not seem to be required for pre-mRNA 3' end cleavage since temperature-sensitive Ceg1p capping enzyme mutants showed no effect on polyadenylation (Fresco and Buratowski, 1996). Moreover, CBC was found to interact with Npl3p, which suppresses recruitment of 3' end cleavage factors, and thus reduce termination of transcription at weak terminators (Wong et al., 2007). This suggests that the function of the CBC in processing the 3' ends of pre-mRNA is not conserved in eukaryotes.

Unlike other mRNAs, histone mRNAs are not polyadenylated but instead carry a conserved stem loop structure at their 3' termini (Marzluff et al., 2008). CBC interacts with NELF-E and Ars2 that mediate recruitment of processing factors required for this stem loop formation (Gruber et al., 2012; Narita et al., 2007). siRNA-mediated depletion of CBC leads to aberrant polyadenylation of the histone mRNA, suggesting its direct involvement in the proper formation of histone mRNA 3' ends (Narita et al., 2007).

1.5.5 Involvement of CBC and eIF4E in snRNA and mRNA export

After transcription by RNA pol II, mRNA and snRNA are exported to the cytoplasm where mRNA is translated, whereas snRNA is modified and assembled into snRNP complexes before translocating back into the nucleus. mRNA and snRNA are exported via two different pathways, both of which involve CBC.

Injection of snRNA into *X. laevis* oocytes demonstrated that snRNA export requires the m7G cap and is mediated by CBC (Hamm and Mattaj, 1990; Izaurralde et al., 1992,

1995a). snRNA bound by CBC was reported to be exported in a complex with the adaptor protein PHAX (Ohno et al., 2000). In the nucleus, PHAX is phosphorylated and forms an export complex with the export receptor CRM1 (Exportin-1), Ran-GTP and snRNA-bound CBC (Kitao et al., 2008; Ohno et al., 2000). The complex is exported in a Ran-GTP-dependent manner to the cytoplasm where PHAX is dephosphorylated, which causes disassembly of the complex and release of the snRNA into the cytoplasm. CBC was also found to interact with Importin-α and *in vitro* studies revealed that CBC, capped-RNA and Importin-α form a complex which is disrupted upon binding by Importin-β (Dias et al., 2009; Görlich et al., 1996). Inhibition of the interaction between Importin-α and Importin-β resulted in the accumulation of microinjected snRNA in the nucleus of *X. laevis* oocytes (Görlich et al., 1996). However, it is unclear whether the interaction of CBC with Importin-α and Importin-β is essential for the export of snRNA *in vivo*.

Similar to snRNA, the export of microinjected mRNA in *X. laevis* oocytes is dependent on the m7G cap and is inhibited by cap analogues (Cheng et al., 2006; Dargemont and Kühn, 1992; Jarmolowski et al., 1994). Experiments in mammalian cells demonstrated that CBC interacts with Aly/REF, which is a component of the TREX complex (Cheng et al., 2006). The TREX complex interacts with the heterodimeric export receptor of mRNA transport, TAP/p15 (Köhler and Hurt, 2007). TREX was found to be most efficiently recruited to spliced mRNA, which is therefore exported more efficiently than unspliced RNA (Cheng et al., 2006). Moreover, RNA lacking introns is also exported in a cap-dependent manner and this was also found to depend on the interaction of CBC with Aly/REF (Nojima et al., 2007). Although the bulk of mRNA is exported in a CBC-dependent manner via the TREX/TAP pathway other TAP-mediated mRNA export pathways do exist. Furthermore, a subset of mRNAs containing AU-rich elements in their 3' UTRs is exported via a CRM1-dependent pathway (Culjkovic-Kraljacic and Borden, 2013).

snRNA and mRNA both carry the m7G cap that is bound by CBC but are exported via two different pathways. A recent study revealed that the RNA length is responsible for determining the export pathway (McCloskey et al., 2012). RNAs smaller than 200 - 300 nt are bound by the nuclear RNA binding protein hnRNP C, which abolishes the interaction of PHAX with CBC and selects the TREX/TAP pathway.

In addition to CBC, eIF4E was also demonstrated to promote mRNA export. It was observed that eIF4E enhances gene-specific nuclear export of mRNAs harbouring a conserved structural motif in their 3' UTR, such as Cyclin D1 mRNA (Culjkovic et al., 2006; Rousseau et al., 1996). eIF4E-mediated export of mRNAs occurs in a cap-dependent manner as a mutant unable to bind to the m7G cap could not promote mRNA export (Culjkovic et al., 2006). Furthermore, addition of promyelocytic leukemia protein (PML), which reduces eIF4E affinity for the cap, also inhibited eIF4E-mediated mRNA export (Cohen et al., 2001; Culjkovic et al., 2006). An eIF4E mutant unable to function in translation initiation could still promote mRNA export suggesting that the function of eIF4E in mRNA export is independent of its function in translation (Culjkovic et al., 2006). In contrast to the bulk of mRNA export, eIF4E-mediated mRNA export is CRM1-dependent but the exact mechanism is unclear.

In yeast, the bulk of mRNA export does not depend on the m7G cap since Ceg1p mutants did not display altered RNA distribution between the nucleus and the cytoplasm (Fresco and Buratowski, 1996). This indicates that the mechanics of RNA export are not conserved in all eukaryotes. However, it should be noted that these results were obtained by fluorescence microscopy analysis at rather low resolution.

1.5.6 The N7-methylguanosine cap is required for eIF4E-mediated translation initiation

From yeast to man, the m7G cap is essential for translation of most mRNAs. Removal of the cap structure from *in vitro* transcribed RNA abolishes translation in

wheat germ cell-free systems (Muthukrishnan et al., 1975; Shimotohno et al., 1977; Zan-Kowalczewska et al., 1977). Unmethylated capped RNA added to wheat germ extracts was only translated upon the addition of the methyl donor S-adenosyl methionine (SAM), whereas translation of methylated RNA did not depend on SAM (Both et al., 1975). Furthermore, incubation with the methylation inhibitor S-adenosyl homocysteine (SAH) inhibited protein synthesis from unmethylated capped RNA but not of methyl-capped RNA, indicating that the methylation of the cap is essential for protein synthesis. Finally, the addition of a cap analogue to wheat germ or HeLa cell extracts inhibited translation and association of ribosomal proteins with the mRNA (Hickey et al., 1976; Weber et al., 1976).

The m7G cap was also found to be required for translation *in vivo*. Temperature-sensitive mutants of the *S. cervisiae* capping enzyme Ceg1p exhibit near loss of translation at the restrictive temperature (Schwer et al., 1998). However, this was accompanied with a strong reduction in transcript levels due to instability of the uncapped mRNA. Contrary to this, the reduction in transcript levels was less prominent in temperature-sensitive mutants of the cap methyltransferase *Abd1p*. However, protein synthesis was nearly abolished in both mutants, thus confirming the function of the methylated cap in translation.

Furthermore, microinjection of *in vitro* transcribed RNA into *X. laevis* oocytes demonstrated that m7GpppG capped RNA is translated more efficiently than GpppG capped or uncapped RNA (Drummond et al., 1985; Gillian-Daniel et al., 1998). Furthermore, the cap analogue m7GpppG but not ApppG inhibited protein synthesis suggesting an involvement of a methyl cap-binding protein in the process (Gillian-Daniel et al., 1998).

The cap-binding protein eIF4E was found to stimulate the translation of m7GpppG capped but not uncapped RNA in cell-free systems suggesting that eIF4E mediates the role of the m7G cap in translation (Sonenberg et al., 1979, 1980). eIF4E is responsible

for the recruitment of eIF4G and eIF4A to the 5' end of mRNA, thus forming the eIF4F complex (Lamphear et al., 1995; Mader et al., 1995). eIF4A is an ATP-dependent RNA helicase that unwinds secondary structures in the RNA and this activity is required for efficient translation (Edery et al., 1984; Koromilas et al., 1992). The scaffolding protein eIF4G interacts with eIF4E, eIF4A, eIF3 and the poly(A)-binding protein (PABP) (Gingras et al., 1999; Hentze, 1997).

The eIF4F complex is required for the recruitment of the translation initiation complex containing the 40S ribosomal subunit and several translation factors. This is mediated by interaction of eIF4G with eIF3, which is part of the 43S initiation complex (Sonenberg and Hinnebusch, 2009; Topisirovic et al., 2011). Furthermore, the eIF4F complex also promotes translation via its interaction with PABP. PABP interacts with the poly(A) tail and eIF4G, which in turn stabilises the association of eIF4E with the cap (Kahvejian et al., 2005) and circularises the mRNA (Wells et al., 1998). The formation of a closed loop, by linking the cap with the poly(A) tail, is believed to increase translation by enhancing recycling of ribosomes on the mRNA and thus facilitating translation re-initiation (Sonenberg and Hinnebusch, 2009; Topisirovic et al., 2011).

However, not all mRNAs are equally dependent on eIF4E-mediated translation initiation (Hsieh et al., 2012; Thoreen et al., 2012). eIF4E function can be inhibited by eIF4-BPs, which in an unphosphorylated state bind to eIF4E and inhibit its ability to interact with eIF4G (Sonenberg and Hinnebusch, 2009; Topisirovic et al., 2011). ATP site-specific inhibition of the kinase mTOR, which is responsible for phosphorylation of eIF4-BPs, was found to reduce global protein synthesis. However, ribosome profiling demonstrated that the translation of a subset of mRNAs was much more impaired than that of others (Hsieh et al., 2012; Thoreen et al., 2012). These mRNAs were shown to harbour a 5' terminal oligopyrimidine tract (TOP) and further experiments found the translation of these 5' TOP mRNAs to be particularly dependent on the interaction of eIF4G with eIF4E.

1.5.7 CBC-mediated pioneer round of translation

The majority of translation is dependent on eIF4E but the translation of m7G capped mRNA can also be mediated by CBC, which is referred to as the pioneer round of translation. As opposed to eIF4E-mediated steady-state translation, which functions to generate large amount of protein, the CBC-mediated pioneer round of translation is thought to serve as a quality control mechanism coordinating nonsense-mediated mRNA decay (NMD) (Maquat et al., 2010; Topisirovic et al., 2011). NMD is a translation-dependent surveillance pathway that recognises and degrades aberrant mRNAs harbouring a premature termination stop codon (Schweingruber et al., 2013).

The mechanism of CBC-mediated translation initiation is not completely clear and is disputed in the field. CBC, similarly to eIF4E, was found to interact with eIF4G in yeast and mammalian cells (Chiu et al., 2004; Fortes et al., 2000; Lejeune et al., 2004; McKendrick et al., 2001). However, this interaction could not be confirmed by other studies and instead it was reported that CBC binds to CTIF, which contains a domain also found in eIF4G (Choe et al., 2012; Kim et al., 2009). CTIF was found to interact directly with eIF3g, which is part of the eIF3 complex responsible for the recruitment of the small ribosomal subunit (Choe et al., 2012). The depletion of CTIF from cell extracts selectively inhibited the translation of CBC-bound mRNA while the addition of recombinant CTIF restored CBC-mediated translation *in vitro* (Kim et al., 2009). Furthermore, CTIF knockdown caused a redistribution of CBC from polysomal to subpolysomal fractions in human cells (Choe et al., 2012; Kim et al., 2009). This suggests that CBC may mediate translation initiation by interacting with CTIF that recruits the eIF3 complex containing the 40S ribosomal subunit.

After mRNA export into the cytoplasm, translation promotes the removal of several nuclear mRNPs, such as the exon-junction complex or PABPN1. However, the exchange of CBC by eIF4E is independent of translation and seems to depend on the

interaction of CBC with the nuclear protein import machinery (Sato and Maquat, 2009). Inhibition of the binding of Importin-β to Importin-α resulted in the accumulation of CBC-bound mRNA and reduced binding of mRNA to eIF4E.

The detailed mechanism and the portion of mRNA that undergoes a pioneer round of translation remain unclear. Furthermore, the exclusive role of the pioneer round of translation in quality control has been questioned since it was revealed that nonsense-mediated mRNA decay (NMD) not only occurs in connection with CBC-mediated translation (Ishigaki et al., 2001; Lejeune et al., 2002) but also during any round of translation including eIF4E or IRES-mediated translation (Durand and Lykke-Andersen, 2013; Maderazo et al., 2003; Rufener and Mühlemann, 2013).

1.5.8 CBC is required for miRNA biogenesis

miRNAs are 21 – 23 nt short RNAs that function to silence expression of specific genes in animals and plants. miRNA genes are transcribed by RNA pol II as primary miRNA (pri-miRNA), which carry a m7G cap and a poly(A) tail. pri-miRNA folds back into stem loop structures, which are cleaved by Drosha in the nucleus producing pre-miRNA and are then processed into short miRNAs by Dicer in the cytoplasm. miRNAs bind to Ago and are incorporated into the RNA-induced silencing complex (RISC), which by pairing with complementary mRNA sequences induces translational repression or degradation of the bound mRNA (Bartel, 2009).

CBC was found to interact with Ars2, which is required for miRNA biogenesis (Gruber et al., 2009; Sabin et al., 2009). Gel shift assays performed with HeLa nuclear extracts demonstrated that Ars2 exists in a complex with CBC and m7G capped RNA *in vivo* (Gruber et al., 2009). siRNA-mediated depletion of CBC in mammalian and fly cells resulted in a reduction of miRNA-mediated silencing (Gruber et al., 2009, 2012; Sabin et al., 2009). Northern-blot analysis revealed a reduction of pri-miRNA levels, suggesting that CBC might stabilise the miRNA precursors. In plants, miRNA

biogenesis was impaired upon deletion of the CBC, however pri-miRNA levels accumulated which suggests a defect in miRNA processing (Laubinger et al., 2008). In agreement with this observation, Ars2 was found to interact with Drosha, and this may explain how CBC promotes processing of miRNAs (Gruber et al., 2009; Sabin et al., 2009). However, the exact details of how CBC regulates miRNA biogenesis remain unclear.

miRNAs act by repressing translation and inducing subsequent mRNA degradation. miRNA-mediated repression of translation occurs during the translation initiation step by interfering with the function of the eIF4F initiation complex (Meijer et al., 2013). Not surprisingly, miRNA silencing of several reporter constructs and *in vitro* transcribed RNA was found to be dependent on the m7G cap whereas IRES-mediated translation was resistant to miRNA-mediated translation inhibition (Iwasaki and Tomari, 2009; Iwasaki et al., 2009; Pillai et al., 2005; Thermann and Hentze, 2007)

1.6 Decapping and RNA degradation

The regulation of mRNA stability is an essential step in gene expression since the steady state level of mRNA is determined not only by transcription but also by mRNA degradation. The removal of the cap structure by decapping enzymes plays a critical role in mRNA decay. The bulk of mRNA decay initiates with the shortening of the poly(A) tail followed by exoribonucleolytic degradation of the mRNA either in 3' to 5' or 5' to 3' direction (Garneau et al., 2007). In the 3' to 5' directed mRNA decay, the mRNA is degraded by the exoribonuclease complex, called the exosome, which functions both in the cytoplasm and the nucleus (Chlebowski et al., 2013). The exosome degrades most of the mRNA leaving a short, capped oligonucleotide behind, which after decapping can be degraded completely. In contrast, the 5' to 3' mRNA decay initiates with the decapping step, which is then followed by mRNA degradation by exoribonucleases such as the cytoplasmic XRN1 and the nuclear XRN2 (Nagarajan et al., 2013).

Five different decapping enzymes have been identified in yeast. The decapping scavenger enzyme, DcpS, was found to be associated with the exosome and is involved in the 3' to 5' mRNA decay pathway (Wang and Kiledjian, 2001). DcpS has decapping activity against capped RNA shorter than 10 nt and it hydrolyses the methylated cap structure releasing m7Gp (Liu et al., 2002).

In contrast to the 3' to 5' pathway, decapping enzymes involved in the 5' to 3' pathway target longer RNA oligonucleotides. The Dcp2p/Dcp1p complex hydrolyses the cap of m7GpppG-RNA longer than 25-29 nt in length into m7Gpp (Dunckley and Parker, 1999; LaGrandeur and Parker, 1998; Steiger et al., 2003). Dcp2p alone possesses decapping activity, but this is strongly stimulated by the interaction with the cofactor Dcp1p. The Dcp2p/Dcp1p complex localise to P-bodies, which are discrete foci in the cytoplasm where mRNA decay occurs (Sheth and Parker, 2003).

Furthermore, Ddp1p, the yeast homologue of mammalian Nudt3, was recently found to be able to decap m7G capped RNA *in vitro* producing m7Gp and m7Gpp, however this activity was not investigated *in vivo* (Song et al., 2013).

Two yeast decapping enzymes were found to exhibit stronger decapping activity towards unmethylated compared to methylated caps. Rai1p functions in the nucleus together with the exoribonuclease Rat1p, a homologue of mammalian XRN2 (Xiang et al., 2009; Xue et al., 2000). It has both decapping and pyrophosphatase activities, but it preferentially targets unmethylated capped RNA and cleaves off the entire cap structure, (m7)GpppG (Jiao et al., 2010; Xiang et al., 2009). The second enzyme, Dxo1, is active in the cytoplasm and possesses both decapping and exoribonuclease activity (Chang et al., 2012). Similar to Rai1p, Dxo1p exhibits stronger decapping activity against unmethylated capped RNA and also removes the entire cap structure. Both Rai1p and Dxo1p are thought to function in a quality control mechanism targeting mRNAs carrying an aberrant cap structure (Chang et al., 2012; Jiao et al., 2010).

Most of the yeast decapping activities are conserved in mammalian cells. As in yeast, DcpS hydrolises the m7G cap structure from short oligonucleotides following 3' to 5' degradation by the exosome (Liu et al., 2002; Wang and Kiledjian, 2001).

Dcp2, the human homologue of the yeast Dcp2p, interacts with Dcp1 and preferentially targets methylated capped RNA and catalyses the release of (m7)Gpp and monophosphorylated RNA (van Dijk et al., 2002; Lykke-Andersen, 2002; Wang et al., 2002). It is mainly cytoplasmic and accumulates in foci, presumably P-bodies (Lykke-Andersen, 2002; Wang et al., 2002). However, recently the Dcp2/Dcp1 complex was also found to associate with the exoribonuclease XRN2 in the nucleus, where it functions to release mRNA from prematurely terminated transcription complexes and possibly limit bidirectional transcription (Brannan et al., 2012).

Dcp2 expression seems to be tissue-specific but another decapping enzyme, Nudt16, was found to be expressed in all tissues (Song et al., 2010). Nudt16 is a

cytoplasmic enzyme that targets both methylated and unmethylated capped RNA catalysing the release of (m7)Gp and m7Gpp (Song et al., 2010, 2013). Nudt16 is a member of the Nudix hydrolase family, which consists of several other proteins demonstrating *in vitro* decapping activity (Song et al., 2013). These include Nudt2, Nudt3, Nudt12, Nudt15, Nudt17 and Nudt19.

DXO, the mammalian homologue of the yeast Rai1p and Dxo1p, has decapping, pyrophosphatase and exoribonucleotase activities (Jiao et al., 2013). DXO exhibits stronger decapping activity towards unmethylated compared to methylated capped RNA and it hydrolyses the entire cap structure releasing (m7)GpppG. Similar to yeast Rai1p and Dxo1p, DXO is involved in a 5' quality control pathway targeting aberrantly capped RNA lacking a functional m7G cap.

1.7 Summary and aims of this thesis

The N7-methylguanosine (m7G) cap structure added to the 5' end of RNAs transcribed by RNA pol II is conserved from yeast to man. The m7G cap is essential for cell viability as it is involved in several steps of eukaryotic gene expression. Most of the effects are mediated via CBC and eIF4E that bind to the m7G cap (Figure 1.4).

The m7G cap is added to the 5' ends of RNA Pol II transcripts co-transcriptionally and in mammalian cells the two enzymes RNGTT and RNMT are required for its synthesis. RNGTT catalyses the addition of an inverted guanosine group to the first transcribed nucleotide, whereas RNMT methylates the cap at the N7 position. Although the capping enzymes were discovered in the 1990s in yeast and subsequently identified in mammalian cells, the mechanistic details and the regulation of m7G cap formation remain elusive. RNMT consists of a catalytic domain and an N-terminal domain that is yet to be characterised. This thesis aims to investigate whether the RNMT N-terminal domain has a biological function in human cells in order to gain better understanding of the mechanics of cap methylation.

In contrast to previous theories, newly synthesised RNA pol II transcripts are not constitutively capped but the formation of the m7G cap is a regulated process. Several studies reported the finding of incompletely capped transcripts lacking the methyl moiety on the cap structure (Chang et al., 2012; Cole and Cowling, 2009; Cowling and Cole, 2007b; Fernandez-Sanchez et al., 2009; Jiao et al., 2010, 2013). Furthermore, it was shown that growth factors and transcription factors essential for cell growth and proliferation can stimulate the synthesis of m7G caps (Aregger and Cowling, 2012; Cole and Cowling, 2009; Cowling and Cole, 2007b; Fernandez-Sanchez et al., 2009; Jiao et al., 2010). Recent studies suggested that m7G cap formation could potentially by targeted for cancer therapeutics: deregulated RNMT expression can induce

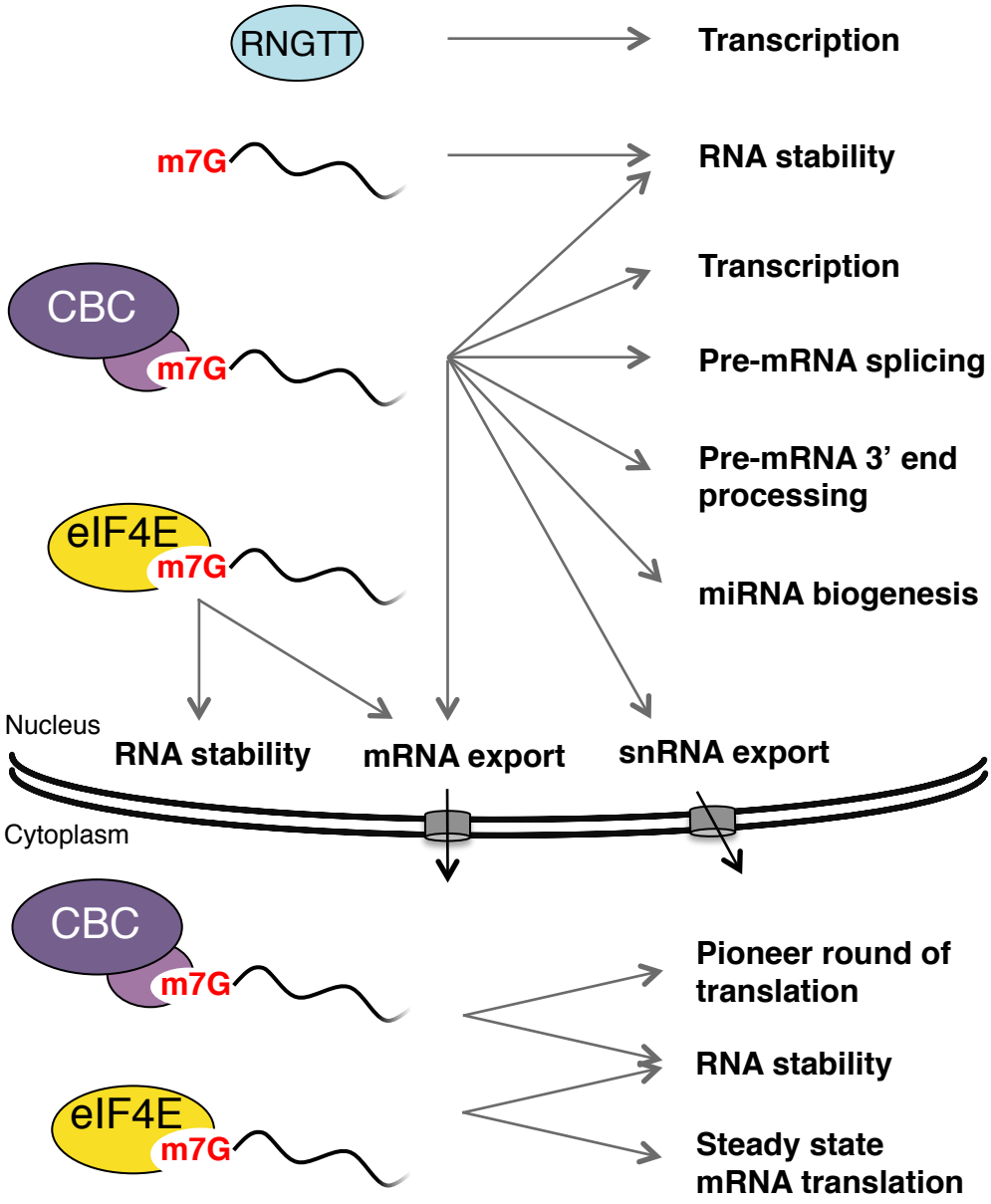

Figure 1.4 Summary of the functions of the N7-methylguanosine cap.

This schematic diagram depicts the functions of the N7-methylguasnosine cap in eukaryotic gene expression. Most of the listed functions are mediated by the two cap-binding proteins, CBC and eIF4E. In the nucleus, CBC promotes transcription, pre-mRNA splicing and 3' end processing, miRNA biogenesis as well as snRNA and mRNA export. After mRNA export, CBC mediates the pioneer round of translation in the cytoplasm. eIF4E promotes the export of specific mRNAs and in the cytoplasm is required for cap-dependent steady state mRNA translation. The N7-methylguasnosine cap structure itself stabilises RNA which is further promoted by the binding of CBC or eIF4E to the cap. Transcription can be promoted by the capping enzymes (e.g. RNGTT) independently of their catalytic activity.

oncogenic cell transformation in cell culture (Cowling, 2010). Moreover, inhibition of cap methylation is synthetically lethal with c-Myc overexpression and can abolish c-Myc induced cell transformation (Fernandez-Sanchez et al., 2009). Therefore, this thesis aims to further elucidate the regulation of m7G formation and in particular aims to investigate whether RNMT is regulated by signalling pathways.

Chapter 2:

Material and Methods

2.1 Material

2.1.1 Laboratory equipment

40C Axivert microscope (Zeiss)

Bioruptor (Diagenode)

Cell Countess (Invitrogen)

Centrifuge Avanti J26 (Beckman Coulter)

Centrifuge 5415R (Eppendorf)

Centrifuge Allegra X-22R (Beckman Coulter)

Ettan IPGphor isolectric focusing system (Amersham)

FACS Calibur (Becton Dickinson)

iQ5 RTPCR (BioRad)

Liquid Scintillation Analyser (Perkin Elmer)

LSM 700 microscope (Zeiss)

Mini Trans-Blot Cell (Bio-Rad).

Mini-Protean Tetra Electrophoresis system (BioRad)

Mini-Sub Cell GT Cell (Bio-Rad)

phosphor screen (FujiFilm)

Phosphorimager FLA-5100 (FujiFilm)

Pipettes (Greiner)

Plate reader (Versamax)

Speed-vacum pump (SciQuip)

Trans-Blot Cell (Bio-Rad)

UV transilluminator (UVP)

2.1.2 Lab consumables

Cell Lifter (Corning Incorporated)

Eppendorf Tubes (Star Lab)

Falcon Tubes (Greiner)

Filter 45 μm (Sartorius)

Filter Units (Thermo Scientific)

Gel Loading Tips (Star Lab)

Pipette Tips (Star Lab)

Syringe needles (Terumo)

2.1.3 Chemicals

2-Mercaptoethanol (Sigma)

3-(N-morpholino)propanesulfonic acid (MOPS) (VWR International)

4-(2-hydroxyethyl)-1-piperazineethanesulfonic acid (Hepes) (Sigma)

Acetic Acid (VWR International)

Calcium Chloride (VWR International)

Dithiothreitol (DTT) (Formedium)

Ethanol (VWR International)

Ethylene glycol tetraacetic acid (EGTA) (VWR International)

Ethylenediamine tetraacetic acid (EDTA) (VWR International)

Formaldehyde (Sigma)

Glycerol (VWR International)

Glycine (VWR International)

Hydrochloric Acid (VWR International)

Isopropanol (VWR International)

Magnesium Chloride (VWR International)

Methanol (VWR International)

piperazine-N,N′-bis(2-ethanesulfonic acid) (PIPES) (Sigma)

Potassium Chloride (VWR International)

Sodium Chloride (VWR International)

Sodium Deoxycholate (Sigma)

Sodium Dodecyl Sulfate (SDS) (Sigma)

Sodium Fluoride (Sigma)

Sodium Hydroxide (VWR International)

Tris-Base (VWR International)

TritonX-100 (VWR International)

Tween 20 (VWR International)

Urea (Fisher Scientific)

2.1.4 Mammalian cell culture and maintenance

100 mm Petri Dishes (Helena)

150 mm Petri Dishes (Helena)

6-Well Plate (Greiner)

Cover Glass 13 mm (VWR International)

Cryovials (Alpha Labs)

DAPI (Sigma)

DPBS (Invitrogen)

Dulbecco's Modified Eagle Medium (DMEM) (Invitrogen)

Dulbecco's Modified Eagle Medium (DMEM) High glucose, pyruvate (Invitrogen)

Dulbecco's Modified Eagle Medium (DMEM) Methionine-, cysteine-free (Invitrogen)

Dulbecco's Modified Eagle Medium (DMEM) Sodium phosphate-free (Invitrogen)

Dulbecco's Modified Eagle Medium Nutrient Mixture F-12 HAM (Sigma)

Epidermal Growth Factor (EGF) (Sigma)

Fetal Bovine Serum (FBS) E.C. Approved (Invitrogen)

Fetal Bovine Serum (FBS) E.C. Approved Dialysed (Invitrogen)

G-418 (Geneticin) (ForMedium)

GeneJuice Transfection Reagent (Novagen)

Hydrocortisone (Sigma)

Insulin Solution Human (Sigma)

Lipofectamine 2000 (Invitrogen)

Penicillin/Streptomycin (Invitrogen)

Polybrene (Sigma)

Puromycin (Sigma)

Trypan Blue solution (0.4%) (Sigma)

Trypsin-EDTA solution (Invitrogen)

2.1.5 Molecular biology

[^{32}P]-orthophosphate (Perkin Elmer)

[γ- ^{32}P]-ATP (Perkin Elmer)

1 Kb DNA Ladder (Invitrogen)

5x Green GoTaq reaction buffer (Promega)

96-well PCR frame Plate (VWR International)

Agarose (Invitrogen)

All Restriction Enzymes (NE BioLabs)

cDNA Synthesis Kit (Quanta Bioscience)

Chromatin immunoprecipitation (ChIP) kit (Millipore)

CIP alkaline phosphatase (NE BioLabs)

DH5α Competent *E.Coli* Cells (DSTT)

dNTPs (Promega)

Ethidium Bromide (Sigma)

Expand High Fidelity PCR System (Roche)

GelRed (Biotium)

Go Taq (Promega)

PCR tubes (Axygen)

Plasmid Maxi Kit (Qiagen)

QIAprep Miniprep Kit (Qiagen)

QIAquick Gel Extraction Kit (Qiagen)

QIAquick PCR Purification Kit (Qiagen)

QuickChange Site-directed Mutagenesis Kit (Stratagene)

RNase A (Sigma)

RNeasy Mini Kit (Qiagen)

SYBR Green Fastmix IQ (Quanta Bioscience)

T4 DNA Ligase (NE Biolabs)

T4 Polynucleotide kinase (PNK) (NE BioLabs)

Transcription Buffer (Promega)

TRIzol Reagent (Invitrogen)

2.1.6 Biochemistry

[^{35}S] Protein Labelling Mix (Perkin Elmer)

[α-^{32}P]-GTP (Perkin Elmer)

Ammonium Acetate (Ambion)

DEPC-Water (Ambion)

DMSO (Merck)

DRB (Sigma)

Nocodazole (Sigma)

P1 nuclease (Sigma)

Phenol/Chloroform Premixed with Isoamyl Alcohol (Ambion)

Propidium iodide (Sigma)

RNasin (Promega)

RO-3306 (Merck)

Roscovitine (Sigma)

S-Adenosyl-Methionine (Sigma)

Saturated Phenol (Ambion)

Sodium Acetate (Ambion)

T7 RNA polymerase (Promega)

Thymidine (Sigma)

TLC PEI Cellulose F Sheets (Merck Milipore)

tRNA (Sigma)

2.1.7 Protein analysis

40% Acrylamide : Bis-acrylamide 29:1 (Flowgen Biosciences)

Ammonium Persulfate (APS) (Sigma)

anti-FLAG antibodies conjugated to agarose (Sigma)

anti-HA antibodies conjugated to agarose (Sigma)

Aprotinin (Sigma)

BenchMark Prestained Protein Ladder (Invitrogen)

Bio-Rad Protein Assay (Bio-Rad)

Bovine Serum Albumin (BSA) (NE BioLabs)

Brilliant Blue g – Colloidal Concentrate (Sigma)

CDK1/Cyclin B1 (NEB)

DAPI Fluorescent Stain (Invitrogen)

Donkey Serum (Sigma)

Dried Skimmed Milk (Marvel)

Gradient SDS-PAGE 4-12% (Invitrogen)

Hydromount (National diagnostics)

Immobilon Transfer Membrane (Millipore)

IPG strip with a pH range of pH 3-10 (BioRad)

Leupeptin Hydrochloride (Sigma)

NNN'N'-Tetramethyletylenediamine (TEMED) (VWR International)

NuPAGE 4-12% Bis-Tris Gel (Invitrogen)

Pepstatin (Sigma)

Phosphatase Inhibitor Cocktail 2 (Sigma)

Phosphatase Inhibitor Cocktail 3 (Sigma)

Protein A/G PLUS-Agarose (Santa Cruz Biotechnology)

Salmon sperm DNA/Protein A agarose (Upstate)

West Pico Chemiluminescent Substrate (of HRP) (Thermo Scientific)

X-RAY FILM (Konica Minolta)

2.1.8 Recombinant protein production

BL21 CodonPlus (DE3)-RIL Competent *E.coli* Cells (Roche)

BL21(DE3) Competent *E.coli* Cells (DSTT)

Cuvettes (Sarstedt)

Glutathione (VWR International)

Glutathione Sepharose 4B (GE Healthcare)

IMAC Sepharose High Performance (GE Healthcare)

Imidazole (Sigma)

LB medium (in house)

Nickel Sepharose (GE Healthcare)

Poly-Prep Chromatography Columns (Bio-Rad)

PreScission Protease (Produced and provided by Daan Van Aalten's lab)

Slide-A-Lyzer Dialysis Cassette (Thermo Scientific)

Snakeskin dialysis tubing 10,000 Mw (Thermo)

Streptavidin Sepharose High Performance beads (GE Healtcare)

Terrific broth (in house)

Vivaspin 20 Concentrator (Sartorius Stedim)

2.1.9 Antibodies

Table 2.1 List of primary antibodies employed in this study for western blot and immunoprecipitation analysis. The antibody name, the species in which the antibody was raised and the supplier are indicated.

Antibody	Species	Supplier
RNMT	Sheep, polyclonal	in house, DSTT
RNMT pT77	Sheep, polyclonal	in house, DSTT
HA (H3663)	Mouse, monoclonal, IgG1	Sigma
RAM	Sheep, polyclonal	in house, DSTT
RNGTT	Sheep, polyclonal	in house, DSTT
β-Tubulin (sc-9104)	Rabbit, polyclonal	Santa Cruz
RNA pol II PAN (sc-899)	Rabbit, polyclonal	Santa Cruz
RNA pol II 3-3 PAN	Mouse, monoclonal, IgG2a	Dirk Eick Lab
RNA pol II 3E10 pS2	Rat monoclonal, IgG1	Dirk Eick Lab
RNA pol II H14 pS5/pS2	Mouse, monoclonal, IgM	Covance
RNA pol II 3E8 pS5	Rat monoclonal, IgG2a	Chromotek
Cyclin B1	Rabbit, monoclonal, IgG	Cell Signalling
Histone 3 pS10	Rabbit, monoclonal, IgG	Abcam
Cyclin D1 (2922)	Rabbit, monoclonal, IgG	Cell Signalling
KPNA2 (PA5-21034)	Rabbit, polyclonal	Thermo
9E10	Sheep, polyclonal	in house, DSTT
9E10	Mouse, monoclonal, IgG	Santa Cruz

Table 2.2 List of HRP-conjugated secondary antibodies employed in this study for western blot analysis. The antibody name, the species in which the antibody was raised and the supplier are indicated.

Antibody	Supplier
Rabbit anti-Sheep	Thermo
Goat anti-Mouse	Thermo
Goat anti-Rabbit	Thermo
Mouse anti-Sheep, light chain specific	Jackson IR

Table 2.3 List of primary antibodies employed in this study for immunofluorescence analysis. The antibody name, the species in which the antibody was raised and the supplier are indicated.

Antibody	Species	Supplier
HA	Sheep	in house, DSTT
RNMT	Sheep	in house, DSTT
Tubulin	Rat	Abcam
Lamin B1	Rabbit	Abcam

Table 2.4 List of fluorescent secondary antibodies employed in this study for immunofluorescence analysis. The antibody name, the species in which the antibody was raised and the supplier are indicated.

Antibody	Species	Supplier
Alexa 488 anti-Sheep	Donkey	Invitrogen
Alexa 594 anti-Sheep	Donkey	Invitrogen
Alexa 642 anti-Sheep	Donkey	Invitrogen

2.1.10 Peptides

Table 2.5 Peptide sequences employed for peptide affinity purification. Peptides were purchased from GL Biochem. T* is the phosphorylated Threonine.

Peptide	Sequence
T77 (4817)	Biotin-C12-RKRKEFEDDLVKESSSCGKDTPSKKRKLDPEIVPE
pT77 (4816)	Biotin-C12-RKRKEFEDDLVKESSSCGKDT*PSKKRKLDPEIVPE

2.1.11 Oligonucleotides

Table 2.6 Oligonucleotide sequence of the siRNA employed in this study. The siRNA was purchased from Dharmacon.

siRNA	Sequence
Human siRNMT	GUUCUAAACUUGUCUCUGA

Table 2.7 Oligonucleotide sequences employed for transcript analysis by RT-PCR. The oligonucleotides were purchased from Eurofins MWG. The transcripts were amplified using each set of primers.

Primer	Sequence
CCNE1 forward	TGAAGCACTTCAGGGGCGTCG
CCNE1 reverse	TGCTCGGGCTTTGTCCAGCAA
MCM2 forward	ACCCCATAGGAGGGCGCTACG
MCM2 reverse	GGTCCACGGTGTCCCTCACCA
PCNA forward	TGAAGCACCAAACCAGGAGAAAGTT
PCNA reverse	ACGTGCAAATTCACCAGAAGGCA

TOP2A forward	GATGCAGGGGGCCGAAACTCC
TOP2A reverse	CCCAACCACACCAAGGCCTGAA
CCNF forward	ACAAGACAGCCCCGACCCCC
CCNF reverse	GGCTGTTCTCCCGCTTCCGTT
KPNA2 forward	GAACGCAGTCGCCCTACAGCC
KPNA2 reverse	GGGAGAAAGCTGCGAAGCGGG
STK15 forward	GTCCCCTGTCGGTTCCTCCGT
STK15 reverse	TCGGTCCATGATGCCTCTAGCTGT
CCNB2 forward	GCAGTCCTAACGGCGCCTCG
CCNB2 reverse	ATCACTGGACACCGTCGGGC
TKK forward	CCGGTTCACTTGGGCATTTACAGA
TKK reverse	CTTGTGGTGGCATGTTCTCTCCAT
PRC1 forward	TCGGGGCCGTGTGGAGTAGG
PRC1 reverse	TCCGCCAGCACCTCACTTCT
TROAP forward	AGGGGCCTCGGTAAGCCATCA
TROAP reverse	CAGTGGGGAAAGGCGTGCGT
CCND1 forward	GCTGGAGGTCTGCGAGGAACA
CCND1 reverse	GGCGGCTCTTTTTCACGGGC
NME1 forward	TCATGCAAGCTTCCGAAGATC
NME1 reverse	GCCCTGAGTGCATGTATTTCAC
RuvBL1 forward	CATTGGGCTGCGAATAAAG
RuvBL1 reverse	TCTGTCTCACACGGAGTT
NPM1 forward	GAAGAGGAGGAGGATGTG

NPM1 reverse	TTCTGTGGAACCTTGCTA
c-Myc forward	TCTGAGGAGGAACAAGAA
c-Myc reverse	GAAGGTGATCCAGACTCT
RNMT 5'UTR forward	TGGGTACTGTACAACTTCAAG
RNMT 5'UTR reverse	TTCAATGACTTTGTGAAGC
RNMT forward	ATTCACTATCACGACGATT
RNMT reverse	GTACTGATATTGCCGATGT

Table 2.8 Oligonucleotide sequences employed for ChIP analysis by RT-PCR. The oligonucleotides were purchased from Eurofins MWG. The DNA segments were amplified using each set of primers.

ChIP-Primer	Sequence
RNMT TSS forward	TGAGTGTGACGGCTGGAACTC (+27)
RNMT TSS reverse	CACGCGTTGGGTAGTGAAG (+164)
RuvBL1 TSS forward	TGTGGCCAGTGGACC (+247)
RuvBL1 TSS reverse	ACTTCCCTGAGGAAATAATGG (+374)
CCND1 TSS forward	AGCTGCCCAGGAAGAGC (+186)
CCND1 TSS reverse	CCGCCTTCAGCATGG (+312)
c-Myc TSS forward	GCACTGGAACTTACAACACC (+390)
c-Myc TSS reverse	ATCCAGCGTCTAAGCAGC (+531)
c-Myc -2000 forward	AAGACGCTTTGCAGCAAAATC
c-Myc -2000 reverse	AGGCCTTTGCCGCAAAC

Table 2.9 Oligonucleotide sequences employed for site-directed mutagenesis. The oligonucleotides were purchased from Eurofins MWG. The constructs were prepared using each set of primers.

Mutagenesis-Primer	Sequence
RNMT WBL forward	AGCCATATCCTGCAAATGAGTCCAGCAAGTTAGTC AGCGAGAAGGTGGATGACTATGAACATGCAGC
RNMT WBL reverse	ATGTTCATAGTCATCCACCTTCTCGCTGACTAACTT GCTGGACTCATTTGCAGGATATGGCTCCAAG
RNMT 5A forward	GCAAAAGCGGCAGTGAATGCTGAAGCAGAGGCTG CATTCAATATTAATG
RNMT 5A reverse	GAATGCAGCCTCTGCTTCAGCATTCACTGCCGCTT TTGCCTGTTCAAG
RNMT 2A forward	GGGAAAGACGCTCCAGCCAAGAAGAGAAAACTTG ATCCTGAAATTGTCCC
RNMT 2A reverse	CAGGATCAAGTTTTCTCTTCTTGGCTGGAGCGTCT TTCCCACAACTAG
RNMT T77A forward	AGTTCTAGTTGTGGGAAAGACGCTCCATCCAAGAA GAGAAAACTTGATCC
RNMT T77A reverse	TGGGACAATTTCAGGATCAAGTTTTCTCTTCTTGGA TGGAGCGTCTTTCC
RNMT T77D forward	AGTTCTAGTTGTGGGAAAGACGATCCATCCAAGAA GAGAAAACTTGATCCA
RNMT T77D reverse	TGGGACAATTTCAGGATCAAGTTTTCTCTTCTTGGA TGGATCGTCTTTCC
RNMT S79A forward	AGTTCTAGTTGTGGGAAAGACACTCCAGCCAAGAA GAGAAAACTTGATCC
RNMT S79A reverse	TGGGACAATTTCAGGATCAAGTTTTCTCTTCTTGGC TGGAGTGTCTTTCC

Table 2.10 Oligonucleotide sequences employed for cloning. The oligonucleotides were purchased from Eurofins MWG. The constructs were prepared using each set of primers.

Cloning primer	Sequence
HA-RNMTcat forward	ACAGGATCCATGTACCCATACGATGTTCCAG ATTACGCTGATGGCACTCAAAATAAGAGA
HA-RNMTcat reverse	ACACTCGAGTCACTGCTGTTTCTCAAAGG CAAA
HA-RNMT-N forward	ACAGGATCCATGTACCCATACGATGTTCCAG ATTACGCTGCAAATTCTGCAAAAGCA
HA-RNMT-N reverse	ACACTCGAGTCATCCAGTAGAAGATTTATCT
6xHIS-RNMT_KasI forward	ACAGGCGCCATGGCAAATTCTGC
6xHIS-RNMT_BamHI reverse	ACAGGATCCCTGCTGTTTCTCAAAGGC

2.1.12 Buffers and solutions

F buffer:

10 mM Tris (pH 7.05), 50 mM NaCl, 30 mM Na pyrophosphate, 50 mM NaF, 10% Glycerol, 0.5% Triton X-100

Buffer A:

20mM HEPES – KOH (pH 7.5), 1.5 mM $MgCl_2$, 10 mM KCl, 1mM EDTA, 1mM EGTA

RIPA buffer:

25 mM Tris-HCl (pH 7.6), 150 mM NaCl, 1% NP-40, 1% sodium deoxycholate, 0.1% SDS

SDS running buffer:

25 mM Tris, 250 mM glycine, 0.1% SDS

Transfer buffer:

25 mM Tris, 192 mM glycine, 20% methanol

TBST:

25 mM Tris (pH 8.1), 155 mM NaCl, 0.1% tween 20

4x Laemmli buffer:

240 mM Tris, 8% SDS, 40% glycerol, bromophenol blue, 100 mM DTT

RNGTT buffer:

50 mM Tris (pH 7.5), 5.5 mM DTT, 1.25 mM $MgCl_2$

MT assay buffer:

50 mM Tris (pH 8.0), 6 mM KCl, 1.25 mM $MgCl_2$

2x HEPES-buffered saline (HBS):

50 mM HEPES (pH 7.05), 1.5 mM Na_2HPO_4, 275 mM NaCl

TAE buffer:

40 mM Tris (pH 8.0), 40 mM acetic acid, 1 mM EDTA

TBE buffer:

89 mM Tris (pH 8.0), 89 mM boric acid, 2.5 mM EDTA

PHEM:

60 mM PIPES, 27 mM HEPES, 10 mM EGTA, 8.22 mM magnesium sulphate

Abdil:

25 mM Tris (pH 8.1), 155 mM NaCl, 0.25 % Tween 20, 0.2% BSA, 0.1 % sodium azide

2D Lysis Buffer:

8M urea, 4% CHAPS, 40 mM Tris

2D rehydration solution:

7M urea, 2M thiourea, 1.2% CHAPS, 0.4% ASB-14, 0.25% ampholytes, 65 mM DTT

2D SDS equilibration solution 1:

50 mM Tris (pH 8.8), 6M Urea, 30% glycerol, 2% SDS, bromophenol blue, containing DTT

2D SDS equilibration solution 2:

50 mM Tris (pH 8.8), 6M Urea, 30% glycerol, 2% SDS, bromophenol blue, 135 mM iodoacetamide

2.2 Methods

2.2.1 Cell culture and maintenance

Cells were maintained at 37 °C under humidified atmosphere containing 5% CO_2 in γ-sterilised tissue culture treated plastic ware. Cells were grown to near confluence in 10 cm dishes and then sub-cultured by removing the old media, washing with PBS and treating with trypsin solution to detach the cells. Cells were diluted in fresh medium and seeded at 5 x 10^5 cells per 10 cm dish. Trypsinised IMEC cells were resuspended in DMEM supplemented with 10% FBS and centrifuged for 3 minutes at 1,800 rpm before diluting the cells in DMEM F-12 HAM medium.

Table 2.11 Cell lines employed for the purpose of this study. The cell line origin and a brief description of their maintenance are indicated.

Cell line	Origin	Maintenance
HEK 293	Human embryonic kidney cells	Adherent cells maintained in DMEM supplemented with 10% FBS, 2 mM L-glutamine and 1mM Sodium Pyruvate
HeLa	Human cervical epithelial carcinoma	Adherent cells maintained in DMEM supplemented with 10% FBS and 2 mM L-glutamine
IMEC	Human immortalised mammary epithelial cells	Adherent cells maintained in DMEM nutrient mixture F-12 HAM supplemented with L-glutamine, 5 µg/ml insulin, 10 ng/ml EGF and 0.5 µg/ml hydrocortisone
A'	Human embryonic kidney cells	Adherent cells maintained in DMEM supplemented with 10% FBS, 2 mM L-glutamine and 1 mM Sodium Pyruvate

2.2.2 Transient plasmid and siRNA transfections

2.2.2.1 DNA transfection using calcium phosphate method

A' and HEK 293 cells were transiently transfected with recombinant DNA vector using the calcium phosphate method. For transfection of A' and HEK 293 cells 4 and 6 µg of DNA vector respectively were added to 500 µl of 250 mM $CaCl_2$ and 500 µl of 2 x HBS was added dropwise to the mixture with continual mixing and incubated for 20 minutes to allow the formation of a fine co-precipitate of DNA-$Ca_3(PO_4)_2$. This mixture was added to 500,000 cells seeded into a 10 cm dish. Fresh media was added 4 hours post-transfection.

2.2.2.2 DNA transfection using transfection reagents

HeLa cells were transiently transfected with recombinant DNA vectors using Gene Juice and Lipofectamine 2000 according to manufacturer's instructions. 1 x 10^6 HeLa cells were seeded in 10 cm dishes and transfected 16 hours later with 4 µg DNA.

2.2.2.3 siRNA transfection

HeLa and IMEC cells were transfected with siRNAs using Lipofectamine 2000 according to manufacturer's instructions. 125,000 cells were seeded in 6-well plates and transfected 16 hours later with 200 pmoles siRNMT (Dharmacon) (Table 2.6). As a control, cells were treated with the transfection reagent alone without addition of any siRNAs.

2.2.3 Stable transfection procedure

HEK-293, HeLa and IMEC cells were stably transfected with recombinant DNA vectors using retroviral infection method. 500,000 Phoenix A' packaging cells were

seeded in a 10 cm plate and transiently transfected 16 hours later using the calcium phosphate method. The medium was changed 24 hours later, collected 48 hours post-transfection, passed through a 45 μm filter and mixed 1:1 with the medium of 500,000 recipient cells which were plated in 10 cm dishes 16 hours earlier. 5 μg/ml of polybrene was added to increase viral infection rates by neutralising the charge repulsion of the virions and the recipient cell surface. Pools of stably transfected cells were selected using 0.5 mg/ml G418.

2.2.4 Cell counting

Cells were counted using a Neubauer chamber. Cells were trypsinised, resuspended in media and diluted 1:1 with trypan blue. The Neubauer chamber was filled with 20 μl of the mixture and cells were counted in four 1x1 mm squares. Average numbers were calculated and multiplied with 20,000 to get the actual cell number/ml media.

Alternatively, cells were counted using a Countess cell counter according to manufacturer's instructions.

2.2.5 Cell synchronisation

2.2.5.1 Double thymidine block

HeLa cells were arrested at G1/S-phase using a double Thymidine block. 1 x 10^6 cells were seeded in 10 cm plates and 16 hours later 2.5 mM thymidine was added. After 16 to 18 hours cells were washed three times with PBS and cells were released into normal medium for 8 to 10 hours. Cells were treated with 2.5 mM thymidine for a second time for 16 to 18 hours. Finally, cells were either harvested or washed three times with PBS and released into normal medium.

2.2.5.2 Nocodazole block

HeLa cells were arrested in M-phase using a double Thymidine block followed by a nocodazole block. 2 x 10^6 cells were seeded in 10 cm plates and 16 hours later 2.5 mM thymidine was added. After 24 hours cells were washed three times with PBS and cells were released into normal medium for 3 hours. 100 ng/ml nocodazole was added for 12 to 13 hours. Finally, cells were either harvested or washed three times with PBS and released into normal medium.

2.2.6 Mammalian protein extraction and analysis

2.2.6.1 Total cell extracts

Culture medium was removed and cells were washed twice with ice-cold PBS. F-Buffer supplemented with 0.1 TIU (trypsin inhibitor unit) aprotinin, 1 µM pepstatin, 10 µM leupeptin and 1% phosphatase inhibitor cocktail 2 and 3 (Sigma) each was used for cell lysis. Cells were scraped in ice-cold F-Buffer using a cell lifter, incubated for 10 to 15 minutes on ice and centrifuged for 10 minutes at 16,000 x g to separate the lysate from cell debris. The supernatant was collected and protein concentration was determined using the Bradford method.

2.2.6.2 Nuclear cell extracts

Culture medium was removed and cells were washed twice with ice-cold PBS and once with ice-cold Buffer A. Cells were scraped in ice-cold Buffer A supplemented with 0.1 TIU (trypsin inhibitor unit) aprotinin, 1 µM pepstatin, 10 µM leupeptin and 1% phosphatase inhibitor cocktail 2 and 3 (Sigma) each using a cell lifter. Cells were left to swell for 10 to 15 minutes on ice before passing through a 45 µm syringe needle ten times. The nuclei were pelleted by centrifugation for 10 minutes at 3,300 x g to separate the cytoplasmic fraction from the nuclei. The supernatant was discarded and

the pellet washed once with Buffer A. The nuclei were pelleted and lysed in F-Buffer supplemented with 0.1 TIU (trypsin inhibitor unit) aprotinin, 1 µM pepstatin, 10 µM leupeptin and 1% phosphatase inhibitor cocktail 2 and 3 (Sigma) for 10 to 15 minutes on ice. Nuclear extracts were centrifuged for 10 minutes at 16,000 x g to separate the lysate from cell debris. The supernatant was collected and protein concentration was determined using the Bradford method.

2.2.6.3 Protein concentration determination

Protein concentration was determined using Bradford reagent with reference to a standard curve obtained with a dilution series of BSA (Bovine Serum Albumin).

For the standard curve BSA was diluted in distilled water and 4 µl of the dilution series was combined with 200 µl of 1x BioRad protein assay reagent in a 96 well plate. Absorbance at 595 nm was measured with a plate reader. Blank measurement of a sample containing distilled water and BioRad protein assay reagent only was subtracted from all other samples. The standard curve was obtained by plotting the absorbance at 595 nm against the BSA concentration (mg/ml).

For estimation of sample protein concentration, cell extracts were diluted in distilled water and analysed as above. A blank measurement of a sample containing F-Buffer diluted in H_2O and BioRad protein assay reagent was subtracted from all other samples. The reading was plotted in the standard curve for estimating the protein concentration of the sample.

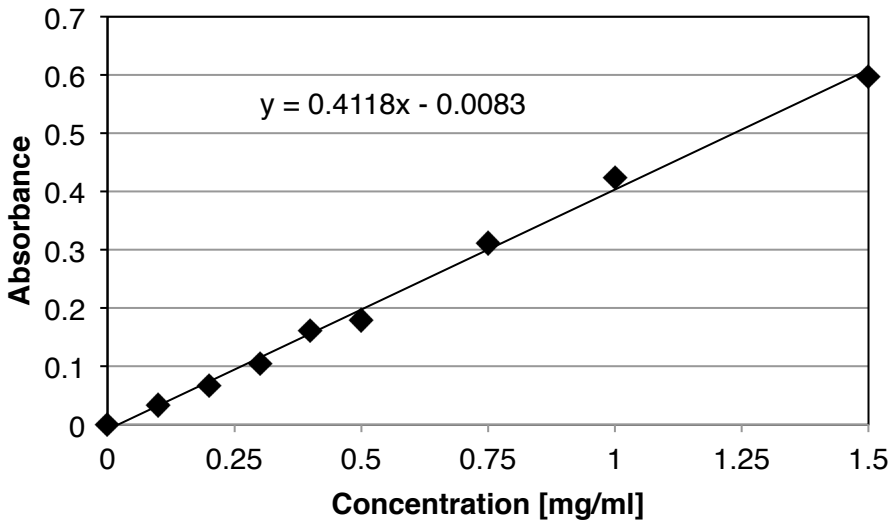

Figure 2.1 Standard curve based on BSA dilutions for the estimation of protein concentration

2.2.6.4 Sodium dodecyl sulphate polyacrylamide gel electrophoresis (SDS-PAGE)

SDS-PAGE was performed to separate proteins according to their molecular weight using a Mini-Protean Tetra Electrophoresis system (BioRad). Polyacrylamide gels were prepared in a final volume of 10 ml by combining 4 ml of 1 M Tris pH 8.8 (final concentration 400 mM), 100 μl 10 % SDS (final concentration 0.1%), acrylamide : bisacrylamide solution and distilled water. The composition of acrylamide : bisacrylamide and water is described in Table 2.12.

Table 2.12 Amount of water and 40% Acrylamide : bisacrylamide used for preparation of different percentage acrylamide gel.

Final Acrylamide concentration	5%	8%	10%	12%	14%
H_2O (ml)	4.5	3.8	3.3	2.8	2.3
40% Acrylamide : bisacrylamide (ml)	1.2	2	2.5	3	3.5

The lower gel described above filled ¾ of the gel whereas the rest was filled with a stacking gel of lower pH and acrylamide content. Stacking gels of 4% and 5% acrylamide were prepared for lower gels containing 5% or more than 5% acrylamide respectively. The stacking gel was made by combining 4 ml 1 M Tris base, pH 6.8 (final concentration 400 mM), 100 µl 10% SDS (final concentration 0.1%), acrylamide : bisacrylamide solution and distilled water. The composition of acrylamide : bisacrylamide and water is described in Table 2.13.

Table 2.13 Amount of water and 40% Acrylamide : bisacrylamide used for preparation of different percentage stacking acrylamide gel.

Final Acrylamide concentration	4%	5%
H_2O (ml)	4.8	4.5
40% Acrylamide : bisacrylamide (ml)	1	1.2

For the polymerization reaction APS and TEMED were added to a final concentration of 0.1% (v/v) and 0.01% (v/v) respectively.

Protein samples were combined with 4x Laemmli buffer complemented with 100 mM DTT and F-buffer to prepare a 1 mg/ml protein sample in 1x Laemmli buffer. Samples were boiled for 2 min and centrifuged at 16,000 x g for 3 min at room temperature. Proteins were resolved alongside molecular weight markers at 180 V. The amount of protein resolved and the percentage of acrylamide gel used for the detection of specific proteins is demonstrated in Table 2.14.

Table 2.14 List of proteins detected by western blot during this study. The amount of total protein extracts analysed and the percentage of SDS-PAGE used are indicated.

Western blot against	Amount of protein analysed (µg)	% Acrylamide gel
RNMT (endogenous + HA-RNMT)	6	8
HA-RNMT	12	8
RAM	18	14
Fg-RAM	12	14
RNGTT	10	8
Tubulin	6.5	8
RNA Pol II	25	5
Cyclin B1	3.5	8
Histone 3	10	14
Cyclin D1	12	12
KPNA2	10	8
9E10-KPNA2	8	8

2.2.6.5 Two-dimensional SDS-PAGE (2D SDS-PAGE)

HA-RNMT was immunoprecipitated overnight from 2 mg HEK-293 cells stably expressing HA-RNMT using 5 µg mouse monoclonal anti-HA antibodies. Immunoprecipitates were resuspended in 25 µl of 2D lysis buffer and incubated with 100 µl of 2D rehydration solution for 2 hours at room temperature. The sample was added into a strip holder and a 7 cm BioRad IPG strip with a pH range of pH 3-10 was

added onto the solution. The IPG strip was overlaid with cover fluid and rehydrated overnight for 13 hours. Isoelectric focusing was performed on an Ettan IPGphor isolectric focusing system using the following three-step protocol: 250 Vhr (0.5 hours at 500 V, 500 Vhr (0.5 hours at 1000 V) and 8000 Vhr (1 hour at 800 V). After isoelectric focusing strips were equilibrated for 10 minutes in 5 ml of 2D SDS equilibration solution 1 and 2 containing iodacematide and DTT respectively. The IPG strip was placed on top of polyacrylamide gel and protein was resolved by SDS-PAGE.

2.2.6.6 Western blot

Protein separated by SDS-PAGE were transferred onto polyvenylfluoride (PVDF) membranes in transfer buffer by wet blotting at 66 V for 90 min at 4 °C using Mini Trans-Blot Cell (Bio-Rad). For RAM western blots, transfer was performed using Trans-Blot Cell (Bio-Rad) at 60 V for 300 min at room temperature.

Protein detection was carried out at room temperature. Membranes were blocked for 45 minutes in TBST containing 5 % milk or 3 % BSA depending on the primary antibody (Table 2.15). Primary antibodies were diluted in blocking solution (Table 2.16) and incubated with the membrane for 60 minutes. For RAM and RNA polymerase II western blots primary antibodies were incubated for 90 and 120 minutes respectively. The membranes were washed four times for 5 minutes with TBST containing 5 % milk. HRP-conjugated secondary antibodies were diluted 1:2000 in TBST containing 5 % milk and incubated with the membrane for 45 minutes. The membranes were washed four times for 5 minutes with TBST. Antibody-bound proteins were visualised on X-ray film using enhanced chemiluminescence reagent according to manufacturer's instructions.

Table 2.15 Concentrations of primary antibodies employed in this study for western blot analysis. The dilution of the antibody and the blocking reagent used are indicated

Antibody	Working concentration	Blocking solution
RNMT	1:1000	Milk
RNMT pT77	1:1000	BSA
HA (H3663)	1:250	BSA
RAM	1:100	Milk
RNGTT	1:1000	Milk
Tubulin (sc-9104)	1:1000	Milk
RNA pol II PAN (sc-899)	1:250	BSA
RNA pol II 3-3 PAN	1:10	BSA
RNA pol II pS2	1:10	BSA
RNA pol II H14 pS5	1:10	BSA
RNA pol II 3E8 pS5	1:10	BSA
Cyclin B1	1:1000	Milk
Histone 3 pS10	1:1000	BSA
Cyclin D1 (2922)	1:1000	Milk
KPNA2 (PA5-21034)	1:1000	Milk
9E10	1:1000	Milk

Table 2.16 Concentrations of HRP-conjugated secondary antibodies employed in this study for western blot analysis. The dilution of the antibody and the blocking reagent used are indicated.

Antibody	Working concentration	Blocking solution
Rabbit anti-Sheep	1:500	Milk
Goat anti-Mouse	1:500	Milk
Goat anti-Rabbit	1:500	Milk
Mouse anti-Sheep, light chain-specific	1:200	Milk

RNMT, RAM, RNGTT and RNMT pT77 antibodies were raised in sheep by the in house Division of Signal Transduction (DSTT) against full-length recombinant human RNMT, RAM, RNGTT and the phosphorylated RNMT peptide CGKDT*PSKKR respectively. Sera were affinity purified on the recombinant protein or phospho-peptide. All other antibodies were acquired commercially or as specified in the material section.

2.2.6.7 Coomassie blue staining

After SDS-PAGE the polyacrylamide gel was washed three times with distilled water for five minutes and protein was stained in Simply Blue Safe stain (Invitrogen) solution for one hour. The gel was washed with distilled water to remove background staining.

2.2.6.8 Immunoprecipitation

Immunoprecipitations were performed at 4 °C with the amount of cell extracts and antibodies stated in the figure legends. In general, cell extracts were precleared with Protein A/G PLUS-Agarose (Santa Cruz) for 45 minutes. Stably expressed exogenous HA-RNMT was immunoprecipitated using mouse monoclonal anti-HA antibody-

conjugated agarose. For endogenous RNMT immunoprecipitation sheep polyclonal anti-RNMT or sheep polyclonal anti-HA (control, DSTT) antibody was used and Protein A/G PLUS-Agarose was added for 1.5 hours to precipitate the antibodies. Immunoprecipitations were performed for 4 hours except for RNMT phosphorylation analysis in which RNMT was immunoprecipitated for 2.5 hours only. Immunoprecipitates were centrifuged at 800 x g for 1.5 minutes washed 4 times with F-Buffer, resuspended in 1x Laemmli dye and resolved by SDS-PAGE.

For exogenous immunoprecipitation 35 and 6.5 % and for endogenous immunoprecipitation 70 and 9 % of immunoprecipitates were resolved to detect RNMT pT77 and total RNMT levels respectively.

2.2.6.9 Large scale immunoprecipitation coupled with mass spectrometry analysis

For RNMT mass spectrometry analysis 40 mg of HEK-293 cell extract was precleared for 5 hours using 50 μl murine IgG-conjugated agarose (Sigma) and 20 μl 50 % slurry Protein A/G PLUS-Agarose (Santa Cruz). HA-RNMT was immunoprecipitated overnight using 20 μg mouse monoclonal anti-HA antibody-conjugated agarose (Sigma) and 20μl protein A/G PLUS-Agarose. Immunoprecipitates were washed and resolved by 4 - 12 % gradient SDS-PAGE. The gel was fixed (40 % methanol, 7 % glacial acetic acid) and stained with brilliant blue G-Colloidal (Sigma) for 2 hours.

Mass spectrometry analysis was performed by the FingerPrints Proteomics Facility located in the College of Life Sciences at the University of Dundee. In brief, Coomassie stained gel bands were excised, washed, and incubated overnight with trypsin. Peptides were extracted and separated by nanoLC-MS/MS on a 4000 QTRAP mass spectrometer for protein identification. Precursor ion scanning was performed before

nanoLC-MS/MS on a LTQ Orbitrap Velos Pro mass spectrometer to identify phosphorylation sites. Results were searched against the SwissProt or IPI human databases using the Mascot Daemon.

2.2.6.10 Peptide affinity purification

Peptide affinity purification was performed at 4 °C with the amount of cell extracts and peptides stated in the figure legends. In general, streptavidine sepharose high performance beads were pelleted at 800 x g for 1.5 minutes and washed five times with F-Buffer. The cell lysate was precleared with 20 µl 50 % slurry streptavidine sepharose five times for 10 minutes. The precleared lysate was incubated with biotinylated peptides (Table 2.5) for 10 minutes and 20 µl 50 % slurry streptavidine-sepharose was added for an additional 5 minutes. The sepharose was pelleted at 800 x g for 1.5 minutes and washed three times with F-Buffer and one time with Buffer A. The precipitates were resuspended in 1x Laemmli dye and resolved by SDS-PAGE

2.2.6.11 Peptide affinity purification coupled to mass spectrometry analysis

For mass spectrometry analysis of peptide-bound proteins, peptide affinity purification was performed as described above. Precipitates were resuspended in 1x LDS sample buffer (Invitrogen) containing 10 mM DTT and boiled for 5 minutes at 70 °C. Iodoactematide was added to 50 mM and the sample was incubated in the dark for 30 minutes at room temperature. The protein was resolved by 4 - 12 % gradient SDS-PAGE and stained with Coomassie blue. Protein bands were extracted as described below and send for mass spectrometry analysis, which was performed by the mass spectrometry facility at the MRC Protein Phosphorylation and Ubiquitylation Unit located in the College of Life Sciences at the University of Dundee. In brief, protein was

trypsinised and peptides separated on a nanoLC system, which was coupled with an LTQ-Orbitrap mass spectrometer (for peptide mass fingerprinting). Results were searched against the SwissProt or IPI human databases using the Mascot Daemon. The mass spectrometry results were subsequently analysed using OLMAT (Online MassSpec data Analysis Tool) available online at www.proteinguru.com.

2.2.6.12 Processing protein bands for mass spectrometry analysis

To minimise contamination with keratin, samples were handled in a laminar flow hood. Indicated gel pieces were cut into small cubes of 1 mm size. The pieces were sequentially washed for 10 minutes in 0.5 ml distilled water, 50% acetonitrile, 0.1 M NH_4HCO_3 and 50 % acetonitrile / 50 mM NH_4HCO_3 on a shaking platform. Gel pieces were briefly spun in a microcentrifuge and all liquid was aspirated. The wash in 50 % acetonitrile / 50 mM NH_4HCO_3 was repeated until the gel pieces were colourless. Next, gel pieces were shrunk by incubating them with 0.3 ml of acetonitrile for 15 minutes at room temperature and subsequently dried with Speed-Vac at 45 °C for 20 to 30 minutes. The gel pieces were swollen with 80 µl 25 mM Triethylammonium bicarbonate buffer containing 5 ug/ml Trypsin and incubated at 30 °C for 16 hours on a shaking platform. Next day, 80 µl of acetonitrile was added and the peptides obtained from the trypsin digestion were extracted for 15 minutes on a shaking platform. The supernatant was frozen on dry ice and dried at 45 °C using Speed-Vac. To further extract the peptides, 100 µl of 50 % acetonitrile supplemented with 2.5 % formic acid were added to the gel pieces and incubated for 15 minutes at room temperature on a shaking platform. The supernatant was combined with the first dried peptide extract, frozen on dry ice and dried using Speed-Vac. Dried peptides were stored at -20 °C and submitted to the mass spectrometry facility at the MRC Protein Phosphorylation and Ubiquitylation Unit located in the College of Life Sciences at the University of Dundee.

2.2.6.13 Affinity purification with nuclear extracts

2 mg of nuclear HeLa cell extracts were incubated for 3 hours at 4 °C with 1.5 μg of purified recombinant GST, GST-RNMT or GST-RNGTT respectively. Recombinant protein was affinity purified with 25 μl of 50% slurry glutathione sepharose and washed five times with F-Buffer. Precipitates were dissolved in 1x Laemmli buffer, separated by SDS-PAGE and analysed by western blot.

2.2.6.14 Immunofluorescence

IMEC cells were seeded on round cover slides and fixed with fresh 4% paraformaldehyde in PHEM for 7 minutes at 37 °C. All other steps were performed at room temperature. Cells were washed in fresh TBST for 5 minutes and permeabilised with 0.02 % Triton X-100 in TBST for 2.5 minutes. After a wash in TBST for 5 minutes cells were blocked with 10 % Donkey serum in Abdil (antibody dilution solution) for 30 minutes. Primary antibodies were incubated in Abdil for 1 hour (Table 2.17) and washed three times in TBST for 5 minutes. Secondary antibodies in Abdil (Table 2.18) were incubated for 50 minutes in the dark. Cells were washed tree times in TBST and stained with 1:50,000 DAPI in Abdil for 20 minutes. Cells were washed in TBST and mounted on glass plates. Fluorescence microscopy was performed on a Zeiss LSM 700.

Table 2.17 Concentrations of primary antibody employed in this study for immunofluorescence analysis.

Antibody	Working concentration
HA	1:2000
RNMT	1:2000
Tubulin	1:500
Lamin B1	1:1000

Table 2.18 Concentrations of secondary antibodies employed in this study for immunofluorescence analysis.

Antibody	Working concentration
Alexa 488 anti-Sheep	1:500
Alexa 594 anti-Sheep	1:500
Alexa 642 anti-Sheep	1:500

2.2.6.15 Orthophosphate labelling

HEK-293 cells were washed twice with PBS and starved in sodium phosphate-free DMEM supplemented with 10 % dialysed FBS for 4 hours at 37 °C. 30 μCi/ml [^{32}P]-orthophosphate (Perkin Elmer) was added and cells were labelled for 2 hours at 37 °C. Cells were lysed in F-Buffer as described before and HA-RNMT was immunoprecipitated for 4 hours from 2 mg of cell extracts using 10 μg of mouse monoclonal anti-HA antibodies. Immunoprecipitates were washed, dissolved in 1x Laemmli dye and resolved by SDS-PAGE. The polyacrylamide gel was fixed (50 %

methanol, 10 % acetic acid and 7 % methanol, 7 % acetic acid, 10 % glycerol), dried and subjected to autoradiography.

2.2.6.16 ^{35}S amino acid labelling

HeLa cells were starved for 15 minutes at 37 °C in methionine- and cysteine-deficient DMEM supplemented with 10 % dialysed FBS. Subsequently cells were labelled for 15 minutes at 37 °C with 33 μCi/ml ^{35}S protein labelling mix (Perkin Elmer) containing ^{35}S-methionine and ^{35}S-cysteine. Cells were lysed in F-Buffer and 12 μg of extracted protein was resolved by 10 % SDS-PAGE. The polyacrylamide gel was fixed (50 % methanol, 10 % acetic acid and 7 % methanol, 7 % acetic acid, 10 % glycerol), dried and subjected to autoradiography.

2.2.6.17 Autoradiography

Radioactive signal was visualised on a phosphor screen using a phosphorimager.

2.2.6.18 Kinase inhibitor treatment

The following kinase inhibitor stock solutions were prepared: DRB (Sigma) was dissolved in EtOH to form a stock solution of 31mM. Roscovitine (Sigma) was dissolved in DMSO to form a stock solution of 10 mM. RO-3306 (Merck) was dissolved in DMSO to form a stock solution of 9 mM. HeLa cells were incubated with these compounds at a concentration and time indicated in the figure legends.

2.2.7 RNA extraction and analysis

2.2.7.1 RNA extraction

RNA from transiently transfected HeLa cells (Figure 3.8) was extracted using QIAGEN RNeasy mini kit according to manufacturer's instructions. RNA from stably transfected HeLa cells (Figure 6.7) was extracted using the TRIzol reagent (Invitrogen) according to manufacturer's instructions.

2.2.7.2 RT-PCR

750 ng of RNA was converted into complementary DNA (cDNA) with random hexamer primers using the qScript cDNA Synthesis Kit (Quanta) according to manufacturer's instructions.

The cDNA was diluted 30 times in distilled water and 2 μl were subjected to real-time polymerase chain reaction (RT-PCR) analysis with a BioRad iQ5 RT-PCR detection system using Quanta Biosciences SYBR Green FastMix for iQ. RT-PCR reactions were performed in a volume of 20 μl using the primers depicted in Table 2.7 at a concentration of 0.3 μM and the following thermo cycle protocol: Cycle 1 (1x) 30 seconds, 95 ºC ; Cycle 2 (40x) 1 second, 95 ºC , 25 seconds 57 ºC.

2.2.8 Biochemical assays

2.2.8.1 *In vitro* cap methyltransferase activity assay

To prepare RNA substrate for the methyl reaction 10 μg of pGEM Cem4 plasmid was linearised with 40 U EcoRI (Roche) in Buffer 3 (NEB) and a 55 nt long transcript driven by a T7 promotor was *in vitro* transcribed using 2 μl TNT T7 RNA polymerase (Promega) in the prescence of 250 μM NTPs, 20 U RNasin (Promega) and Transcription Buffer (Promega) for 2 hours at 37 °C. The transcript was purified by

phenol:chloroform extraction, precipitated in ethanol and dissolved in 50 μl nuclease-free water. 200 ng of *in vitro* transcribed RNA was capped with 10 μCi [α-^{32}P] GTP (Perkin Elmer) in the presence of 2 μg recombinant RNGTT, 40 U RNasin and RNGTT Buffer for 1 hour at 37 °C. The capped transcript was purified by phenol:chloroform extraction, acetate precipitated and dissolved in 50 μl nuclease-free water.

For cap methylation assays the indicated amount of immunoprecipitated RNMT or total cell extract was incubated in a total volume of 10 μl with 2 ng of RNA substrate, 200 μM S-adenosyl methionine, 20 U RNasin and MT Buffer at 37 °C for the indicated time.

Cap methylation assays with recombinant RNMT were performed at 30 °C with the amount and time indicated in the figure legend.

Following the reaction, RNA was purified by phenol:chloroform extraction, acetate precipitated, and resuspended in 4 μl of 50 mM NaAcetate (pH 5.5) and incubated with 0.75 U P1 nuclease (Sigma) for 60 minutes at 37 °C to release free GpppG and m7GpppG. Cap structures were resolved by 0.4 M ammonium sulphate on PEI cellulose plates. Labelled GpppG and m7GpppG spots were visualized and quantified by autoradiography.

2.2.8.2 Phenol/Chloroform extraction

RNA was purified by phenol/chloroform extraction to remove any protein contamination. An equal amount of phenol/chloroform was added to the nucleic acid solution and shaken for 10 seconds to form an emulsion. The aqueous and organic fractions were separated by centrifugation at 16,000 x g for 10 minutes. The upper aqueous phase was transferred into a new tube and mixed with 1/10 volume of 5 M Ammonium acetate and 2 volumes of Ethanol and incubated at -20 °C overnight. For RNA purification from capping reaction and methyltransferase activity assay, 1/10

volume of 2 mg/ml polyU or 1/50 volume of 1 mg/ml tRNA was added respectively as a carrier. The precipitated RNA was pelleted by centrifugation at 16,000 x g for 60 minutes at 4 °C and washed with 70 % Ethanol. The pellet was dried for 20 minutes and dissolved in the solution specified.

2.2.8.3 Chromatin immunoprecipitation (ChIP)

For chromatin immunoprecipitations presented in chapter 3, 1 x 10^6 HeLa cells were transfected with i)1.5 μg pcDNA4, ii) 0.75 μg pcDNA4 HA-RNMT and 0.75 μg pcDNA4 FLAG-RAM, iii) 0.53 μg pcDNA4 HA-RNMTcat, 0.75 μg pcDNA4 FLAG-RAM and 0.22μg pcDNA4, iv) 0.2 μg pcDNA4 HA-RNMT-N, 0.75 μg pcDNA4 FLAG-RAM and 0.55 μg pcDNA4 using Lipofectamine 2000 (Invitrogen).

For chromatin immunoprecipitations presented in chapter 6, 1 x 10^6 HeLa cells were transfected with i) 4 μg pcDNA5, ii) 2 μg pcDNA5 HA-RNMT WT and 2 μg pcDNA5 FLAG-RAM and iii) 1.6 μg pcDNA5 HA-RNMT T77A, 2 μg pcDNA4 FLAG-RAM and 0.4 μg pcDNA5 using Lipofectamine 2000 (Invitrogen).

Chromatin immunoprecipitations were performed using the Millipore ChIP kit according to manufacturer's instructions. In brief, cells were crosslinked with formaldehyde for 10 minutes at 37 °C, washed with PBS and lysed in SDS lysis buffer. The lysate was sonicated to shear the DNA to lengths between 200 and 500 basepairs using a bioruptor (Diagenode) at medium amplitude at cycles of 30 seconds ON/OFF for 10 minutes. Lysates were centrifuged at 16,000 x g for 10 minutes and the supernatant was diluted in ChIP dilution buffer. After preclearing with salmon sperm DNA/Protein A agarose 1 % of the sample was kept as input sample. The remaining solution was incubated overnight at 4 °C with 15 μg anti-HA or anti-FLAG antibodies conjugated to agarose (both Sigma) to immunoprecipitate HA-RNMT and FLAG-RAM proteins. Immunoprecipitates were subsequently washed with low salt immune

complex wash buffer, high salt immune complex wash buffer, LiCl immune complex wash buffer and TE buffer. Protein was eluted in 1 % SDS, 0.1 M $NaHCO_3$ at room temperature, histone-DNA crosslink was reversed in 200 mM NaCl at 65 °C for 4 hours and protein was digested with 0.1 mg/ml proteinase K. The DNA was purified with a QIAquick PCR purification kit (Qiagen) and eluted in 50 μl distilled water. 2μl of input and immunoprecipitated DNA were subjected to RT-PCR analysis with a BioRad iQ5 RT-PCR detection system using Quanta Biosciences SYBR Green FastMix for iQ. RT-PCR reactions were performed in a volume of 20 μl using the primers depicted in Table 2.8 at a concentration of 0.3 μM and the following thermo cycle protocol: Cycle 1 (1x) 30 seconds, 95 ºC ; Cycle 2 (40x) 1 second, 95 ºC , 25 seconds 57 ºC. ChIP signal was determined relative to input.

2.2.8.4 Flow cytometry analysis

HeLa cells were trypsinised, resuspended in medium and washed in PBS. Cells were resuspended in 430 μl PBS and fixed by dropwise addition of 1 ml cold Ethanol whilst vortexing to avoid clumping cells. Cells were washed twice in 3 ml PBS, 1 % FBS and stained in 300 to 500 μl PI solution (PBS, 1 % FBS, 50 μg/ml RNase A, 50 μg/ml propidium iodide) for 30 minutes at room temperature in the dark. DNA content was assessed by flow cytometry using a FACS Calibur (Becton Dickinson). 10,000 events were counted per sample and the fluorescence data (DNA content) was plotted on a histogram from channel number 0 to 1023 using the FlowJo software. The G1 peak was set to 200 to allow good resolution of the G1, S and G2/M phase distribution. Cell cycle distribution was estimated with FlowJo using the Watson distribution model.

2.2.8.5 *In vitro* phosphorylation

In vitro phosphorylation was performed with purified recombinant HIS-RNMT WT or T77A in complex with GST-RAM 1-90 and activated CDK1/Cyclin B1 (NEB) or CDK2/Cyclin A2 (DSTT). 0.33 μM HIS-RNMT/GST-RAM 1-90 was incubated with 0.01 μM CDK1/Cyclin B1, 100 μM non-radioactive or [γ-^{32}P]-ATP (500 cpm/pmol) (Perkin Elmer), 10 mM $MgCl_2$, 2 mM DTT, 50 mM Tris pH 7.5 and 0.1 mM EGTA. Kinase assays were performed in total volumes of 20 or 30 μl at 30 °C in a shaking incubator at 1200 rpm for the time indicated in the figure legends. Reactions were stopped by addition of 4x Laemmli dye. Samples were separated by SDS-PAGE and analysed by western blot or stained with Coomassie blue and subjected to autoradiography. To estimate the stoichiometry of [^{32}P] incorporation into RNMT, RNMT bands were excised and counted for 60 seconds using a scintillation counter. At the same time the specific activity of the input [γ-^{32}P]-ATP was measured by scintillation counting. The RNMT counts were divided by the specific activity of the [γ-^{32}P]-ATP and by the amount of RNMT used for the *in vitro* phosphorylation reaction.

2.2.8.6 *In vitro* phosphorylation coupled to methyltransferase activity assay

In vitro phosphorylation was performed as described above in the presence or absence of cold ATP or CDK1/Cyclin B1 for 30 minutes. After *in vitro* phosphorylation the reaction mix was diluted in F-Buffer and 900 ng of HIS-RNMT in complex with GST-RAM 1-90 was subjected to glutathione affinity purification using 20 μl 50 % slurry glutathione sepharose for 1.5 hours. Precipitates were washed in F-Buffer and MT-Buffer and dissolved in 150 μl MT-Buffer supplemented with 0.05 % Triton X-100. 5 μl (1/30) was used to perform *in vitro* cap methyltransferase assays.

2.2.8.7 *In vitro* affinity assay

1.5 or 2 μg of purified recombinant proteins were mixed in RIPA buffer (Figure 3.6) or F-Buffer (Figure 5.6) and incubated with 25 μl 50% slurry glutathione sepharose for 3 hours at 4 °C. GST tagged protein was affinity purified with glutathione sepharose and washed precipitates were resolved in 1x Laemmli buffer, separated by SDS-PAGE and stained by Coomassie blue or analysed by western blot.

2.2.9 Recombinant protein production

2.2.9.1 Preparation of HIS-RNMT

A pNIFTY-based vector expressing RNMT fused N-terminally to a 6 x HIS tag was transduced into BL21 CodonPlus (DE3)-RIL *E. coli*. A single colony was expanded to a 1 L culture in terrific broth. At an OD_{600} of 1.2, expression of recombinant protein was induced with 1 M IPTG (isopropyl-β-D-thiogalactopyranoside) for 18 hours at 14 °C. Cells were harvested by centrifugation at 4,000 x g, washed in PBS and frozen at -80 °C. Pellets were resuspended in 25 ml lysis buffer [50 mM Tris/HCl (pH 7.5), 250 mM NaCl, 0.5 mM EGTA, 0.5 mM EDTA, 0.5 % Triton X-100, 1 mM DTT, 20 μg/ml leupeptin, 1 mM Pefabloc, 0.5 mM TCEP, 20 mM immidazole] and sonicated six times on ice for 30 sec. Insoluble material was removed by centrifugation for 25 min at 60,000 x g. 250 μl Ni^{2+} resin was incubated with the soluble material for 1.5 hours at 4 °C and washed in 25 ml wash buffer [50 mM Tris/HCl (pH 7.5), 250 mM NaCl, 0.03% Brij-35, 40 mM immidazole]. HIS-RNMT was eluted from the Ni^{2+} resin in 2 ml elution buffer [50 mM HEPES, 150 mM NaCl, 0.03% Brij-35, 400 mM immidazole]. The purified protein was dialysed overnight at 4 °C in dialysis buffer (50 mM HEPES, 150 mM NaCl, 0.03% Brij-35) using 10,000 Mw snakeskin dialysis tubing (Thermo).

2.2.9.2 Preparation of GST-RNMT

A pGEX6P1-based vector expressing RNMT fused N-terminally to a GST tag was transduced into BL21 (DE3) *E. coli*. A single colony was expanded to a 1 L culture in LB medium. At an OD_{600} of 0.6, expression of recombinant protein was induced with 1 M IPTG (isopropyl-β-D-thiogalactopyranoside) for 18 hours at 16 °C. Cells were harvested by centrifugation at 4,000 x g, washed in PBS and frozen at -80 °C. Pellets were resuspended in 12 ml lysis buffer [50 mM Tris/HCl (pH 7.5), 150 mM NaCl, 0.1 mM EGTA, 0.1 mM EDTA, 0.1 % Triton X-100, 0.1 % β-mercaptoethanol, 0.2 mM PMSF, 1 mM benzamidine, 20 µg/ml leupeptin, 1 mg/ml lysozyme] and sonicated six times on ice for 30 sec. Insoluble material was removed by centrifugation for 25 min at 60,000 x g. 1 ml glutathione sepharose was incubated with the soluble material for 1.5 hours at 4 °C and washed five times in 25 ml wash buffer [50 mM Tris/HCl (pH 7.5), 150 mM NaCl, 0.1 mM EGTA, 0.1 mM EDTA]. GST-RNMT was eluted from the glutathione sepharose in 5 ml elution buffer [50 mM Tris/HCl (pH 7.5), 150 mM NaCl, 0.1 mM EGTA, 0.1 mM EDTA, 0.1 % β-mercaptoethanol, 0.2 mM PMSF, 1 mM benzamidine, 20 µg/ml leupeptin 50 mM glutathione]. The purified protein was buffer-exchanged in elution buffer without glutathione and concentrated to 2 ml using a diafiltration column.

The GST tag was removed by incubating GST-RNMT bound to glutathione sepharose overnight in wash buffer containing 200 µg of precision protease.

2.2.9.3 Preparation of other recombinant protein

The following recombinant proteins were purified in house by the Division of Signal Transduction Therapy (DSTT): HIS-RNMT/GST-RAM 1-90 (DU42422), HIS-RNMT T77A/GST-RAM 1-90 (DU43251), GST, GST-RNGTT, GST-KPNA2 and KPNA2 GST-OFF (DU42444).

2.2.10 Cloning methodology

All constructs prepared for this study are presented in Table 2.20.

2.2.10.1 Site-directed mutagenesis

DNA vectors were subjected to site-directed mutagenesis using the QuickChange site-directed mutagenesis kit (Stratagene) according to manufacturer's instructions. In brief, 50 and 5 ng of DNA templates were combined with a 50 µl reaction mixture containing 1x site-directed mutagenesis buffer, 200 µM dNTPs, 0.5 µM of each primer (Table 2.9) and 5 U of high fidelity DNA polymerase. PCR reactions were performed in a DNA Engine Dyad Peltier Thermal Cycler (Bio-Rad). DNA was first denatured at 95 °C for 30 seconds before entering a cycle of denaturation at 95 °C for 30 seconds, primer annealing at 55 °C for 30 seconds and extension at 68 °C for 7 minutes. After a total of 18 cycles the original methylated and non-mutated plasmid derived from bacterial source was digested by the addition of 2 U *Dpn*I to the PCR products and incubation for 1 hour at 37 °C. Products from the two PCR reactions were combined and purified with a QIAquick PCR purification kit (Qiagen) and used for *E. coli* cell transformation.

2.2.10.2 PCR

DNA was amplified using polymerase chain reaction (PCR) from vector templates using Expand High Fidelity PCR System (Roche) according to manufacturer's instruction. In brief, 100 ng vector was combined with a 100 µl reaction mixture containing 1x High Fidelity PCR System buffer supplemented with 1.5 mM $MgCl_2$, 200 µM dNTPs, 0.5 µM of each primer (Table 2.10) and 5 U of high fidelity DNA polymerase. PCR reactions were performed in a DNA Engine Dyad Peltier Thermal Cycler (Bio-Rad). DNA was first denatured at 95 °C for 2 minutes before entering a

cycle of denaturation at 95 °C for 30 seconds, annealing at 55 °C for 30 seconds and extension at 72 °C for 30 (RNMT-N), 60 (RNMTcat) or 90 seconds (HIS-RNMT). After a total of 28 cycles the reaction entered a final extension phase at 72 °C for 2 minutes. The PCR products were purified with a QIAquick PCR purification kit (Qiagen).

2.2.10.3 PCR purification

PCR products were purified using the QIAquick PCR purification kit (Qiagen) according to manufacturer's instructions. DNA was eluted in 50 µl distilled water.

2.2.10.4 Restriction enzyme digestion

Restriction digests of DNA were performed with restriction enzymes using the buffers recommended by the manufacturer. Typically, digestions were performed for 4 hours at 37 °C in a total volume of 50 µl containing two different restriction enzymes and 1x NEB buffer compatible for both enzymes. In general 2 µg of backbone vector, 6 µg of insert-containing vector or 15 µl of insert-containing PCR product was digested with 20 U of restriction enzymes. For the backbone vector digestion, after 3 hours digestion, 10 U CIP phosphatase (NE biolabs) was added to the reaction mixture in order to dephosphorylate 5'-phosphate ends created by the restriction digestion and reduce self-ligation of vector during cloning. Digestion products were analysed by agarose gel electrophoresis and purified using QIAquick gel extraction kit (Qiagen).

2.2.10.5 Agarose gel electrophoresis

Double stranded DNA was purified after restriction digestion by agarose gel electrophoresis. Typically, 1% (w/v) Agarose was dissolved in 1x TAE buffer by heating up the solution. Gels were cast into a gel tray after addition of 0.1 % gel red (Biotium).

DNA samples were combined with 5x Green GoTaq reaction (Promega) buffer as loading dye. Electrophoresis was performed in a Mini-Sub Cell GT Cell (Bio-Rad) in 1x TAE buffer at 120 V for approximately 40 minutes. DNA was visualised with a UV transilluminator, extracted and purified by QIAquick Gel Extraction Kit (Qiagen).

2.2.10.6 Gel extraction

DNA was purified after agarose gel electrophoresis using QIAquick Gel Extraction Kit (Qiagen) according to manufacturer's instructions. DNA was eluted in 50 µl distilled water.

2.2.10.7 Ligation

Digested insert DNA and vector backbones were ligated in a molar ration of 3:1 using T4 DNA ligase (NE BioLabs) according to manufacturer's instruction. In general, 10 µl ligation reaction containing 1 µl vector, 3 µl insert, 1x T4 ligation buffer and 1 U T4 DNA ligase were incubated for 1 hour at room temperature. 5 µl of the reaction were used to transform competent DH5α *E. coli* cells.

2.2.10.8 Transformation of *E. coli* cells with plasmids

Competent *E. coli* cells (Table 2.19) were thawed on ice and mixed with 50 to 200 ng DNA or 5 µl ligation mix. After 20 minutes on ice cells were heat-shocked for 45 seconds at 42 °C and incubated on ice for 2 minutes. The bacteria were plated on selective LB agar plates containing the appropriate antibiotic (50 µg/ml ampicillin or 50 µg/ml kanamycin) and incubated overnight at 37 °C.

Table 2.19 *E. coli* strains and their genotype used in this study.

Bacterial strain	Genotype
DH5α	*F' ϕ80dlacZΔM15 Δ(lacZYA-argF) U169 deoR recA1 endA1 hsdR17 phoA supE44 λ- thi-1 gyrA96 reA1*
BL21 (DE3)	*B F⁻ ompT hsdS($r_B^-m_B^-$) dcm$^+$ Tet^r gal endA*
BL21 CodonPlus (DE3)-RIL	*B F⁻ ompT hsdS($r_B^-m_B^-$) dcm$^+$ Tet^r gal endA Hte [argU ileY leuW Cam^r]*

2.2.10.9 Plasmid preparation

Plasmid DNA was purified from DH5α *E. coli* cells growing overnight at 37 °C. DNA QIAprep Miniprep Kit (Qiagen) was used to purify 5-10 µg DNA eluted in 50 µl distilled water according to manufacturer's instructions.

To produce large amount of plasmids DNA Maxi Kit (Qiagen) was used according to manufacturer's instructions. Typically 500-1000 µg DNA were resuspended in 700 µl distilled water.

Table 2.20 Table of all constructs generated

Construct	Backbone	Cloning method
HA-RNMTcat	pcDNA4	HA-RNMT 121-476 was amplified from pBMN RNMT-GFP construct by PCR using primers described at Table 2.13. *Bam*HI and *Xho*I restriction enzymes in NEB 2 buffer were used for double digestion of vector and insert.
HA-RNMT-N	pcDNA4	HA-RNMT was amplified from pBMN RNMT-GFP construct by PCR using primers described in Table 2.13. *Bam*HI and *Xho*I restriction enzymes in NEB 2 buffer were used for double digestion of vector and insert.

HA-RNMT WBL	pcDNA5	HA-RNMT was cut out from INI HA-RNMT WBL with *Bam*HI and *Not*I in NEB 3 and ligated into pcDNA5 that was digested with the same enzymes.
HA-RNMT T77A WBL	pcDNA5	Site-directed mutagenesis with mutagenesis primers (Table 2.12) using pcDNA5 HA-RNMT WBL as template.
HA-RNMT 5A	pBMN-Z-IRES-NEO (INI)	Site-directed mutagenesis with mutagenesis primers (Table 2.12) using INI HA-RNMT as template.
HA-RNMT 2A	pBMN-Z-IRES-NEO (INI)	Site-directed mutagenesis with mutagenesis primers (Table 2.12) using INI HA-RNMT as template.
HA-RNMT 7A	pBMN-Z-IRES-NEO (INI)	Site-directed mutagenesis with mutagenesis primers (Table 2.12) using INI HA-RNMT 5A as template.
INI HA-RNMT T77A WBL	pBMN-Z-IRES-NEO (INI)	Site-directed mutagenesis with mutagenesis primers (Table 2.12) using INI HA-RNMT WBL as template.
HA-RNMT T77D WBL	pBMN-Z-IRES-NEO (INI)	Site-directed mutagenesis with mutagenesis primers (Table 2.12) using INI HA-RNMT WBL as template.
HA-RNMT S79A WBL	pBMN-Z-IRES-NEO (INI)	Site-directed mutagenesis with mutagenesis primers (Table 2.12) using INI HA-RNMT WBL as template.
HIS-RNMT	pNIFTY	RNMT was amplified from pBMN RNMT-GFP by PCR using primers described in Table 2.13. *Kas*I and *BamH*I restriction enzymes in NEB 2 buffer were used for double digestion of vector and insert.

2.2.10.10 Additional constructs used in this study

The following constructs used in this study were cloned in the Cowling lab: pcDNA4 HA-RNMT, pcDNA4 Fg-RAM, pcDNA5 Fg-RAM, INI HA-RNMT WBL, pGEX6P1 GST-RNMT.

The following construct used in this study was cloned in the Division of Signal Transduction (DSTT): pcDNA5 9E10-KPNA2, pGEX6P1 GST-KPNA2, pGEX6P1 GST-RNMT T77A, pGEX6P1 GST-RNMT T77D.

Chapter 3:

Human cap methyltransferase (RNMT) N-terminal non-catalytic domain mediates recruitment to transcription initiation start sites

3.1 Introduction

The N7-methylguanosine cap is a structure found on the 5' end of RNAs transcribed by RNA polymerase II. The N7-methylguanosine cap is conserved in eukaryotes and is essential for cell viability. It protects transcripts from degradation, and via interactions with cap-binding proteins, mediates several RNA processing events and ensures efficient translation of mRNAs. In mammals, two enzymes are required for the formation of the N7-methylguanosine cap: the capping enzyme, RNA guanylyltransferase and 5' triphosphatase (RNGTT), removes the terminal phosphate from the 5' end of nascent RNA and catalyses the addition of a reverse guanosine group (referred to as cap) and the RNA guanine-7 methyltransferase, RNMT, methylates the cap at the N-7 position. Furthermore, RNMT functions in a complex with the small RNMT-activating mini protein RAM.

RNMT contains a catalytic domain, which is conserved to yeast, responsible for the transfer of a methyl group from S-adenosyl methionine to the N7 position of the cap. Several studies with yeast cap methyltransferases as well as with human RNMT have identified essential amino acids that are required for cell viability and *in vitro* catalytic activity (Mao et al., 1996; Saha et al., 1999; Schwer et al., 2000; Wang and Shuman, 1997). Crystal structure analysis of the cap methyltransferase of *Encephalitozoon*

cuniculi and the catalytic domain of human RNMT localised these essential amino acids in the two binding pockets for the methyl donor, S-adenosyl methionine, and for the cap structure (Fabrega et al., 2004; Wu et al., 2007; Zeng et al., 2008).

In addition to the highly conserved catalytic domain, mammalian RNMT contains a N-terminal domain of approximately 144 amino acids that is absent or not conserved in lower eukaryotes. The N-terminus is not required for catalytic activity since human RNMT 120-476 was able to complement cap methyltransferase-deficient yeast and both recombinant RNMT 120-476 and 144-476 retained cap methyltransferase activity *in vitro* (Saha et al., 1999; Wen and Shatkin, 2000). Furthermore, the N-terminal domain is dispensable for the RNMT-RAM interaction which is essential for cell viability in mammalian cells (Gonatopoulos-Pournatzis et al., 2011). However, the RNMT N-terminus carries three functionally redundant nuclear localisation signals (NLS) that ensure nuclear localisation required for RNMT function *in vivo* and thus for cell viability (Shafer et al., 2005). The three NLS 80KKRK, 103KKRKR and 126KRK are all located towards the 3' end of the N-terminus and thus the biological role of the upstream amino acids remains elusive. Thus, this chapter aims to elucidate whether the RNMT N-terminus has a molecular function besides mediating nuclear localisation.

3.2 Results

3.2.1 Influence of the RNMT N-terminus on cap methyltransferase activity

Human RNMT consists of a well-characterised catalytic domain and a N-terminal domain without a defined function. To elucidate the function of the non-catalytic N-terminal domain HA-tagged constructs expressing wild type RNMT and a N-terminal truncation mutant, RNMTcat, that lacks the first 120 amino acids were made (Figure 3.1). RNMTcat lacks most of the N-terminus but still contains a functional NLS at amino acid 126. In addition, a construct expressing the N-terminus alone, RNMT-N, consisting of the first 120 amino acids was created (Figure 3.1).

RNMT functions in the nucleus and its nuclear localisation is essential for cell viability (Shafer et al., 2005). Immunofluorescence analysis of endogenous RNMT confirmed nuclear localisation of the cap methyltransferase (Figure 3.2a). The three NLS have been shown to be functionally redundant in studies performed with GFP-tagged constructs (Shafer et al., 2005). To confirm nuclear localisation of full-length HA-RNMT and the N-terminal truncation mutant RNMTcat, containing all three or only one NLS respectively, immunofluorescence studies were performed with HeLa cells transiently transfected with HA-tagged constructs (Figure 3.2b). As expected, HA-RNMT wild type, HA-RNMTcat and the N-terminus alone (HA-RNMT-N) were observed to be nuclear.

In an attempt to investigate the role of the RNMT N-terminus we compared cap methyltransferase activities of cellular wild type RNMT and the N-terminal truncation mutant, RNMTcat. The cap methyltransferase activity of RNMT can be assessed *in vitro* in an assay first described by the Shuman laboratory (Mao et al., 1995). Briefly, recombinant RNMT, immunoprecipitated cellular RNMT or total cell extracts are combined with the methyl donor S-adenosyl methionine (SAM) and an *in vitro*

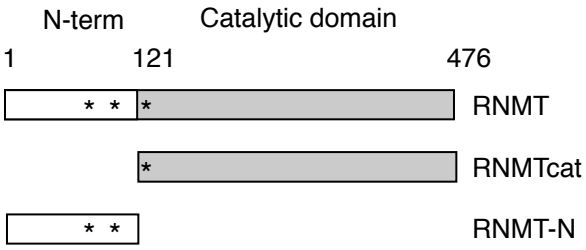

Figure 3.1. RNMT consists of a catalytic domain and a N-terminal domain of unknown function. Human RNMT consists of a catalytic domain (amino acids 121-476, represented by a grey box) and a uncharacterised N-terminal domain (amino acids 1-120, represented by a white box). This schematic diagram represents the constructs used in this chapter; full length RNMT (1-476), RNMTcat (121-476) and RNMT-N (1-120). The position of nuclear localisation signals (NLS) are indicated with an asterisk.

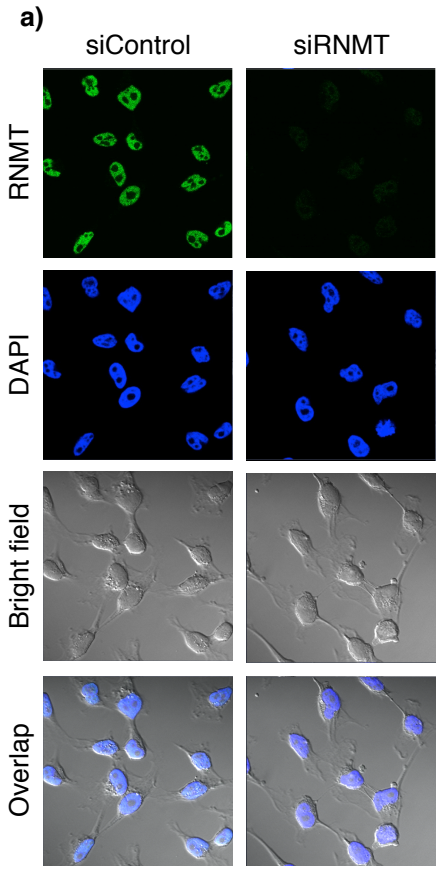

Figure 3.2 RNMT nuclear localisation does not require the N-terminal domain. a) Immunofluorescence analysis was performed on HeLa cells transfected with siRNAs against RNMT or a control for 48 hours. The subcellular localisation of RNMT was detected with an anti-RNMT antibody. DAPI was used to stain DNA to detect nuclei and a bright field view to detect the cell membrane.

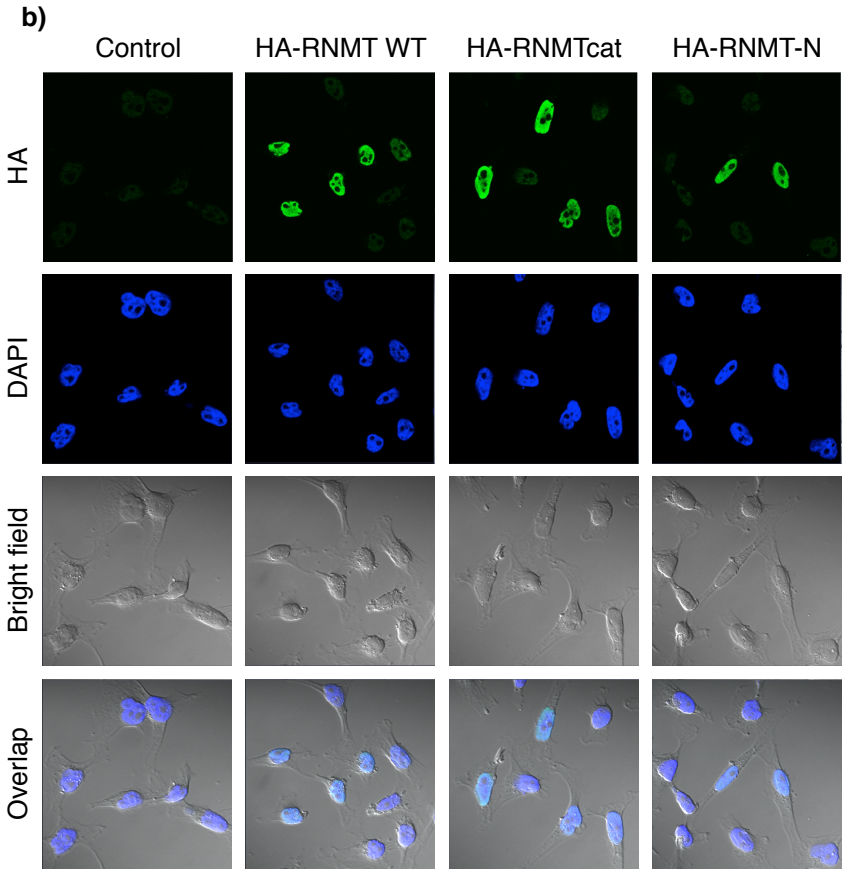

Figure 3.2 RNMT nuclear localisation does not require the N-terminal domain. b) Immunofluorescence analysis was performed on HeLa cells transiently transfected with pcDNA4 (control) or pcDNA4 HA-RNMT, HA-RNMTcat, HA-RNMT-N plus pcDNA4 FLAG-RAM. The subcellular localisation of RNMT was detected via the HA tag. DAPI stain was used to detect nuclei and a bright field view to detect the cell membrane.

transcribed short piece of RNA containing a radioactively labelled cap. After incubation with RNMT the RNA is digested with a nuclease to cleave off the cap and the nucleotide mixture is resolved by thin layer chromatography (TLC). The guanosine cap and N7-methylguanosine cap are resolved differentially on the TLC plate and thus are separated. After exposure to autoradiography, the conversion of radioactively labelled guanosine to N7-methylguoanosine cap can be quantified using a phosphorimager (Figure 3.3).

To assess whether the RNMT N-terminus influences cap methyltransferase activity of cellular RNMT, HEK-293 cells were transiently transfected with constructs expressing full-length RNMT or the catalytic domain only. Western blots were performed to detect expression of transiently transfected constructs and the transfection protocol was optimised for equal protein levels of the two RNMT variants. HA-RNMT and HA-RNMTcat were immunoprecipitated from HEK-293 cells using mouse monoclonal anti-HA antibody (Figure 3.4a). *In vitro* cap methyltransferase activity assays were performed with immunoprecipitates over a time course of 15 minutes (Figure 3.4b) or with a titration of immunoprecipitates obtained from 5 to 40 μg of cell extracts (Figure 3.4c). In agreement with data published with recombinant RNMT (Saha et al., 1999), RNMTcat retained cap methyltransferase activity. However, whereas recombinant RNMTcat showed a 2-fold reduction in activity, RNMTcat immunoprecipitated from human cells exhibited a 1.5 to 2-fold increase in cap methylation compared to full-length RNMT.

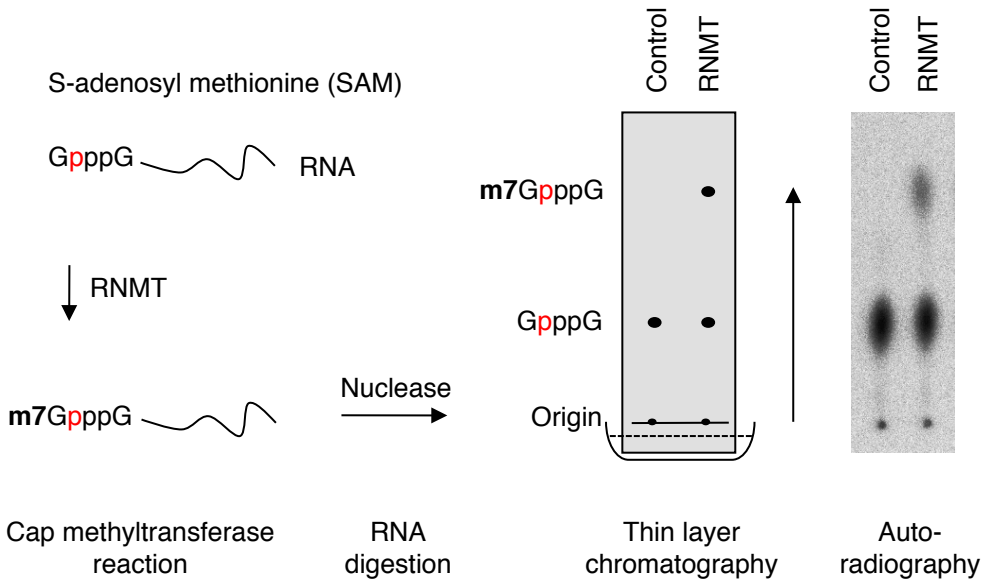

Figure 3.3 *In vitro* cap methyltransferase activity assay. RNMT activity was assessed in a *in vitro* cap methyltransferase activity assay. This schematic diagram represents the major steps of the assay. A typical picture of an autoradiography exposure is shown on the right.

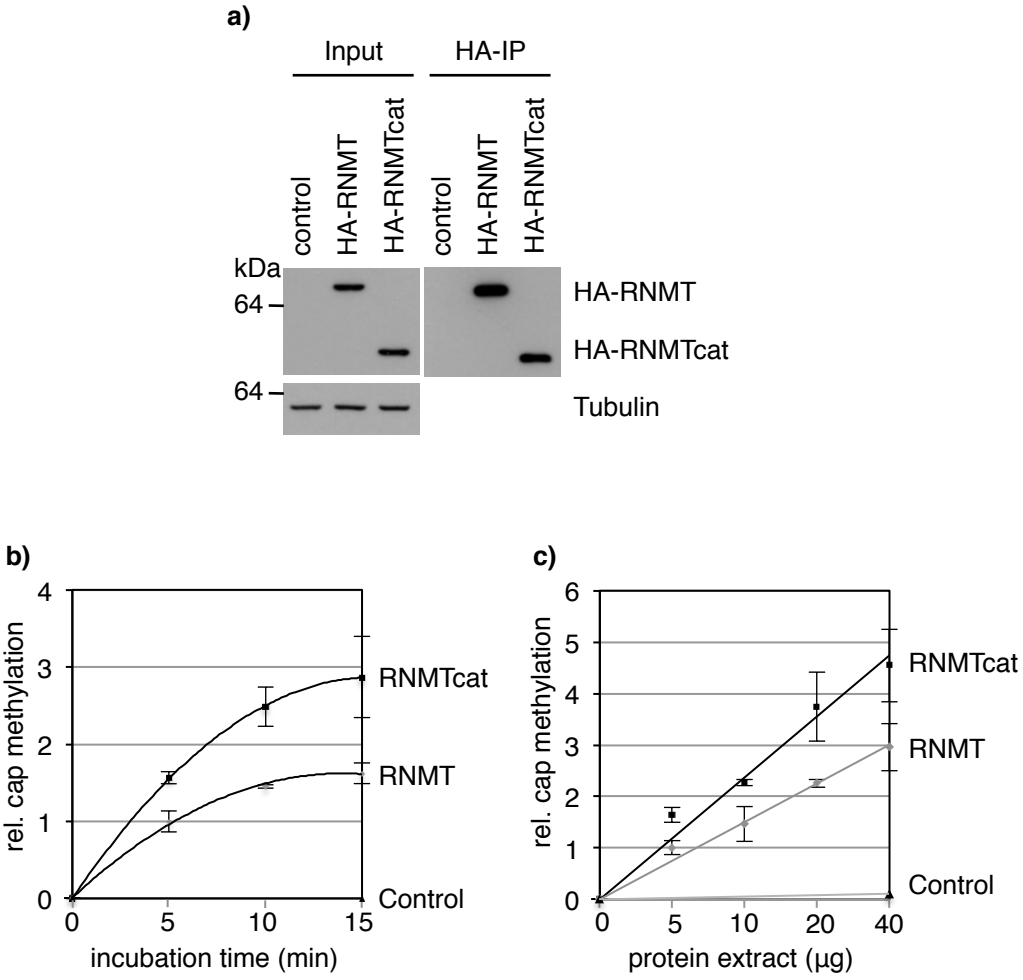

Figure 3.4 RNMT amino acids 1-120 are not required for catalytic activity.

a) HEK-293 cells were transiently transfected by the calcium phosphate method with 6 µg pcDNA4 HA-RNMT or HA-RNMTcat or vector control. Western blots were performed with an anti-HA antibody to detect expression of HA-RNMT and HA-RNMTcat in 10 µg cell extracts or after immunoprecipitation from 50 µg cell extracts using 1.5 µg anti-HA antibody. Tubulin was detected as a loading control.

b) HA-RNMT and HA-RNMTcat were immunoprecipitated from 50 µg of cell extracts of transiently transfected HEK-293 cells using 1.5 µg anti-HA antibody. Following immunoprecipitation cap methyltransferase assays were performed for the time points indicated.

c) As for b) but HA-RNMT and HA-RNMTcat were immunoprecipitated from the quantity of cell extracts indicated and cap methyltransferase assays were performed for 5 minutes. The charts depict the average and standard deviation of three independent experiments (T-test p-values of data series <0.001 for both charts).

3.2.2 Analysis of RNMT recruitment to transcription start sites by chromatin immunoprecipitation (ChIP)

The formation of the N7-methylguanosine cap occurs predominantly at transcription start sites (TSS) (Coppola et al., 1983; Rasmussen and Lis, 1993). The capping enzyme, RNGTT, has been shown to be recruited to Serine-5 phosphorylated CTD of RNA Pol II, an interaction which was shown to activate RNGTT (Ghosh et al., 2011; Ho and Shuman, 1999). RNMT is also recruited to TSS and interactions with RNGTT and RNA pol II, in combination with RNGTT, have been detected with recombinant proteins *in vitro* (Glover-Cutter et al., 2008; Pillutla et al., 1998b). To test whether the RNMT N-terminus is required for RNMT recruitment to TSS, chromatin immunoprecipitation (ChIP) were performed.

HeLa cells were transiently transfected with HA-RNMT or HA-RNMTcat together with FLAG-RAM. Western blots were performed to optimise equal protein levels of the two RNMT variants (Figure 3.5a). ChIP was performed with both anti-HA (Figure 3.5b) and anti-FLAG (Figure 3.5c) antibodies to provide independent confirmation of RNMT-RAM recruitment to chromatin. Recruitment of RNMT and RAM to four c-Myc responsive genes, RNMT, CCND1, RuvBL1 and c-Myc, was measured. qPCR was performed with primers that bind to the promoter proximal regions of the described genes. ChIP with both HA-RNMT and FLAG-RAM showed strongly impaired recruitment of RNMTcat to TSS compared to full-length RNMT. The signal of RNMTcat was comparable to that of the negative control ChIP whereas full-length RNMT showed significant, although low, recruitment to chromatin. As a negative control recruitment of RNMT-RAM 2000 bases upstream of the c-Myc transcription initiation site (-2000) was measured (Figure 3.5b and c). c-Myc -2000 is a location which had previously been demonstrated to have reduced RNMT binding (Glover-Cutter et al., 2008).

a)

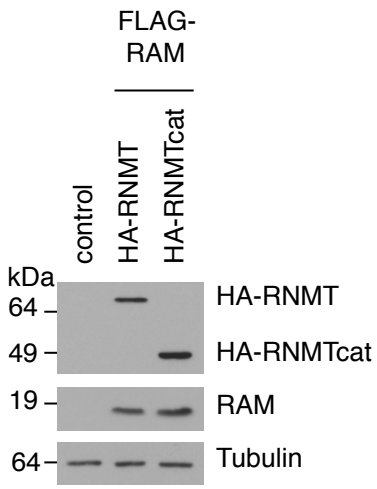

Figure 3.5 RNMT N-terminus is required for recruitment to transcription initiation sites.

a) HeLa cells were transiently transfected with pcDNA4 HA-RNMT or HA-RNMTcat plus pcDNA4 FLAG-RAM or with pcDNA4 (control). Western blots were performed with anti-HA antibody to detect expression of HA-RNMT and HA-RNMTcat. Anti-RAM antibodies were used to detect FLAG-RAM and Tubulin was detected as a loading control.

b) Chromatin immunoprecipitation was performed using HeLa cells transiently transfected with pcDNA4 HA-RNMT or HA-RNMTcat plus pcDNA4 FLAG-RAM or with pcDNA4 (control). Anti-HA antibody was used to immunoprecipitate RNMT. PCR analysis was performed against promoter proximal regions of the genes indicated or 2000 bases upstream of the transcription start site of c-Myc (-2000). The charts depict the average mean signal relative to input and normalised to control for three independent experiments and the error bars represent the standard deviation. T-test p-value <0.05 is indicated with an asterisk.

c) As in b) but immunoprecipitations were performed with anti-FLAG antibody to detect RAM.

Acknowledgement of contribution: Cell transfections and immunoprecipitations were performed by Victoria Cowling.

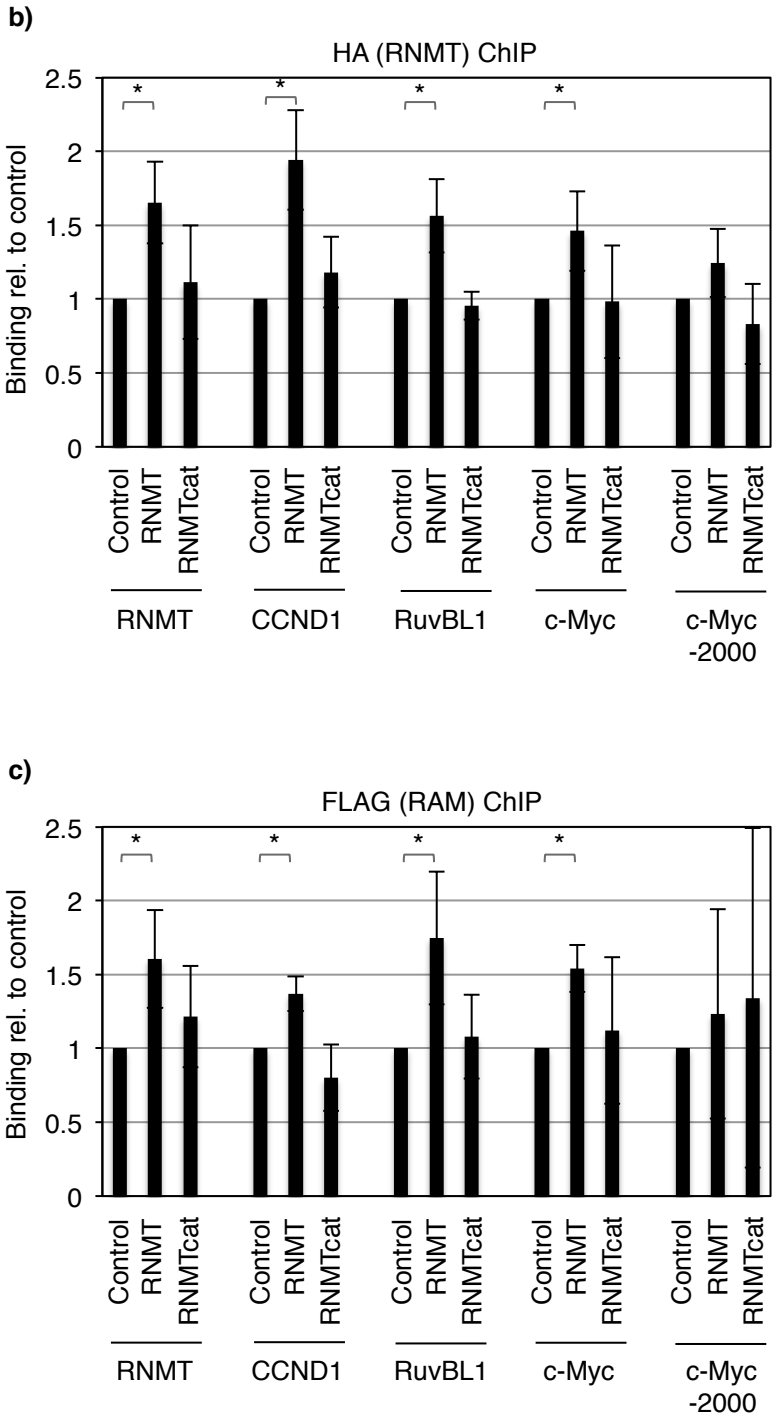

Figure 3.5 RNMT N-terminus is required for recruitment to transcription initiation sites.

No significant ChIP signal was detected at c-Myc -2000 for either RNMT or RNMTcat compared to vector control.

The most likely explanation of the observation that RNMTcat is not efficiently recruited to chromatin is that the first 120 amino acids are required for recruitment to TSS. To investigate whether the RNMT N-terminus alone is sufficient for chromatin recruitment, the experiments were repeated with full length and the N-terminal domain of RNMT. HeLa cells were transiently transfected with HA-RNMT or HA-tagged N-terminal domain, HA-RNMT- N (amino acids 1-120, Figure 3.1) and western blots were performed to optimise equal protein levels of the two RNMT variants (Figure 3.6a). ChIP was performed with anti-HA antibody to detect chromatin recruitment of RNMT (Figure 3.6b). Interestingly, RNMT-N exhibited a strong ChIP signal for all tested genes. For three out of the four genes the recruitment was even higher than full-length RNMT. These experiments show that the RNMT N-terminus is not only essential but sufficient for RNMT recruitment to TSS.

Cellular RNMT exists as a heterodimer with its activating subunit, RAM, and thus, an obvious question is whether RAM is required for RNMT recruitment. Since RAM binds to RNMTcat but does not bind to RNMT-N (Gonatopoulos-Pournatzis et al., 2011) it should follow that RAM is not required for RNMT recruitment to TSS (Figure 3.5b and 3.6b).

3.2.3 Investigating the molecular mechanism for RNMT chromatin recruitment

RNMT recruitment to TSS is mediated by its first 120 amino acids. Unlike RNGTT, no direct interaction with RNA pol II has been demonstrated for RNMT, however, recombinant RNMT was immunoprecipitated with recombinant RNGTT alone or in a tertiary complex with RNA pol II (Pillutla et al., 1998b). To test whether the RNMT N-terminus mediates an interaction with RNGTT and/or RNA pol II CTD affinity

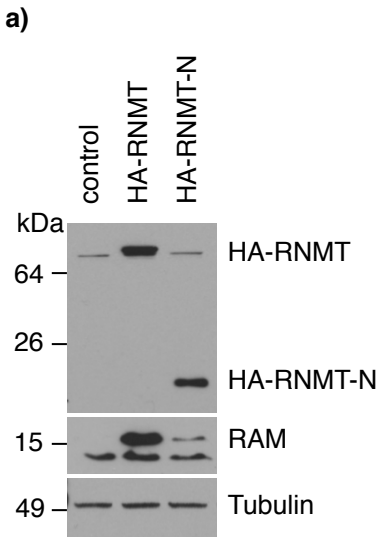

Figure 3.6 RNMT is recruited to chromatin via the N-terminus.

a) HeLa cells were transiently transfected with pcDNA4 HA-RNMT or HA-RNMT-N plus pcDNA4 FLAG-RAM or with pcDNA4 (control) and lysates were subjected to SDS-PAGE and western blot were performed. Anti-HA, anti-RAM and anti-Tubulin antibodies were used to detect HA-RNMT, RAM and Tubulin from cell extracts.

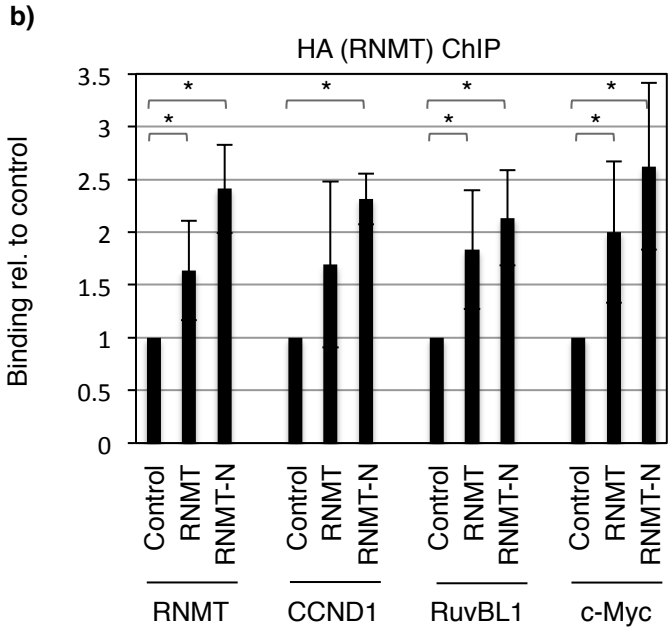

Figure 3.6 RNMT is recruited to chromatin via the N-terminus.

b) Chromatin immunoprecipitation was performed with lysates of HeLa cells transiently transfected as in a). Anti-HA antibody was used to immunoprecipitate RNMT. PCR analysis was performed against promoter proximal regions of the genes indicated. The charts depict the average mean signal relative to input and normalised to control of three independent experiments and the error bars represent the standard deviation. T-test p-value <0.05 is indicated with an asterisk.

Acknowledgement of contribution: Cell transfection and immunoprecipitation were performed by Victoria Cowling.

purification assays and immunoprecipitations were performed with recombinant HIS-RNMT and GST-RNGTT. However, despite extensive effort using a range of buffers (RIPA buffer, F-Buffer, Dignam C and Dignam C + 0.1 % NP40) no direct and specific interaction could be detected (Figure 3.7). Furthermore, previous attempts to detect an interaction with cellular RNMT and RNGTT were not successful (data not shown).

Finally, it was tested whether RNMT interacts directly with RNA pol II. Due to previous unsuccessful attempts to co-immunoprecipitate cellular exogenous or endogenous RNMT and RNA pol II, affinity purification with recombinant protein was attempted. Recombinant GST, GST-RNGTT and GST-RNMT were incubated with HeLa nuclear cell extracts and affinity purified using glutathione sepharose. Precipitated proteins were analysed by SDS-PAGE and western blotting (Figure 3.8). A robust interaction of RNGTT with Serine-5 phosphorylated but not unphosphorylated RNA pol II CTD was detected, confirming the results of previous publications (Yue et al., 1997). However, no interaction was detected between recombinant GST-RNMT and RNA pol II. Furthermore, no interaction was observed between recombinant GST-RNMT or GST-RNGTT with cellular RNGTT or RNMT respectively (Figure 3.8). These data indicate that RNMT may not be recruited to chromatin via a direct interaction with either RNGTT or RNA pol II. However, a transient interaction between RNMT and RNGTT or RNA pol II, or the requirement of additional proteins for mediating such an interaction cannot be excluded.

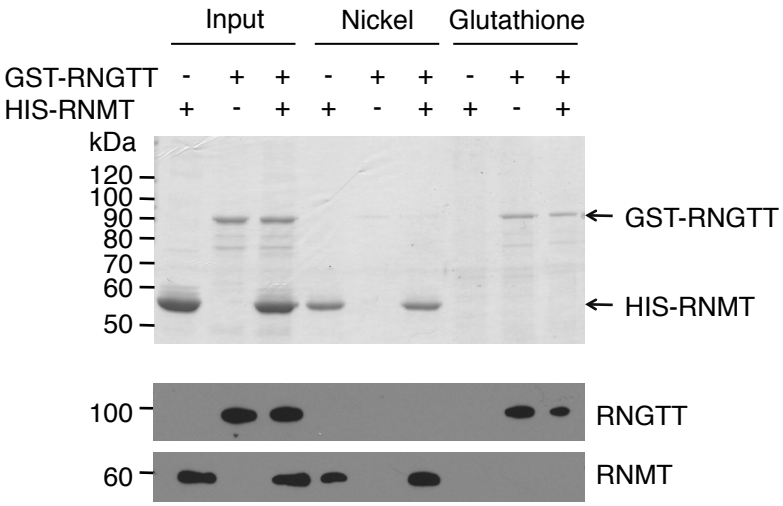

Figure 3.7 An interaction between RNMT and RNGTT is not detectable.

2 µg of purified recombinant HIS-RNMT was incubated with 1.5 µg of purified recombinant GST-RNGTT and affinity purified with nickel agarose or glutathione sepharose. Proteins eluted were resolved by SDS-PAGE and stained by Coomassie blue (upper panel) or analysed by western blot using anti-RNGTT or anti-RNMT antibodies (lower panel).

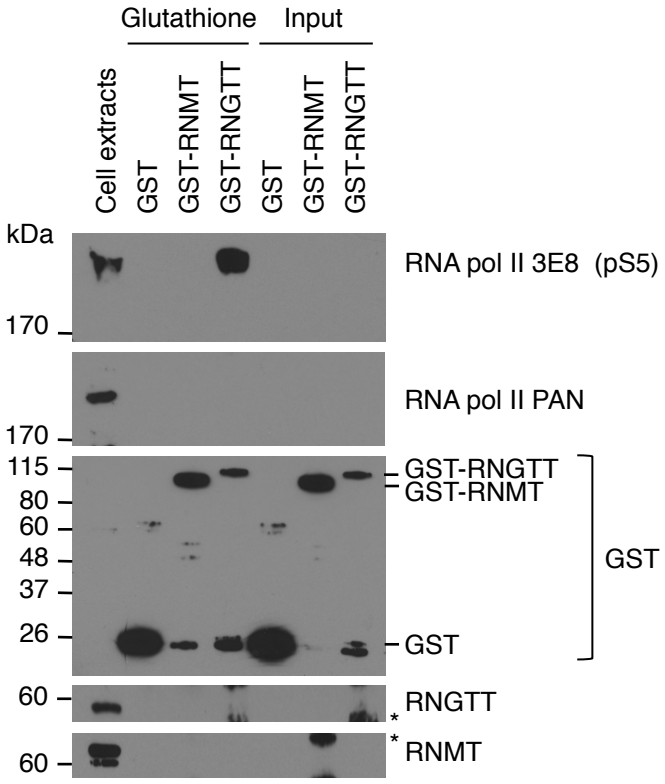

Figure 3.8 A direct interaction between RNMT and phosphorylated RNA polymerase II is not detectable.

1.5 µg of purified recombinant GST, GST-RNMT or GST-RNGTT was incubated with 2 mg of HeLa nuclear cell extracts and affinity purified with glutathione sepharose. Proteins eluted were resolved by SDS-PAGE and analysed by western blotting to detect Serine-5 phosphorylated (pS5) or total (PAN) RNA polymerase II CTD, GST, RNGTT or RNMT. Nonspecific bands are indicated with an asterisk.

3.3 Discussion

Human RNMT consists of a well-characterised catalytic domain at the C-terminus and an uncharacterised N-terminal domain. While the catalytic domain is conserved to yeast the N-terminal domain is only found in mammalian RNMT. The N-terminus is not required for complementing cap methyltransferase deficient yeast cells and it is also dispensable for recombinant RNMT activity (Saha et al., 1999). Human RNMT carries three nuclear localisation signals (NLS) that ensure nuclear localisation and are required for cell viability (Shafer et al., 2005). Two of the NLS are located within the first 120 amino acids whereas the third one is located immediately next to the N-terminus in the catalytic domain. Previous work using GFP-tagged constructs has demonstrated that the three NLS are functionally redundant (Shafer et al., 2005). Thus not surprisingly, our immunofluorescence analysis confirmed nuclear localisation of wild type RNMT and also RNMTcat, which only contains the 126 KKKR NLS.

In order to characterise the function of the human RNMT N-terminus it was investigated whether the N-terminal domain regulates cellular cap methyltransferase activity. As observed with recombinant protein, RNMT purified from HeLa cells did not require the first 120 amino acids for its catalytic activity. However, in contrast to previously described measurements made with recombinant RNMTcat, which exhibited a 2-fold decrease in cap methyltransferase activity (Saha et al., 1999), cellular RNMTcat was 1.5 - 2-fold more active than full-length RNMT. This contrast between recombinant and cellular RNMT may be due to differences in protein folding, post-translational modifications or interactions with other proteins.

The recruitment of RNMT to TSS is essential since N7-methylguanosine cap formation occurs co-transcriptionally (Chiu et al., 2002; Coppola et al., 1983; Moteki and Price, 2002; Rasmussen and Lis, 1993). ChIP analysis of both yeast cap methyltransferase Abd1p and human RNMT have demonstrated that the cap

methyltransferase links to promoters, coding regions or even 3' ends (Glover-Cutter et al., 2008; Komarnitsky et al., 2000; Schroeder et al., 2000). To test whether the N-terminus is required for RNMT recruitment to chromatin ChIP analysis was performed using exogenously expressed proteins. RNMT was observed to be recruited to TSS, though the ChIP signal was low. Interestingly, RNMTcat was not recruited to chromatin. Furthermore, ChIP of RNMT-N demonstrated that the RNMT N-terminus is sufficient to mediate the recruitment to TSS.

The yeast methyltransferase Abd1p recruitment to chromatin was demonstrated to be dependent on phosphorylated RNA pol II CTD (Schroeder et al., 2000). However, to date no direct interaction has been observed between mammalian RNMT and RNA pol II. In contrast, a direct interaction between mammalian RNGTT and phosphorylated RNA pol II CTD has been reported and confirmed by several laboratories (Ghosh et al., 2011; McCracken et al., 1997; Yue et al., 1997). It was found that recombinant RNMT can interact with RNGTT *in vitro* and a trimeric complex was detected when recombinant RNMT, RNGTT and cellular RNA pol II were incubated together (Pillutla et al., 1998b). However, despite exploiting different experimental approaches a direct interaction between RNMT and RNGTT could not be confirmed. Abundant nonspecific immunoprecipitation of RNMT was observed in control experiments using antibodies alone. Such control experiments were not shown in Pillutla *et al.*, 1998. In the present study a robust interaction between RNGTT and phosphorylated RNA pol II was observed but no direct interaction was detectable between RNMT and RNA pol II. Further work in the Cowling laboratory demonstrated however that recruitment of RNMT and RNMT-N is dependent on phosphorylated RNA Pol II CTD (Aregger and Cowling, 2013). 5,6-dichloro-1-β-D-ribofuranosylbenzimidazole (DRB) was demonstrated to inhibit the transcription-regulating subset of CDKs including CDK7, CDK8 and CDK9 leading to inhibition of RNA pol II CTD phosphorylation (Dubois et al., 1994; Yankulov et al., 1995). ChIP experiments with DRB-treated cells demonstrated

that inhibition of RNA pol II CTD phosphorylation significantly reduces recruitment of RNMT to transcription initiation sites (Aregger and Cowling, 2013). However, the precise molecular details of how RNMT is recruited to TSS still remain unclear.

The RNMT N-terminus is not conserved in yeast homologs but yeast Abd1p was demonstrated to be recruited to chromatin in an RNA pol II-dependent manner (Komarnitsky et al., 2000; Schroeder et al., 2000). Although we could not detect an interaction with RNA pol II additional data from our laboratory suggests that chromatin recruitment of human RNMT is also dependent on RNA pol II, thus sharing a common mechanism with yeast. Whereas in yeast the catalytic domain is sufficient for recruitment to TSS the mammalian cap methyltransferase requires the N-terminus for efficient recruitment. The transcription machinery is much more complex in vertebrates and thus it can be speculated that the RNMT N-terminus may have evolved to maintain recruitment of RNMT to TSS when confronted with the mammalian RNA pol II complex. It is also possible that the N-terminal domain may have evolved to regulate RNMT recruitment to chromatin.

Chapter 4:

RNMT is phosphorylated at Threonine-77 in a cell cycle-dependent manner by CDK1/Cyclin B

4.1 Introduction

Until recently, the addition of the N7-methylguanosine cap to the 5' termini of RNA pol II transcripts was thought to be a ubiquitous process and the three enzymatic reactions required for N7-methylguanosine cap formation (triphosphate, guanylyltransferase and methyltransferase) always occur to completion producing a functional N7-methylguanosine cap. However, recent evidence suggests that methyl cap formation can be regulated. Several studies identified incompletely capped mRNAs lacking the methyl moiety on the cap structure and also revealed a special machinery targeting these aberrantly capped mRNAs (Chang et al., 2012; Cole and Cowling, 2009; Cowling and Cole, 2007c; Fernandez-Sanchez et al., 2009; Jiao et al., 2010, 2013). Furthermore, it was observed that growth factors can stimulate formation of the N7-methylguanosine cap. In addition, the Myc and E2F1 transcription factors, which are essential for cell growth and proliferation, were found to upregulate N7-methylguanosine cap formation of specific target genes (Aregger and Cowling, 2012; Cole and Cowling, 2009; Cowling and Cole, 2007a; Fernandez-Sanchez et al., 2009). All these studies suggest that N7-methylguanosine cap formation can be regulated in cells and this chapter aims to investigate whether signalling pathways directly regulate the cap methyltransferase RNMT.

Enzymatic function can be modulated in response to signalling cascades, which results in the addition or removal of chemical moieties to the protein. These post-translational modifications often alter protein properties and are widely used in signalling pathways. One of the most frequently observed and arguably the most widespread type of post-translational modification used in signalling pathways is protein phosphorylation. Protein phosphorylation was found to regulate most eukaryotic cellular processes and it is thought that 30% of all proteins are phosphorylated in human cells (Cohen, 2002). Not all phosphorylation events necessarily have a biological role, however the addition or removal of phosphate groups can modify the function of a protein in several different ways; it can increase or decrease catalytic activity, alter protein movement and thus localisation, increase protein stability or mark proteins for degradation and inhibit or create protein-protein interactions.

In chapter 3 the RNMT N-terminus was observed to negatively regulate cellular RNMT activity contradicting previous studies with recombinant protein (Saha et al., 1999). Thus, an intriguing possibility is that cellular signaling pathways use the N-terminal domain to regulate RNA cap methylation. Several studies exploiting large-scale phosphoproteomic analysis have identified phosphorylated RNMT peptides in mouse and human cells (Hornbeck et al., 2012). However, no site-specific analysis was reported to date characterising sites and functions of any RNMT post-translational modifications. Therefore, the aim of this chapter is to investigate whether RNMT carries post-translational modifications and if so to determine their nature and localisation.

4.2 Results

4.2.1 Biochemical analysis of RNMT to detect post-translational modifications

For the identification of post-translational modifications HEK-293 cells stably transfected with retroviral constructs expressing HA-RNMT to levels equivalent to endogenous RNMT or vector control were used (Figure 4.1a).

Initially, two-dimensional gel electrophoresis (2D SDS-PAGE) analysis was performed to separate RNMT by its molecular weight and its isoelectric point (pI) (the pH at which the protein carries no electrical charge). Unmodified HA-RNMT has a theoretical pI of 5.94, which can be altered by post-translational modifications; for example, one phospho-group would lower the pI of RNMT to 5.81.

Stably expressed HA-RNMT was immunoprecipitated from HEK-293 cells, subjected to 2D SDS-PAGE and analysed by western blot (Figure 4.1a and b). RNMT was found to exist with more than one isoelectric point indicating that it is post-translationally modified. The fact that several spots are visible suggests that RNMT carries several post-translational modifications.

Preliminary work in the Cowling laboratory using orthophosphate-labelling showed that endogenous RNMT is phosphorylated. In order to confirm this work with exogenous RNMT, HEK-293 cells stably expressing HA-RNMT were labelled with [^{32}P]-orthophosphate and HA-RNMT was immunoprecipitated and subjected to autoradiography (Figure 4.2). A specific radiolabelled band was visible after immunoprecipitation with anti-HA antibody suggesting that HA-RNMT is phosphorylated and thus confirming the observation obtained with endogenous RNMT.

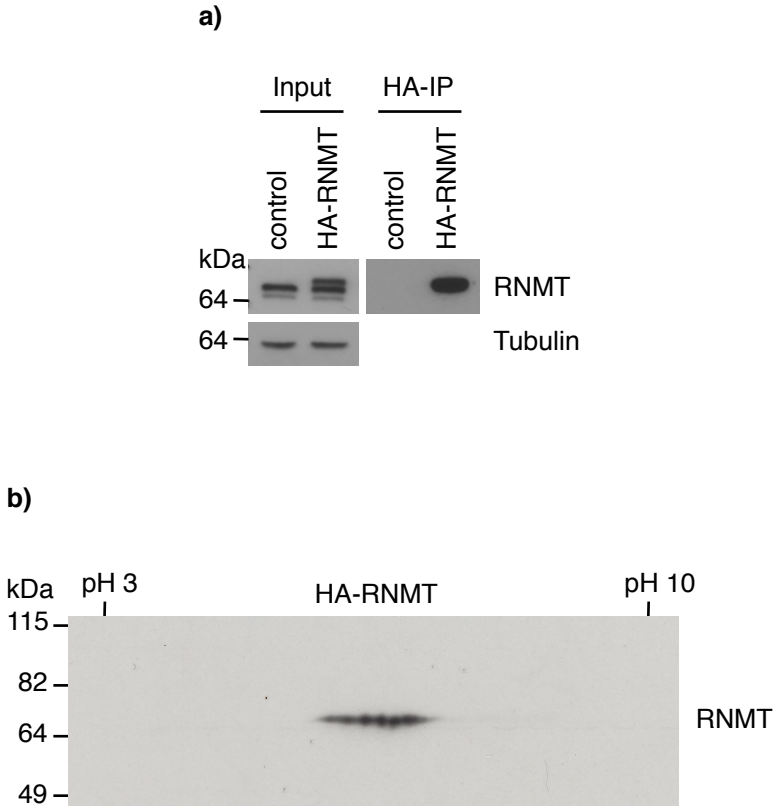

Figure 4.1 Analysis by two-dimensional gel electrophoresis demonstrates that RNMT is post-translationally modified.

a) HA-RNMT was immunoprecipitated from extracts of HEK-293 cells stably expressing HA-RNMT or vector control using anti-HA antibody. Western blots were performed to detect RNMT and Tubulin.

b) Immunoprecipitated HA-RNMT was analysed by two-dimensional gel electrophoresis using a pH range from 3 to 10 and separated protein was subsequently detected by western blotting using anti-RNMT antibody.

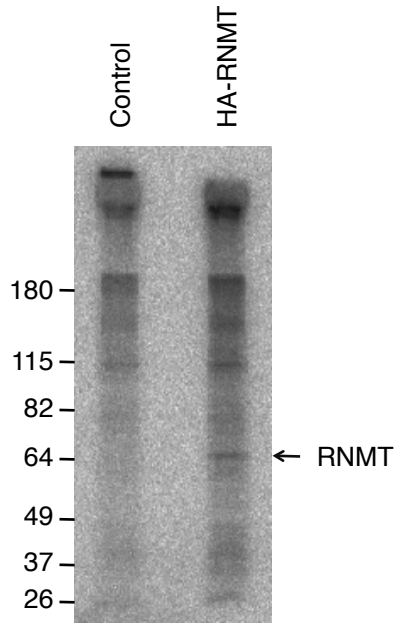

Figure 4.2 Exogenous RNMT is phosphorylated. HEK-293 cells stably expressing HA-RNMT or a vector control were incubated with ^{32}P-orthophosphate and HA-RNMT was immunoprecipitated with anti-HA antibody, resolved by SDS-PAGE and subjected to autoradiography.

4.2.2 Mass spectrometry analysis of RNMT post-translational modifications

Having observed that RNMT is phosphorylated and possibly carries several post-translational modifications, we wanted to identify the modified sites and the nature of the post-translational modifications. To this end, mass spectrometry analysis was performed with HA-RNMT immunoprecipitated from HEK-293 cells. Immunoprecipitates were resolved by SDS-PAGE and stained with Coomassie blue (Figure 4.3a). After trypsin-digestion of the visible protein band mass spectrometry analysis was performed in house by the Fingerprints Proteomics Facility. The samples were analysed by LC-MS/MS on a 4000 QTrap mass spectrometer for protein identification. A protein coverage of 66% of total RNMT amino acids was obtained. Having identified RNMT in the immunoprecipitates, precursor ion scanning was performed to identify phosphorylated peptides. This technique detects phosphopeptides prior to generation of MS/MS data. Precursor ion scanning followed by LC-MS/MS was run on a more sensitive LTQ Orbitrap Velos Pro mass spectrometer. The MS/MS data was subsequently searched against the SwissProt or IPI human databases using the Mascot Daemon to identify the site(s) of phosphorylation. Precursor ion scanning identified two phosphopeptides located at the RNMT N-terminus carrying one phospho group each (Figure 4.3b and c). The Mascot probability based score of the first peptide was statistically significant (p-value < 0.05) whereas the score for the second peptide was not significant but still relatively high compared to its expected value. The exact phosphorylation sites could not be determined by mass spectrometry since both peptides contained multiple candidate phosphorylated amino acids with high scores (Figure 4.3b).

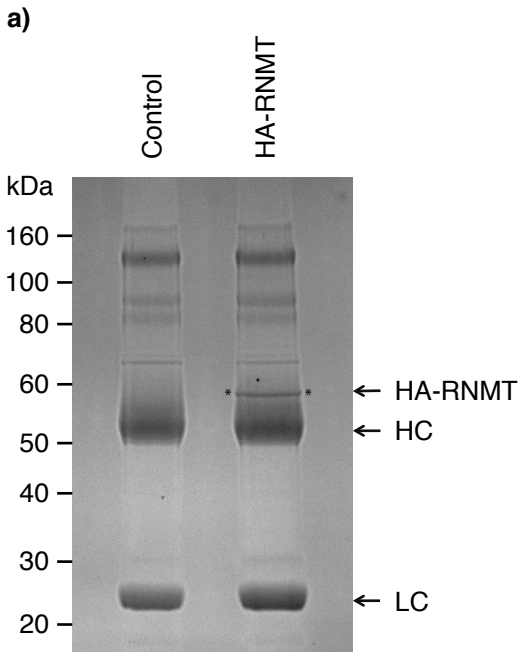

Figure 4.3 RNMT is phosphorylated at the N-terminus.

a) HA-RNMT was immunoprecipitated from 40 mg cell extracts of HEK-293 cells stably expressing HA-RNMT or an empty vector control using 40 μg of anti-HA antibody. Immunoprecipitates were resolved by SDS-PAGE and stained by Coomassie blue. The band marked with an asterisk (HA-RNMT) was excised and analysed by mass spectrometry. HA-RNMT, antibody heavy chain (HC) and light chain (LC) are indicated.

b)

Phosphopeptide	Score	Expected
ASVNSE**T**ESSFNINENTTASGTGLSEK	42	0.057
ASVN**S**ETESSFNINENTTASGTGLSEK	40.1	0.088
A**S**VNSETESSFNINENTTASGTGLSEK	40.1	0.088
ASVNSETES**S**FNINENTTASGTGLSEK	30.6	0.77
ASVNSETE**S**SFNINENTTASGTGLSEK	30.6	0.77
EFEDDLVKESSSCGKD**T**PSK	30.3	0.67
EFEDDLVKESSSCGKDTP**S**K	19.2	8.6

c)

```
MANSAKAEEY EKMSLEQAKA SVNSETESSF NINENTTASG TGLSEKTSVC RQVDIARKRK 60
EFEDDLVKES SSCGKDTPSK KRKLDPEIVP EEKDCGDAEG NSKKRKRETE DVPKDKSSTG 120
DGTQNKRKIA LEDVPEKQKN LEEGHSSTVA AHYNELQEVG LEKRSQSRIF YLRNFNNWMK 180
SVLIGEFLEK VRQKKKRDIT VLDLGCGKGG DLLKWKKGRI NKLVCTDIAD VSVKQCQQRY 240
EDMKNRRDSE YIFSAEFITA DSSKELLIDK FRDPQMCFDI CSCQFVCHYS FESYEQADMM 300
LRNACERLSP GGYFIGTTPN SFELIRRLEA SETESFGNEI YTVKFQKKGD YPLFGCKYDF 360
NLEGVVDVPE FLVYFPLLNE MAKKYNMKLV YKKTFLEFYE EKIKNNENKM LLKRMQALEP 420
YPANESSKLV SEKVDDYEHA AKYMKNSQVR LPLGTLSKSE WEATSIYLVF AFEKQQ 476
```

Figure 4.3 RNMT is phosphorylated at the N-terminus.

b) Mass spectrometry analysis using LC-MS/MS precursor ion search identified two phosphorylated RNMT peptides. The table depicts the amino acid sequence of the two peptides with the candidate phosphorylated amino acid underlined and lists the mascot score and expected value for each candidate. Mascot probability based scores higher than 38 are considered to be significant (p-value < 0.05).

c) The diagram depicts the human RNMT amino acid sequence. The two phosphorylated peptides identified by mass spectrometry are underlined and candidate phosphorylated amino acids are marked with grey shadows.

In addition to phosphorylation, mass spectrometry analysis also identified acetylated and methylated RNMT peptides. The highest acetylation scores were obtained for K83 and K348 whereas the highest methylation scores were detected on E25 and D97. However, due to time constrains the acetylation and methylation sites were not validated or investigated further in order to focus on understanding RNMT phosphorylation.

4.2.3 Identification of the major RNMT phosphorylation site

In order to validate the phosphoproteomic analysis and more specifically determine the exact phosphorylation sites, orthophosphate labelling was performed in combination with a site-specific mutation approach. Candidate phosphorylated amino acids located on the phosphopeptides identified by mass spectrometry were mutated to Alanine, which cannot be phosphorylated (Figure 4.4a). Initially, all possible phosphorylation sites were mutated and stably expressed in HEK-293 cells. HA-RNMT 5A contains mutations of the five candidates of the first phosphopeptide, HA-RNMT 2A carries two mutations of the second phosphorylated peptide and HA-RNMT 7A has all possible candidates mutated to Alanine. The cells were incubated with P^{32}-orthophosphate and HA-RNMT was immunoprecipitated and subjected to autoradiography (Figure 4.4b, left panel). Interestingly, the mutation of the phosphorylation candidates of the first phosphopeptides (HA-RNMT 5A) did not abolish the radioactive signal whereas mutation of all candidates (7A) or the ones from the second phosphorylated peptide (2A) resulted in the loss of the radiolabelled band. This suggests that the major phosphorylation site(s) reside on the second identified peptide. To investigate the contribution of the candidate amino acid of the second phospho peptide to total RNMT phosphorylation, the single Alanine mutants T77A and S79A were created and P^{32}-orthophosphate labelling was repeated with these single mutants (Figure 4.4b, right panel). Mutation of Threonine-77 reduced the radioactive signal in

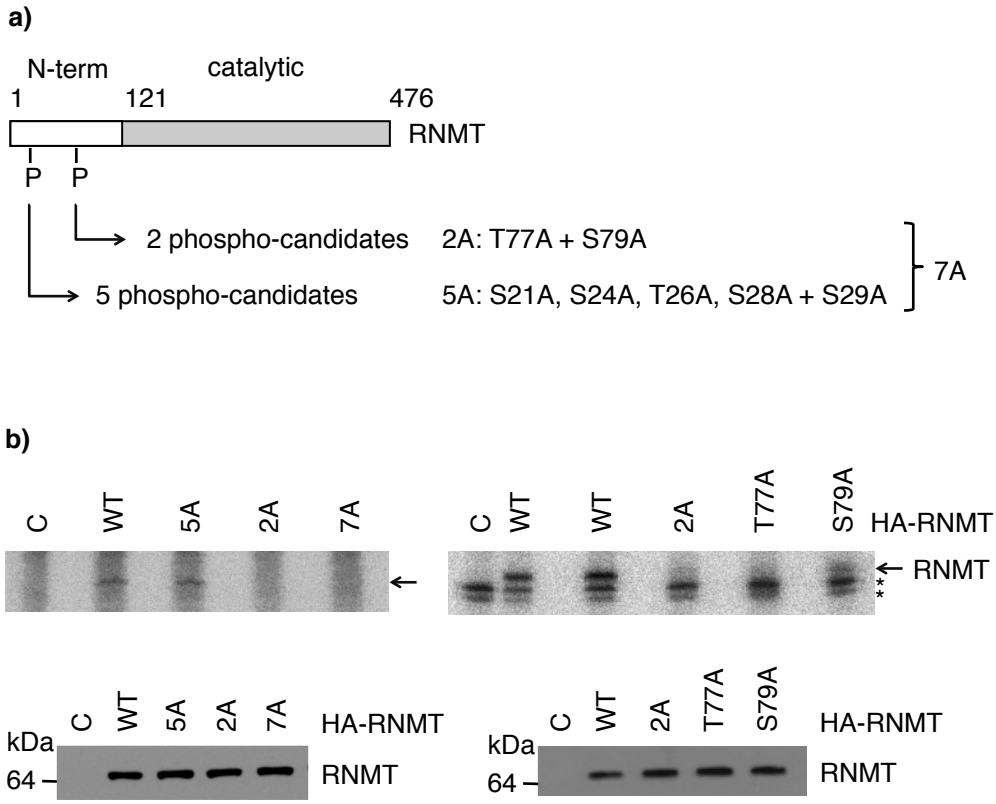

Figure 4.4 RNMT is predominantly phosphorylated at Threonine-77.

a) Schematic diagram depicting the two identified phosphorylation sites and RNMT candidate phosphorylation mutants. Candidate phosphorylated amino acids were mutated to Alanine. RNMT 5A contains the five mutations S21A, S24A, T26A, S28A and S29A whereas RNMT 2A contains the two mutations T77A and T79A. RNMT 7A has all seven phosphorylation candidates mutated to Alanine while RNMT T77A and RNMT S79A contain single amino acid mutations.

b) HEK-293 cells stably expressing HA-RNMT WT, 5A, 2A, 7A, T77A and S79A or an empty vector control (C) were incubated with ^{32}P-orthophosphate. HA-RNMT was immunoprecipitated from 2.5 mg of cell extracts using 10 μg of anti-HA antibody, resolved by SDS-PAGE and subjected to autoradiography (upper panel). HA-RNMT is indicated with an arrow and an asterisk indicates nonspecific bands. Immunoprecipitates were analysed by western blotting to detect RNMT (lower panel).

average by 70 % whereas mutation of Serine-79 only reduced the signal by 52 %. The observation that mutation of a single amino acid led to loss of incorporation of [^{32}P]-orthophosphate suggests that in the cell system studied there is only one major phosphorylation site. Although a second phosphorylation event has been observed by mass spectrometry this site seems to be phosphorylated less abundantly or its phosphorylation may be dependent on Threonine-77. Overall we concluded that Threonine-77 (T77) is the major phosphorylation site of RNMT.

In order to test whether this phosphorylation site has a biological function cell proliferation assays were performed by Victoria Cowling. Endogenous RNMT-RAM was depleted from HeLa cells using siRNAs and RNMT-RAM was replaced with HA-RNMT wild type or T77A in combination with FLAG-RAM (data not shown). Depletion of RNMT-RAM results in loss of cell accumulation (Gonatopoulos-Pournatzis et al., 2011). While wild type RNMT-RAM could rescue proliferation RNMT T77A-RAM did not. This suggests that RNMT T77 phosphorylation is required for normal cell proliferation and thus has a biological function in cells.

4.2.4 Development of a phospho-specific antibody against RNMT Threonine-77

To more efficiently and specifically investigate RNMT T77 phosphorylation a phospho-specific antibody against the T77 phosphorylation site was raised in sheep and affinity purified against phosphorylated peptides by the Division of Signal Transduction Therapy (DSTT) at the College of Life Sciences, Dundee. To characterise the antibody and test whether it was phospho-specific HA-RNMT WT or T77A was immunoprecipitated from HeLa cells and SDS-PAGE and western blots were performed (Figure 4.5a). The phospho-specific antibody only detected wild type protein but not the mutant. Furthermore, when RNMT was immunoprecipitated in the absence of phosphatase inhibitors no signal was detected for phosphorylated T77 (Figure 4.5b).

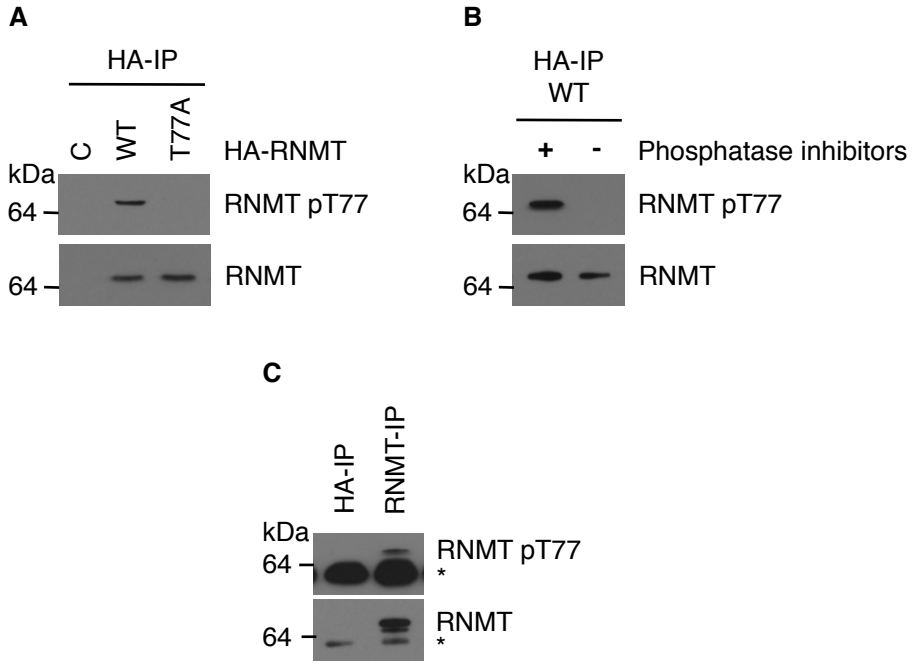

Figure 4.5 Characterisation of a phospho-specific antibody against RNMT Threonine-77.

a) HA-RNMT was immunoprecipitated from 0.6 mg HeLa cells stably expressing HA-RNMT WT, T77A or an empty vector control (C) using 7 μg anti-HA antibody. Immunoprecipitates were resolved by SDS-PAGE and analysed by western blotting to detect T77-phosphorylated and total RNMT.

b) As in a) but HA-RNMT WT was immunoprecipitated in the presence or absence of phosphatase inhibitors.

c) Endogenous RNMT was immunoprecipitated from 0.6 mg HeLa cells using 1.5 μg anti-RNMT antibody. Anti-HA antibody was used as a control. Immunoprecipitates were resolved by SDS-PAGE and analysed by western blotting to detect phosphorylated and total RNMT.

Finally, endogenous RNMT was immunoprecipitated using anti-RNMT antibodies and the phospho-specific antibody also recognised phosphorylation of the immunoprecipitated endogenous protein (Figure 4.5c). Therefore, the produced antibody specifically recognises T77 phosphorylated RNMT.

4.2.5 Identification of a Cyclin-dependent kinase and cyclin consensus sequence

Protein kinase substrate specificity is based not only on the phosphorylation site but also on a short consensus sequence flanking the phosphorylation site. The identification of a consensus sequence near a phosphorylated amino acid can indicate the kinase responsible for phosphorylation. The RNMT T77 phosphorylation site was analysed using the online motif search tools Scansite (http://scansite.mit.edu) and Eukaryotic Linear Motif (ELM) resource (http://elm.eu.org). Both resources compare user-submitted protein sequences with experimentally validated motifs and thus provide a tool to discover putative linear motifs in a target protein (Dinkel et al., 2012; Obenauer et al., 2003). Using these online resources the T77 site was recognised as a proline-directed Serine/Threonine kinase group and more specifically as a Cyclin-dependent kinase motif (S/T-P-x-K/R). Furthermore, immediately adjacent to the T77 phosphorylation site a cyclin recognition site (R-x-L) was predicted (Figure 4.6).

It should be noted that further upstream of the T77 phosphorylation site, the RNMT sequence 62FEDDL resembles the mTOR signalling (TOS) motif (F-E/D/Q/S-M/I/L/V-E/D-M/I/L/V) which is required for interacting with the mTORC1 subunit Raptor (Schalm and Blenis, 2002). However, the sequence does not match the TOS motif completely and incubation with the mTORC1 inhibitor Rapamycin did not affect RNMT T77 phosphorylation (data not shown).

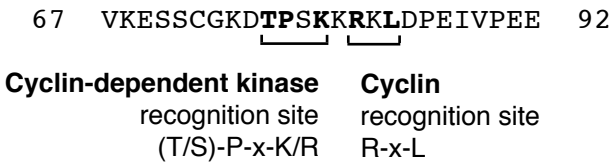

Figure 4.6 RNMT Threonine-77 resides within a Cyclin-dependent kinase recognition site.

Schematic diagram depicting the RNMT amino acid sequence around Threonine-77. Cyclin-dependent kinase and cyclin recognition sites are underlined and marked in bold and the consensus sequences are indicated below (Dinkel et al., 2012; Obenauer et al., 2003).

4.2.6 Cyclin-dependent kinases

Cyclin-dependent kinases (CDKs) are a group of Serine-/Threonine-kinases that form complexes with cyclin proteins. Formation of the CDK-cyclin complex results in a conformational change that is required for the kinase activity. Substrate specificity of the complex is conferred by both the CDK and the cyclin; CDKs recognise a consensus sequence of S/T-P-x-K/R (x is any amino acid, phosphorylation site underlined) and cyclins bind a R-x-L motif in close proximity of the phosphorylation site providing further specificity (Adams et al., 1996; Chen et al., 1996; Songyang et al., 1994).

CDKs in complex with cyclin are the main regulators of the eukaryotic cell cycle, which can be divided into four phases: G1, S, G2 and M-phase. During G1 or gap-phase the cell prepares for DNA replication. S-phase is defined as the stage during which DNA synthesis occurs. After replication cells enter a second gap phase, G2, which is required to prepare for division. The last phase is called M-phase, which stands for mitosis. In M-phase the replicated chromosomes segregate into two new nuclei and finally the cell undergoes cytokinesis to form two daughter cells (Johnson and Walker, 1999).

CDKs coordinate the events of the cell cycle and integrate extracellular and intracellular signals. They are activated during specific points during the cell cycle and when activated they phosphorylate selected proteins to induce downstream processes that control progression through the cell cycle. In humans nine CDKs have been identified of which four are active during the cell cycle (Figure 4.7a). CDK4/Cyclin D and CDK6/Cyclin D are active during G1 phase and are required for progression through G1 due to their ability to suppress the anti-proliferative effects of the retinoblastoma tumour suppressor protein (Rb). CDK2/Cyclin E controls the transition from G1 into S-phase and CDK2/Cyclin A is required for entry and completion of S-phase. Cyclin A also associates with CDK1, which regulates the G2/M-phase transition. M-phase itself is mainly regulated by CDK1/Cyclin B, which phosphorylates targets

a)

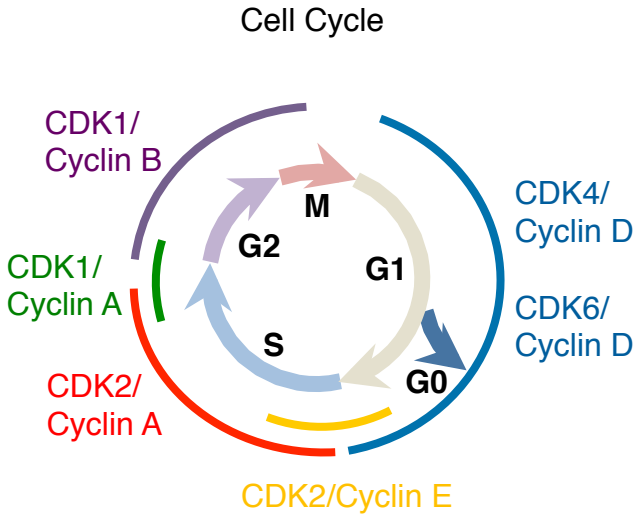

b)

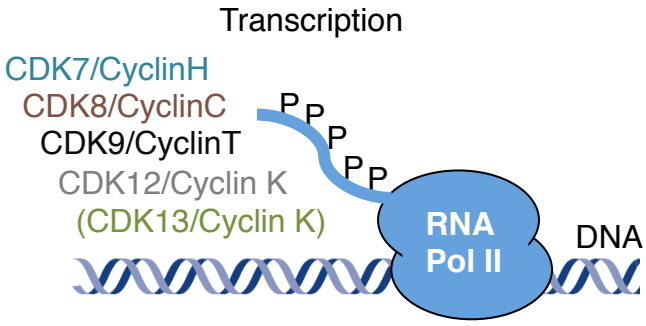

Figure 4.7 RNMT Cyclin-dependent kinases regulate the cell cycle and transcription.

a) This schematic diagram illustrate the stages of the eukaryotic cell cycle (coloured arrows) and the CDK/Cyclin complexes (coloured lines) that are active during a specific phase of the cell cycle.

b) This schematic diagram illustrate the major CDK/Cyclin complexes that regulate transcription by phosphorylating the C-terminal domain of RNA polymerase II.

such as lamins, histones or components of the mitotic spindle. Finally, to exit mitosis cyclin A and B must be degraded leading to the inactivation of CDK1 (Johnson and Walker, 1999).

As described in chapter 1, CDKs also play an important role in the regulation of transcription. RNA polymerase II function is highly dependent on sequential phosphorylation of several amino acids of its C-terminal domain (CTD) during transcription initiation, elongation and termination. Several CDKs have been implicated in CTD phosphorylation (Figure 4.7b): during transcription initiation the CTD is phosphorylated by CDK7/Cyclin H/MAT1, which is part of the general transcription factor TFIIH, and to some extent by CDK8/Cyclin C, which forms a subunit of the mediator complex. CTD phosphorylation by CDK9/Cyclin T, which is the catalytic subunit of the positive transcription elongation factor p-TEFb, is required for transcription elongation. Furthermore, there is initial evidence that CDK12 is also involved in CTD phosphorylation and CDK13 expressed CTD kinase activity *in vitro*. The phosphorylation pattern of the CTD mediates recruitment of many transcription and RNA processing factors and thus not only regulates transcription itself but also RNA maturation (Hsin and Manley, 2012).

4.2.7 Regulation of the CDK/Cyclin complexes

CDKs are regulated in many different ways including subunit binding and phosphorylation events. In an unmodified monomeric state CDKs are catalytically inactive. A flexible loop, called the T-loop or activation segment, blocks the substrate binding at the entrance of the active site cleft. Furthermore, several key residues in the ATP binding site are not correctly positioned. Thus, the primary mechanism of CDK activation is mediated by the binding of the cyclin subunit, which causes a major change in the conformation of the CDK active site (Jeffrey et al., 1995). The most obvious change is the orientation of the T-loop, which lies almost flat at the entrance of

the active site upon cyclin-binding. Furthermore, the residues of the active site are positioned in a way that allows interaction with ATP (Jeffrey et al., 1995). As mentioned above, CDK-cyclin binding is specific since CDKs do not bind all cyclins. The expression of most cyclins oscillates throughout the cell cycle. This is in part achieved by induction of transcription of many cyclins during G1/S transition and often involves positive feedback loops leading to a rapid rise in cyclin levels (Morgan, 1997). Furthermore, regulated ubiquitin-dependent proteolysis controls the levels of cyclins; mitotic cyclins are rapidly degraded towards the end of mitosis and this is necessary to prepare for the next cell cycle (King et al., 1996). Finally, cyclins can be regulated by subcellular localisation; the levels of mitotic cyclin B increase in S and G2 phase but remain in the cytoplasm and CDK1/Cyclin B is unable to phosphorylate its nuclear target proteins. Only during mitosis does cyclin B become phosphorylated which causes translocation of the complex into the nucleus (Li et al., 1997).

In addition to cyclin binding, CDKs are activated by phosphorylation at a conserved site in the t-loop of the kinase domain. Phosphorylation of the t-loop does not substantially alter the conformation of the CDK/Cyclin complex but flattens the t-loop, which stabilises the interaction of the complex which may lead to improved protein-substrate binding (Russo et al., 1996a). The t-loop phosphorylation is catalysed by the CDK-activating kinase (CAK), which is composed of CDK7/Cyclin H/MAT1. As mentioned above, in addition to its role as CAK, CDK7/Cyclin H/MAT1 also exists as a subunit in the TFIIH complex regulating transcription (Fisher, 2012).

Phosphorylation of CDKs does not always lead to kinase activation. Phosphorylation of Tyrosine-15 or Threonine-14 inhibits CDK activation. The side chains of these amino acids form the roof of the ATP binding pocket and phosphorylation may alter their orientation (De Bondt et al., 1993; Jeffrey et al., 1995; Morgan, 1997). For example, CDK1 is kept inactive by Tyrosine-15 and Threonine-14 phosphorylation catalysed by

WEE1 and MYT1. During mitosis WEE1 and MYT1 activity drops and CDK1 inhibitory phosphorylation is removed by the phosphatase CDC25 (Boutros et al., 2006).

Finally, the activity of many CDKs is inhibited by CDK-inhibitory subunits that interact with both cyclin and CDKs and occupy the ATP-binding site (Russo et al., 1996b). These inhibitors, such as p21 or p27, control CDK activity in response to extracellular and intracellular signals.

4.2.8 Identification of the signaling pathway regulating RNMT Threonine-77 phosphorylation

As the RNMT T77 phosphorylation site resides within a CDK recognition site and next to a cyclin binding motif the possibility that CDK/Cyclin complexes regulate RNMT phosphorylation was explored using kinase inhibitors. The transcription-regulating subset of CDKs including CDK7, CDK8 and CDK9 can be inhibited by 5,6-dichloro-1-β-D-ribofuranosylbenzimidazole (DRB) which leads to a reduction in RNA pol II CTD phosphorylation (Dubois et al., 1994; Yankulov et al., 1995). As RNMT is thought to function co-transcriptionally initial experiments were performed to investigate whether RNMT becomes phosphorylated by transcription-regulating CDKs by inhibiting CDK7, CDK8 and CDK9 activity with DRB. HeLa cells were stably transfected with HA-RNMT WT and T77A and incubated over a time course with 50 μM DRB at 37 °C. Immunoprecipitated HA-RNMT was resolved by SDS-PAGE and total and T77 phosphorylated RNMT was analysed by western blot (Figure 4.8, upper panel). Unexpectedly, RNMT phosphorylation levels did not change upon DRB treatment. To confirm that CDK7, CDK8 and CDK9 were inhibited levels of RNA pol II CTD phosphorylation was detected by western blots (Figure 4.8, lower panel). While total RNA pol II levels did not change upon incubation with DRB, the phosphorylation pattern of Serine-2 and Serine-5 was altered which is indicative for inhibition of RNA pol II

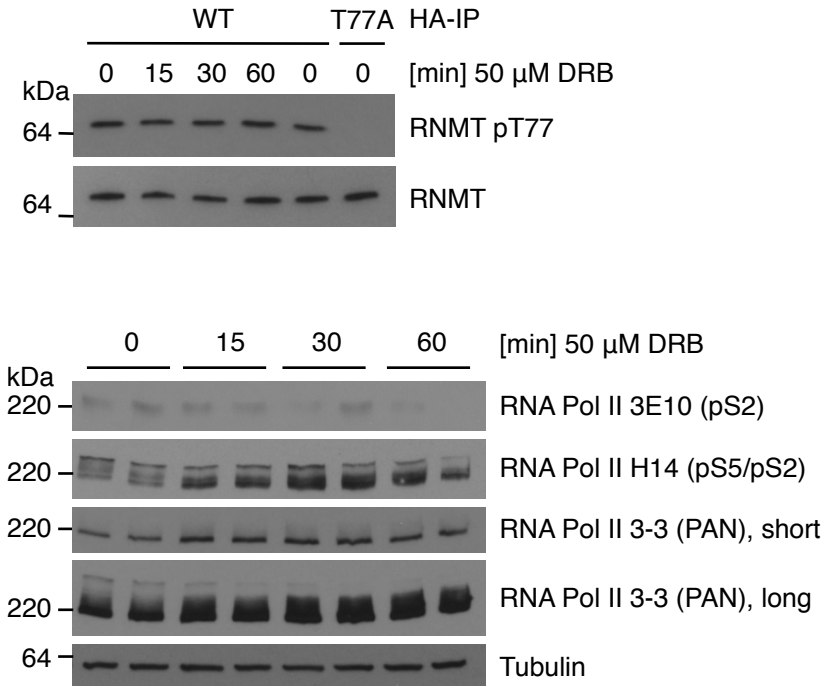

Figure 4.8 DRB does not inhibit RNMT Threonine-77 phosphorylation.

HeLa cells stably expressing HA-RNMT WT or T77A were incubated with 50 µM 5,6-Dichlorobenzimidazole-1-β-D-ribofuranoside (DRB) for the indicated time points. HA-RNMT was immunoprecipitated from 0.6 mg cell extracts using 7µg anti-HA antibody. Immunoprecipitates were resolved by SDS-PAGE and analysed by western blotting to detect Threonine-77 phosphorylated and total RNMT (upper panel). The same cell extracts were resolved by SDS-PAGE and western blots were performed to detect total (PAN), CTD Serine-2 phosphorylated (pS2) and Serine-5 phosphorylated (pS5) RNA polymerase II and Tubulin (lower panel). For total RNA polymerase II (PAN) short and long exposures are shown.

phosphorylation by DRB. RNA pol II was detected as a ladder with antibodies against both total (PAN) and CTD Serine-5/Serine-2 phosphorylated (pS5/pS2) RNA Pol II, which upon DRB treatment was shifted towards decreased molecular weight suggesting reduced phosphorylation levels of the CTD. Therefore, these experiments are indicating that transcription-regulating CDKs do not regulate RNMT T77 phosphorylation.

The remaining CDK/Cyclin complexes regulate the cell cycle. In order to investigate whether they phosphorylate RNMT T77 specific inhibitors were used. Roscovitine is an ATP-analogue that inhibits CDK1, CDK2, CDK5, CDK7, and CDK9 (Meijer and Raymond, 2003). Stably transfected HeLa cells were treated with a titration of Roscovitine for 20 minutes at 37°C. HA-RNMT was immunoprecipitated and western blots were performed (Figure 4.9a). Interestingly, a clear reduction in RNMT phosphorylation was observed upon incubation with Roscovitine. A time course over 60 minutes with 50 μM Roscovitine also showed that T77 phosphorylation is impaired suggesting that cell cycle-regulating CDKs are responsible for RNMT phosphorylation (Figure 4.9b).

One of few specific CDK inhibitors available is RO-3306 which shows very high specificity against CDK1 with an inhibitor constant (Ki) of 35 nM (Vassilev et al., 2006). Thus, RO-3306 was used to test whether specific inhibition of CDK1 would result in reduced RNMT T77 phosphorylation. Stably transfected HeLa cells were incubated with 9 μM RO-3306 over a time course of 120 minutes at 37°C. HA-RNMT was immunoprecipitated and western blots were performed (Figure 4.10). RO-3306 strongly impaired T77 phosphorylation within 5 minutes. Interestingly, when cells were treated with this compound for 30 minutes or longer, phosphorylation levels started to recover suggesting that other CDKs can partially compensate for CDK1 inhibition. Overall the kinase inhibitor experiments indicate that RNMT is phosphorylated by CDK1 and possibly additional cell cycle-regulating CDKs.

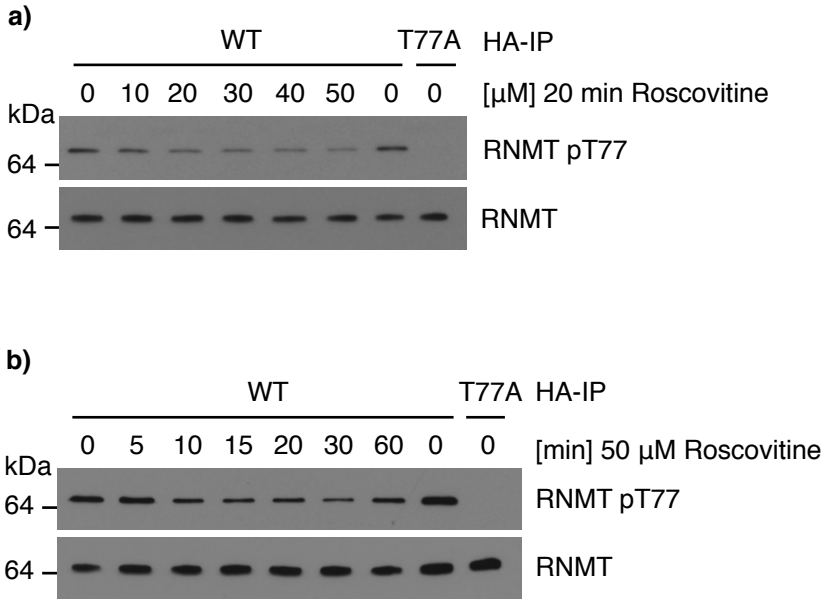

Figure 4.9 Roscovitine inhibits RNMT Threonine-77 phosphorylation.

a) HeLa cells stably expressing HA-RNMT WT or T77A were incubated for 20 min with the indicated concentration of Roscovitine. HA-RNMT was immunoprecipitated from 0.6 mg cell extracts using 7 μg anti-HA antibody, immunoprecipitates were resolved by SDS-PAGE and analysed by western blotting to detect Threonine-77 phosphorylated and total RNMT.

b) As above but cells were incubated with 50 μM Roscovitine for the indicated time points.

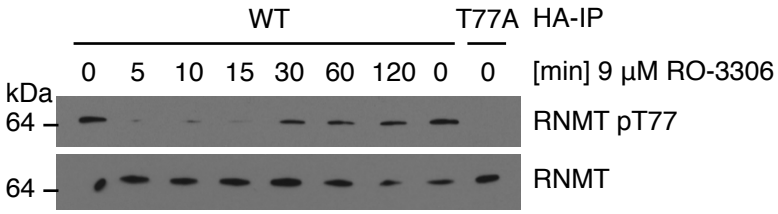

Figure 4.10 RO-3306 inhibits RNMT Threonine-77 phosphorylation.

HeLa cells stably expressing HA-RNMT WT or T77A were incubated for the indicated time points with 9 μM RO-3306. HA-RNMT was immunoprecipitated from 0.6 mg cell extracts using 7μg anti-HA antibody, immunoprecipitates were resolved by SDS-PAGE and analysed by western blotting to detect Threonine-77 phosphorylated and total RNMT.

4.2.9 Analysis of RNMT Threonine-77 phosphorylation in synchronised cells

In order to confirm that RNMT phosphorylation is cell cycle-regulated, experiments were performed with cells synchronised to the same point of the cell cycle. Initially, cells were synchronised at the entrance to S-phase using a double thymidine block. High concentrations of thymidine reversibly interrupt the deoxynucleotide metabolism pathway and hence inhibit DNA replication (Banfalvi, 2011). During the first treatment cells are arrested throughout S-phase. To get a synchronous population arrested at early S-phase cells are released from the block and treated with thymidine for a second time.

HeLa cells stably expressing HA-RNMT were synchronised with a double thymidine block and released into the cell cycle for 0 to 12 hours. Cells were harvested every two hours and RNMT was immunoprecipitated and analysed by western blot (Figure 4.11a, upper panel). A clear cell cycle-dependent pattern in T77 phosphorylation could be observed. Very low levels of phosphorylation were detected in cells blocked in early S-phase but the phospho-specific signal started to increase after 4 hours and peaked at around 8 hours after cells were released from the thymidine block. The signal was then rapidly lost after 12 hours. Cell synchronisation was monitored by western blot by observing levels of: Cyclin B1, which accumulates towards and is destroyed after G2/M-phase; Histone 3 Serine-10 phosphorylation, which is a marker of mitotic cells; Cyclin D1, which is synthesised during G1 (Figure 4.11a, lower panel) (Hendzel et al., 1997; Johnson and Walker, 1999). A similar pattern of RNMT T77 phosphorylation was observed with endogenous protein confirming that this was not an artifact of ectopically expressed HA-RNMT (Figure 4.11b). Finally, cell cycle distribution of synchronised cells was analysed by flow cytometry (Figure 4.11c). In nonsynchronous cells (control) a typical cell cycle distribution was observed with a first peak of G1 cells containing one set of chromosomes followed by S-phase cells that gradually replicate their DNA and

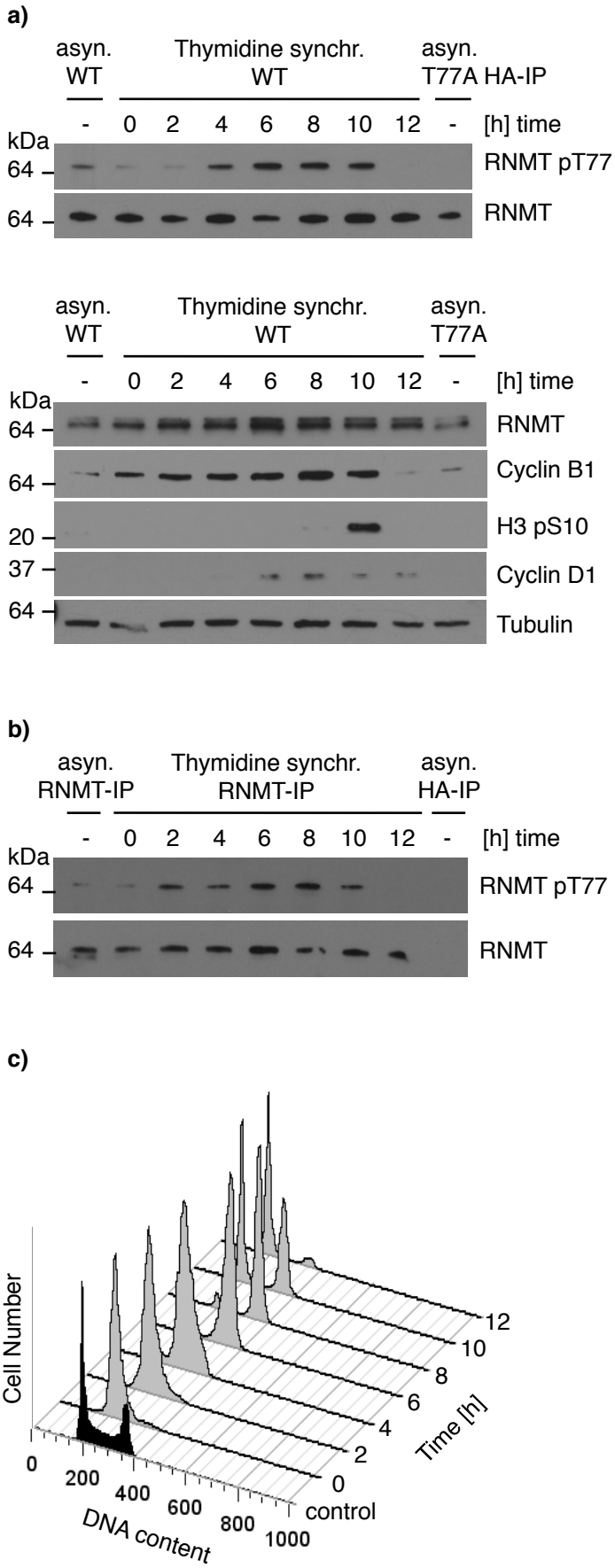
a)
asyn. WT
Thymidine synchr. WT
asyn. T77A
HA-IP
- 0 2 4 6 8 10 12 - [h] time
kDa
64
RNMT pT77
64
RNMT
asyn. WT
Thymidine synchr. WT
asyn. T77A
- 0 2 4 6 8 10 12 - [h] time
kDa
64
RNMT
64
Cyclin B1
20
H3 pS10
37
Cyclin D1
64
Tubulin
b)
asyn. RNMT-IP
Thymidine synchr. RNMT-IP
asyn. HA-IP
- 0 2 4 6 8 10 12 - [h] time
kDa
64
RNMT pT77
64
RNMT
c)
Cell Number
0
200
400
600
800
1000
DNA content
control
0
2
4
6
8
10
12
Time [h]

Figure 4.11 RNMT is predominantly phosphorylated during G2/M phase of the cell cycle.

a) HeLa cells stably expressing HA-RNMT WT were synchronised by a double thymidine block and released into normal growth medium for the indicated time points. Asynchronous HeLa cells expressing HA-RNMT WT or T77A were used as controls. HA-RNMT was immunoprecipitated from 0.6 mg cell extracts using 7μg anti-HA antibody. Immunoprecipitates were resolved by SDS-PAGE and analysed by western blotting to detect Threonine-77 phosphorylated and total RNMT (upper panel). The same cell extracts were analysed by western blotting to detect RNMT, Cyclin B1, phosphorylated Histone 3 Serine-10 (H3 pS10), Cyclin D1 and Tubulin (lower panel).

b) Untransfected HeLa cells were synchronised as above and released into normal growth medium for the indicated time points. RNMT was immunoprecipitated from 0.5 mg extracts using 1.5 μg anti-RNMT antibody. Immunoprecipitations with asynchronous HeLa cells using anti-HA and anti-RNMT antibodies were used as controls.

c) HeLa cells were synchronised as above and released into normal growth medium for the indicated time points. Cells were stained with propidium iodide and cell synchrony was monitored by flow cytometry. DNA content and relative cell numbers are depicted in the diagram.

finally a second peak of cells in G2/M-phase that have two sets of chromosomes but have not yet undergone cytokinesis. The analysis of thymidine-treated cells (0 - 12 hours) confirmed synchronous progression of the cell population from S into G2/M-phase and finally into G1-phase. By comparing this analysis with the western blots it can be concluded that RNMT T77 phosphorylation is first detected when cells leave S-phase and enter G2-phase. The peak of phosphorylation is reached when almost all cells are in G2/M phase and is abruptly lost after cells have completed mitosis and entered G1-phase.

To independently confirm cell cycle-dependent phosphorylation of RNMT during G2/M-phase, cell synchronisation using a nocodazole block was performed. Nocodazole interferes with the polymerisation of microtubules and thus prevents formation of the mitotic spindle (Banfalvi, 2011). The absence of microtubule attachment to kinetochores results in activation of the spindle assembly checkpoint and thus arrest in prometaphase. Initially, cells were treated with thymidine to arrest cells throughout S-phase. After release from the thymidine block cells were allowed to initiate mitosis before the addition of nocodazole arrested the cells in mitosis.

Stably transfected HeLa cells were synchronised with nocodazole and HA-RNMT was immunoprecipitated and analysed by western blot (Figure 4.12a, upper panel). A strong phosphorylation signal was observed in cells arrested in mitosis. When cells were released from the nocodazole block the phosphorylation levels decreased at first but started to accumulate after 10 - 12 hours. Western blot analysis of cell extracts of the corresponding samples confirmed mitotic arrest and subsequent progression into G1 of the synchronised cells (Figure 4.12a, lower panel). Analysis of endogenous RNMT showed the same pattern as exogenous HA-RNMT (Figure 4.12b) confirming high levels of T77 phosphorylation during mitosis and loss of the signal in G1. Lastly, flow cytometry analysis was performed which confirmed synchronous progression of the cell population from mitosis into G1, S and G2/M-phase. At the time points when no

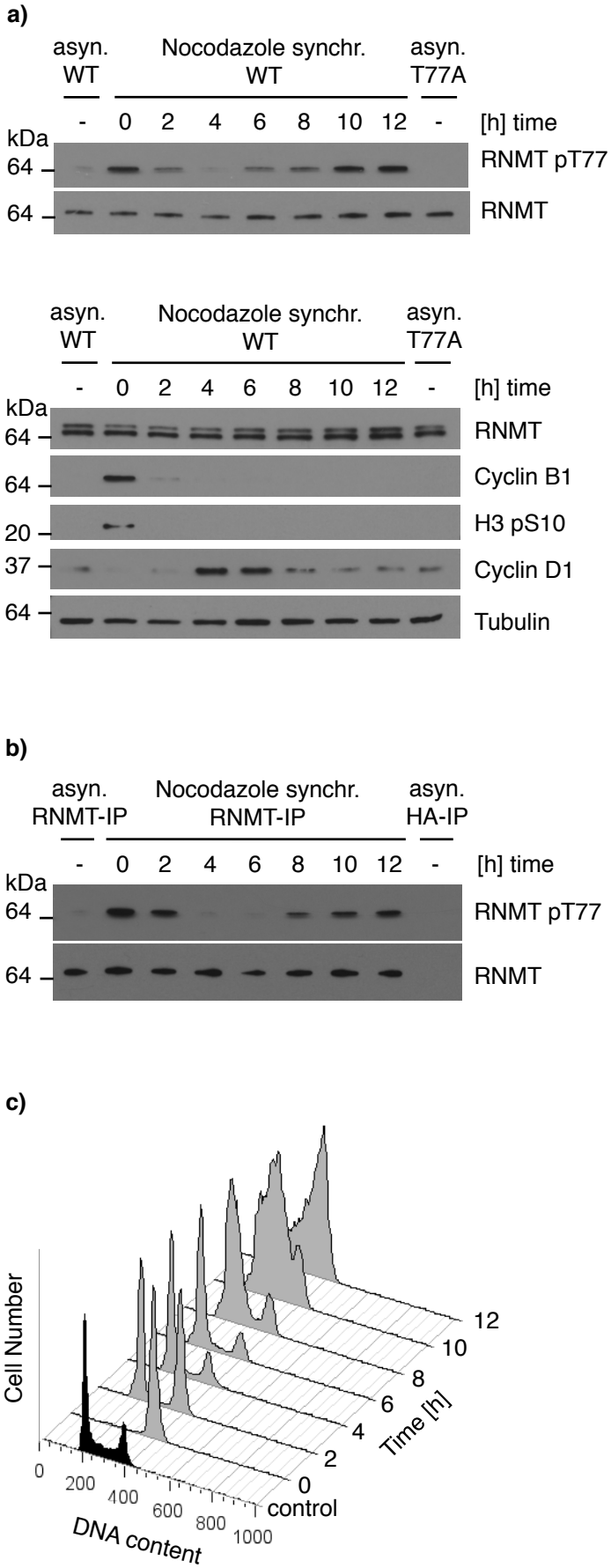
a)
asyn. WT
Nocodazole synchr. WT
asyn. T77A
- 0 2 4 6 8 10 12 -
[h] time
kDa
64
RNMT pT77
64
RNMT
asyn. WT
Nocodazole synchr. WT
asyn. T77A
- 0 2 4 6 8 10 12 -
[h] time
kDa
64
RNMT
64
Cyclin B1
20
H3 pS10
37
Cyclin D1
64
Tubulin
b)
asyn. RNMT-IP
Nocodazole synchr. RNMT-IP
asyn. HA-IP
- 0 2 4 6 8 10 12 -
[h] time
kDa
64
RNMT pT77
64
RNMT
c)
Cell Number
0
200
400
600
800
1000
DNA content
control
0
2
4
6
8
10
12
Time [h]

Figure 4.12 Nocodazole block confirms G2/M-phase specific phosphorylation of RNMT Threonine 77.

a) HeLa cells stably expressing HA-RNMT WT were synchronised by a thymidine block followed by a nocodazole block and released into normal growth medium for the indicated time points. Asynchronous HeLa cells expressing HA-RNMT WT or T77A were used as controls. HA-RNMT was immunoprecipitated from 0.6 mg cell extracts using 7μg anti-HA antibody. Immunoprecipitates were resolved by SDS-PAGE and analysed by western blotting to detect Threonine-77 phosphorylated and total RNMT (upper panel). The same cell extracts were analysed by western blotting to detect RNMT, Cyclin B1, phosphorylated Histone 3 Serine-10 (H3 pS10), Cyclin D1 and Tubulin (lower panel).

b) Untransfected HeLa cells were synchronised as above and released into normal growth medium for the indicated time points. RNMT was immunoprecipitated from 0.5 mg extracts using 1.5 μg anti-RNMT antibody. Immunoprecipitations with asynchronous HeLa cells using anti-HA and anti-RNMT antibodies were used as controls.

c) HeLa cells were synchronised as above and released into normal growth medium for the indicated time points. Cells were stained with propidium iodide and cell synchrony was monitored by flow cytometry. DNA content and relative cell numbers are depicted in the diagram.

phospho-signal was detected by western blots most cells were in G1-phase. The phosphorylation levels started to increase when cells progressed through S-phase and entered G2/M phase.

Overall, the two independent cell synchronisation methods performed demonstrated that RNMT is phosphorylated at T77 in a cell cycle-dependent manner and peaks during G2/M-phase.

4.2.10 *In vitro* phosphorylation of RNMT by CDK1/Cyclin B

CDK1/Cyclin B is the most active CDK in G2/M-phase and is efficiently inhibited by RO-3306 and Roscovitine. Thus, the cell synchronisation experiments showing high RNMT phosphorylation during G2/M-phase, together with the results obtained with kinase inhibitors suggest that RNMT T77 is a substrate of CDK1/Cyclin B. To test whether CDK1/Cyclin can phosphorylate RNMT, *in vitro* phosphorylation experiments were performed. Recombinant RNMT/RAM was incubated with CDK1/Cyclin B and [^{32}P]-ATP, resolved by SDS-PAGE and subjected to autoradiography (Figure 4.13a). As expected, RNMT WT was radioactively labeled whereas RNMT T77A was not. Furthermore, no radioactive signal was detected for RAM (data not shown). This confirms that the RNMT T77 site can be specifically phosphorylated by CDK1/Cyclin B *in vitro*. The same result was obtained when the assays were performed with cold ATP and the phosphorylation status was detected by western blot instead (Figure 4.13b).

Finally, in order to determine the stoichiometry of RNMT phosphorylation by CDK1/Cyclin B, *in vitro* phosphorylation was performed with [^{32}P]-ATP over a time course experiment of 2 hours. RNMT phosphorylation reached saturation of [^{32}P] incorporation after 80 minutes and, considering the specific activity of [^{32}P]-ATP and the radioactive label of RNMT, a maximum stoichiometry of 65% was calculated (Figure 4.13c).

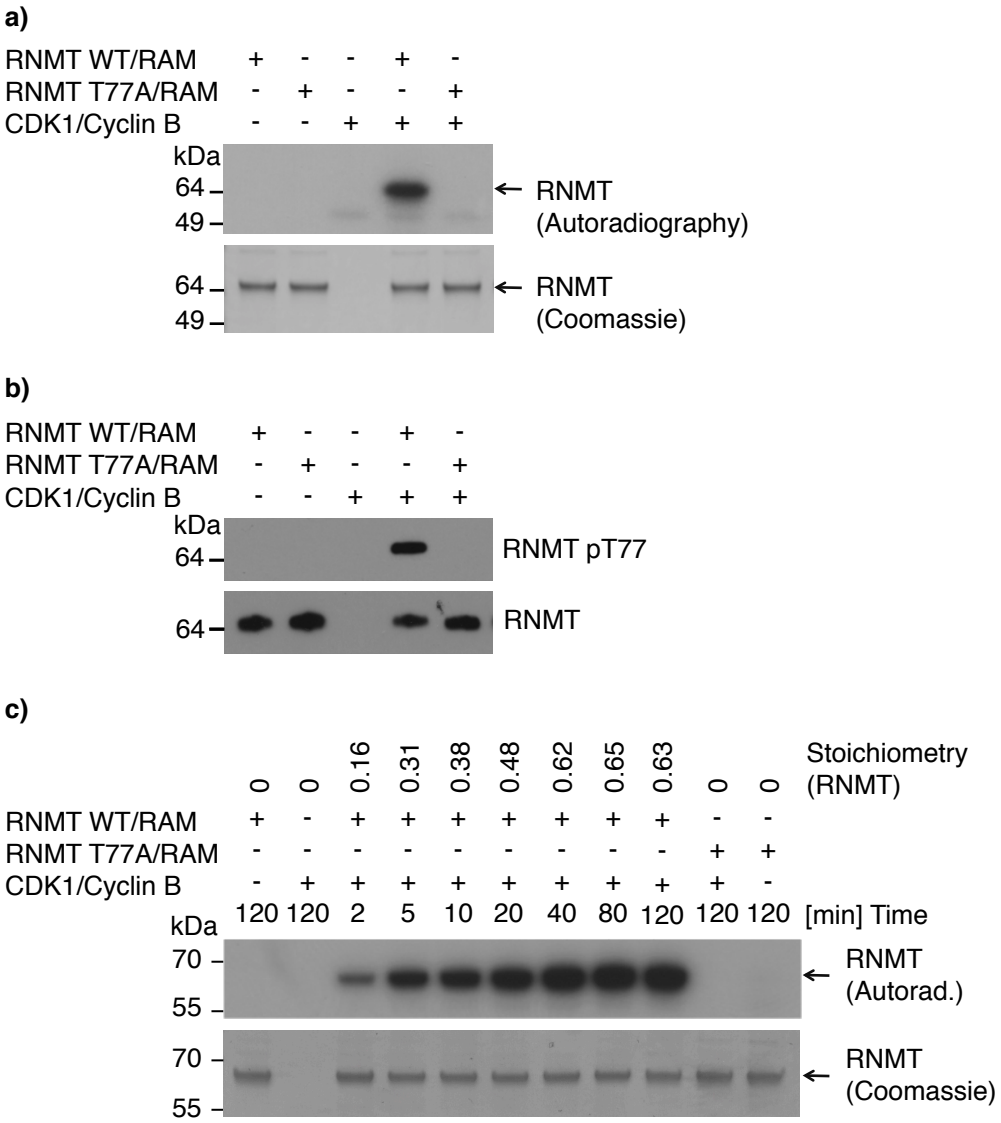

Figure 4.13 RNMT Threonine-77 is phosphorylated by CDK1/Cyclin B *in vitro*.

In vitro phosphorylation of recombinant HIS-RNMT WT or T77A in complex with GST-RAM 1-90 was performed with the kinase complex CDK1/Cyclin B.

a) RNMT/RAM and CDK1/Cyclin B were incubated with [γ-^{32}P]-ATP for 30 min, separated by SDS-PAGE and detected by autoradiography (upper panel) or stained with Coomassie blue (lower panel).

b) RNMT/RAM and CDK1/Cyclin B were incubated with cold ATP for 30 min, separated by SDS-PAGE and western blots were performed to detect Threonine-77 phosphorylated or total RNMT.

c) RNMT/RAM and CDK1/Cyclin B were incubated with radioactive [γ-^{32}P]-ATP for indicated time points, separated by SDS-PAGE and detected by autoradiography (upper panel) or stained with Coomassie blue (lower panel). The stoichiometry of the reaction is indicated on the top.

4.2.11 *In vitro* phosphorylation of RNMT by CDK2/Cyclin A

The peak of RNMT T77 phosphorylation was observed in G2/M phase but lower levels of RNMT phosphorylation were also detected during S-phase. CDK2/Cyclin A is the major kinase controlling progression through S-phase and therefore it was tested whether CDK2/Cyclin A can phosphorylate RNMT *in vitro*. *In vitro* phosphorylation assays were performed with CDK2/Cyclin A as described before for CDK1/Cyclin B. Recombinant RNMT/RAM was incubated with CDK2/Cyclin A and [^{32}P]-ATP, resolved by SDS-PAGE and subjected to autoradiography (Figure 4.14a). RNMT WT exhibited a radioactive signal whereas RNMT T77A did not. Furthermore, incubation of RNMT/RAM with CDK2/Cyclin A in the presence or absence of cold ATP followed by SDS-PAGE and analysis by western blot confirmed the specificity of CDK2/Cyclin A *in vitro* (Figure 4.14b). A phospho-specific signal was only detected when CDK2/Cyclin A was incubated in the presence of ATP with RNMT WT but not with RNMT T77A. Finally, the stoichiometry of RNMT phosphorylation by CDK2/Cyclin A was estimated over a time course of 2 hours and a maximum stoichiometry of 59% was observed after 120 minutes (Figure 4.14c).

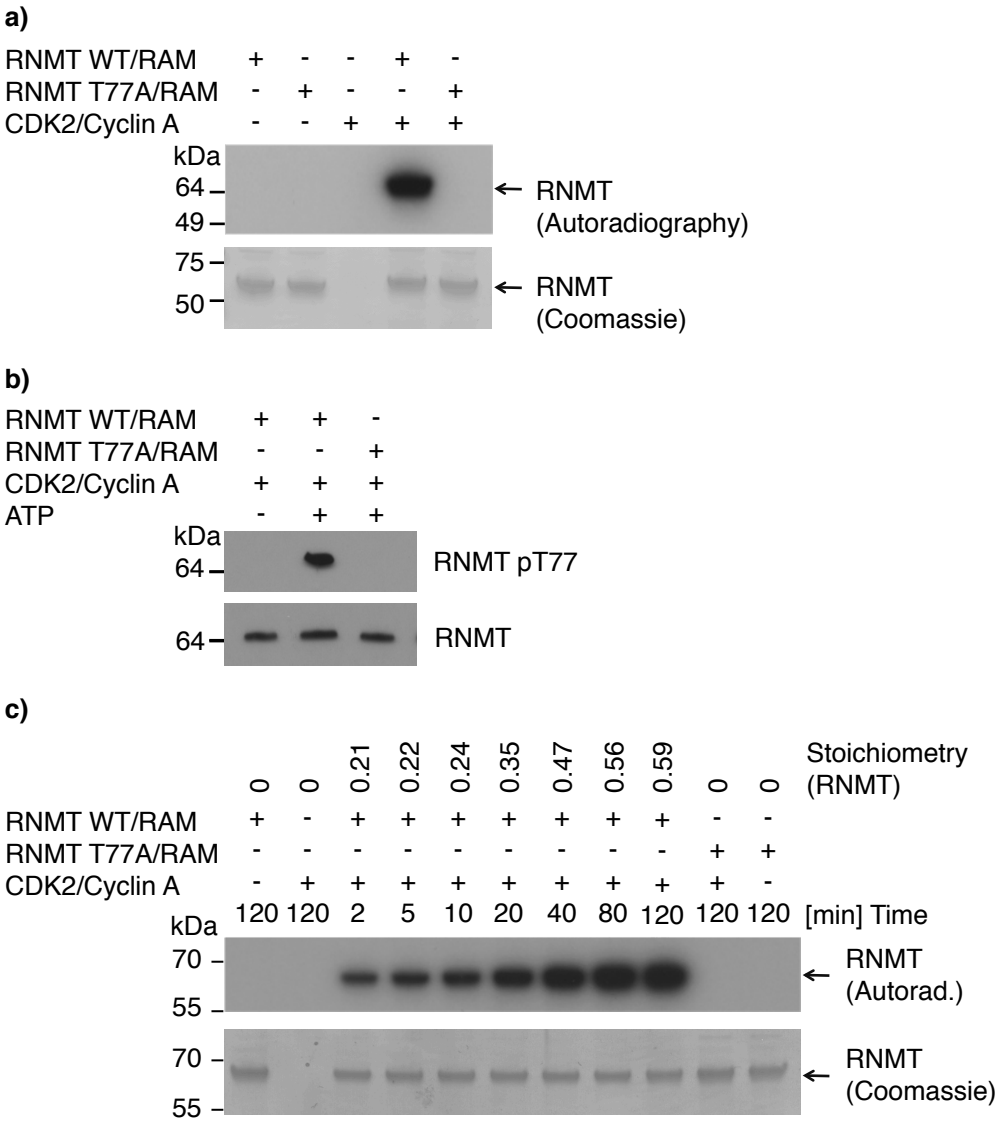

Figure 4.14 RNMT Threonine-77 is phosphorylated by CDK2/Cyclin A *in vitro*.

In vitro phosphorylation of recombinant HIS-RNMT WT or T77A in complex with GST-RAM 1-90 was performed with the kinase complex CDK2/Cyclin A.

a) RNMT/RAM and CDK2/Cyclin A were incubated with [γ-^{32}P]-ATP for 30 min, separated by SDS-PAGE and detected by autoradiography (upper panel) or stained with Coomassie blue (lower panel).

b) RNMT/RAM and CDK2/Cyclin A were incubated with or without cold ATP for 30 min, separated by SDS-PAGE and western blots were performed to detect Threonine-77 phosphorylated or total RNMT.

c) RNMT/RAM and CDK2/Cyclin A were incubated with radioactive [γ-^{32}P]-ATP for indicated time points, separated by SDS-PAGE and detected by autoradiography (upper panel) or stained with Coomassie blue (lower panel). The stoichiometry of the reaction is indicated on the top.

4.3 Discussion

In order to elucidate how the cap methyltransferase is regulated we investigated whether RNMT is post-translationally modified. Initial analysis by 2D gel electrophoresis suggested that RNMT carries several post-translational modifications. Orthophosphate labelling demonstrated that RNMT is phosphorylated and we identified two phosphorylation sites by mass spectrometry. To date no validated RNMT phosphorylation sites have been reported but studies exploiting high-throughput phosphoproteomic analysis have detected several phosphorylation sites in mouse (Hornbeck et al., 2012). Furthermore, high-throughput data from Cell Signalling Technology available on the PhosphoSitePlus resource lists a number of phosphorylation sites identified in human Jurkat cells (Hornbeck et al., 2012). The two phospho-peptides identified in our study have been detected both in mouse and human high-throughput analyses.

Our mass spectrometry analysis suggested that only a small portion of exogenous HA-RNMT is phosphorylated as the phospho-peptides were only detected with highly sensitive mass spectrometers and the overall Mascot scores were not very high. The exact phosphorylation sites could not be determined by mass spectrometry analysis as the phospho-peptide contained several candidate amino acids that could potentially be phosphorylated.

Mutation of candidate phosphorylated amino acids combined with orthophosphate labelling was performed to identify and validate the exact phosphorylation sites. This analysis revealed Threonine-77 as the predominant RNMT phosphorylation site in our experimental system. Mutation of Threonine-77 abolished orthophosphate incorporation whereas mutation of Serine-79 and candidates of the first phosphorylation sites only modestly reduced or did not alter the [^{32}P] signal respectively. Though the RNMT S79A mutation resulted in a reduction of

orthophosphate labelling it is likely that T77 is the major phosphorylation site due to the much higher Mascot score in the mass spectrometry analysis and additional reports of this site by other studies (Hornbeck et al., 2012). Furthermore, T77 resides within a CDK recognition site and T77 but not S79 is predicted to be targeted for Proline-directed phosphorylation by CDKs. Finally, S79 is located immediately next to the T77 phosphorylation site and thus the reduced orthophosphate signal in S79A could have been caused by reduced kinase recruitment to T77.

Due to the location of the RNMT T77 within a CDK consensus motif and next to a cyclin binding site the possibility that this site was recognised by a CDK/Cyclin complex was explored. RNMT T77 phosphorylation was strongly reduced after incubation with compounds inhibiting cell cycle-regulating CDKs and more specifically CDK1/Cyclin B. In addition, cell synchronisation experiments revealed that RNMT phosphorylation is cell cycle-dependent and peaks in G2/M-phase. This data together demonstrates that, in the experimental system used, RNMT T77 is phosphorylated in a cell-cycle dependent manner by CDK1/Cyclin B. *In vitro* kinase experiments demonstrated that CDK1/Cyclin B specifically phosphorylates RNMT at T77. However, the possibility that other CDK/Cyclin complexes active during late S-phase or early G2-phase may also contribute to RNMT phosphorylation cannot be excluded. For example, CDK2/Cyclin A2, which is expressed during S-phase was also able to specifically phosphorylate RNMT T77 *in vitro* and the stoichiometry of RNMT phosphorylation reached similar values as observed with CDK1/Cyclin B.

Chapter 5:

RNMT Threonine-77 phosphorylation activates cap methyltransferase activity and negatively regulates the interaction of RNMT with KPNA2

5.1 Introduction

In mammalian cells RNMT exists in a complex with a 14 kDa protein termed RNMT activating miniprotein (RAM) (Gonatopoulos-Pournatzis et al., 2011). In addition to RAM, a second RNMT-binding protein has been identified; Wen and Shatkin (2000) demonstrated that KPNA2 directly binds to RNMT both *in vitro* and *in vivo*. KPNA2 is a member of the Importin-α family that together with Importin-β mediates nuclear import of protein cargos carrying a classical nuclear localisation signal (NLS). KPNA2 was described to bind to the N-terminal region of RNMT, which contains three NLSs. KPNA2 was also demonstrated to bind to RNA and to activate cap methyltransferase activity *in vitro* by increasing RNMT-binding to capped RNA. The interaction partner of KPNA2, Importin-β, did not inhibit KPNA2-RNMT complex formation but it disrupted KPNA2-RNMT-RNA complexes and blocked the stimulatory effect of KPNA2 on RNMT (Wen and Shatkin, 2000).

As discussed above, RNMT activity can be regulated by an interaction with RAM and KPNA2. Furthermore, it is possible that cap methyltransferase activity is regulated by RNMT phosphorylation. The addition of a negatively charged phosphate group often causes conformational changes in the protein, which can be caused by electrostatic attraction or repulsion between the phospho group and charged amino acids. This in

turn can alter the catalytic properties of the enzyme or affect the interaction with other proteins. Hence, this chapter aims to elucidate whether RNMT phosphorylation regulates cap methyltransferase activity or protein-protein interactions.

5.2 Results

5.2.1 Investigation of the effect of RNMT Threonine-77 phosphorylation on cellular RNMT activity

To address whether RNMT T77 phosphorylation could regulate cellular RNMT activity, cap methyltransferase activity assays were performed with HA-RNMT constructs immunoprecipitated from stably expressed HeLa cells (Figure 5.1a). RNMT T77A exhibited reduced activity suggesting that loss of phosphorylation reduces cellular RNMT activity. The drop in activity was only about 25 % but these experiments were performed with non-synchronised cells and thus, only a minor portion of wild type RNMT was expected to be in G2/M-phase and hence to be phosphorylated. To mimic constitutive phosphorylation Threonine-77 was replaced with Aspartate (D). Unlike the loss of phosphorylation mutant RNMT T77A, the phosphorylation-mimicking mutant RNMT T77D did not show any change in activity compared to RNMT WT.

To increase the phosphorylated portion of RNMT, cap methyltransferase assays were performed with synchronised cell extracts. Cells were arrested in S-phase using a double thymidine block and subsequently released into the cell cycle for 8 hours. According to previous results, cells are in G2/M-phase at this time point and show maximal phosphorylation levels. Cell extracts in G2/M-phase (T8) exhibited increased cap methyltransferase activity compared to cells arrested in S-phase (T0) (Figure 5.1b). This increase was prevented by incubation with the CDK-inhibitors Roscovitine and RO-3306. Together, these experiments suggest that phosphorylation of RNMT T77 increases cellular RNMT activity. However, whether the activation is directly caused by the phosphorylation itself, for example via a conformational change, or whether it is mediated via interaction with other proteins is not known. Furthermore, the exact stoichiometry of RNMT T77 phosphorylation during G2/M-phase is unknown and thus it is not clear to what extent RNMT is activated by phosphorylation.

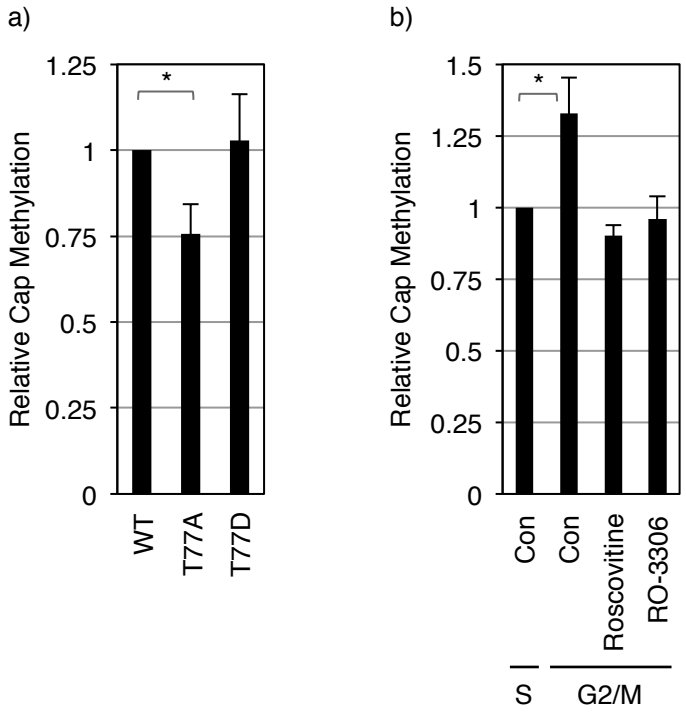

Figure 5.1: Loss of Threonine-77 phosphorylation reduces cellular RNMT activity.

a) Cellular HA-RNMT was immunoprecipitated from 100 µg cell extracts HeLa cells stably expressing HA-RNMT WT, T77A or T77D using 1 µg anti-HA antibody and cap methyltransferase assays were performed for 5 min with the immunoprecipitates. Charts depict the average and standard deviation of three independent experiments. Samples were normalised to RNMT WT. T-test p-value <0.05 is indicated by an asterisk.

b) HeLa cells were synchronised by a double thymidine block and released into normal growth medium for 0 hour (S) or 8 hours (G2/M). Cells released for 8 hours were treated with 50 µM Roscovitine or 9 µM RO-3306 for 15 minutes prior to lysing. Cap methyltransferase assays were performed with 2 µg of cell extracts for 10 minutes. The activity normalised to T0 control is depicted for the average and standard deviation of four independent experiments. T-test p-value <0.05 is indicated by asterisk.

5.2.2 Analysis of RNMT activity after *in vitro* phosphorylation

In order to elucidate and quantify whether T77 phosphorylation directly activates RNMT activity, methyltransferase activity assays were performed with recombinant RNMT/RAM after *in vitro* phosphorylation. RNMT/RAM was incubated in the presence or absence of CDK1/Cyclin B and ATP, affinity purified and washed before activity assays were performed (Figure 5.2a). Incubation of RNMT with CDK1/Cyclin B or ATP alone did not alter basal cap methyltransferase activity of unphosphorylated RNMT. However, when RNMT was incubated with both CDK1/Cyclin B and ATP, a 35 - 45 % increase in activity was observed. The stoichiometry of RNMT T77 phosphorylation after 30 minutes under the conditions used in this experiment was determined as 40 % (Figure 5.2b). Therefore, these experiments suggest that RNMT T77 phosphorylation increases the cap methyltransferase activity of RNMT/RAM by two-fold in the *in vitro* assay.

5.2.3 Investigation of phosphorylation-dependent protein interactions

Next, the possibility that RNMT T77 phosphorylation may influence RNMT protein interactions was explored. To test this hypothesis peptide affinity purification with unphosphorylated and phosphorylated RNMT peptides containing the T77 site were performed. Biotinylated peptides of 35 amino acids in length were incubated with HeLa cell extracts and affinity purified. Precipitated protein was resolved by SDS-PAGE and stained with Coomassie blue (Figure 5.3a, left panel). Two bands of around 130 and 80 kDa in size were enriched in pull-downs with unphosphorylated peptides and were further investigated as proteins that interact with RNMT in a phosphorylation-dependent manner. The candidate gel bands from the unphosphorylated T77 peptide pull-down and the corresponding bands form the phosphorylated T77 peptide pull-

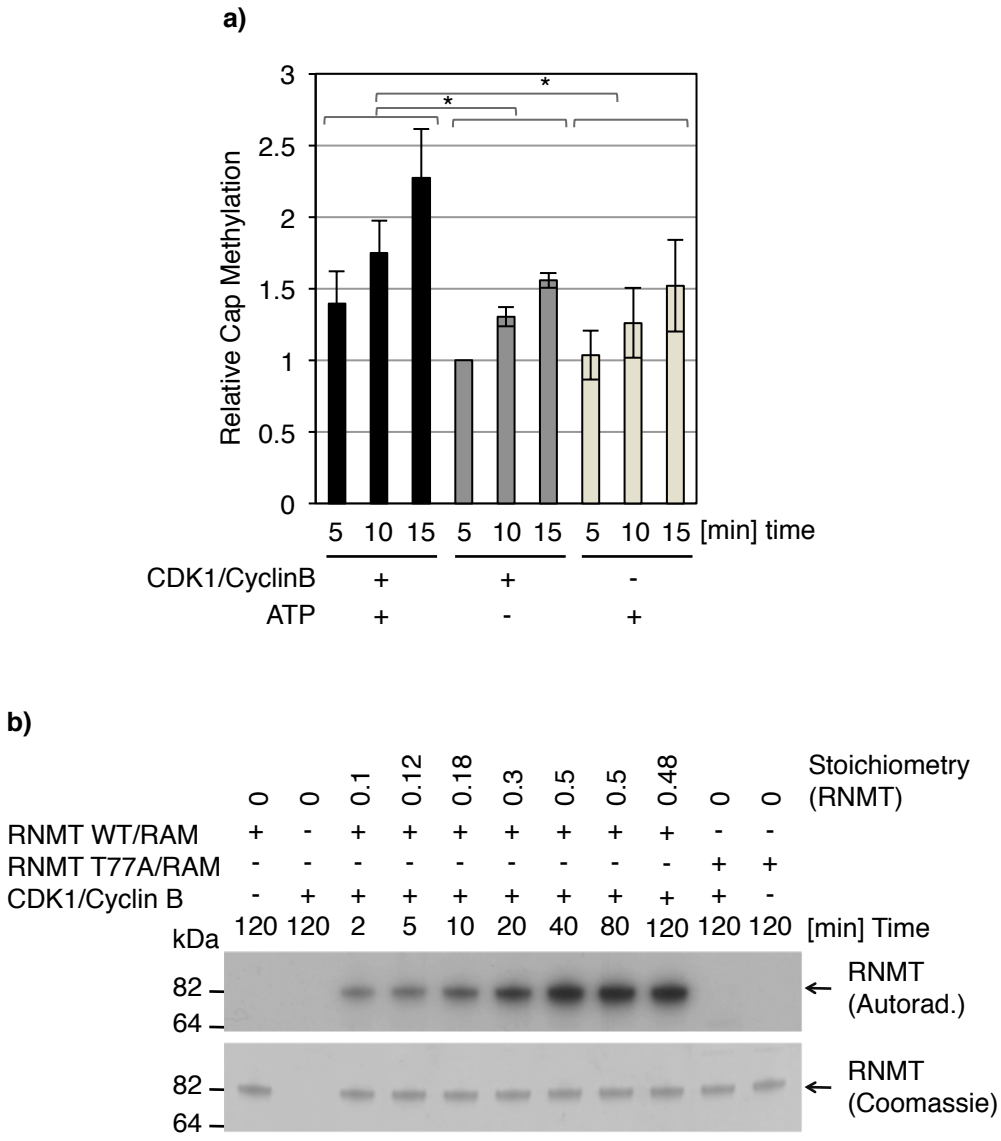

Figure 5.2: Phosphorylation of RNMT Threonine-77 increases RNMT activity.
a) 900 ng recombinant purified His-RNMT/GST-RAM 1-90 was incubated in the presence or absence of 10 ng CDK1/Cyclin B and 100 µM ATP. After *in vitro* phosphorylation, His-RNMT/GST-RAM 1-90 was affinity purified using glutathione sepharose and 3.33 % of purified RNMT was assessed in a cap methyltransferase assay for the time points indicated. Charts depict the average and standard deviation of three independent experiments performed in triplicate. T-test p-value <0.05 is indicated with an asterisk.
b) RNMT/RAM and CDK1/Cyclin B were incubated with radioactive [^{32}P]-ATP for the indicated time points, separated by SDS-PAGE and detected to autoradiography (upper panel) or stained with Coomassie blue (lower panel). The stoichiometry of the reaction is indicated above.

a)

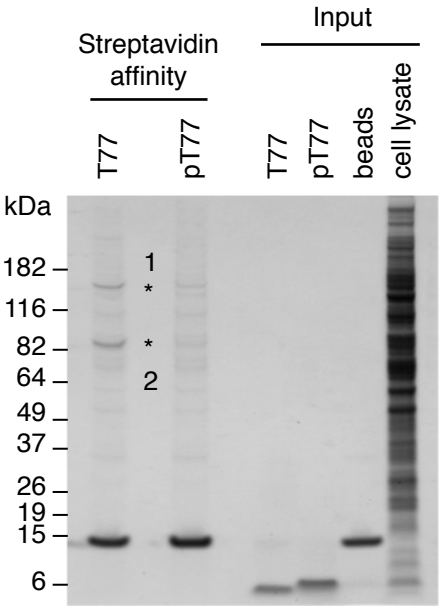

	Proteins enriched with T77 peptide	Score T77	Score pT77
1 *	Importin Subunit Beta-1 (KPNB1)	6623	2999
	Nuclear pore complex protein 153 (NUP153)	726	34
* 2	Importin Subunit Alpha-2 (KPNA2)	4414	2732
	Importin Subunit Alpha-3 (KPNA3)	667	105
	Importin Subunit Alpha-4 (KPNA4)	959	144

Figure 5.3: KPNA2 preferentially binds to unphosphorylated RNMT Threonine-77 peptide.

a) 10 mg of HeLa cell extracts were incubated with 3 µg of biotinylated RNMT peptides containing either unphosphorylated (T77) or phosphorylated (pT77) Threonine-77. The peptides were affinity purified using streptavidin beads and the bound proteins were separated by SDS-PAGE and stained with Coomassie blue (left panel). The gel bands marked with an asterisk were excised and proteins identified by mass spectrometry analysis. The most abundant proteins enriched in the T77 peptide pull-down are listed with their Mascot score (right panel).

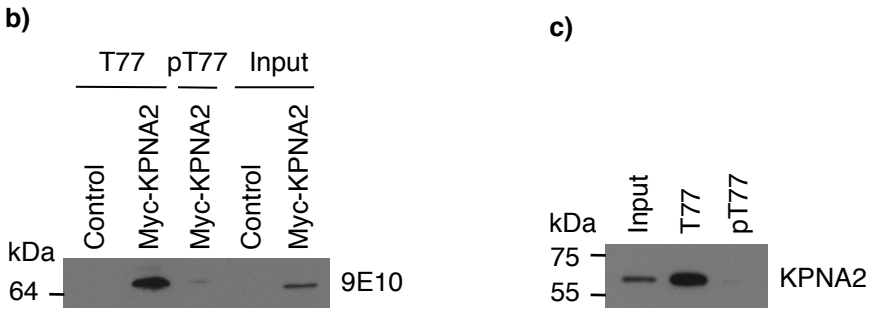

Figure 5.3: KPNA2 preferentially binds unphosphorylated RNMT Threonine-77 peptide.

b) HeLa cells were transiently transfected with pcDNA5 Myc-KPNA2 or vector control. 2.2 mg of cell extracts were incubated with 1 µg of biotinylated RNMT T77 or pT77 peptides and affinity purified using streptavidin beads. Bound proteins were separated by SDS-PAGE and western blot was performed to detect exogenous Myc-KPNA2 using anti-9E10 antibodies.

c) 3 mg of HeLa cell extracts were incubated with 1.5 µg of biotinylated RNMT T77 or pT77 peptides and affinity purified using streptavidin beads. Bound proteins were separated by SDS-PAGE and western blot was performed to detect endogenous KPNA2 using KPNA2-antibodies.

down were extracted and proteins identified by mass spectrometry. In the upper gel band two proteins were detected to be enriched with the unphosphorylated T77 peptide: Importin-β (Importin Subunit Beta-1, KPNB1) and the nuclear pore complex protein 153 (NUP153) (Figure 5.3a, right panel). The Mascot score of NUP153 was much lower than that of Importin-β. In the lower gel band three proteins were identified to be enriched with the unphosphorylated T77 peptide: Importin Subunit Alpha-2 (KPNA2), Importin Subunit Alpha-3 (KPNA3) and Importin Subunit Alpha-4 (KPNA4). The protein with the highest Mascot score was KPNA2. All identified proteins are part of the classical nuclear protein import machinery, which recognizes nuclear localisation signals (NLS). There is a NLS immediately adjacent to the RNMT T77 and hence it was not completely surprising that parts of the nuclear import machinery were purified with the peptides. However, the fact that these proteins expressed differential affinity to unphosphorylated and phosphorylated RNMT peptides raises the possibility that RNMT T77 phosphorylation regulates the interaction with the nuclear import machinery.

It is well established that the KPNA protein family interacts with KPNB1 and binding of both KPNA2 and KPNB1 to NUP153 was reported (Moroianu et al., 1997; Shah et al., 1998). Of the proteins identified in the peptide pull-downs only KPNA2 was previously described to directly interact with RNMT (Wen and Shatkin, 2000). Due to these previous reports further investigation focused on KPNA2. Peptide affinity purification was repeated with HeLa cells transfected with Myc-tagged KPNA2. Precipitates were analysed by western blot to detect exogenous Myc-KPNA2 using anti-9E10 antibody, which recognises the Myc-tag (Figure 5.3b). Myc-KPNA2 was strongly enriched in the unphosphorylated T77 peptide pull-down and only a very weak signal was detected with phosphorylated T77 peptide. The experiment was repeated with untransfected cells and endogenous KPNA2 was strongly enriched in the unphosphorylated peptide pull-down compared to the phosphorylated peptide pull-down confirming the mass spectrometry result (Figure 5.3c).

5.2.4 Characterisation of RNMT interaction with KPNA2

To confirm that the KPNA2-interaction occurs with full-length RNMT, HeLa cells were transfected with pcDNA5 Myc-KPNA2 and immunoprecipitations were performed with anti-RNMT, anti-9E10 and control antibodies (Figure 5.4a, for untransfected control 9E10-IP see 5.4c). Immunoprecipitation of Myc-tagged KPNA2 resulted in the co-purification of RNMT. However, Myc-KPNA2 was not detected when RNMT was immunoprecipitated. The co-immunoprecipitation experiments were repeated with untransfected HeLa cells and endogenous protein was detected by western blot (Figure 5.4b). Endogenous KPNA2 immunoprecipitation resulted in co-purification of RNMT but KPNA2 was not detected in RNMT immunoprecipitates.

In order to test whether the interaction observed between RNMT and KPNA2 is dependent on the phosphorylation status of RNMT, HeLa cells stably expressing HA-RNMT WT, HA-RNMT T77A, HA-RNMT T77D or vector control were transfected with Myc-KPNA2. Exogenous KPNA2 was immunoprecipitated and the interaction with the RNMT constructs detected by western blot (Figure 5.4c). As observed with endogenous RNMT, HA-RNMT co-immunoprecipitated with Myc-KPNA2. A much stronger interaction was detected with the unphosphorylated HA-RNMT T77A. In contrast, the signal for the phospho-mimicking mutant HA-RNMT T77D was very weak in the Myc-KPNA2 immunoprecipitates. This suggests that the interaction with KPNA2 is reduced when RNMT T77 is phosphorylated.

The experiments were repeated using anti-KPNA2 antibodies to immunoprecipitate endogenous KPNA2 (Figure 5.4d). As with exogenous KPNA2 immunoprecipitation of endogenous KPNA2 resulted in the co-immunoprecipitation of RNMT WT and T77A but a much lower signal of RNMT T77D was observed (see top band of RNMT western blots in Figure 5.4d). Together, co-immunoprecipitation of KPNA2 confirmed the interaction with RNMT and furthermore, demonstrated a strong preference of KPNA2 binding to unphosphorylated RNMT T77.

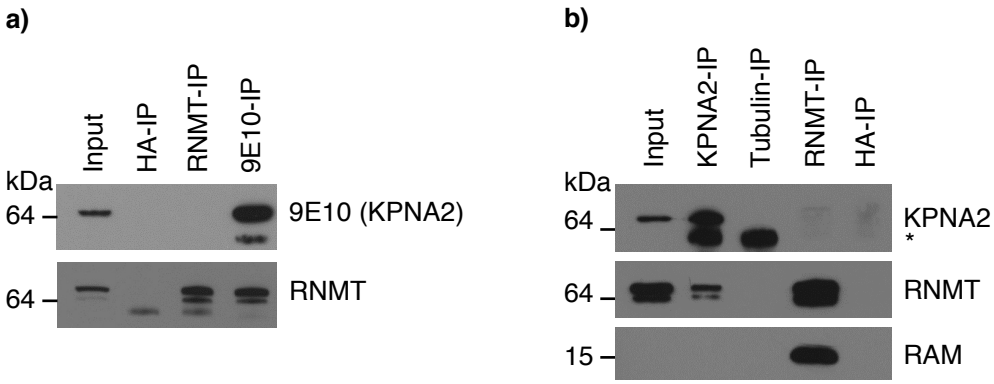

Figure 5.4: KPNA2 preferentially interacts with RNMT T77A.

a) HeLa cells were transiently transfected with pcDNA5 Myc-KPNA2. RNMT and Myc-KPNA2 were immunoprecipitated from 1.5 mg of cell extract using 1.5 µg anti-RNMT and anti-9E10 antibodies respectively. Immunoprecipitation with anti-HA antibody was used as a control. Immunoprecipitates were separated by SDS-PAGE and western blots were performed to detect Myc-KPNA2 and RNMT.

b) KPNA2 and RNMT was immunoprecipitated from 1.5 mg of untransfected HeLa cell extracts with 1.5 µg anti-KPNA2 or anti-RNMT antibodies respectively. Immunoprecipitations with anti-Tubulin or anti-HA antibodies were used as a control. Immunoprecipitates were separated by SDS-PAGE and western blots were performed to detect KPNA2, RNMT and RAM. Nonspecific bands are indicated with an asterisk.

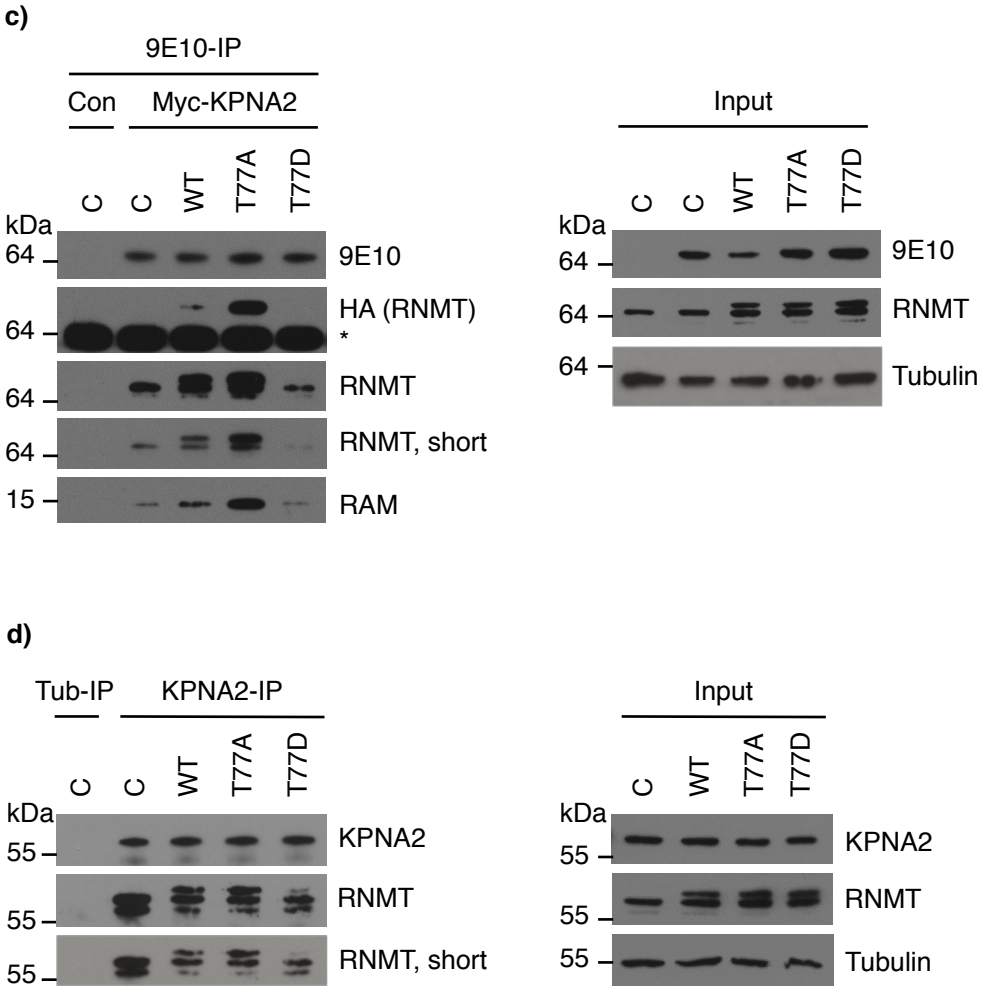

Figure 5.4: KPNA2 preferentially interacts with RNMT T77A.

c) HeLa cells stably expressing HA-RNMT WT, T77A, T77D or a vector control (C) were transiently transfected with pcDNA5 Myc-KPNA2 or vector control (Con). Myc-KPNA2 was immunoprecipitated from 1.5 mg of cell extract using 1.5 µg anti-9E10 antibodies. Immunoprecipitates were separated by SDS-PAGE and western blots were performed to detect Myc-KPNA2, HA-RNMT, RNMT and RAM (left panel). The same extracts were analysed by western blotting to detect Myc-KPNA2, RNMT and Tubulin (right panel). Nonspecific bands are indicated with an asterisk.

d) KPNA2 was immunoprecipitated from 1.5 mg of extracts from HeLa cells stably expressing HA-RNMT WT, T77A, T77D or a vector control (C) using 1.5 µg anti-KPNA2 antibodies. Immunoprecipitates were separated by SDS-PAGE and western blots were performed to detect KPNA2 and RNMT. The same extracts were analysed by western blotting to detect KPNA2, RNMT and Tubulin (right panel).

5.2.5 Analysis of RNMT-KPNA2 interaction during the cell cycle

As KPNA2 was demonstrated to preferentially interact with unphosphorylated RNMT, this association was monitored throughout the phases of the cell cycle when RNMT phosphorylation changes. HeLa cells were transfected with Myc-KPNA2 and synchronised using a double thymidine block. Cells were released into the cell cycle and harvested after 2 hours when cells were in S-phase and RNMT T77 exhibited low phosphorylation or released for 8 hours when cells were in G2/M-phase and RNMT T77 exhibited high phosphorylation. Myc-KPNA2 was immunoprecipitated from extracts at different stages of the cell cycle and binding to endogenous RNMT was detected by western blot (Figure 5.5a). As expected, a weaker interaction between KPNA2 and RNMT was observed during G2/M-phase compared to S-phase. Interestingly, inhibiting CDK1/Cyclin B by treatment with RO-3306 increased the binding of RNMT to KPNA2 during G2/M-phase. This suggests that the interaction during G2/M-phase is interrupted by RNMT T77 phosphorylation.

A similar experiment was repeated with untransfected cells (Figure 5.5b). Again, reduced association of RNMT with KPNA2 during G2/M-phase was observed, which could be increased by treatment with the compounds RO-3306 or Roscovitine.

5.2.6 Affinity purification of recombinant RNMT and KPNA2

In order to test whether the interaction between RNMT and KPNA2 is direct, affinity purifications with recombinant proteins were performed. Untagged RNMT was specifically co-purified with GST-KPNA2 but not with GST (Figure 5.6a). A specific interaction was also observed when KPNA2 was co-purified with GST-RNMT (Figure 5.6b). This result confirms the previous report of a direct association between RNMT and KPNA2 performed with *in vitro* translated protein (Wen and Shatkin, 2000).

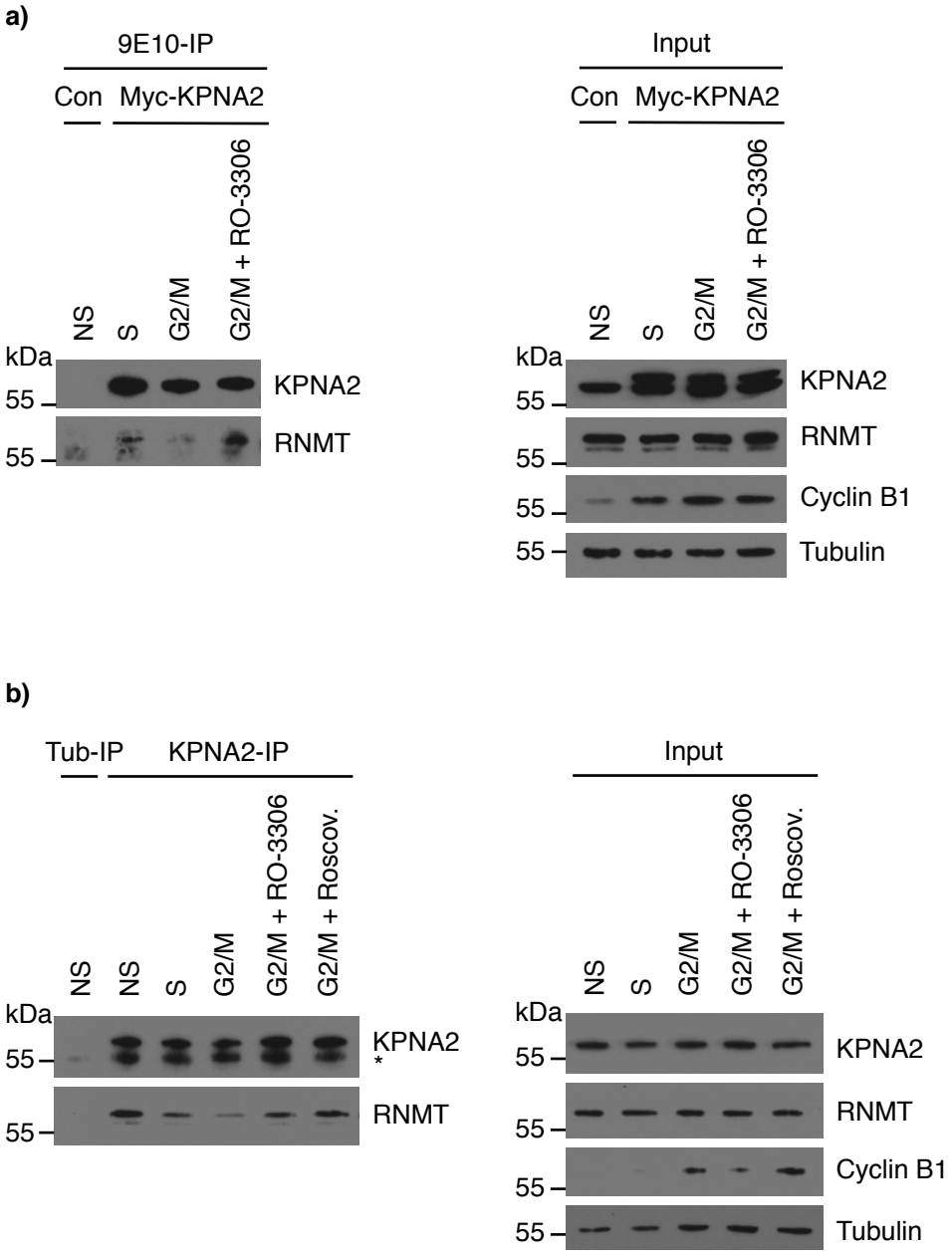
a)
9E10-IP
Con
Myc-KPNA2
NS
S
G2/M
G2/M + RO-3306
kDa
55
KPNA2
55
RNMT
Input
Con
Myc-KPNA2
NS
S
G2/M
G2/M + RO-3306
kDa
55
KPNA2
55
RNMT
55
Cyclin B1
55
Tubulin
b)
Tub-IP
KPNA2-IP
NS
NS
S
G2/M
G2/M + RO-3306
G2/M + Roscov.
kDa
55
KPNA2
*
55
RNMT
Input
NS
S
G2/M
G2/M + RO-3306
G2/M + Roscov.
kDa
55
KPNA2
55
RNMT
55
Cyclin B1
55
Tubulin

Figure 5.5: KPNA2-RNMT interaction is reduced in G2/M phase but can be rescued using CDK1 inhibitors.

a) HeLa cells were transiently transfected with pcDNA5 Myc-KPNA2. Cells were synchronised using a double-thymidine block and released into normal growth media for 2 (S) or 8 hours (G2/M) and incubated with 9 μM RO-3306 for 15 minutes (G2/M + RO-3306). Nonsynchronous (NS) vector control (Con) transfected cells were used as a control. Myc-KPNA2 was immunoprecipitated from 1.5 mg of cell extract using 1.5 μg anti-9E10 antibodies. Immunoprecipitates were separated by SDS-PAGE and western blots were performed to detect KPNA2 and RNMT (left panel). The same extracts were analysed by western blotting to detect KPNA2, RNMT, Cyclin B1 and Tubulin (right panel).

b) Untransfected HeLa cells were synchronised using a double-thymidine block and released into normal growth media for 2 (S) or 8 hours (G2/M) and incubated with 9 μM RO-3306 (G2/M + RO-3306) or 50 μM Roscovitine (G2/M + Roscov.) for 15 minutes. KPNA2 was immunoprecipitated from 1.5 mg of cell extracts from untransfected HeLa cells using 1.5 μg anti-KPNA2 antibodies. Immunoprecipitations with nonsynchronous cells (NS) using anti-Tubulin (Tub) and anti-KPNA2 antibodies were used as a control. Immunoprecipitates were separated by SDS-PAGE and western blots were performed to detect KPNA2 and RNMT (left panel). The same extracts were analysed by western blotting to detect KPNA2, RNMT, Cyclin B1 and Tubulin (right panel). Nonspecific bands are indicated with an asterisk.

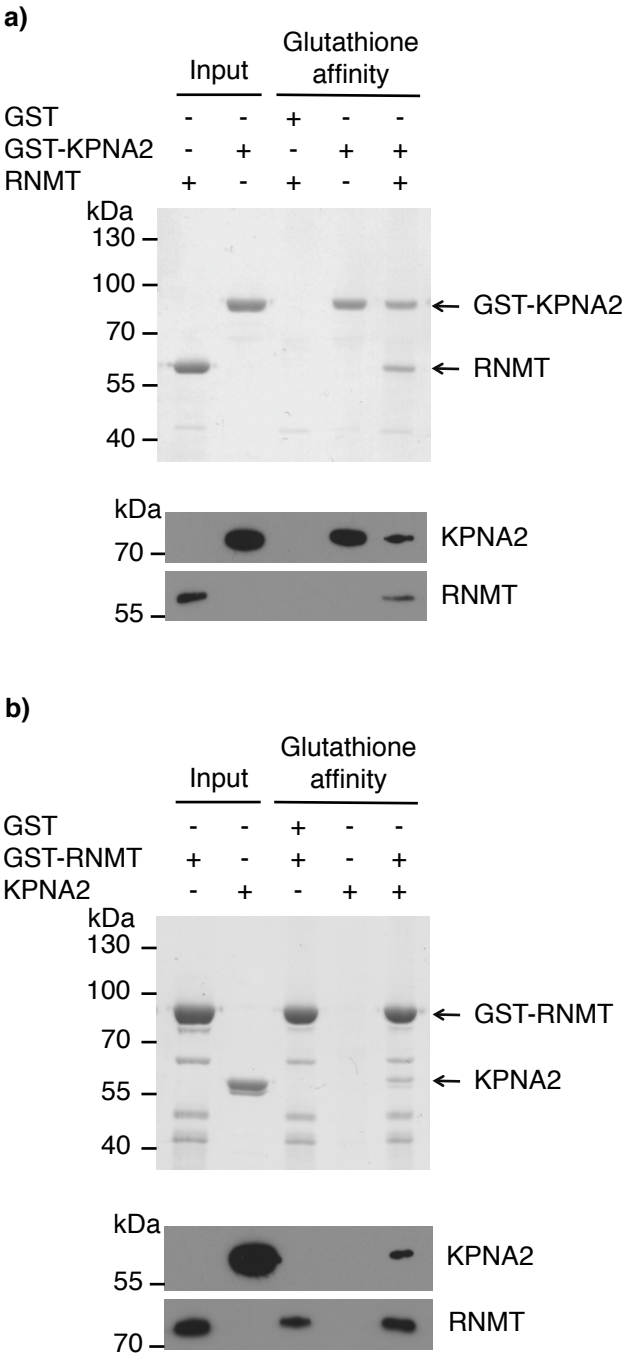

Figure 5.6: KPNA2 and RNMT interact directly.

a) 2 µg of purified recombinant GST-KPNA2 was incubated with purified recombinant RNMT and affinity purified with glutathione-sepharose. Proteins eluted were resolved by SDS-PAGE and stained by Coomassie blue (upper panel) or analysed by western blot to detect KPNA2 and RNMT (lower panel). GST-KPNA2 and RNMT are indicated in the upper panel.

b) As above but 2 µg of purified recombinant GST-RNMT was incubated with purified recombinant KPNA2 and affinity purified with glutathione-sepharose.

5.2.7 *In vitro* cap methyltransferase assays with RNMT and KPNA2

In addition to the direct interaction between RNMT and KPNA2, Wen and Shatkin (2000) also reported that KPNA2 enhanced RNMT binding to capped RNA and stimulated cap methyltransferase activity. Therefore, activity assays were performed to confirm this result and to investigate how KPNA2 might modify the activity of phosphorylated RNMT.

In vitro cap methyltransferase assays were performed with recombinant RNMT and a titration of recombinant KPNA2 or BSA (Figure 5.7). Addition of BSA only had a subtle effect and increasing the molar ratio did not alter RNMT activity. However, increasing the molar ratio of KPNA2:RNMT strongly inhibited RNMT activity. Whereas an equal amount of RNMT and KPNA2 did not affect RNMT activity, a five-fold excess of KPNA2 decreased the activity by over 50 % and a ten-fold excess of KPNA2 led to a reduction of RNMT activity by 90 %. This result was unexpected and contradicts the previous study reporting that KPNA2 activates RNMT with an increasing molar ratio (Wen and Shatkin, 2000).

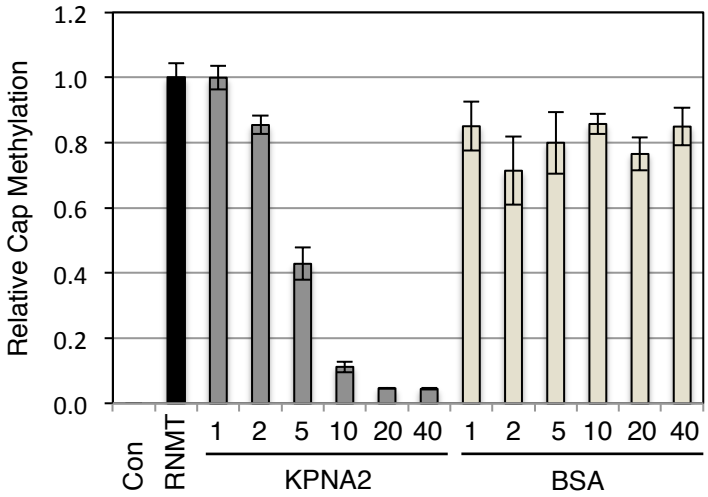

Figure 5.7: KPNA2 inhibits RNMT activity.

Cap methyltransferase assays were performed using 40 nM of purified recombinant RNMT and a titration of purified recombinant KPNA2 or BSA. The molar ratio of KPNA2:RNMT is indicated in the diagram. Charts depict the average and standard deviation of three experiments.

5.3 Discussion

In order to elucidate the function of RNMT T77 phosphorylation initial experiments were performed to determine whether it regulates cap methyltransferase activity. Immunoprecipitation of cellular HA-RNMT demonstrated that loss of phosphorylation reduces RNMT activity. The reduction in RNMT T77A is relatively small but it should be considered that this experiment was performed with nonsynchronous cells and thus only a small portion of RNMT WT was actually phosphorylated. Interestingly, the T77D phospho-mimicking mutant was more active than the T77A mutant but did not show an increase in activity compared to wild type protein. Thus, T77D mutation might not fully represent the properties of phosphorylated T77.

Performing activity assays with synchronised cell extracts also suggested that phosphorylation of RNMT increases cap methyltransferase activity. G2/M-phase extracts showed increased activity compared to S-phase extracts and this increase could be blocked with CDK inhibitors. The activation in G2/M-phase was minor but despite observing maximal phosphorylation levels in G2/M-phase it is unknown what proportion of total RNMT is phosphorylated during that stage of the cell cycle.

To test whether phosphorylation of T77 activates RNMT directly and to quantify a change in activity we performed *in vitro* phosphorylation assays before assessing RNMT activity. These experiments demonstrated that T77 phosphorylation activates RNMT directly by two-fold. It should be mentioned that this analysis was performed with RNMT/RAM complexes and RAM itself activates RNMT five-fold (Gonatopoulos-Pournatzis et al., 2011). Thus, the phosphorylation-mediated increase in activity represents a further increase by two-fold. Further investigation is required to determine the mechanism of this activation. The RNMT-RAM interaction does not seem to be affected by T77 phosphorylation (data not shown) but it is possible that the phosphorylation causes a conformational change of the N-terminus. Crystal structures

from human and fungal RNMT are only available for the catalytic domain (Fabrega et al., 2003; Wu et al., 2007; Zeng et al., 2008) and thus there is no information about the orientation of the N-terminal domain.

In addition to assessing the influence of T77 phosphorylation on RNMT activity the ability of RNMT phosphorylation to regulate interactions with other proteins was investigated. As expected, the interaction of RNMT with RAM was not affected by RNMT T77 phosphorylation (data not shown) since RAM directly binds to the catalytic domain of RNMT (Gonatopoulos-Pournatzis et al., 2011). However, affinity purification with phosphorylated or unphosphorylated RNMT T77 peptides revealed that phosphorylation reduces an interaction with the nuclear import machinery. Mass spectrometry analysis identified Importin-β (Importin Subunit Beta-1, KPNB1) and KPNA2 (Importin Subunit Alpha-2) as the most abundant proteins enriched with unphosphorylated T77 peptides. Both proteins are part of the classical nuclear protein import pathway in which cargos carrying classical NLSs are bound by Importin-α that serves as an adaptor between the cargo and Importin-β. Importin-β then mediates translocation through the nuclear pore complex. In the nucleus Importin-β dissociates from Importin-α and the cargo is then released from Importin-α. Since Importin-α is the component that directly binds the cargo and an interaction between KPNA2 and RNMT has been previously reported (Wen and Shatkin, 2000) we aimed to further characterise this interaction. Co-immunoprecipitation experiments confirmed a specific interaction with RNMT. However, the interaction between RNMT and KPNA2 could only be detected after immunoprecipitation of KPNA2 but not *vice versa*. Since it is possible that the antibody used for immunoprecipitation of RNMT could interrupt the association with KPNA2 we used both antibodies against the HA-tag or against RNMT itself but no KPNA2 was detected after RNMT immunoprecipitation with either antibody. However, a direct interaction was confirmed with both KPNA2 and RNMT affinity purifications using recombinant RNMT and KPNA2. Furthermore, the interaction of cellular KPNA2 with

RNMT was found to be negatively regulated by T77 phosphorylation. This result was observed with both endogenous and exogenous protein.

Wen and Shatkin (2000) mapped the RNMT and KPNA2 interaction domains using truncation mutants and reported that KPNA2 binds to RNMT between amino acid 96-144. In contrast, our analysis suggests that the major KPNA2-binding site is located further towards the N-terminus. However, since RNMT contains three NLS it is likely that KPNA2 can bind RNMT at more than one site. However, although the data is not shown, Wen and Shatkin (2000) reported that KPNA2 interacts with RNMT via its C-terminal domain and not via its NLS-binding domain. To the contrary, our data shows that phosphorylation of RNMT T77 located next to a NLS disrupts the interaction with KPNA2 and thus indicates an NLS-directed interaction.

Furthermore, KPNA2 was reported to increase RNMT-binding to GpppG-RNA and to increase cap methyltransferase activity (Wen and Shatkin, 2000). Thus, we tested whether activation of RNMT by KPNA2 can be confirmed and whether phosphorylation would abolish this effect. Unexpectedly, it was found that KPNA2 reduces RNMT activity, which contradicts the data shown by Wen and Shatkin. The exact mechanism of RNMT inhibition by KPNA2 is unclear. KPNA2 was demonstrated to bind to RNA (Wen and Shatkin, 2000) and thus KPNA2 could titrate RNA away from RNMT. Alternatively, binding of KPNA2 to RNMT could inhibit RNMT catalytic activity by blocking the active site or causing a conformational change. Theoretically, this could be addressed by repeating the activity assay with the phospho-mimicking RNMT T77D mutant that doesn't bind to KPNA2. Thus, recombinant RNMT WT, T77A and T77D were purified and *in vitro* affinity purifications were performed. However, unlike cellular RNMT, all recombinant RNMT constructs interacted with KPNA2 (data not shown). Hence, further work is required to elucidate the molecular mechanism of negative regulation of RNMT by KPNA2. Cap methyltransferase assays could be performed with KPNA2 mutants deficient in RNA-binding (KPNA2 72-529) or RNMT-binding (KPNA2

1-455) (Wen and Shatkin, 2000). Furthermore, *in vitro* phosphorylated RNMT could be assessed for its interaction with KPNA2 instead and subsequently be used in RNMT activity assays.

Experiments performed with cell extracts demonstrated that KPNA2 and RNMT interact with each other and further *in vitro* data showed that this leads to the inhibition of RNMT catalytic activity. However, it remains unclear whether this interaction occurs at the site where RNA guanosine caps are methylated *in vivo* and thus KPNA2 directly regulates RNMT activity *in vivo*. KPNA2 is expected to dissociate from its cargo after nuclear translocation due to the high Ran-GTP content in the nucleus. However, it is possible that a pool of KPNA2 may exhibit additional functions in the nucleus.

Finally, at an equimolar ratio of RNMT and KPNA2 no effect was observed on RNMT catalytic activity. Only with increasing amounts of KPNA2 cap methyltransferase activity was inhibited *in vitro*. Therefore, in order to exhibit an effect on RNMT activity *in vivo*, KPNA2 would need to accumulate at high stoichiometry around RNMT. Further experiments are required to investigate the biological relevance of the inhibition of RNMT by KPNA2. For example, gel filtration experiments may reveal information about the molar ratio of the RNMT-KPNA2 interaction.

Together, this work has identified cell cycle-dependent phosphorylation of RNMT T77 and shown that this phosphorylation activates RNMT activity *in vitro*. Furthermore, a phosphorylation-dependent interaction with KPNA2 was identified and it was demonstrated that at high stoichiometry KPNA2 can act as an inhibitor of RNMT activity *in vitro*. Thus, experiments performed in cells and *in vitro* suggest that RNMT phosphorylation can act as a direct activator of RNMT but also indirectly via decreasing RNMT interaction with the negative regulator KPNA2.

Chapter 6:

Investigation of the biological function of RNMT Threonine-77 phosphorylation

6.1 Introduction

The previous chapters described cell-cycle dependent phosphorylation of the human cap methyltransferase RNMT and how the effect of this post-transcriptional modification was investigated *in vitro*. This final chapter aims to elucidate the biological function of the T77 phosphorylation site in cells.

The RNMT phosphorylation site identified in chapter 4 resides next to a nuclear localisation signal (NLS). Furthermore, experiments described in chapter 5 demonstrated that T77 phosphorylation negatively regulates the interaction of RNMT with the nuclear import machinery. Thus, RNMT T77 phosphorylation may regulate subcellular localisation during the cell cycle. It has been demonstrated that phosphorylation can regulate nuclear protein import in many different ways (Nardozzi et al., 2010); directly by increasing the affinity of a protein with importins or by causing a conformational change, which exposes a previously inaccessible NLS. Examples for enhanced nuclear import after phosphorylation have been described for the Epstein-Barr virus nuclear antigen 1 (EBNA-1) or for the capsid surface protein PKC of the human hepatitis virus (Kann et al., 1999; Kitamura et al., 2006). Phosphorylation in the proximity of a NLS may also disrupt the interaction with importins, as is the case for the nuclear factor of activated T-cells (NFAT) or the yeast Swi6p transcription factor that is

phosphorylated in a cell cycle specific manner (Belfield et al., 2006; Sidorova et al., 1995).

Maximum RNMT T77 phosphorylation levels were observed in G2/M-phase and the localisation of several factors functioning at chromatin is regulated during this stage of the cell cycle. The majority of the gene expression machinery is displaced from mitotic chromatin but some gene promoters remain associated with transcription factors. The retention of specific transcriptional regulatory factors at target gene promoters on mitotic chromatin is a form of gene bookmarking (Zaidi et al., 2011). It is thought that mitotic retention of nuclear factors enables rapid transcriptional reactivation during M/G1-transition or early G1-phase and it could also serve to maintain lineage and differentiation-specific gene expression patterns (Kadauke and Blobel, 2013). For example, during mitosis the lineage-specific transcription factor Runx2 binds to particular genes to ensure the expression of lineage specific genes in daughter cells (Young et al., 2007a, 2007b). Moreover, Brd4 binds acetylated histones and marks specific genes for post-mitotic transcription (Dey et al., 2009). Phosphorylation plays a critical role in the functional regulation of some transcription factors during mitosis. For instance, phosphorylation of the transcription factor Oct1 displaces it from mitotic chromosomes while TFIID remains associated with mitotic chromosomes but its activity is inhibited by phosphorylation (Roberts et al., 1991; Segil et al., 1991, 1996). Thus, this represents another example of how cell cycle-dependent phosphorylation can affect the subcellular localisation or function of target proteins.

6.2 Results

6.2.1 Experimental system employing siRNA-resistant HA-RNMT

The aim of this chapter is to further investigate the biological function of RNMT T77 phosphorylation in cells. To study the effect of exogenously expressed RNMT phosphorylation mutants in the absence of endogenous RNMT expression, siRNA-resistant HA-RNMT constructs were designed and stably expressed in IMEC or HeLa cells. Upon treatment with siRNAs targeting RNMT, endogenous RNMT was depleted while exogenous HA-RNMT expression remained unaltered (Figure 6.1). Thus, this experimental system allowed partial replacement of endogenous RNMT with HA-RNMT mutants expressed at endogenous levels.

6.2.2 Study of RNMT localisation during mitosis

RNMT was previously described as a nuclear protein with three nuclear localisation signals (NLS) in its N-terminal region (Shafer et al., 2005). The RNMT T77 phosphorylation site resides immediately next to one of the three NLSs and results described in chapter 5 revealed that RNMT T77 phosphorylation negatively regulates an interaction with KPNA2, which is part of the nuclear import machinery. Moreover, RNMT phosphorylation peaks during G2/M-phase and, as described above, the localisation of several proteins is regulated by mitotic phosphorylation. To determine whether RNMT T77 phosphorylation affects RNMT localisation immunofluorescence experiments were performed to monitor subcellular localisation of RNMT during interphase and different stages of mitosis.

Mitosis can be divided into five different stages: at prophase the replicated chromosomes condense and the mitotic spindle starts to assemble; at prometaphase the nuclear envelope breaks down and the chromosomes attach to the mitotic spindle;

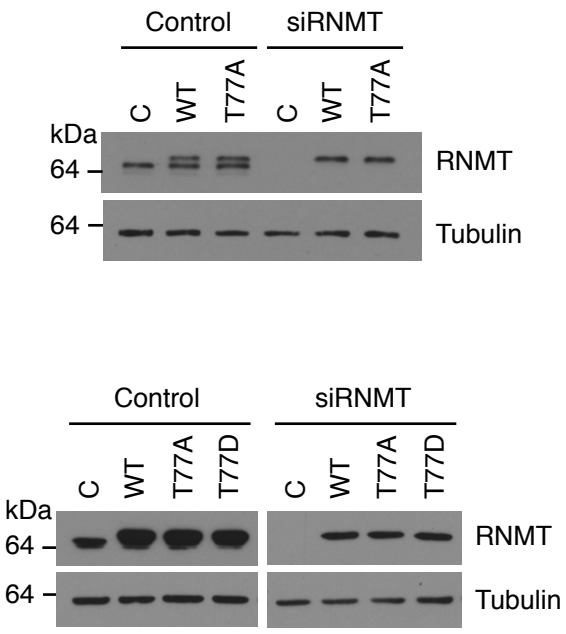

Figure 6.1: Experimental system to study the biological function of RNMT Threonine-77 phosphorylation.

HeLa cells (upper panel) or IMEC cells (lower panel) stably expressing siRNA-resistant HA-RNMT WT, T77A and T77D constructs or vector control (C) were transfected with siRNAs against RNMT or control-treated with transfection reagent. 48 hours post-transfection western blots were performed to detect RNMT and Tubulin.

at metaphase the chromosomes align in the middle of the cells; at anaphase the daughter chromosomes are separated and moved towards the spindle pole and at telophase the chromosomes arrive at the spindle poles and the nuclear envelope reassembles forming two nuclei to complete mitosis. Finally, after mitosis the cell undergoes cytokinesis in which the cytoplasm is divided and two daughter cells are formed.

Initially, localisation of endogenous RNMT during mitosis was characterized by immunofluorescence in IMEC cells using an anti-RNMT antibody (Figure 6.2). DAPI-stained chromosomes and the mitotic spindle, detected with an anti-Tubulin antibody, served to determine mitotic stages in the nonsynchronous cell pool. As expected, non-mitotic cells exhibited nuclear localisation of RNMT and the same was observed at entrance of mitosis (prophase). When the mitotic spindle started to form in prometaphase RNMT did not perfectly colocalise with DAPI staining but started to show a cytoplasmic signal. At metaphase RNMT was completely delocalised from mitotic chromosomes and this remained unaltered during anaphase. In telophase RNMT and DAPI staining started to colocalise and the nuclear RNMT signal was perfectly restored at the end of telophase. Thus, the immunofluorescence analysis suggests that RNMT disperses into the cytoplasm when the nuclear envelope breaks down after prophase. Furthermore, RNMT remains delocalized from condensed mitotic chromosomes and moves back into the nucleus once it is reformed in telophase.

To investigate whether loss or gain of RNMT T77 phosphorylation would alter RNMT localisation IMEC cells stably expressing siRNA-resistant HA-RNMT constructs were transfected with siRNMT or control-treated with transfection reagent for 72 hours. Immunofluorescence analysis was performed to detect RNMT and Tubulin as well as nuclear envelope component Lamin B1 which was used to monitor the status of the nuclear envelope throughout mitosis. Compared to control-treated cells the RNMT signal detected in siRNMT-treated vector control cells was strongly depleted confirming

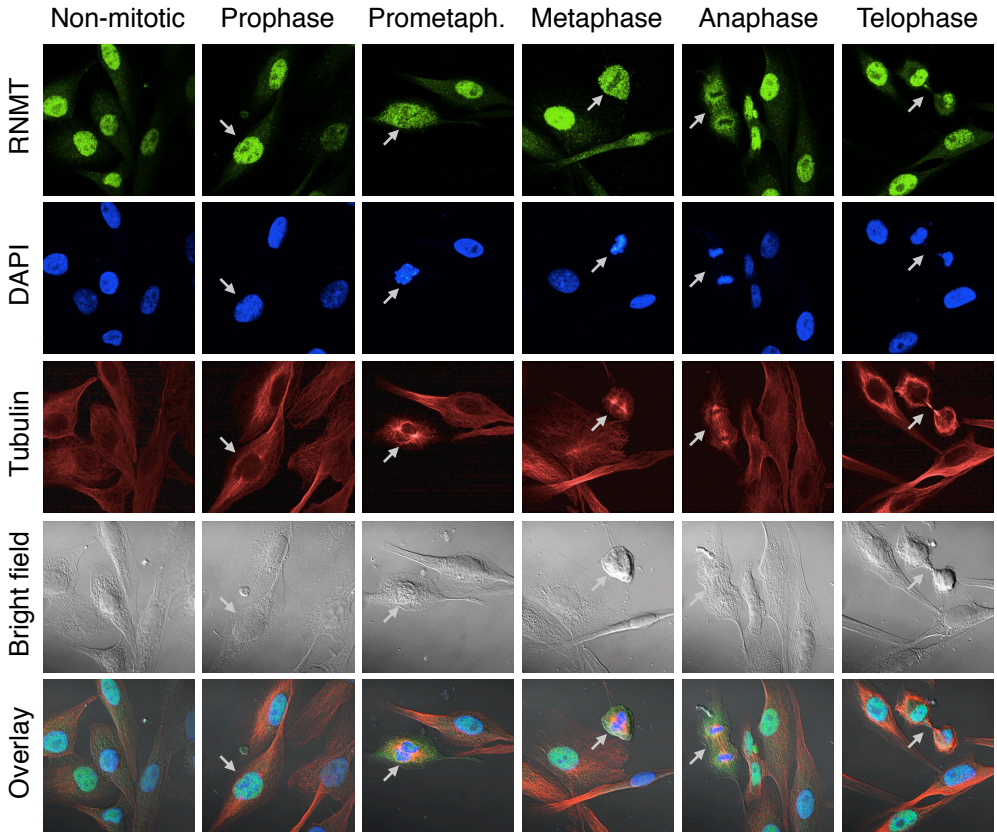

Figure 6.2: RNMT is delocalised from chromatin during mitosis.
Immunofluorescence analysis was performed to detect the subcellular localisation of RNMT and Tubulin during mitosis in IMECs. DNA staining by DAPI was used to detect nuclei and a bright field view to detect the cell membrane. Arrows mark cells in the mitotic stage indicated on the top of the diagram. Representative pictures of three independent experiments are shown

efficient knockdown of endogenous RNMT (Figure 6.3a). Immunofluorescence analysis of siRNMT-transfected cells stably expressing siRNA-resistant HA-RNMT WT showed a similar pattern as observed for endogenous RNMT (Figure 6.3b): in non-mitotic cells HA-RNMT is a nuclear protein. When the nuclear envelope starts to break down HA-RNMT is dispersed into the cytoplasm and stays delocalised from mitotic chromosomes. In telophase when the nuclear envelope is reformed HA-RNMT re-establishes nuclear localisation. Immunofluorescence analysis was also performed on cells stably expressing RNMT with the loss of phosphorylation mutation T77A or the gain of phosphorylation mutation T77D and no difference was observed with either mutant compared to HA-RNMT WT (Figure 6.3c and d). Hence, RNMT T77 phosphorylation during G2/M-phase does not seem to regulate RNMT subcellular localisation or bookmark the protein to mitotic chromosomes.

6.2.3 Cell cycle progression of HA-RNMT WT and T77A expressing cells

Replacement of endogenous RNMT with RNMT T77A resulted in reduced cell proliferation compared to cells expressing wild type RNMT (proliferation experiments performed by Victoria Cowling, data not shown). Since T77 phosphorylation is regulated during the cell cycle and loss of phosphorylation reduced cell proliferation it was tested whether cells expressing the phosphorylation mutant T77A show a defect in cell cycle progression. HeLa cells stably expressing siRNA-resistant HA-RNMT constructs were transfected with siRNAs against RNMT for 48 hours. Cells were stained with propidium iodide and were analysed by flow cytometry to quantify the cell cycle distribution (Figure 6.4a and b). Depletion of RNMT with siRNA did not alter the normal cell cycle distribution and no change was observed in cells expressing RNMT T77A compared to RNMT WT.

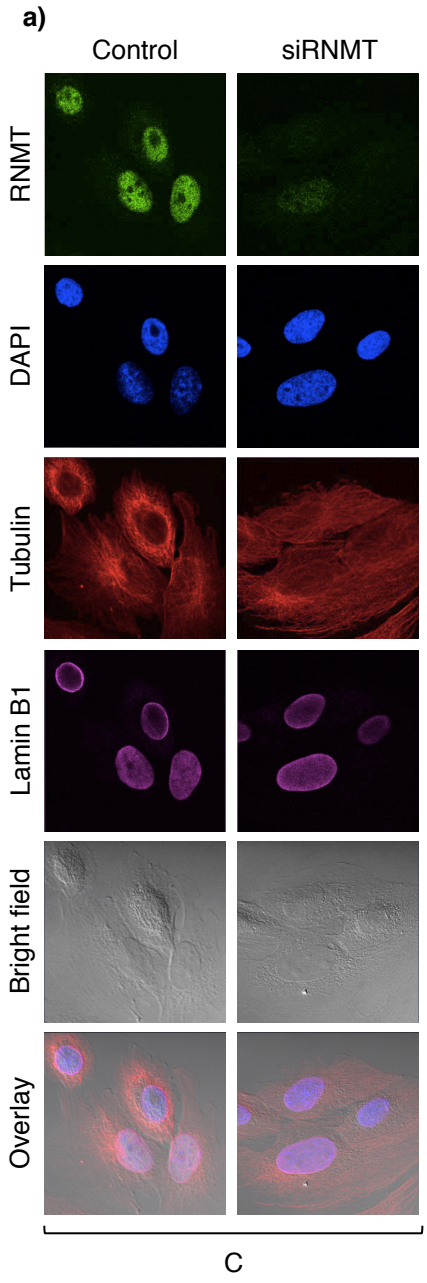

Figure 6.3: Mutation of RNMT Threonine-77 did not influence RNMT localisation during mitosis.

Immunofluorescence analysis was performed to detect the subcellular localisation of RNMT, Tubulin and Lamin B1 during mitosis in IMEC cells. DNA staining by DAPI was used to detect nuclei and a bright field view to detect the cell membrane. Arrows mark cells in the mitotic stage indicated on the top of the diagram. Representative pictures of three independent experiments are shown.

a) IMEC cells expressing vector control (C) were transfected with siRNAs against RNMT or control-treated with transfection reagent for 72 hours and immunofluorescence analysis was performed.

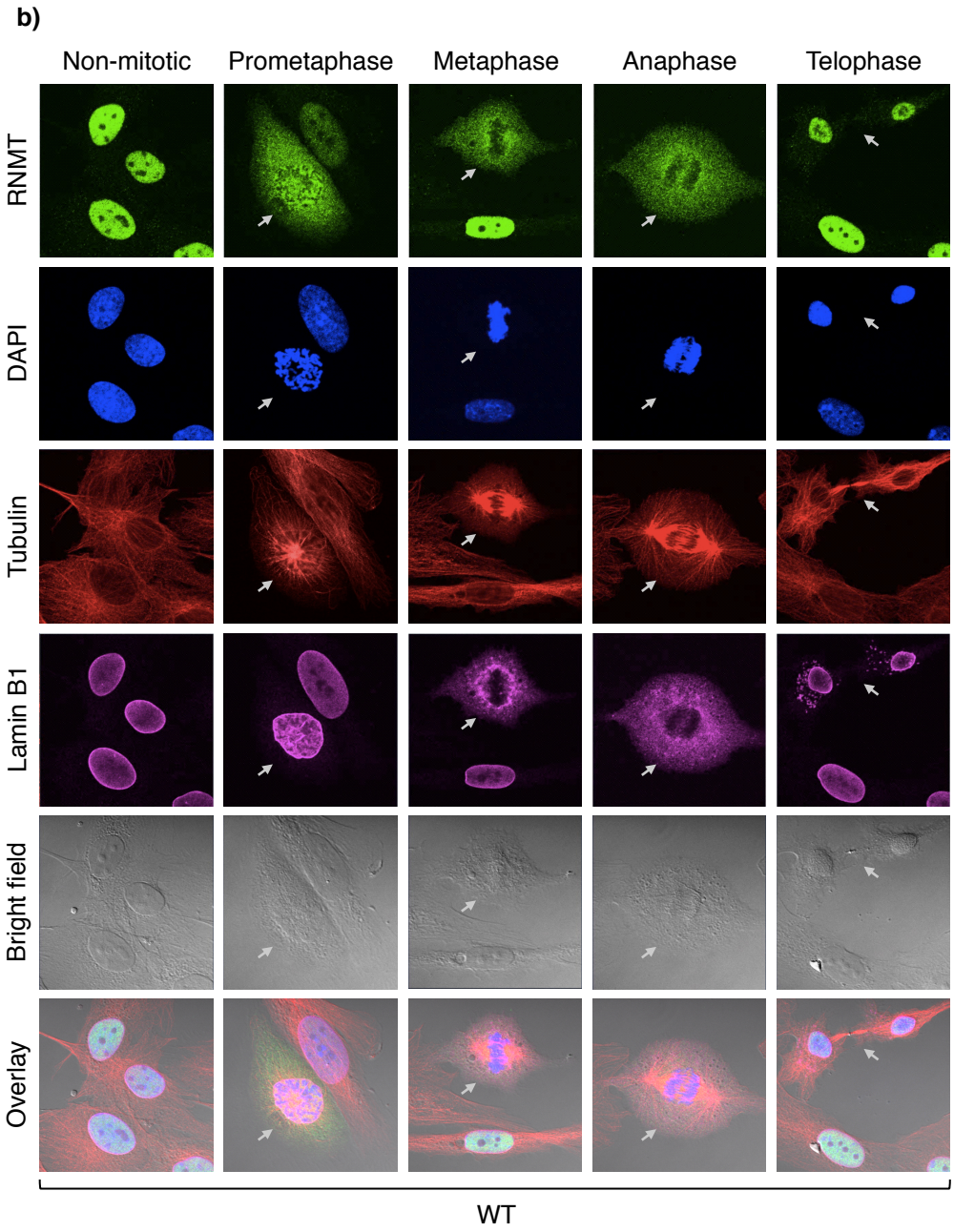

Figure 6.3: Mutation of RNMT Threonine-77 did not influence RNMT localisation during mitosis.

b) IMEC cells expressing siRNA-resistant HA-RNMT WT were transfected with siRNAs against RNMT for 72 hours and immunofluorescence analysis was performed.

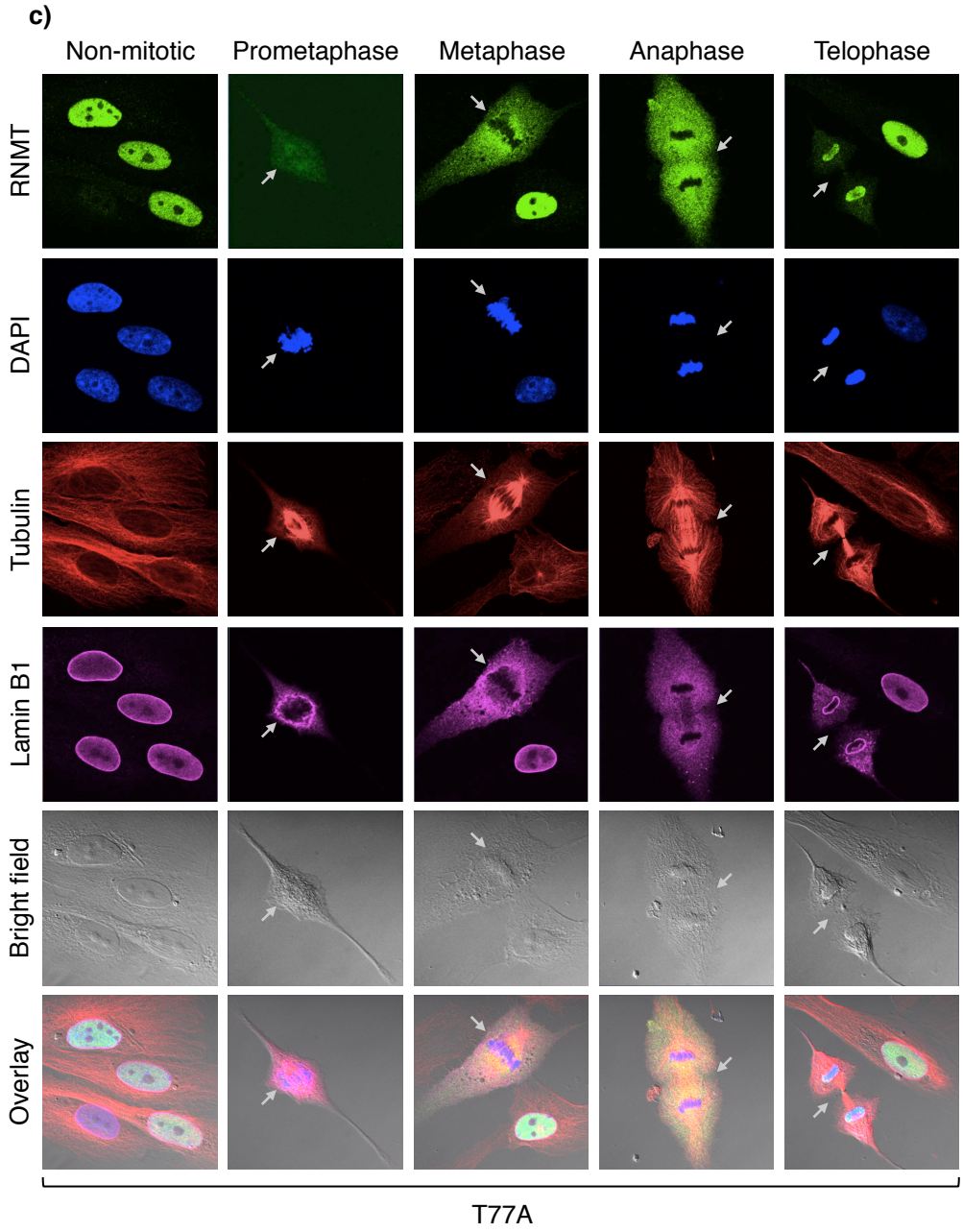

Figure 6.3: Mutation of RNMT Threonine-77 did not influence RNMT localisation during mitosis.

c) IMEC cells expressing siRNA-resistant HA-RNMT T77A were transfected with siRNAs against RNMT for 72 hours and immunofluorescence analysis was performed.

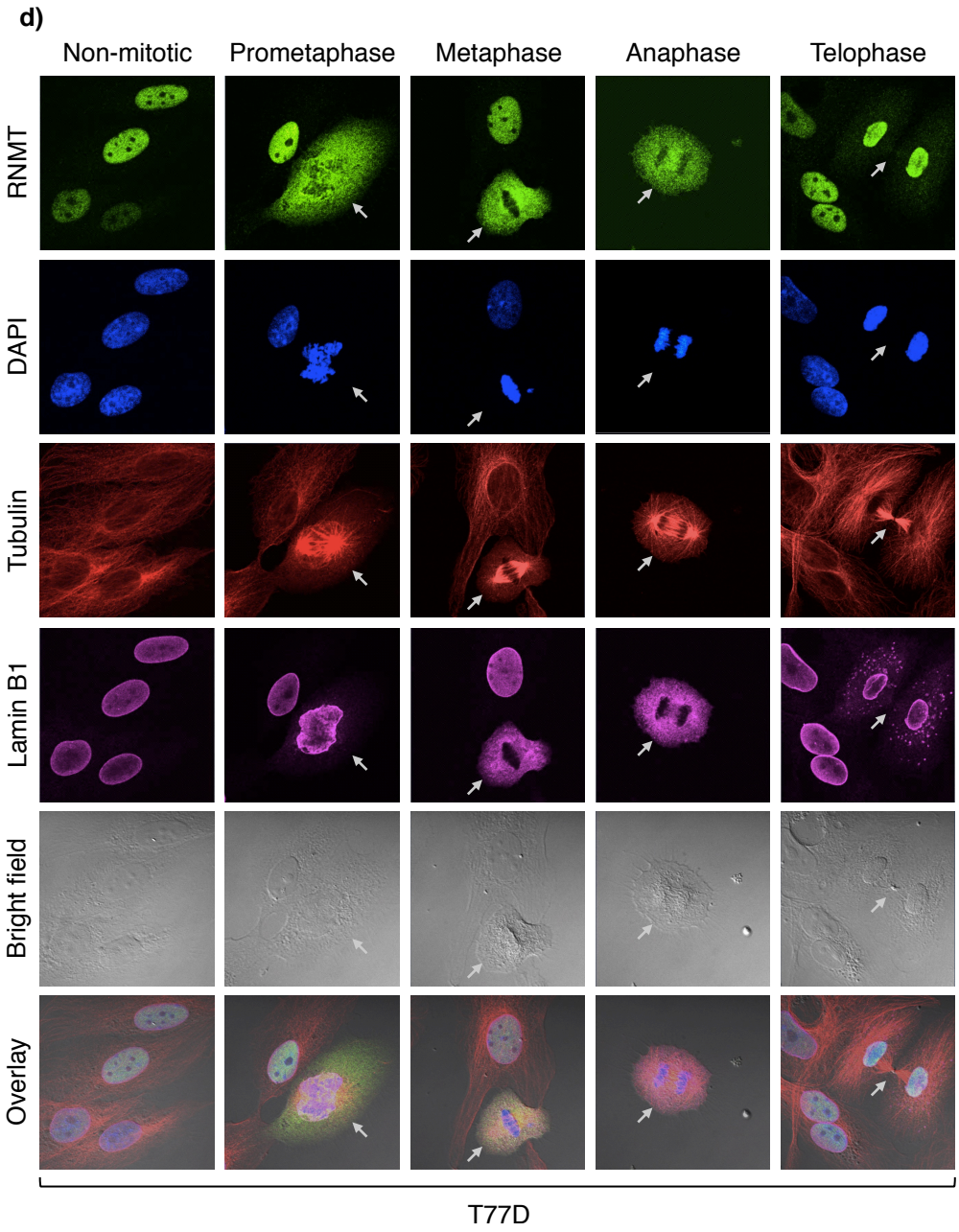

Figure 6.3: Mutation of RNMT Threonine-77 did not influence RNMT localisation during mitosis.

d) IMEC cells expressing siRNA-resistant HA-RNMT T77D were transfected with siRNAs against RNMT for 72 hours and immunofluorescence analysis was performed.

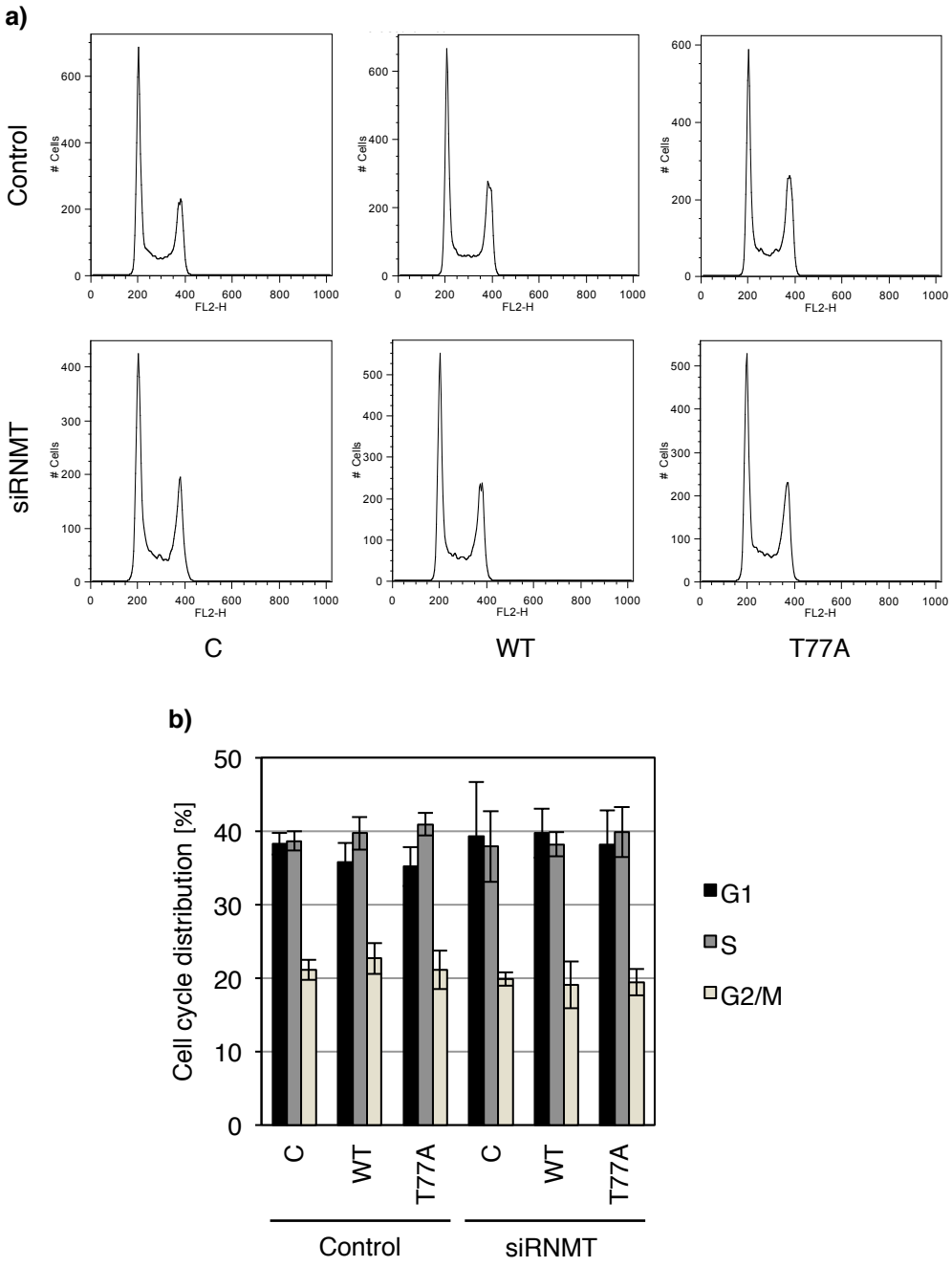

Figure 6.4: Loss of RNMT Threonine-77 phosphorylation does not affect cell cycle progression.

HeLa cells stably expressing siRNA-resistant HA-RNMT WT, T77A or vector control (C) were transfected with siRNAs against RNMT or control-treated with transfection reagent. 48 hours post-transfection cells were stained with propidium iodide and cell cycle distribution was monitored by flow cytometry.

a) DNA content and cell numbers of a representative experiment are depicted.

b) Cell cycle distribution was estimated using the Watson model. The chart depicts average and standard deviation of three independent experiments.

6.2.4 Measurement of chromatin recruitment of RNMT T77A

Work presented in chapter 3 demonstrated that the N-terminal 120 amino acids of RNMT are essential for its recruitment to chromatin. To test whether RNMT T77 phosphorylation regulates recruitment to transcription start sites (TSS), chromatin immunoprecipitation (ChIP) experiments were performed as described in chapter 3: HeLa cells were transiently transfected with HA-RNMT WT or T77A and FLAG-RAM or vector control and, after crosslinking nucleic acid-protein complexes with formaldehyde, RNMT-RAM complexes were purified with anti-HA and anti-FLAG antibodies. ChIP analysis with anti-HA antibody showed that RNMT T77A is recruited to similar or slightly higher levels compared to WT protein (Figure 6.5a). A similar result was obtained after performing FLAG-RAM ChIP with FLAG-antibodies (Figure 6.5b). Thus, these experiments suggest that RNMT T77 phosphorylation is not required for recruitment of RNMT to TSS.

6.2.5 Introduction to the regulation of gene expression during the cell cycle

Several *in vitro* experiments described in chapters 4 and 5 demonstrated that RNMT phosphorylation on T77 increased cap methyltransferase activity in a direct manner and indirectly by interrupting the inhibitory interaction of RNMT with KPNA2. As described in detail in chapter 1, the N7-methylguanosine cap is essential for eukaryotic gene expression and cell proliferation. It stabilises RNA pol II transcripts by protecting them from 5' to 3' exoribonucleolytic degradation, and interacts with the cap-binding complex (CBC) and the eukaryotic translation initiation factor 4E (eIF4E), thus promoting transcription, splicing, polyadenylation, nuclear export and translation initiation (Cowling, 2009; Topisirovic et al., 2011). However, cell cycle-regulated formation or functions of the N7-methylguanosine cap have not been reported to date.

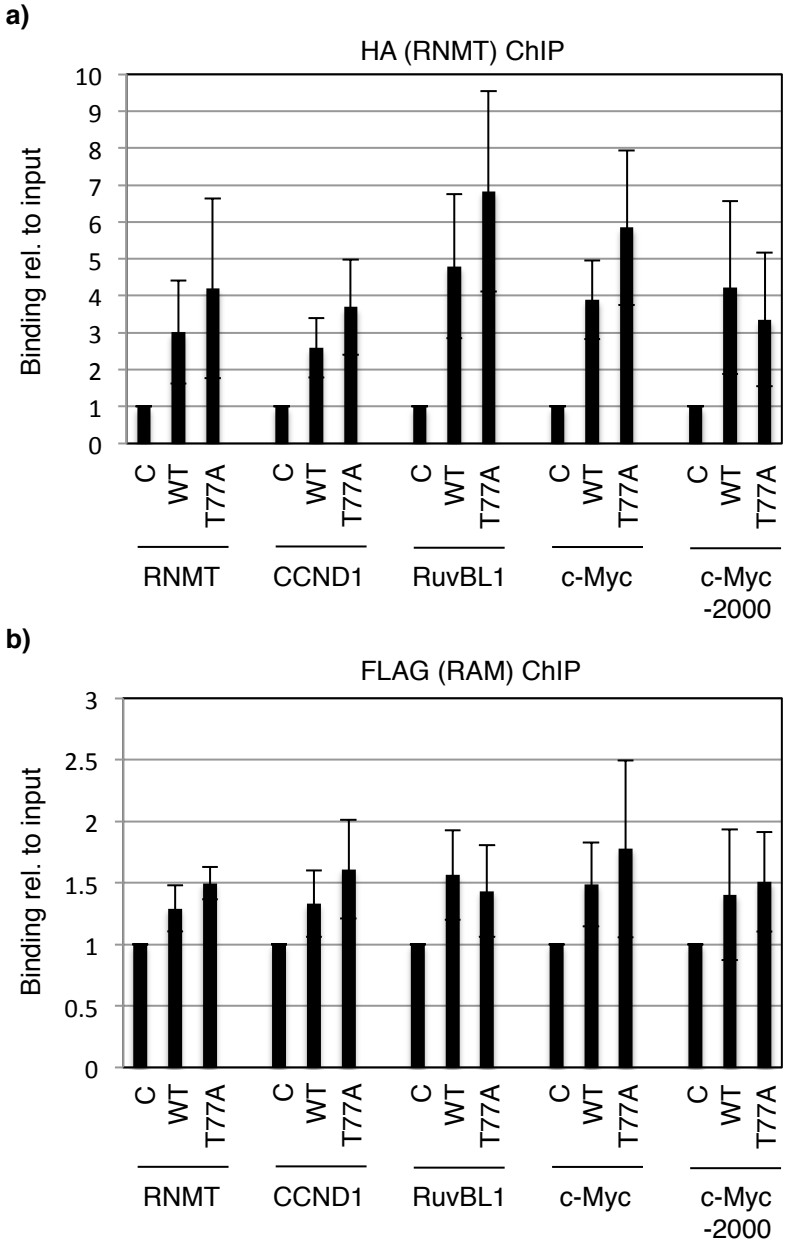

Figure 6.5: Loss of RNMT Threonine-77 phosphorylation did not alter chromatin recruitment of RNMT.

a) Chromatin immunoprecipitation was performed on HeLa cells transiently transfected with pcDNA4 HA-RNMT WT or T77A plus pcDNA4 FLAG-RAM or with pcDNA4 (C). An anti-HA antibody was used to immunoprecipitate RNMT. PCR analysis was performed against promoter proximal regions of the genes indicated or 2000 bases upstream of the transcription start site of c-Myc (-2000). The charts depict the average mean signal relative to input and normalised to control for five independent experiments and the error bars represent the standard deviation.

b) As in a) but immunoprecipitations were performed with anti-FLAG antibodies to detect RAM.

A study of the transcriptional profile of human fibroblasts progressing through the cell cycle identified approximately 700 genes that displayed expressional periodicity (Cho et al., 2001). Furthermore, the expression of over 800 transcripts in HeLa cells has been shown to exhibit periodic variation throughout the cell cycle, of which 24 % peaked during G2/M-phase and 17 % at M/G1-phase (Whitfield et al., 2002). Cyclic transcription ensures that proteins required for different cell cycle phases are produced at the appropriate time. Not surprisingly, many of the periodically expressed genes encode proteins that are directly involved in various aspects of the cell cycle such as DNA replication or cell division.

With the exception of specific genes required during M-phase, basal gene expression is strongly impaired during mitosis through the inhibition of both RNA and protein synthesis. The reduction in transcription during mitosis was shown by the reduced incorporation of radioactive RNA precursors into nascent transcripts from the end of prophase to telophase (Prescott and Bender, 1962; Taylor, 1960). Transcriptional inhibition may be caused by the condensation of mitotic chromatin, physically blocking the association of the transcription machinery with DNA, or by the inactivation of transcription initiation factors. Immunofluorescence and ChIP experiments revealed that the majority of RNA pol II is displaced from mitotic chromatin (Blobel et al., 2009; Christova and Oelgeschläger, 2002; Parsons and Spencer, 1997; Spencer et al., 2000). However, loss of mitotic transcription can occur independently of chromatin condensation as shown by the inhibition of transcription of non-condensed viral DNA (Spencer et al., 2000). This suggests that inactivation of certain transcription factors may be sufficient to block transcription.

Several factors involved in transcription initiation are targeted for phosphorylation during mitosis. The RNA pol II CTD kinase TFIIH is repressed during mitosis, which is mediated through phosphorylation of the CDK7 subunit at the T-loop by CDK1/Cyclin B (Akoulitchev and Reinberg, 1998; Long et al., 1998). Furthermore, TFIID, which

contains the TATA box-binding protein, is phosphorylated during mitosis abolishing its function in transcription activation (Segil et al., 1996). In addition to RNA pol II, transcription mediated by RNA pol I and RNA pol III is also inhibited by mitotic phosphorylation events (Hartl et al., 1993; Heix et al., 1998; Klein and Grummt, 1999; White et al., 1995).

The rate of protein synthesis varies throughout the cell cycle; translation in mitotic cells is reduced by 60 - 80 % (Bonneau and Sonenberg, 1987; Fan and Penman, 1970). Reduction of protein synthesis during mitosis is predominantly achieved through reduced translation initiation. During mitosis eIF4E phosphorylation is impaired reducing its affinity for the N7-methylguanosine cap and the translation initiation complex, eiF4F, is disrupted through the sequestering of eIF4E by the 4E-BPs as a result of hypophosphorylation of 4E-BPs. These events lead to a rapid reduction of cap-dependent translation (Pyronnet et al., 2001). Furthermore, several other translation initiation factors, polyadenylation proteins and RNA binding factors have been found to be regulated by mitotic phosphorylation, which may also contribute to reduced translation rates during mitosis (Le Breton et al., 2005). Moreover, the tumour suppressor 14-3-3σ inhibits cap-dependent translation during mitosis through binding to several translation initiation factors (Wilker et al., 2007). Several studies suggest that IRES-mediated translation could be utilised by the cell to bypass the suppression of cap-dependent translation during mitosis. A growing list of mRNAs, such as $p58^{PITSLRE}$ (CDK11B) or c-Myc, have been demonstrated to be translated via cap-independent IRES-mediated translation during M-phase (Cornelis et al., 2000; Kim et al., 2003; Pyronnet et al., 2000). After the completion of mitosis, total protein synthesis rate rapidly increases. Interestingly, 4E-BP1 phosphorylation has been observed to increase towards the end of mitosis which may act to restimulate cap-dependent translation as cells enter G1 (Heesom et al., 2001).

6.2.6 Analysis of gene expression in cells expressing HA-RNMT WT or T77A

To investigate whether cell cycle-dependent RNMT phosphorylation regulates gene expression, transcript and protein levels were studied in HeLa cells stably expressing siRNA-resistant HA-RNMT WT or T77A. Initially, ^{35}S-labelling experiments were performed to estimate global protein synthesis (Figure 6.6). Knockdown of endogenous RNMT decreased ^{35}S-incorporation however this effect could not be rescued by the stable expression of RNMT WT. Unexpectedly, a lower ^{35}S-signal was detected in control-treated cells expressing both endogenous and exogenous RNMT. Although RNMT T77A expressing cells showed reduced ^{35}S-incorporation compared to RNMT WT expressing cells this difference was not significant.

As the experiment measuring global protein synthesis was not successful the possibility that RNMT T77 phosphorylation regulates gene expression in a gene- or cell cycle-specific manner was investigated. This hypothesis was tested by measuring transcript levels of genes that are periodically expressed during the cell cycle or that are cell cycle independent (Whitfield et al., 2002). HeLa cells stably expressing siRNA-resistant HA-RNMT were transfected with siRNMT or control-treated with transfection reagent for 48 hours and RNA was extracted and analysed by RT-PCR (Figure 6.7). The depletion of RNMT was monitored by using primers recognising endogenous RNMT (5' UTR) or total RNMT (RNMT). As expected, RNMT mRNA was significantly reduced in siRNMT-treated vector control cells. However, the other investigated transcripts were largely unaffected by the knockdown of RNMT, though CCDN1 showed a significant increase in siRNMT-treated control cells. No significant changes in periodically expressed genes were observed between cells expressing HA-RNMT WT and T77A. Interestingly, the transcript levels of two non-periodically expressed genes were found to be significantly reduced in T77A cells: NME1 and c-Myc.

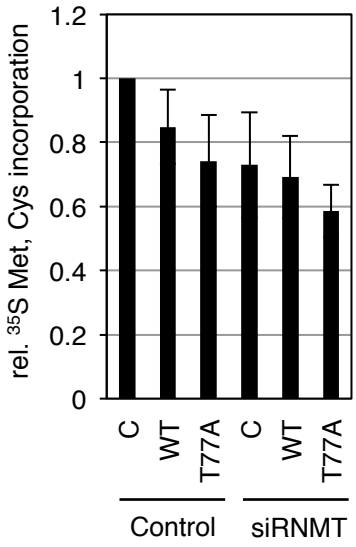

Figure 6.6: Loss of RNMT Threonine-77 phosphorylation modestly reduces total protein synthesis.

HeLa cells stably expressing siRNA-resistant HA-RNMT WT or T77A were transfected with siRNAs against siRNMT or control-treated with transfection reagent. 48 hours post-transfection cells were labelled with ^{35}S Methionine and Cysteine for 15 minutes and total cell extracts were separated by SDS-PAGE and subjected to autoradiography. Charts depict the average mean and standard deviation of four independent experiments.

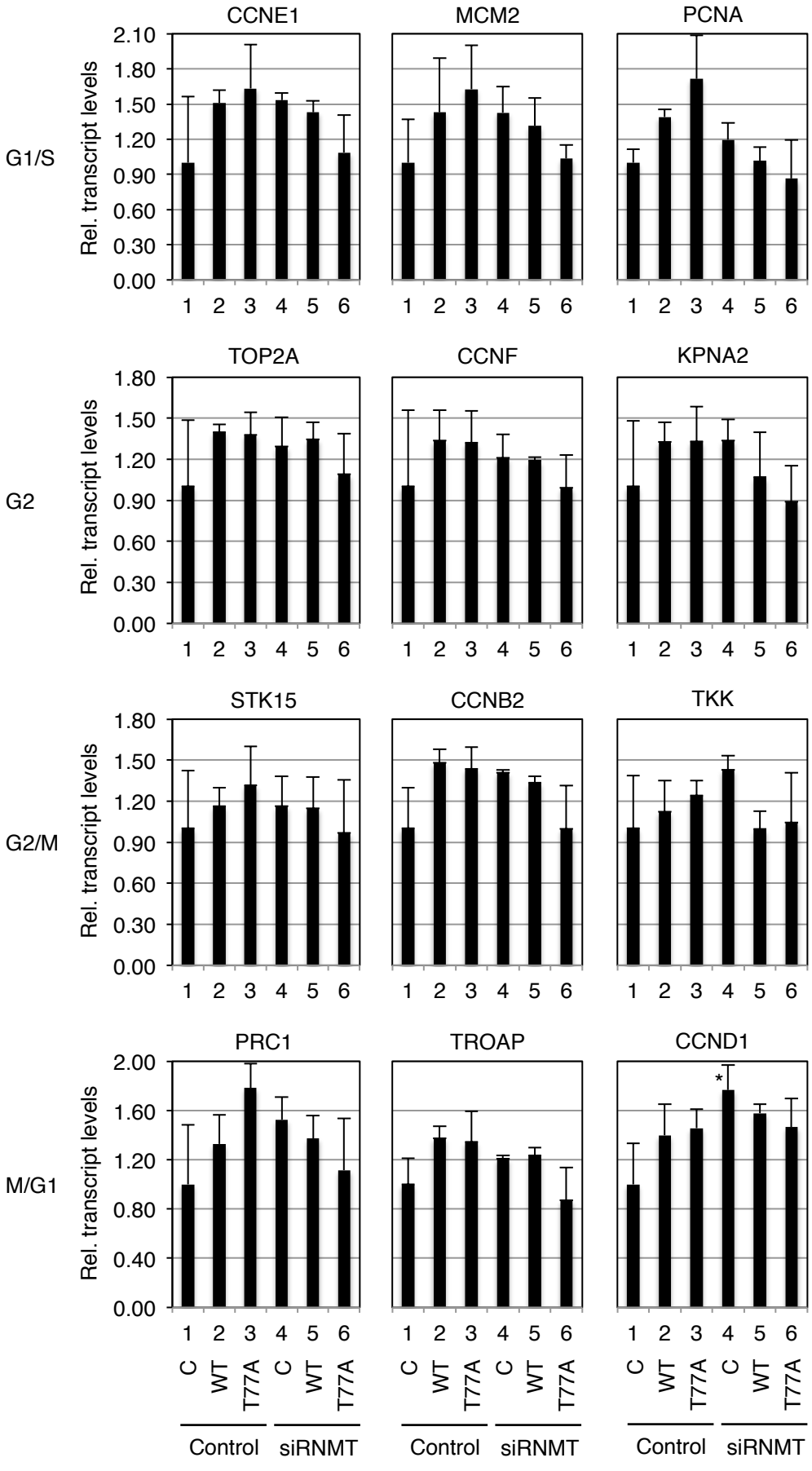
G1/S
G2
G2/M
M/G1
CCNE1
MCM2
PCNA
TOP2A
CCNF
KPNA2
STK15
CCNB2
TKK
PRC1
TROAP
CCND1
Rel. transcript levels
2.10
1.80
1.50
1.20
0.90
0.60
0.30
0.00
2.00
1.60
0.80
0.40
1 2 3 4 5 6
C
WT
T77A
Control
siRNMT
*

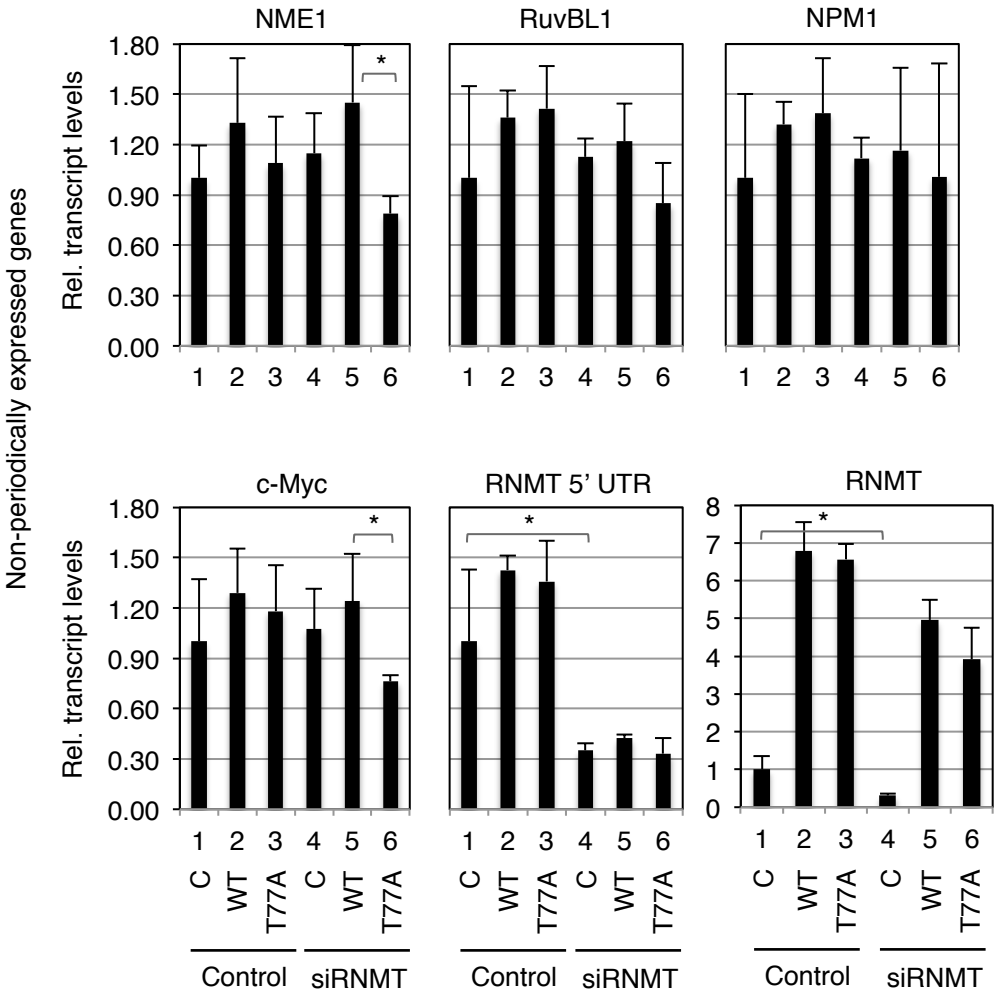

Figure 6.7: Loss of RNMT Threonine-77 phosphorylation reduces specific transcript levels.

HeLa cells stably expressing vector control (1,4) or siRNA-resistant HA-RNMT WT (2,5) or T77A (3,6) were transfected with siRNAs against RNMT (4-6) or control-treated with transfection reagent (1-3). 48 hours post-transfection RNA was extracted and reverse transcribed into cDNA. RT-PCR analysis was performed to detect periodically (G1/S, G2, G2/M, M/G1) and non-periodically expressed transcripts as indicated on top of each chart. Charts depict the average mean and standard deviation of three independent experiments. T-Test p-value < 0.05 are indicated with an asterisk.

6.3 Discussion

To investigate the biological function of RNMT T77 phosphorylation cell lines stably expressing siRNA-resistant RNMT WT or T77A phosphorylation mutant at levels similar to endogenous protein were used. Upon treatment with siRNMT endogenous RNMT levels were depleted whereas the expression of exogenous was not affected. This system enabled the effect of exogenous RNMT T77A phosphorylation mutant to be studied whilst RNMT levels were strongly reduced. Although siRNMT treatment resulted in depletion of the majority of endogenous RNMT it must be noted that low levels of endogenous RNMT remained.

Subcellular localisation of RNMT was analysed throughout mitosis. In contrast to the other stages of the cell cycle, mitotic cells can be relatively easily identified by immunofluorescence microscopy due to their characteristic architecture including condensed chromatin, formation of the mitotic spindle and rounded cells underging cytokinesis towards the end of mitosis. Immunofluorescence analysis of endogenous RNMT confirmed nuclear localisation throughout interphase but revealed displacement from chromatin and cytoplasmic localisation during mitosis. At prometaphase, probably when the nuclear envelope breaks down, RNMT starts to disperse into the cytoplasm and is completely displaced from chromatin in meta- and anaphase. Towards the end of telophase RNMT is localised to the reformed nucleus and colocalises with chromatin.

Phosphorylation of certain proteins has been described to ‘bookmark’ proteins to chromatin throughout mitosis and it was investigated whether RNMT phosphorylation during G2/M-phase has a ‘bookmarking’ effect. The localisation of RNMT during the cell cycle may also be affected by T77 phosphorylation negatively regulating the interaction of RNMT with the protein import machinery, which possibly is due to the T77 phosphorylation site interfering with an adjacent NLS. To address these two

possibilities subcellular localisation of the phosphorylation mutants T77A and T77D were compared with RNMT WT, however, no change in the localisation pattern throughout mitosis was detected. This indicates that T77 phosphorylation does not 'bookmark' RNMT to chromatin in this experimental system, however it should be noted that the phospho-mimetic aspartic acid does not fully represent the characteristics of phosphorylation. Since RNMT T77D, which does not efficiently interact with KPNA2, translocates to the nucleus at the end of M-phase it is likely that the NLS starting at K81 does not play an essential role for nuclear import in telophase but may be redundant with the other two NLS present in RNMT.

Although reduced cell proliferation was observed in RNMT T77A expressing cells when endogenous RNMT was depleted, no effect was detected on cell cycle distribution of HeLa cells upon treatment with siRNMT or when comparing cells stably expressing RNMT WT to T77A. This suggests that RNMT depleted cells or cells lacking RNMT T77 phosphorylation either display a slower proliferation rate or increased apoptosis. Indeed, knockdown of RNMT in HeLa cells was previously reported to induce apoptosis (Chu and Shatkin, 2008).

The identified T77 phosphorylation site resides on the RNMT N-terminus and experiments described in chapter 3 demonstrated that this domain is essential for recruitment of RNMT to chromatin. Thus, ChIP experiments were performed with HA-RNMT WT and T77A in order to test whether RNMT phosphorylation is important for recruitment of RNMT to TSS. No significant difference was observed between wild type RNMT and the phosphorylation mutant T77A detected at a number of gene transcription start sites indicating that RNMT phosphorylation does not seem to be required for chromatin recruitment. This was expected since N7-methylguanosine cap formation occurs co-transcriptionally and RNMT exists in an unphosphorylated state throughout most of the cell cycle. Immunofluorescence analysis performed with RNMT T77A and T77D showed that the phosphorylation mutants are displaced from mitotic

chromatin in a similar manner to wild type RNMT. However, it is possible that RNMT T77 phosphorylation may regulate RNMT recruitment to specific genes that remain associated with RNA pol II during mitosis.

Since the N7-methylguanosine cap is essential for eukaryotic gene expression it was investigated whether RNMT T77 phosphorylation affects transcript or protein levels. ^{35}S-labelling experiments showed no significant changes in global protein synthesis rates between cells expressing RNMT WT or T77A. However, a trend in reduced translation detected upon depletion of RNMT in vector control cells was not rescued by the expression of wild type HA-RNMT. This was unexpected and suggests that the experimental system used was not ideal for this assay. The stress caused by RNMT depletion together with amino acid starvation may have impacted protein synthesis in an unpredicted way.

Finally, whether RNMT T77 phosphorylation affects gene expression in a gene-specific way was investigated by measuring the transcript levels of various genes. The N7-methylguanosine cap structure is thought to stabilize transcripts and also promote various RNA processing events, which is mediated mainly by the cap-binding complex (Topisirovic et al., 2011). Thus, depletion of RNMT was expected to reduce transcript levels. However, the levels of most transcripts investigated were not reduced upon treatment with siRNAs against RNMT for 48 hours. Although RNMT transcript levels dropped by over 60 % the remaining RNMT pool may have been sufficient to keep normal gene expression intact. Furthermore, previous work in the Cowling laboratory demonstrated that the effect of RNMT depletion on transcript levels is not uniform but certain transcripts are more sensitive than others.

Since RNMT T77 is phosphorylated in a cell cycle dependent manner it was tested whether mRNA levels of periodically expressed genes were affected by the loss of RNMT phosphorylation. No change was observed in any cell cycle-regulated transcript investigated. RNMT T77 phosphorylation may have no effect on cell cycle-specific

transcripts or remaining endogenous RNMT may have rescued any phenotype. Interestingly, a significant reduction in NME1 and c-Myc mRNAs in cells expressing RNMT T77A was observed. These genes were not identified as periodically expressed but are involved in cell proliferation, which may partially explain the reduction in cell proliferation observed in cells stably expressing RNMT T77A. Overall, the transcript analysis suggests that RNMT T77 phosphorylation may regulate gene expression in a gene-specific manner but a genome-wide study is required to identify target genes regulated by RNMT T77 phosphorylation. Furthermore, an improved experimental system allowing more efficient depletion or complete replacement of endogenous RNMT is required to study the effects of RNMT phosphorylation mutants on gene expression.

Chapter 7:

Final discussion and future work

7.1 Summary

The N7-methylguanosine (m7G) cap structure is essential for cell viability from yeast to man as it influences several steps of eukaryotic gene expression such as mRNA processing, RNA export and mRNA translation. The m7G cap is added co-transcriptionally to the 5' end of nascent RNA transcribed by RNA pol II. In mammalian cells two enzymes catalyse its synthesis: RNGTT adds the guanosine cap to the 5' end of the transcript and RNMT methylates the cap structure at the N7-position, which is required for the recognition of the cap by the cap-binding proteins CBC and eIF4E.

RNMT consists of two domains: a C-terminal catalytic domain (amino acids 121-476) in which the active site essential for cap methyltransferase activity resides and an N-terminal domain (amino acids 1-120) that contains two nuclear localisation sequences (NLS) towards the C-terminal end but remains functionally uncharacterised. Thus, an aim of this thesis was to investigate whether the RNMT N-terminal domain has a biological function in mammalian cells.

In vitro cap methyltransferase activity assays performed with cellular RNMT and an N-terminal deletion mutant (RNMTcat, amino acids 121-476) demonstrated that the N-terminus is not required for catalytic activity. However, cell proliferation was reduced in mammalian cells expressing RNMTcat compared to RNMT WT indicating that the N-terminus has a biological function in cells (Aregger and Cowling, 2013). To investigate whether the N-terminal domain is involved in RNMT recruitment to transcription start sites (TSS), chromatin immunoprecipitation (ChIP) was performed with cells expressing

RNMT WT, RNMTcat or RNMT-N (amino acids 1-120). These experiments revealed that the N-terminal domain is required and is sufficient for RNMT recruitment to TSS. Further ChIP experiments suggested that RNMT recruitment is dependent on phosphorylated RNA pol II CTD as DRB-treatment abolished RNMT recruitment to TSS (Aregger and Cowling, 2013). However, no direct interaction of RNMT with RNA pol II could be detected and thus, the exact molecular mechanism of RNMT recruitment to chromatin remains unclear.

There is accumulated evidence that m7G cap synthesis is not a constitutive but a regulated process (Cowling, 2009). Therefore, another aim of this thesis was to elucidate whether RNMT is regulated by signalling pathways. Two-dimensional gel electrophoresis, orthophosphate labelling and mass spectrometry analysis revealed that RNMT carries post-translational modifications including phosphorylation. Site-specific mutations in combination with orthophosphate labelling revealed that in the human cell lines utilised in this study RNMT is predominantly phosphorylated at Threonine-77 (T77). A phospho-specific antibody was raised against this phosphorylation site, which was subsequently used to detect RNMT T77 phosphorylation levels in cells.

The RNMT T77 phosphorylation site resides within a Cyclin-dependent kinase (CDK) recognition site and next to a Cyclin-binding motif. Incubation of cells with specific inhibitors against cell cycle-regulating kinases, including the CDK1-targeting compound RO-3306, reduced RNMT T77 phosphorylation. The analysis of RNMT T77 phosphorylation levels throughout several stages of the cell cycle confirmed that RNMT T77 is phosphorylated in a cell cycle-dependent manner and maximal phosphorylation levels were detected during G2/M-phase. Furthermore, CDK1/Cyclin B specifically phosphorylated RNMT T77 *in vitro*.

In vitro phosphorylation followed by cap methyltransferase activity assays demonstrated that T77 phosphorylation stimulates RNMT activity *in vitro* by two-fold.

Furthermore, peptide pull-downs and immunoprecipitation experiments revealed that T77 phosphorylation negatively regulates the interaction between RNMT and KPNA2 (Importin-α). *In vitro* cap methyltransferase activity assays with recombinant RNMT and KPNA2 revealed that KPNA2 inhibits RNMT activity.

To investigate the biological function of RNMT T77 phosphorylation *in vivo*, siRNA-resistant exogenous wild type RNMT or phosphorylation mutants were stably expressed while endogenous RNMT was depleted with siRNAs against RNMT. Immunofluorescence analysis confirmed the nuclear localisation of RNMT throughout interphase and revealed that RNMT is dispersed into the cytoplasm once the nuclear envelope breaks down at the beginning of mitosis. It was found that RNMT stays delocalised from mitotic chromatin throughout M-phase and only translocates back to the nucleus at the end of M-phase when the nuclear envelope reforms. RNMT loss (T77A) or gain (T77D) of phosphorylation mutants did not express an altered localisation pattern indicating that T77 phosphorylation does not regulate subcellular RNMT localisation throughout G2/M-phase or interphase.

Cells transiently expressing RNMT T77A displayed reduced cell proliferation compared to RNMT WT expressing cells. However, analysis of the cell cycle distribution of cells stably expressing exogenous RNMT constructs while endogenous RNMT was depleted did not reveal any evidence that RNMT T77 phosphorylation is required for progression through the cell cycle. Furthermore, no changes in RNMT recruitment to TSS were observed in ChIP experiments when the T77 phosphorylation site was mutated. Since the m7G cap is essential for eukaryotic gene expression the impact of RNMT T77 phosphorylation on transcript levels or translation was investigated. However, the experimental system described above proved not to be suitable for these analysis. Exogenous RNMT could not rescue the drop in translation observed upon depletion of endogenous RNMT. Furthermore, depletion of endogenous RNMT did not result in reduced transcript levels indicating that remaining RNMT levels

were sufficient to maintain normal transcript levels. Nonetheless, a significant reduction in c-Myc and NME1 transcript levels was observed in RNMT T77A expressing cells indicating that RNMT T77 phosphorylation may specifically regulate certain transcripts rather than acting globally.

In summary, the previously uncharacterised N-terminal domain of RNMT was found to mediate RNMT recruitment to TSS and to be targeted at T77 for cell cycle-dependent phosphorylation (Figure 7). RNMT T77 phosphorylation activates RNMT *in vitro* and negatively regulates the interaction of RNMT with KPNA2. The biological role of RNMT T77 phosphorylation during G2/M-phase remains unclear and further experiments are required to investigate its function *in vivo*.

7.2 Regulation of N7-methylguanosine cap formation

Several recent studies suggested that the synthesis of the m7G cap is not a constitutive but a regulated process. A pool of incompletely capped mRNA, lacking the methyl moiety on the cap or lacking the entire cap structure, was detected both in yeast and mammalian cells (Chang et al., 2012; Cole and Cowling, 2009; Cowling and Cole, 2007b; Fernandez-Sanchez et al., 2009; Jiao et al., 2010, 2013). In addition, the finding that eukaryotic cells possess a 5' quality control mechanism that selectively degrades aberrantly capped transcripts suggests that m7G cap formation does not always occur to completion (Chang et al., 2012; Jiao et al., 2010, 2013). Furthermore, it was found that growth factors stimulate m7G cap levels in yeast (Jiao et al., 2010). Finally, the Myc and E2F1 transcription factors can promote the formation of the m7G cap on specific transcripts in mammalian cells (Aregger and Cowling, 2012; Cole and Cowling, 2009; Cowling and Cole, 2007b; Fernandez-Sanchez et al., 2009).

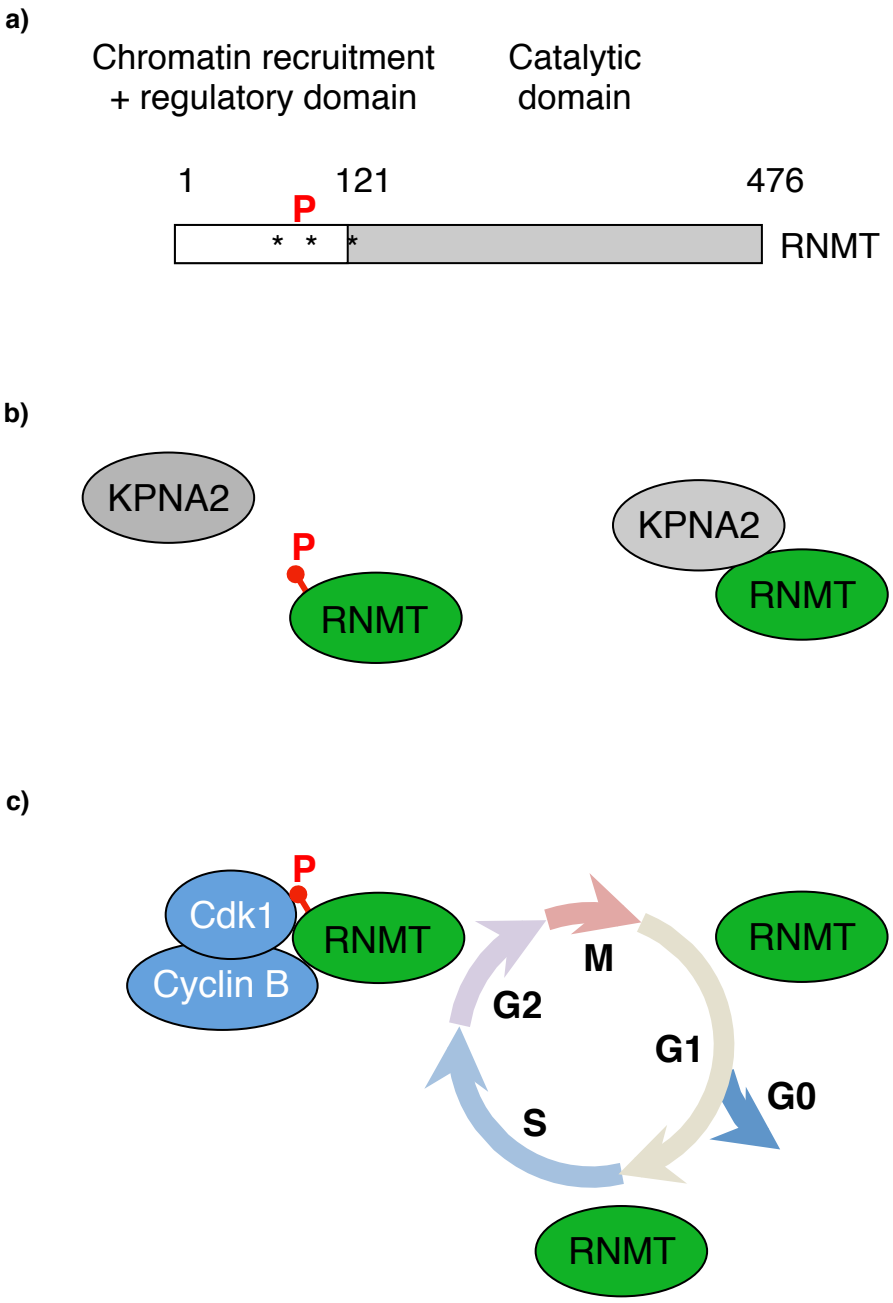

Figure 7: The N-terminal domain of RNMT is required for RNMT recruitment to chromatin and is targeted for cell cycle-dependent phosphorylation.

a) The RNMT N-terminal domain mediates RNMT recruitment to chromatin and is phosphorylated at Threonine-77. Nuclear localisation signals are indicated with an asterisk and the Threonine-77 phosphorylation site is indicated with a red P.

b) RNMT T77 phosphorylation negatively regulates the interaction of RNMT with KPNA2 (Importin-α).

c) RNMT T77 is phosphorylated in a cell cycle-dependent manner during G2/M-phase by CDK1/Cyclin B.

The identification of cell cycle-dependent phosphorylation of RNMT further supports the notion that m7G cap synthesis is regulated in cells. Whereas previous studies described the regulation of proteins influencing cap methylation, this thesis presents the first evidence that the capping machinery itself can be regulated. *In vitro* data suggests that phosphorylation of RNMT T77 activates cap methyltransferase activity. It can be speculated that this increased activity may be required to methylate a dormant pool of incompletely capped RNA during G2/M-phase in order to efficiently translate these transcripts upon exit of mitosis or during entrance of G1-phase. When the nuclear envelope breaks down during mitosis RNMT is dispersed into the cytoplasm. It is possible that increased RNMT catalytic activity and delocalisation of RNMT from KPNA2 may be required for RNMT to function in the absence of a nucleus and dissociated from chromatin.

Interestingly, the disassembly of the nucleus during mitosis is not a conserved eukaryotic feature. Many lower eukaryotes such as fungi or protists undergo a 'closed mitosis' in which the daughter chromosomes migrate to opposite poles of the intact nucleus, which subsequently divides into two (De Souza and Osmani, 2007). The cap methyltransferase of these organisms does not encounter a cytoplasmic environment during mitosis, which correlates with the absence of a cap methyltransferase N-terminal domain in lower eukaryotes. However, it is unlikely the RNMT N-terminus has solely evolved for a possible mitotic function since open mitosis occurs in most metazoans (Güttinger et al., 2009) but the RNMT T77 phosphorylation site is only conserved in mammals. Furthermore, the N-terminal domain was shown to not only regulate RNMT activity but also mediate recruitment to TSS in mammalian cells.

7.3 The N7-methylguanosine cap and cancer

mRNA translation is a highly regulated process with the initiation phase as the rate-limiting step. Translation initiation is regulated by the PI3K and MAPK signalling pathways (Blagden and Willis, 2011). PI3K is activated by nutrient and energy signals and via Akt activates mTORC1. mTORC1 phosphorylates 4E-BPs and S6K, which promotes the formation of the eIF4F complex and increases translation initiation. The MAPK pathway is activated by stress, growth factors, hormones and other factors and via p38 and ERK activates Mnk1. Activated Mnk1 phosphorylates eIF4E which increases eIF4E cap-binding activity and thus promotes translation initiation (Blagden and Willis, 2011).

Deregulation of the components of the PI3K and MAPK pathway are often associated with cancer. In addition, aberrant expression of several translation initiation factors has been demonstrated to cause tumour growth. Overexpression of eIF4E was found to promote tumorigenic transformation of fibroblasts and to cause tumour formation in mice, which was further promoted by Mnk1-mediated phosphorylation of eIF4E (Lazaris-Karatzas et al., 1990; Ruggero et al., 2004; Wendel et al., 2007). Increased eIF4E expression was detected in several cancers such as breast, head and neck, bladder, colon, cervix, lung and prostate cancers when compared with normal tissues (Blagden and Willis, 2011). Furthermore, increased phosphorylation of 4E-BPs correlates with poor clinical outcome (Petricoin et al., 2007; Rojo et al., 2007). Since increased translation rates play a critical role in tumourigenesis, eIF4E and other translation initiation factors have been targeted for drug screening and several new drugs inhibiting cap-dependent translation are currently in clinical trial (Blagden and Willis, 2011).

Recently, the formation the m7G cap has also been associated with oncogenic cell transformation. Overexpression of RNMT in fibroblasts increases Cyclin D1 expression

and promotes cell transformation (Cowling, 2010). Furthermore, the proto-oncogenes c-Myc and E2F1 were found to upregulate m7G cap levels of specific transcripts (Cole and Cowling, 2009; Cowling and Cole, 2007b; Fernandez-Sanchez et al., 2009). Upon elevated c-Myc expression transcript levels were typically increased by 2-fold whereas m7G cap levels of specific transcripts were found to be upregulated by up to 8-fold. Furthermore, increased cap methylation was required for c-Myc to promote protein synthesis, cell proliferation and cell transformation, and inhibition of cap methylation is synthetically lethal with elevated c-Myc expression (Fernandez-Sanchez et al., 2009). Therefore, formation of the m7G cap is rate limiting for Myc-induced cell transformation and thus the capping machinery potentially provides a novel therapeutic target in Myc-overexpressing tumours.

Several different approaches to target cap methylation are currently being investigated in the Cowling laboratory. RAM was found to activate RNMT and to be essential for cap methylation in cells (Gonatopoulos-Pournatzis et al., 2011). Therefore, targeting the interface between RAM and RNMT to disrupt the RNMT-RAM interaction may be a promising approach to inhibit m7G cap formation in cells. Furthermore, the Cowling laboratory is currently screening compounds that would inhibit cap methyltransferase activity of RNMT. The findings that RNMT is phosphorylated during the cell cycle and that mutation of the T77 phosphorylation site reduces cell proliferation indicate that RNMT phosphorylation contributes to driving cell proliferation. This novel information may potentially be exploited to develop drugs directed against cap methyltransferase function in the future.

7.4 Future work

To investigate the biological function of RNMT T77 phosphorylation an experimental system is required that allows efficient replacement of wild type proteins with phosphorylation mutant constructs (RNMT T77A or RNMT T77D). Several novel techniques allowing sequence-specific 'genome editing' such as zinc finger nucleases (ZFNs), transcription activator like effector nucleases (TALENs) and the clustered regularly interspaced short palindromic repeats (CRISPRs)/Cas-system (Gaj et al., 2013), could be exploited to completely replace wild type RNMT with phosphorylation mutants.

To investigate the biological role of RNMT T77 phosphorylation in mammalian cells one of the experimental systems described above could be exploited to compare gene expression patterns between cells expressing RNMT WT, T77A or T77D. The combination of the following genome-wide experiments would identify direct gene-specific effects of RNMT T77 phosphorylation:

1. ChIP-sequencing

   RNMT T77 is phosphorylated during the cell cycle, which activates RNMT *in vitro*. As discussed above it is possible that RNMT functions in the cytoplasm during mitosis, however, it is thought that RNMT functions predominantly near chromatin. Thus, it would be interesting to investigate the chromatin distribution of wild type RNMT during the cell cycle to reveal any direct targets of capping during G2/M-phase when RNMT maximal T77 phosphorylation levels are observed. To address this, ChIP experiments can be performed in combination with DNA sequencing.

2. CLIP-sequencing

   RNMT crosslinking-immunoprecipitation (CLIP) during G2/M-phase combined with RNA sequencing could provide a genome-wide overview of nascent or

incompletely capped transcripts that are bound by RNMT. This analysis could reveal specific transcripts that are targeted for cap methylation during G2/M-phase and thus may be regulated by RNMT T77 phosphorylation.

3. m7G-IP combined with RNA sequencing

   If phosphorylation of RNMT T77 affects cap methyltransferase activity *in vivo* this would ultimately result in changes of m7G cap levels. This hypothesis can be investigated with an anti-N7-methylguanosine antibody (Cowling and Cole, 2007b), which specifically binds to the methylated cap structure but not the unmethylated cap. Thus, m7G-capped transcripts can be immunoprecipitated using this antibody and subsequently be identified by RNA sequencing. By comparing the sequencing profile between cells expressing wild type RNMT or T77 mutant RNMT, specific transcripts could be identified that are targeted for regulation by RNMT T77 phosphorylation.

4. RNA sequencing of total mRNA

   Since the m7G cap is essential for RNA stability and influences transcription, detection of total mRNA levels can be used as a means to identify transcripts that are regulated by RNMT T77 phosphorylation. Total mRNA levels can be selected by poly(A) purification and can subsequently be analysed by RNA sequencing. As above, the sequencing profile can be compared between RNMT wild type or phosphorylation mutant expressing cells to identify transcripts regulated by T77 phosphorylation.

The combination of the above proposed genome-wide experiments would allow to discriminate between direct and indirect effects such as increased m7G cap formation and increased transcription, respectively.

If the above experiments reveal gene expression patterns that are regulated by RNMT T77 phosphorylation, an RNMT T77A or T77D knock-in mouse would provide an excellent model to investigate the biological relevance of RNMT T77 phosphorylation. The experiments performed in this thesis and discussed above were performed in human cell lines, however, it would be interesting to test the effects of RNMT T77 phosphorylation in an animal model. This would reveal possible effects during development or allow to assess the oncogenic potential of this phosphorylation site.

References

Abovich, N., Liao, X.C., and Rosbash, M. (1994). The yeast MUD2 protein: an interaction with PRP11 defines a bridge between commitment complexes and U2 snRNP addition. Genes Dev. *8*, 843–854.

Adams, P.D., Sellers, W.R., Sharma, S.K., Wu, A.D., Nalin, C.M., and Kaelin, W.G. (1996). Identification of a cyclin-cdk2 recognition motif present in substrates and p21-like cyclin-dependent kinase inhibitors. Mol. Cell. Biol. *16*, 6623–6633.

Akoulitchev, S., and Reinberg, D. (1998). The molecular mechanism of mitotic inhibition of TFIIH is mediated by phosphorylation of CDK7. Genes Dev. *12*, 3541–3550.

Altmann, M., Edery, I., Sonenberg, N., and Trachsel, H. (1985). Purification and characterization of protein synthesis initiation factor eIF-4E from the yeast Saccharomyces cerevisiae. Biochemistry *24*, 6085–6089.

Altmann, M., Handschin, C., and Trachsel, H. (1987). mRNA cap-binding protein: cloning of the gene encoding protein synthesis initiation factor eIF-4E from Saccharomyces cerevisiae. Mol. Cell. Biol. *7*, 998–1003.

Aregger, M., and Cowling, V.H. (2012). E2F1-dependent methyl cap formation requires RNA pol II phosphorylation. Cell Cycle *11*, 2146–2148.

Aregger, M., and Cowling, V.H. (2013). Human cap methyltransferase (RNMT) N-terminal non-catalytic domain mediates recruitment to transcription initiation sites. Biochem. J. *455*, 67–73.

Balatsos, N.A.A., Nilsson, P., Mazza, C., Cusack, S., and Virtanen, A. (2006). Inhibition of mRNA deadenylation by the nuclear cap binding complex (CBC). J. Biol. Chem. *281*, 4517–4522.

Balvay, L., Soto Rifo, R., Ricci, E.P., Decimo, D., and Ohlmann, T. (2009). Structural and functional diversity of viral IRESes. Biochim. Biophys. Acta *1789*, 542–557.

Banfalvi, G. (2011). Overview of cell synchronization. Methods Mol. Biol. *761*, 1–23.

Bartel, D.P. (2009). MicroRNAs: target recognition and regulatory functions. Cell *136*, 215–233.

Bartkowiak, B., Liu, P., Phatnani, H.P., Fuda, N.J., Cooper, J.J., Price, D.H., Adelman, K., Lis, J.T., and Greenleaf, A.L. (2010). CDK12 is a transcription elongation-associated CTD kinase, the metazoan ortholog of yeast Ctk1. Genes Dev. *24*, 2303–2316.

Bélanger, F., Stepinski, J., Darzynkiewicz, E., and Pelletier, J. (2010). Characterization of hMTr1, a human Cap1 2'-O-ribose methyltransferase. J. Biol. Chem. *285*, 33037–33044.

Belfield, J.L., Whittaker, C., Cader, M.Z., and Chawla, S. (2006). Differential effects of Ca2+ and cAMP on transcription mediated by MEF2D and cAMP-response element-binding protein in hippocampal neurons. J. Biol. Chem. *281*, 27724–27732.

Beretta, L., Gingras, A.C., Svitkin, Y. V, Hall, M.N., and Sonenberg, N. (1996). Rapamycin blocks the phosphorylation of 4E-BP1 and inhibits cap-dependent initiation of translation. EMBO J. *15*, 658–664.

Blagden, S.P., and Willis, A.E. (2011). The biological and therapeutic relevance of mRNA translation in cancer. Nat. Rev. Clin. Oncol. *8*, 280–291.

Blazek, D., Kohoutek, J., Bartholomeeusen, K., Johansen, E., Hulinkova, P., Luo, Z., Cimermancic, P., Ule, J., and Peterlin, B.M. (2011). The Cyclin K/Cdk12 complex maintains genomic stability via regulation of expression of DNA damage response genes. Genes Dev. *25*, 2158–2172.

Blobel, G.A., Kadauke, S., Wang, E., Lau, A.W., Zuber, J., Chou, M.M., and Vakoc, C.R. (2009). A reconfigured pattern of MLL occupancy within mitotic chromatin promotes rapid transcriptional reactivation following mitotic exit. Mol. Cell *36*, 970–983.

De Bondt, H.L., Rosenblatt, J., Jancarik, J., Jones, H.D., Morgan, D.O., and Kim, S.H. (1993). Crystal structure of cyclin-dependent kinase 2. Nature *363*, 595–602.

Bonneau, A.M., and Sonenberg, N. (1987). Involvement of the 24-kDa cap-binding protein in regulation of protein synthesis in mitosis. J. Biol. Chem. *262*, 11134–11139.

Both, G.W., Banerjee, A.K., and Shatkin, A.J. (1975). Methylation-dependent translation of viral messenger RNAs in vitro. Proc Natl Acad Sci U S A *72*, 1189–1193.

Boutros, R., Dozier, C., and Ducommun, B. (2006). The when and wheres of CDC25 phosphatases. Curr. Opin. Cell Biol. *18*, 185–191.

Brannan, K., Kim, H., Erickson, B., Glover-Cutter, K., Kim, S., Fong, N., Kiemele, L., Hansen, K., Davis, R., Lykke-Andersen, J., et al. (2012). mRNA Decapping Factors and the Exonuclease Xrn2 Function in Widespread Premature Termination of RNA Polymerase II Transcription. Mol. Cell *46*, 311–324.

Braunschweig, U., Gueroussov, S., Plocik, A.M., Graveley, B.R., and Blencowe, B.J. (2013). Dynamic integration of splicing within gene regulatory pathways. Cell *152*, 1252–1269.

Le Breton, M., Cormier, P., Bellé, R., Mulner-Lorillon, O., and Morales, J. (2005). Translational control during mitosis. Biochimie *87*, 805–811.

Brunn, G.J., Hudson, C.C., Sekulić, A., Williams, J.M., Hosoi, H., Houghton, P.J., Lawrence, J.C., and Abraham, R.T. (1997). Phosphorylation of the translational repressor PHAS-I by the mammalian target of rapamycin. Science (80-.). *277*, 99–101.

Calero, G., Wilson, K.F., Ly, T., Rios-Steiner, J.L., Clardy, J.C., and Cerione, R.A. (2002). Structural basis of m7GpppG binding to the nuclear cap-binding protein complex. Nat. Struct. Biol. *9*, 912–917.

Cao, Q., Padmanabhan, K., and Richter, J.D. (2010). Pumilio 2 controls translation by competing with eIF4E for 7-methyl guanosine cap recognition. RNA *16*, 221–227.

Chang, J.H., Jiao, X., Chiba, K., Oh, C., Martin, C.E., Kiledjian, M., and Tong, L. (2012). Dxo1 is a new type of eukaryotic enzyme with both decapping and 5'-3' exoribonuclease activity. Nat. Struct. Mol. Biol. *19*, 1011–1017.

Changela, A., Ho, C.K., Martins, A., Shuman, S., and Mondragón, A. (2001). Structure and mechanism of the RNA triphosphatase component of mammalian mRNA capping enzyme. EMBO J. *20*, 2575–2586.

Chapman, R.D., Heidemann, M., Hintermair, C., and Eick, D. (2008). Molecular evolution of the RNA polymerase II CTD. Trends Genet. *24*, 289–296.

Chen, J., Saha, P., Kornbluth, S., Dynlacht, B.D., and Dutta, A. (1996). Cyclin-binding motifs are essential for the function of p21CIP1. Mol. Cell. Biol. *16*, 4673–4682.

Cheng, H., Dufu, K., Lee, C.-S., Hsu, J.L., Dias, A., and Reed, R. (2006). Human mRNA export machinery recruited to the 5' end of mRNA. Cell *127*, 1389–1400.

Chiu, S.-Y., Lejeune, F., Ranganathan, A.C., and Maquat, L.E. (2004). The pioneer translation initiation complex is functionally distinct from but structurally overlaps with the steady-state translation initiation complex. Genes Dev. *18*, 745–754.

Chiu, Y.-L., Ho, C.K.K., Saha, N., Schwer, B., Shuman, S., and Rana, T.M. (2002). Tat stimulates cotranscriptional capping of HIV mRNA. Mol. Cell *10*, 585–597.

Chlebowski, A., Lubas, M., Jensen, T.H., and Dziembowski, A. (2013). RNA decay machines: the exosome. Biochim. Biophys. Acta *1829*, 552–560.

Cho, E.-J., Takagi, T., Moore, C.R., and Buratowski, S. (1997). mRNA capping enzyme is recruited to the transcription complex by phosphorylation of the RNA polymerase II carboxy-terminal domain. Genes Dev. *11*, 3319–3326.

Cho, E.J., Rodriguez, C.R., Takagi, T., and Buratowski, S. (1998). Allosteric interactions between capping enzyme subunits and the RNA polymerase II carboxy-terminal domain. Genes Dev. *12*, 3482–3487.

Cho, R.J., Huang, M., Campbell, M.J., Dong, H., Steinmetz, L., Sapinoso, L., Hampton, G., Elledge, S.J., Davis, R.W., and Lockhart, D.J. (2001). Transcriptional regulation and function during the human cell cycle. Nat. Genet. *27*, 48–54.

Chodosh, L.A., Fire, A., Samuels, M., and Sharp, P.A. (1989). 5,6-Dichloro-1-beta-D-ribofuranosylbenzimidazole inhibits transcription elongation by RNA polymerase II in vitro. J. Biol. Chem. *264*, 2250–2257.

Choe, J., Oh, N., Park, S., Lee, Y.K., Song, O.-K., Locker, N., Chi, S.-G., and Kim, Y.K. (2012). Translation initiation on mRNAs bound by nuclear cap-binding protein complex CBP80/20 requires interaction between CBP80/20-dependent translation initiation factor and eukaryotic translation initiation factor 3g. J. Biol. Chem. *287*, 18500–18509.

Christova, R., and Oelgeschläger, T. (2002). Association of human TFIID-promoter complexes with silenced mitotic chromatin in vivo. Nat. Cell Biol. *4*, 79–82.

Chu, C., and Shatkin, A.J. (2008). Apoptosis and autophagy induction in mammalian cells by small interfering RNA knockdown of mRNA capping enzymes. Mol. Cell. Biol. *28*, 5829–5836.

Chu, C., Das, K., Tyminski, J.R., Bauman, J.D., Guan, R., Qiu, W., Montelione, G.T., Arnold, E., and Shatkin, A.J. (2011). Structure of the guanylyltransferase domain of human mRNA capping enzyme. Proc. Natl. Acad. Sci. U. S. A. *108*, 10104–10108.

Chuang, T.-W., Chang, W.-L., Lee, K.-M., and Tarn, W.-Y. (2013). The RNA-binding protein Y14 inhibits mRNA decapping and modulates processing body formation. Mol. Biol. Cell *24*, 1–13.

Cingolani, G., Petosa, C., Weis, K., and Müller, C.W. (1999). Structure of importin-beta bound to the IBB domain of importin-alpha. Nature *399*, 221–229.

Cohen, P. (2002). The origins of protein phosphorylation. Nat. Cell Biol. *4*, E127–30.

Cohen, N., Sharma, M., Kentsis, A., Perez, J.M., Strudwick, S., and Borden, K.L. (2001). PML RING suppresses oncogenic transformation by reducing the affinity of eIF4E for mRNA. EMBO J. *20*, 4547–4559.

Cole, M.D., and Cowling, V.H. (2009). Specific regulation of mRNA cap methylation by the c-Myc and E2F1 transcription factors. Oncogene *28*, 1169–1175.

Colot, H. V, Stutz, F., and Rosbash, M. (1996). The yeast splicing factor Mud13p is a commitment complex component and corresponds to CBP20, the small subunit of the nuclear cap-binding complex. Genes Dev. *10*, 1699–1708.

Conti, E., and Kuriyan, J. (2000). Crystallographic analysis of the specific yet versatile recognition of distinct nuclear localization signals by karyopherin alpha. Structure *8*, 329–338.

Conti, E., Uy, M., Leighton, L., Blobel, G., and Kuriyan, J. (1998). Crystallographic analysis of the recognition of a nuclear localization signal by the nuclear import factor karyopherin alpha. Cell *94*, 193–204.

Cooke, C., and Alwine, J.C. (1996). The cap and the 3' splice site similarly affect polyadenylation efficiency. Mol. Cell. Biol. *16*, 2579–2584.

Coppola, J.A., Field, A.S., and Luse, D.S. (1983). Promoter-proximal pausing by RNA polymerase II in vitro: transcripts shorter than 20 nucleotides are not capped. Proc. Natl. Acad. Sci. U. S. A. *80*, 1251–1255.

Cornelis, S., Bruynooghe, Y., Denecker, G., Van Huffel, S., Tinton, S., and Beyaert, R. (2000). Identification and characterization of a novel cell cycle-regulated internal ribosome entry site. Mol. Cell *5*, 597–605.

Cowling, V.H. (2009). Regulation of mRNA cap methylation. Biochem J *425*, 295–302.

Cowling, V.H. (2010). Enhanced mRNA cap methylation increases cyclin D1 expression and promotes cell transformation. Oncogene *29*, 930–936.

Cowling, V.H., and Cole, M.D. (2007a). The Myc transactivation domain promotes global phosphorylation of the RNA polymerase II carboxy-terminal domain independently of direct DNA binding. Mol Cell Biol *27*, 2059–2073.

Cowling, V.H., and Cole, M.D. (2007b). The Myc transactivation domain promotes global phosphorylation of the RNA polymerase II carboxy-terminal domain independently of direct DNA binding. Mol. Cell. Biol. *27*, 2059–2073.

Cowling, V.H., and Cole, M.D. (2007c). HATs off to capping: a new mechanism for Myc. Cell Cycle *6*, 907–909.

Crick, F. (1970). Central dogma of molecular biology. Nature *227*, 561–563.

Crick, F.H. (1958). Ideas on Protein Synthesis. In Symp. Soc. Exp. Biol., The Biological Replication of Marcromolecules, XII,.

Culjkovic, B., Topisirovic, I., Skrabanek, L., Ruiz-Gutierrez, M., and Borden, K.L.B. (2006). eIF4E is a central node of an RNA regulon that governs cellular proliferation. J. Cell Biol. *175*, 415–426.

Culjkovic-Kraljacic, B., and Borden, K.L.B. (2013). Aiding and abetting cancer: mRNA export and the nuclear pore. Trends Cell Biol. *23*, 328–335.

Dargemont, C., and Kühn, L.C. (1992). Export of mRNA from microinjected nuclei of Xenopus laevis oocytes. J. Cell Biol. *118*, 1–9.

Das, B., Guo, Z., Russo, P., Chartrand, P., and Sherman, F. (2000). The role of nuclear cap binding protein Cbc1p of yeast in mRNA termination and degradation. Mol. Cell. Biol. *20*, 2827–2838.

Dehlin, E., Wormington, M., Körner, C.G., and Wahle, E. (2000). Cap-dependent deadenylation of mRNA. EMBO J. *19*, 1079–1086.

Deribe, Y.L., Pawson, T., and Dikic, I. (2010). Post-translational modifications in signal integration. Nat. Struct. Mol. Biol. *17*, 666–672.

Dey, A., Nishiyama, A., Karpova, T., McNally, J., and Ozato, K. (2009). Brd4 marks select genes on mitotic chromatin and directs postmitotic transcription. Mol. Biol. Cell *20*, 4899–4909.

Dias, S.M.G., Wilson, K.F., Rojas, K.S., Ambrosio, A.L.B., and Cerione, R.A. (2009). The molecular basis for the regulation of the cap-binding complex by the importins. Nat. Struct. Mol. Biol. *16*, 930–937.

Van Dijk, E., Cougot, N., Meyer, S., Babajko, S., Wahle, E., and Séraphin, B. (2002). Human Dcp2: a catalytically active mRNA decapping enzyme located in specific cytoplasmic structures. EMBO J. *21*, 6915–6924.

Dingwall, C., Sharnick, S. V, and Laskey, R.A. (1982). A polypeptide domain that specifies migration of nucleoplasmin into the nucleus. Cell *30*, 449–458.

Dinkel, H., Michael, S., Weatheritt, R.J., Davey, N.E., Van Roey, K., Altenberg, B., Toedt, G., Uyar, B., Seiler, M., Budd, A., et al. (2012). ELM--the database of eukaryotic linear motifs. Nucleic Acids Res. *40*, D242–51.

Drummond, D.R., Armstrong, J., and Colman, A. (1985). The effect of capping and polyadenylation on the stability, movement and translation of synthetic messenger RNAs in Xenopus oocytes. Nucleic Acids Res. *13*, 7375–7394.

Dubois, M.F., Nguyen, V.T., Bellier, S., and Bensaude, O. (1994). Inhibitors of transcription such as 5,6-dichloro-1-beta-D-ribofuranosylbenzimidazole and isoquinoline sulfonamide derivatives (H-8 and H-7) promote dephosphorylation of the carboxyl-terminal domain of RNA polymerase II largest subunit. J. Biol. Chem. *269*, 13331–13336.

Dunckley, T., and Parker, R. (1999). The DCP2 protein is required for mRNA decapping in Saccharomyces cerevisiae and contains a functional MutT motif. EMBO J. *18*, 5411–5422.

Durand, S., and Lykke-Andersen, J. (2013). Nonsense-mediated mRNA decay occurs during eIF4F-dependent translation in human cells. Nat. Struct. Mol. Biol. *20*, 702–709.

Edery, I., and Sonenberg, N. (1985). Cap-dependent RNA splicing in a HeLa nuclear extract. Proc. Natl. Acad. Sci. U. S. A. *82*, 7590–7594.

Edery, I., Lee, K.A., and Sonenberg, N. (1984). Functional characterization of eukaryotic mRNA cap binding protein complex: effects on translation of capped and naturally uncapped RNAs. Biochemistry *23*, 2456–2462.

Endicott, J.A., Noble, M.E.M., and Johnson, L.N. (2012). The structural basis for control of eukaryotic protein kinases. Annu. Rev. Biochem. *81*, 587–613.

Fabrega, C., Shen, V., Shuman, S., and Lima, C.D. (2003). Structure of an mRNA capping enzyme bound to the phosphorylated carboxy-terminal domain of RNA polymerase II. Mol. Cell *11*, 1549–1561.

Fabrega, C., Hausmann, S., Shen, V., Shuman, S., and Lima, C.D. (2004). Structure and mechanism of mRNA cap (guanine-N7) methyltransferase. Mol. Cell *13*, 77–89.

Fan, H., and Penman, S. (1970). Regulation of protein synthesis in mammalian cells. II. Inhibition of protein synthesis at the level of initiation during mitosis. J. Mol. Biol. *50*, 655–670.

Feaver, W.J., Gileadi, O., Li, Y., and Kornberg, R.D. (1991). CTD kinase associated with yeast RNA polymerase II initiation factor b. Cell *67*, 1223–1230.

Fernandez-Sanchez, M.E., Gonatopoulos-Pournatzis, T., Preston, G., Lawlor, M. a, and Cowling, V.H. (2009). S-adenosyl homocysteine hydrolase is required for Myc-induced mRNA cap methylation, protein synthesis, and cell proliferation. Mol. Cell. Biol. *29*, 6182–6191.

Fisher, R.P. (2012). The CDK Network: Linking Cycles of Cell Division and Gene Expression. Genes Cancer *3*, 731–738.

Flaherty, S.M., Fortes, P., Izaurralde, E., Mattaj, I.W., and Gilmartin, G.M. (1997). Participation of the nuclear cap binding complex in pre-mRNA 3' processing. Proc. Natl. Acad. Sci. U. S. A. *94*, 11893–11898.

Fontes, M.R., Teh, T., and Kobe, B. (2000). Structural basis of recognition of monopartite and bipartite nuclear localization sequences by mammalian importin-alpha. J. Mol. Biol. *297*, 1183–1194.

Fortes, P., Kufel, J., Fornerod, M., Polycarpou-Schwarz, M., Lafontaine, D., Tollervey, D., and Mattaj, I.W. (1999). Genetic and physical interactions involving the yeast nuclear cap-binding complex. Mol. Cell. Biol. *19*, 6543–6553.

Fortes, P., Inada, T., Preiss, T., Hentze, M.W., Mattaj, I.W., and Sachs, A.B. (2000). The yeast nuclear cap binding complex can interact with translation factor eIF4G and mediate translation initiation. Mol. Cell *6*, 191–196.

Fresco, L.D., and Buratowski, S. (1996). Conditional mutants of the yeast mRNA capping enzyme show that the cap enhances, but is not required for, mRNA splicing. RNA *2*, 584–596.

Furuichi, Y., and Miura, K. (1975). A blocked structure at the 5' terminus of mRNA from cytoplasmic polyhedrosis virus. Nature *253*, 374–375.

Furuichi, Y., and Shatkin, A.J. (2000). Viral and cellular mRNA capping: past and prospects. Adv. Virus Res. *55*, 135–184.

Furuichi, Y., Morgan, M., Muthukrishnan, S., and Shatkin, A.J. (1975a). Reovirus messenger RNA contains a methylated, blocked 5'-terminal structure: m-7G(5')ppp(5')G-MpCp. Proc Natl Acad Sci U S A *72*, 362–366.

Furuichi, Y., Morgan, M., Shatkin, A.J., Jelinek, W., Salditt-Georgieff, M., and Darnell, J.E. (1975b). Methylated, blocked 5 termini in HeLa cell mRNA. Proc. Natl. Acad. Sci. U. S. A. *72*, 1904–1908.

Furuichi, Y., LaFiandra, A., and Shatkin, A.J. (1977). 5'-Terminal structure and mRNA stability. Nature *266*, 235–239.

Gaj, T., Gersbach, C.A., and Barbas, C.F. (2013). ZFN, TALEN, and CRISPR/Cas-based methods for genome engineering. Trends Biotechnol. *31*, 397–405.

Galbraith, M.D., Donner, A.J., and Espinosa, J.M. (2010). CDK8: a positive regulator of transcription. Transcription *1*, 4–12.

Gao, M., Fritz, D.T., Ford, L.P., and Wilusz, J. (2000). Interaction between a poly(A)-specific ribonuclease and the 5' cap influences mRNA deadenylation rates in vitro. Mol. Cell *5*, 479–488.

Garneau, N.L., Wilusz, J., and Wilusz, C.J. (2007). The highways and byways of mRNA decay. Nat. Rev. Mol. Cell Biol. *8*, 113–126.

Georgiev, O., Mous, J., and Birnstiel, M.L. (1984). Processing and nucleo-cytoplasmic transport of histone gene transcripts. Nucleic Acids Res. *12*, 8539–8551.

Ghosh, A., Shuman, S., and Lima, C.D. (2011). Structural Insights to How Mammalian Capping Enzyme Reads the CTD Code. Mol. Cell *43*, 299–310.

Di Giammartino, D.C., Nishida, K., and Manley, J.L. (2011). Mechanisms and consequences of alternative polyadenylation. Mol. Cell *43*, 853–866.

Gilchrist, D., Mykytka, B., and Rexach, M. (2002). Accelerating the rate of disassembly of karyopherin.cargo complexes. J. Biol. Chem. *277*, 18161–18172.

Gillian-Daniel, D.L., Gray, N.K., Aström, J., Barkoff, A., and Wickens, M. (1998). Modifications of the 5' cap of mRNAs during Xenopus oocyte maturation: independence from changes in poly(A) length and impact on translation. Mol. Cell. Biol. *18*, 6152–6163.

Gilmartin, G.M., McDevitt, M.A., and Nevins, J.R. (1988). Multiple factors are required for specific RNA cleavage at a poly(A) addition site. Genes Dev. *2*, 578–587.

Gingras, A.C., Raught, B., and Sonenberg, N. (1999). eIF4 initiation factors: effectors of mRNA recruitment to ribosomes and regulators of translation. Annu. Rev. Biochem. *68*, 913–963.

Glover-Cutter, K., Kim, S., Espinosa, J., and Bentley, D.L. (2008). RNA polymerase II pauses and associates with pre-mRNA processing factors at both ends of genes. Nat Struct Mol Biol *15*, 71–78.

Goldfarb, D.S., Corbett, A.H., Mason, D.A., Harreman, M.T., and Adam, S.A. (2004). Importin alpha: a multipurpose nuclear-transport receptor. Trends Cell Biol. *14*, 505–514.

Gonatopoulos-Pournatzis, T., Dunn, S., Bounds, R., and Cowling, V.H. (2011). RAM/Fam103a1 Is Required for mRNA Cap Methylation. Mol. Cell *44*, 585–596.

Görlich, D., Kraft, R., Kostka, S., Vogel, F., Hartmann, E., Laskey, R.A., Mattaj, I.W., and Izaurralde, E. (1996). Importin provides a link between nuclear protein import and U snRNA export. Cell *87*, 21–32.

Green, M.R., Maniatis, T., and Melton, D.A. (1983). Human beta-globin pre-mRNA synthesized in vitro is accurately spliced in Xenopus oocyte nuclei. Cell *32*, 681–694.

Gross, J.D., Moerke, N.J., von der Haar, T., Lugovskoy, A.A., Sachs, A.B., McCarthy, J.E.G., and Wagner, G. (2003). Ribosome loading onto the mRNA cap is driven by conformational coupling between eIF4G and eIF4E. Cell *115*, 739–750.

Gruber, J.J., Zatechka, D.S., Sabin, L.R., Yong, J., Lum, J.J., Kong, M., Zong, W.-X., Zhang, Z., Lau, C.-K., Rawlings, J., et al. (2009). Ars2 links the nuclear cap-binding complex to RNA interference and cell proliferation. Cell *138*, 328–339.

Gruber, J.J., Olejniczak, S.H., Yong, J., La Rocca, G., Dreyfuss, G., and Thompson, C.B. (2012). Ars2 promotes proper replication-dependent histone mRNA 3' end formation. Mol. Cell *45*, 87–98.

Grudzien, E., Kalek, M., Jemielity, J., Darzynkiewicz, E., and Rhoads, R.E. (2006). Differential inhibition of mRNA degradation pathways by novel cap analogs. J. Biol. Chem. *281*, 1857–1867.

Gu, M., Rajashankar, K.R., and Lima, C.D. (2010). Structure of the Saccharomyces cerevisiae Cet1-Ceg1 mRNA capping apparatus. Structure *18*, 216–227.

Guenther, M.G., Levine, S.S., Boyer, L.A., Jaenisch, R., and Young, R.A. (2007). A chromatin landmark and transcription initiation at most promoters in human cells. Cell *130*, 77–88.

Guiguen, A., Soutourina, J., Dewez, M., Tafforeau, L., Dieu, M., Raes, M., Vandenhaute, J., Werner, M., and Hermand, D. (2007). Recruitment of P-TEFb (Cdk9-Pch1) to chromatin by the cap-methyl transferase Pcm1 in fission yeast. EMBO J. *26*, 1552–1559.

Güttinger, S., Laurell, E., and Kutay, U. (2009). Orchestrating nuclear envelope disassembly and reassembly during mitosis. Nat. Rev. Mol. Cell Biol. *10*, 178–191.

Haghighat, A., and Sonenberg, N. (1997). eIF4G dramatically enhances the binding of eIF4E to the mRNA 5'-cap structure. J. Biol. Chem. *272*, 21677–21680.

Haghighat, A., Mader, S., Pause, A., and Sonenberg, N. (1995). Repression of cap-dependent translation by 4E-binding protein 1: competition with p220 for binding to eukaryotic initiation factor-4E. EMBO J. *14*, 5701–5709.

Håkansson, K., and Wigley, D.B. (1998). Structure of a complex between a cap analogue and mRNA guanylyl transferase demonstrates the structural chemistry of RNA capping. Proc. Natl. Acad. Sci. U. S. A. *95*, 1505–1510.

Håkansson, K., Doherty, A.J., Shuman, S., and Wigley, D.B. (1997). X-ray crystallography reveals a large conformational change during guanyl transfer by mRNA capping enzymes. Cell *89*, 545–553.

Hamm, J., and Mattaj, I.W. (1990). Monomethylated cap structures facilitate RNA export from the nucleus. Cell *63*, 109–118.

Hartl, P., Gottesfeld, J., and Forbes, D.J. (1993). Mitotic repression of transcription in vitro. J. Cell Biol. *120*, 613–624.

Heesom, K.J., Gampel, a, Mellor, H., and Denton, R.M. (2001). Cell cycle-dependent phosphorylation of the translational repressor eIF-4E binding protein-1 (4E-BP1). Curr. Biol. *11*, 1374–1379.

Heidemann, M., Hintermair, C., Voß, K., and Eick, D. (2013). Dynamic phosphorylation patterns of RNA polymerase II CTD during transcription. Biochim. Biophys. Acta *1829*, 55–62.

Heix, J., Vente, A., Voit, R., Budde, A., Michaelidis, T.M., and Grummt, I. (1998). Mitotic silencing of human rRNA synthesis: inactivation of the promoter selectivity factor SL1 by cdc2/cyclin B-mediated phosphorylation. EMBO J. *17*, 7373–7381.

Hendzel, M.J., Wei, Y., Mancini, M.A., Van Hooser, A., Ranalli, T., Brinkley, B.R., Bazett-Jones, D.P., and Allis, C.D. (1997). Mitosis-specific phosphorylation of histone H3 initiates primarily within pericentromeric heterochromatin during G2 and spreads in an ordered fashion coincident with mitotic chromosome condensation. Chromosoma *106*, 348–360.

Hentze, M.W. (1997). eIF4G: a multipurpose ribosome adapter? Science (80-.). *275*, 500–501.

Hickey, E.D., Weber, L.A., and Baglioni, C. (1976). Inhibition of initiation of protein synthesis by 7-methylguanosine-5'-monophosphate. Proc. Natl. Acad. Sci. U. S. A. *73*, 19–23.

Ho, C.K., and Shuman, S. (1999). Distinct roles for CTD Ser-2 and Ser-5 phosphorylation in the recruitment and allosteric activation of mammalian mRNA capping enzyme. Mol. Cell *3*, 405–411.

Ho, C.K., Sriskanda, V., McCracken, S., Bentley, D., Schwer, B., and Shuman, S. (1998). The guanylyltransferase domain of mammalian mRNA capping enzyme binds to the phosphorylated carboxyl-terminal domain of RNA polymerase II. J Biol Chem *273*, 9577–9585.

Hocine, S., Singer, R.H., and Grünwald, D. (2010). RNA processing and export. Cold Spring Harb. Perspect. Biol. *2*, a000752.

Hornbeck, P. V, Kornhauser, J.M., Tkachev, S., Zhang, B., Skrzypek, E., Murray, B., Latham, V., and Sullivan, M. (2012). PhosphoSitePlus: a comprehensive resource for investigating the structure and function of experimentally determined post-translational modifications in man and mouse. Nucleic Acids Res. *40*, D261–70.

Hoskins, A.A., and Moore, M.J. (2012). The spliceosome: a flexible, reversible macromolecular machine. Trends Biochem. Sci. *37*, 179–188.

Hossain, M.A., Chung, C., Pradhan, S.K., and Johnson, T.L. (2013). The yeast cap binding complex modulates transcription factor recruitment and establishes proper histone H3K36 trimethylation during active transcription. Mol. Cell. Biol. *33*, 785–799.

Hsieh, A.C., Liu, Y., Edlind, M.P., Ingolia, N.T., Janes, M.R., Sher, A., Shi, E.Y., Stumpf, C.R., Christensen, C., Bonham, M.J., et al. (2012). The translational landscape of mTOR signalling steers cancer initiation and metastasis. Nature *485*, 55–61.

Hsin, J.-P., and Manley, J.L. (2012). The RNA polymerase II CTD coordinates transcription and RNA processing. Genes Dev. *26*, 2119–2137.

Iaquinta, P.J., and Lees, J.A. (2007). Life and death decisions by the E2F transcription factors. Curr. Opin. Cell Biol. *19*, 649–657.

Inoue, K., Ohno, M., Sakamoto, H., and Shimura, Y. (1989). Effect of the cap structure on pre-mRNA splicing in Xenopus oocyte nuclei. Genes Dev. *3*, 1472–1479.

Ishigaki, Y., Li, X., Serin, G., and Maquat, L.E. (2001). Evidence for a pioneer round of mRNA translation: mRNAs subject to nonsense-mediated decay in mammalian cells are bound by CBP80 and CBP20. Cell *106*, 607–617.

Iwasaki, S., and Tomari, Y. (2009). Argonaute-mediated translational repression (and activation). Fly (Austin). *3*, 204–206.

Iwasaki, S., Kawamata, T., and Tomari, Y. (2009). Drosophila argonaute1 and argonaute2 employ distinct mechanisms for translational repression. Mol. Cell *34*, 58–67.

Izaurralde, E., Stepinski, J., Darzynkiewicz, E., and Mattaj, I.W. (1992). A cap binding protein that may mediate nuclear export of RNA polymerase II-transcribed RNAs. J. Cell Biol. *118*, 1287–1295.

Izaurralde, E., Lewis, J., McGuigan, C., Jankowska, M., Darzynkiewicz, E., and Mattaj, I.W. (1994). A nuclear cap binding protein complex involved in pre-mRNA splicing. Cell *78*, 657–668.

Izaurralde, E., Lewis, J., Gamberi, C., Jarmolowski, A., McGuigan, C., and Mattaj, I.W. (1995a). A cap-binding protein complex mediating U snRNA export. Nature *376*, 709–712.

Izaurralde, E., McGuigan, C., and Mattaj, I.W. (1995b). Nuclear localization of a cap-binding protein complex. Cold Spring Harb. Symp. Quant. Biol. *60*, 669–675.

Jackson, R.J., Hellen, C.U.T., and Pestova, T. V (2010). The mechanism of eukaryotic translation initiation and principles of its regulation. Nat. Rev. Mol. Cell Biol. *11*, 113–127.

Jarmolowski, A., Boelens, W.C., Izaurralde, E., and Mattaj, I.W. (1994). Nuclear export of different classes of RNA is mediated by specific factors. J Cell Biol *124*, 627–635.

Jeffrey, P.D., Russo, A.A., Polyak, K., Gibbs, E., Hurwitz, J., Massagué, J., and Pavletich, N.P. (1995). Mechanism of CDK activation revealed by the structure of a cyclinA-CDK2 complex. Nature *376*, 313–320.

Jiao, X., Xiang, S., Oh, C., Martin, C.E., Tong, L., and Kiledjian, M. (2010). Identification of a quality-control mechanism for mRNA 5'-end capping. Nature *467*, 608–611.

Jiao, X., Chang, J.H., Kilic, T., Tong, L., and Kiledjian, M. (2013). A Mammalian Pre-mRNA 5' End Capping Quality Control Mechanism and an Unexpected Link of Capping to Pre-mRNA Processing. Mol. Cell *50*, 104–115.

Johnson, D.G., and Walker, C.L. (1999). Cyclins and cell cycle checkpoints. Annu. Rev. Pharmacol. Toxicol. *39*, 295–312.

Jove, R., and Manley, J.L. (1984). In vitro transcription from the adenovirus 2 major late promoter utilizing templates truncated at promoter-proximal sites. J. Biol. Chem. *259*, 8513–8521.

Kadauke, S., and Blobel, G.A. (2013). Mitotic bookmarking by transcription factors. Epigenetics Chromatin *6*, 6.

Kahvejian, A., Svitkin, Y. V, Sukarieh, R., M'Boutchou, M.-N., and Sonenberg, N. (2005). Mammalian poly(A)-binding protein is a eukaryotic translation initiation factor, which acts via multiple mechanisms. Genes Dev. *19*, 104–113.

Kalderon, D., Richardson, W.D., Markham, A.F., and Smith, A.E. (1984). Sequence requirements for nuclear location of simian virus 40 large-T antigen. Nature *311*, 33–38.

Kann, M., Sodeik, B., Vlachou, A., Gerlich, W.H., and Helenius, A. (1999). Phosphorylation-dependent binding of hepatitis B virus core particles to the nuclear pore complex. J. Cell Biol. *145*, 45–55.

Kataoka, N., Ohno, M., Moda, I., and Shimura, Y. (1995). Identification of the factors that interact with NCBP, an 80 kDa nuclear cap binding protein. Nucleic Acids Res. *23*, 3638–3641.

Khaleghpour, K., Pyronnet, S., Gingras, A.C., and Sonenberg, N. (1999). Translational homeostasis: eukaryotic translation initiation factor 4E control of 4E-binding protein 1 and p70 S6 kinase activities. Mol. Cell. Biol. *19*, 4302–4310.

Khanna, R., and Kiledjian, M. (2004). Poly(A)-binding-protein-mediated regulation of hDcp2 decapping in vitro. EMBO J. *23*, 1968–1976.

Kim, J.H., Paek, K.Y., Choi, K., Kim, T.-D., Hahm, B., Kim, K.-T., and Jang, S.K. (2003). Heterogeneous nuclear ribonucleoprotein C modulates translation of c-myc mRNA in a cell cycle phase-dependent manner. Mol. Cell. Biol. *23*, 708–720.

Kim, K.M., Cho, H., Choi, K., Kim, J., Kim, B.-W., Ko, Y.-G., Jang, S.K., and Kim, Y.K. (2009). A new MIF4G domain-containing protein, CTIF, directs nuclear cap-binding protein CBP80/20-dependent translation. Genes Dev. *23*, 2033–2045.

Kim, T.H., Barrera, L.O., Zheng, M., Qu, C., Singer, M.A., Richmond, T.A., Wu, Y., Green, R.D., and Ren, B. (2005). A high-resolution map of active promoters in the human genome. Nature *436*, 876–880.

King, R.W., Deshaies, R.J., Peters, J.M., and Kirschner, M.W. (1996). How proteolysis drives the cell cycle. Science (80-.). *274*, 1652–1659.

Kitamura, R., Sekimoto, T., Ito, S., Harada, S., Yamagata, H., Masai, H., Yoneda, Y., and Yanagi, K. (2006). Nuclear Import of Epstein-Barr Virus Nuclear Antigen 1 Mediated by NPI-1 (Importin 5) Is Up- and Down-Regulated by Phosphorylation of the Nuclear Localization Signal for Which Lys379 and Arg380 Are Essential. J. Virol. *80*, 1979–1991.

Kitao, S., Segref, A., Kast, J., Wilm, M., Mattaj, I.W., and Ohno, M. (2008). A compartmentalized phosphorylation/dephosphorylation system that regulates U snRNA export from the nucleus. Mol. Cell. Biol. *28*, 487–497.

Klein, J., and Grummt, I. (1999). Cell cycle-dependent regulation of RNA polymerase I transcription: the nucleolar transcription factor UBF is inactive in mitosis and early G1. Proc. Natl. Acad. Sci. U. S. A. *96*, 6096–6101.

Kobe, B. (1999). Autoinhibition by an internal nuclear localization signal revealed by the crystal structure of mammalian importin alpha. Nat. Struct. Biol. *6*, 388–397.

Köhler, A., and Hurt, E. (2007). Exporting RNA from the nucleus to the cytoplasm. Nat. Rev. Mol. Cell Biol. *8*, 761–773.

Komar, A.A., and Hatzoglou, M. (2011). Cellular IRES-mediated translation: the war of ITAFs in pathophysiological states. Cell Cycle *10*, 229–240.

Komarnitsky, P., Cho, E.-J., and Buratowski, S. (2000). Different phosphorylated forms of RNA polymerase II and associated mRNA processing factors during transcription. Genes Dev. *14*, 2452–2460.

Konarska, M.M., Padgett, R.A., and Sharp, P.A. (1984). Recognition of cap structure in splicing in vitro of mRNA precursors. Cell *38*, 731–736.

Koromilas, A.E., Lazaris-Karatzas, A., and Sonenberg, N. (1992). mRNAs containing extensive secondary structure in their 5' non-coding region translate efficiently in cells overexpressing initiation factor eIF-4E. EMBO J. *11*, 4153–4158.

LaGrandeur, T.E., and Parker, R. (1998). Isolation and characterization of Dcp1p, the yeast mRNA decapping enzyme. EMBO J. *17*, 1487–1496.

Lahudkar, S., Shukla, A., Bajwa, P., Durairaj, G., Stanojevic, N., and Bhaumik, S.R. (2011). The mRNA cap-binding complex stimulates the formation of pre-initiation complex at the promoter via its interaction with Mot1p in vivo. Nucleic Acids Res. *39*, 2188–2209.

Lamphear, B.J., Kirchweger, R., Skern, T., and Rhoads, R.E. (1995). Mapping of functional domains in eukaryotic protein synthesis initiation factor 4G (eIF4G) with picornaviral proteases. Implications for cap-dependent and cap-independent translational initiation. J. Biol. Chem. *270*, 21975–21983.

Laubinger, S., Sachsenberg, T., Zeller, G., Busch, W., Lohmann, J.U., Rätsch, G., and Weigel, D. (2008). Dual roles of the nuclear cap-binding complex and SERRATE in pre-mRNA splicing and microRNA processing in Arabidopsis thaliana. Proc. Natl. Acad. Sci. U. S. A. *105*, 8795–8800.

Lazaris-Karatzas, A., Montine, K.S., and Sonenberg, N. (1990). Malignant transformation by a eukaryotic initiation factor subunit that binds to mRNA 5' cap. Nature *345*, 544–547.

Lejeune, F., Ishigaki, Y., Li, X., and Maquat, L.E. (2002). The exon junction complex is detected on CBP80-bound but not eIF4E-bound mRNA in mammalian cells: dynamics of mRNP remodeling. EMBO J. *21*, 3536–3545.

Lejeune, F., Ranganathan, A.C., and Maquat, L.E. (2004). eIF4G is required for the pioneer round of translation in mammalian cells. Nat. Struct. Mol. Biol. *11*, 992–1000.

Lenasi, T., Peterlin, B.M., and Barboric, M. (2011). Cap-binding protein complex links pre-mRNA capping to transcription elongation and alternative splicing through positive transcription elongation factor b (P-TEFb). J. Biol. Chem. *286*, 22758–22768.

Lewis, J.D., Izaurralde, E., Jarmolowski, A., McGuigan, C., and Mattaj, I.W. (1996). A nuclear cap-binding complex facilitates association of U1 snRNP with the cap-proximal 5' splice site. Genes Dev. *10*, 1683–1698.

Li, J., Meyer, A.N., and Donoghue, D.J. (1997). Nuclear localization of cyclin B1 mediates its biological activity and is regulated by phosphorylation. Proc. Natl. Acad. Sci. U. S. A. *94*, 502–507.

Lidschreiber, M., Leike, K., and Cramer, P. (2013). Cap completion and CTD kinase recruitment underlie the initiation-elongation transition of RNA polymerase II. Mol. Cell. Biol. *33*.

Lim, S.K., and Maquat, L.E. (1992). Human beta-globin mRNAs that harbor a nonsense codon are degraded in murine erythroid tissues to intermediates lacking regions of exon I or exons I and II that have a cap-like structure at the 5' termini. EMBO J. *11*, 3271–3278.

Lima, C.D., Wang, L.K., and Shuman, S. (1999). Structure and mechanism of yeast RNA triphosphatase: an essential component of the mRNA capping apparatus. Cell *99*, 533–543.

Lindstrom, D.L., Squazzo, S.L., Muster, N., Burckin, T.A., Wachter, K.C., Emigh, C.A., McCleery, J.A., Yates, J.R., and Hartzog, G.A. (2003). Dual roles for Spt5 in pre-mRNA processing and transcription elongation revealed by identification of Spt5-associated proteins. Mol. Cell. Biol. *23*, 1368–1378.

Listerman, I., Sapra, A.K., and Neugebauer, K.M. (2006). Cotranscriptional coupling of splicing factor recruitment and precursor messenger RNA splicing in mammalian cells. Nat. Struct. Mol. Biol. *13*, 815–822.

Liu, H., Rodgers, N.D., Jiao, X., and Kiledjian, M. (2002). The scavenger mRNA decapping enzyme DcpS is a member of the HIT family of pyrophosphatases. EMBO J. *21*, 4699–4708.

Liu, P., Kenney, J.M., Stiller, J.W., and Greenleaf, A.L. (2010). Genetic organization, length conservation, and evolution of RNA polymerase II carboxyl-terminal domain. Mol. Biol. Evol. *27*, 2628–2641.

Long, J.J., Leresche, A., Kriwacki, R.W., and Gottesfeld, J.M. (1998). Repression of TFIIH transcriptional activity and TFIIH-associated cdk7 kinase activity at mitosis. Mol. Cell. Biol. *18*, 1467–1476.

Lu, H., Flores, O., Weinmann, R., and Reinberg, D. (1991). The nonphosphorylated form of RNA polymerase II preferentially associates with the preinitiation complex. Proc. Natl. Acad. Sci. U. S. A. *88*, 10004–10008.

Lu, H., Zawel, L., Fisher, L., Egly, J.M., and Reinberg, D. (1992). Human general transcription factor IIH phosphorylates the C-terminal domain of RNA polymerase II. Nature *358*, 641–645.

Lykke-Andersen, J. (2002). Identification of a human decapping complex associated with hUpf proteins in nonsense-mediated decay. Mol. Cell. Biol. *22*, 8114–8121.

Mader, S., Lee, H., Pause, A., and Sonenberg, N. (1995). The translation initiation factor eIF-4E binds to a common motif shared by the translation factor eIF-4 gamma and the translational repressors 4E-binding proteins. Mol. Cell. Biol. *15*, 4990–4997.

Maderazo, A.B., Belk, J.P., He, F., and Jacobson, A. (2003). Nonsense-containing mRNAs that accumulate in the absence of a functional nonsense-mediated mRNA decay pathway are destabilized rapidly upon its restitution. Mol. Cell. Biol. *23*, 842–851.

Mandal, S.S., Chu, C., Wada, T., Handa, H., Shatkin, A.J., and Reinberg, D. (2004). Functional interactions of RNA-capping enzyme with factors that positively and negatively regulate promoter escape by RNA polymerase II. Proc. Natl. Acad. Sci. U. S. A. *101*, 7572–7577.

Manning, G., Whyte, D.B., Martinez, R., Hunter, T., and Sudarsanam, S. (2002). The protein kinase complement of the human genome. Science (80-.). *298*, 1912–1934.

Mao, X., Schwer, B., and Shuman, S. (1995). Yeast mRNA cap methyltransferase is a 50-kilodalton protein encoded by an essential gene. Mol. Cell. Biol. *15*, 4167–4174.

Mao, X., Schwer, B., and Shuman, S. (1996). Mutational analysis of the Saccharomyces cerevisiae ABD1 gene: cap methyltransferase activity is essential for cell growth. Mol. Cell. Biol. *16*, 475–480.

Maquat, L.E., Tarn, W.-Y., and Isken, O. (2010). The pioneer round of translation: features and functions. Cell *142*, 368–374.

Marcotrigiano, J., Gingras, A.C., Sonenberg, N., and Burley, S.K. (1997). Cocrystal structure of the messenger RNA 5' cap-binding protein (eIF4E) bound to 7-methyl-GDP. Cell *89*, 951–961.

Marcotrigiano, J., Gingras, A.C., Sonenberg, N., and Burley, S.K. (1999). Cap-dependent translation initiation in eukaryotes is regulated by a molecular mimic of eIF4G. Mol. Cell *3*, 707–716.

Marshall, N.F., Peng, J., Xie, Z., and Price, D.H. (1996). Control of RNA polymerase II elongation potential by a novel carboxyl-terminal domain kinase. J. Biol. Chem. *271*, 27176–27183.

Martin, D.M.A., Miranda-Saavedra, D., and Barton, G.J. (2009). Kinomer v. 1.0: a database of systematically classified eukaryotic protein kinases. Nucleic Acids Res. *37*, D244–50.

Martinez, J., Ren, Y.G., Thuresson, A.C., Hellman, U., Astrom, J., and Virtanen, A. (2000). A 54-kDa fragment of the Poly(A)-specific ribonuclease is an oligomeric, processive, and cap-interacting Poly(A)-specific 3' exonuclease. J. Biol. Chem. *275*, 24222–24230.

Marzluff, W.F., Wagner, E.J., and Duronio, R.J. (2008). Metabolism and regulation of canonical histone mRNAs: life without a poly(A) tail. Nat. Rev. Genet. *9*, 843–854.

Matsuura, Y., and Stewart, M. (2005). Nup50/Npap60 function in nuclear protein import complex disassembly and importin recycling. EMBO J. *24*, 3681–3689.

Matsuura, Y., Lange, A., Harreman, M.T., Corbett, A.H., and Stewart, M. (2003). Structural basis for Nup2p function in cargo release and karyopherin recycling in nuclear import. EMBO J. *22*, 5358–5369.

Max, T., Søgaard, M., and Svejstrup, J.Q. (2007). Hyperphosphorylation of the C-terminal repeat domain of RNA polymerase II facilitates dissociation of its complex with mediator. J. Biol. Chem. *282*, 14113–14120.

Mazza, C., Ohno, M., Segref, A., Mattaj, I.W., and Cusack, S. (2001). Crystal structure of the human nuclear cap binding complex. Mol. Cell *8*, 383–396.

Mazza, C., Segref, A., Mattaj, I.W., and Cusack, S. (2002). Co-crystallization of the human nuclear cap-binding complex with a m7GpppG cap analogue using protein engineering. Acta Crystallogr. D. Biol. Crystallogr. *58*, 2194–2197.

McCloskey, a., Taniguchi, I., Shinmyozu, K., and Ohno, M. (2012). hnRNP C Tetramer Measures RNA Length to Classify RNA Polymerase II Transcripts for Export. Science (80-.). *335*, 1643–1646.

McCracken, S., Fong, N., Rosonina, E., Yankulov, K., Brothers, G., Siderovski, D., Hessel, A., Foster, S., Shuman, S., and Bentley, D.L. (1997). 5'-Capping enzymes are targeted to pre-mRNA by binding to the phosphorylated carboxy-terminal domain of RNA polymerase II. Genes Dev *11*, 3306–3318.

McKendrick, L., Thompson, E., Ferreira, J., Morley, S.J., and Lewis, J.D. (2001). Interaction of eukaryotic translation initiation factor 4G with the nuclear cap-binding complex provides a link between nuclear and cytoplasmic functions of the m(7) guanosine cap. Mol. Cell. Biol. *21*, 3632–3641.

Meijer, L., and Raymond, E. (2003). Roscovitine and other purines as kinase inhibitors. From starfish oocytes to clinical trials. Acc. Chem. Res. *36*, 417–425.

Meijer, H.A., Kong, Y.W., Lu, W.T., Wilczynska, A., Spriggs, R. V., Robinson, S.W., Godfrey, J.D., Willis, A.E., and Bushell, M. (2013). Translational Repression and eIF4A2 Activity Are Critical for MicroRNA-Mediated Gene Regulation. Science (80-.). *340*, 82–85.

Meyer, N., and Penn, L.Z. (2008). Reflecting on 25 years with MYC. Nat. Rev. Cancer *8*, 976–990.

Minich, W.B., Balasta, M.L., Goss, D.J., and Rhoads, R.E. (1994). Chromatographic resolution of in vivo phosphorylated and nonphosphorylated eukaryotic translation initiation factor eIF-4E: increased cap affinity of the phosphorylated form. Proc. Natl. Acad. Sci. U. S. A. *91*, 7668–7672.

Morgan, D.O. (1997). Cyclin-dependent kinases: engines, clocks, and microprocessors. Annu. Rev. Cell Dev. Biol. *13*, 261–291.

Moroianu, J., Blobel, G., and Radu, A. (1997). RanGTP-mediated nuclear export of karyopherin alpha involves its interaction with the nucleoporin Nup153. Proc. Natl. Acad. Sci. U. S. A. *94*, 9699–9704.

Moteki, S., and Price, D. (2002). Functional Coupling of Capping and Transcription of mRNA. Mol. Cell *10*, 599–609.

Mukherjee, C., Patil, D.P., Kennedy, B.A., Bakthavachalu, B., Bundschuh, R., and Schoenberg, D.R. (2012). Identification of cytoplasmic capping targets reveals a role for cap homeostasis in translation and mRNA stability. Cell Rep. *2*, 674–684.

Murthy, K.G., Park, P., and Manley, J.L. (1991). A nuclear micrococcal-sensitive, ATP-dependent exoribonuclease degrades uncapped but not capped RNA substrates. Nucleic Acids Res *19*, 2685–2692.

Muthukrishnan, S., Both, G.W., Furuichi, Y., and Shatkin, A.J. (1975). 5'-Terminal 7-methylguanosine in eukaryotic mRNA is required for translation. Nature *255*, 33–37.

Nagarajan, V.K., Jones, C.I., Newbury, S.F., and Green, P.J. (2013). XRN 5'→3' exoribonucleases: structure, mechanisms and functions. Biochim. Biophys. Acta *1829*, 590–603.

Nardozzi, J.D., Lott, K., and Cingolani, G. (2010). Phosphorylation meets nuclear import: a review. Cell Commun. Signal. *8*, 32.

Narita, T., Yung, T.M.C., Yamamoto, J., Tsuboi, Y., Tanabe, H., Tanaka, K., Yamaguchi, Y., and Handa, H. (2007). NELF interacts with CBC and participates in 3' end processing of replication-dependent histone mRNAs. Mol. Cell *26*, 349–365.

Nie, Z., Hu, G., Wei, G., Cui, K., Yamane, A., Resch, W., Wang, R., Green, D.R., Tessarollo, L., Casellas, R., et al. (2012). c-Myc is a universal amplifier of expressed genes in lymphocytes and embryonic stem cells. Cell *151*, 68–79.

Niedzwiecka, A., Marcotrigiano, J., Stepinski, J., Jankowska-Anyszka, M., Wyslouch-Cieszynska, A., Dadlez, M., Gingras, A.C., Mak, P., Darzynkiewicz, E., Sonenberg, N., et al. (2002). Biophysical studies of eIF4E cap-binding protein: recognition of mRNA 5' cap structure and synthetic fragments of eIF4G and 4E-BP1 proteins. J. Mol. Biol. *319*, 615–635.

Nojima, T., Hirose, T., Kimura, H., and Hagiwara, M. (2007). The interaction between cap-binding complex and RNA export factor is required for intronless mRNA export. J. Biol. Chem. *282*, 15645–15651.

Obenauer, J.C., Cantley, L.C., and Yaffe, M.B. (2003). Scansite 2.0: Proteome-wide prediction of cell signaling interactions using short sequence motifs. Nucleic Acids Res. *31*, 3635–3641.

Ohno, M., Sakamoto, H., and Shimura, Y. (1987). Preferential excision of the 5' proximal intron from mRNA precursors with two introns as mediated by the cap structure. Proc. Natl. Acad. Sci. U. S. A. *84*, 5187–5191.

Ohno, M., Segref, A., Bachi, A., Wilm, M., and Mattaj, I.W. (2000). PHAX, a mediator of U snRNA nuclear export whose activity is regulated by phosphorylation. Cell *101*, 187–198.

Orphanides, G. (2002). A Unified Theory of Gene Expression. Cell *108*, 439–451.

Orphanides, G., Lagrange, T., and Reinberg, D. (1996). The general transcription factors of RNA polymerase II. Genes Dev. *10*, 2657–2683.

Otsuka, Y., Kedersha, N.L., and Schoenberg, D.R. (2009). Identification of a cytoplasmic complex that adds a cap onto 5'-monophosphate RNA. Mol. Cell. Biol. *29*, 2155–2167.

Pabis, M., Neufeld, N., Steiner, M.C., Bojic, T., Shav-Tal, Y., and Neugebauer, K.M. (2013). The nuclear cap-binding complex interacts with the U4/U6·U5 tri-snRNP and promotes spliceosome assembly in mammalian cells. RNA *19*, 1054–1063.

Pan, Q., Shai, O., Lee, L.J., Frey, B.J., and Blencowe, B.J. (2008). Deep surveying of alternative splicing complexity in the human transcriptome by high-throughput sequencing. Nat. Genet. *40*, 1413–1415.

Parsons, G.G., and Spencer, C.A. (1997). Mitotic repression of RNA polymerase II transcription is accompanied by release of transcription elongation complexes. Mol. Cell. Biol. *17*, 5791–5802.

Patzelt, E., Thalmann, E., Hartmuth, K., Blaas, D., and Kuechler, E. (1987). Assembly of pre-mRNA splicing complex is cap dependent. Nucleic Acids Res. *15*, 1387–1399.

Pause, A., Belsham, G.J., Gingras, A.C., Donzé, O., Lin, T.A., Lawrence, J.C., and Sonenberg, N. (1994). Insulin-dependent stimulation of protein synthesis by phosphorylation of a regulator of 5'-cap function. Nature *371*, 762–767.

Pei, Y., and Shuman, S. (2002). Interactions between fission yeast mRNA capping enzymes and elongation factor Spt5. J. Biol. Chem. *277*, 19639–19648.

Pei, Y., Schwer, B., Hausmann, S., and Shuman, S. (2001). Characterization of Schizosaccharomyces pombe RNA triphosphatase. Nucleic Acids Res. *29*, 387–396.

Pei, Y., Schwer, B., and Shuman, S. (2003). Interactions between fission yeast Cdk9, its cyclin partner Pch1, and mRNA capping enzyme Pct1 suggest an elongation checkpoint for mRNA quality control. J. Biol. Chem. *278*, 7180–7188.

Petricoin, E.F., Espina, V., Araujo, R.P., Midura, B., Yeung, C., Wan, X., Eichler, G.S., Johann, D.J., Qualman, S., Tsokos, M., et al. (2007). Phosphoprotein pathway mapping: Akt/mammalian target of rapamycin activation is negatively associated with childhood rhabdomyosarcoma survival. Cancer Res. *67*, 3431–3440.

Pillai, R.S., Bhattacharyya, S.N., Artus, C.G., Zoller, T., Cougot, N., Basyuk, E., Bertrand, E., and Filipowicz, W. (2005). Inhibition of translational initiation by Let-7 MicroRNA in human cells. Science (80-.). *309*, 1573–1576.

Pillutla, R.C., Shimamoto, A., Furuichi, Y., and Shatkin, A.J. (1998a). Human mRNA capping enzyme (RNGTT) and cap methyltransferase (RNMT) map to 6q16 and 18p11.22-p11.23, respectively. Genomics *54*, 351–353.

Pillutla, R.C., Yue, Z., Maldonado, E., and Shatkin, A.J. (1998b). Recombinant human mRNA cap methyltransferase binds capping enzyme/RNA polymerase IIo complexes. J Biol Chem *273*, 21443–21446.

Poulin, F., Gingras, A.C., Olsen, H., Chevalier, S., and Sonenberg, N. (1998). 4E-BP3, a new member of the eukaryotic initiation factor 4E-binding protein family. J. Biol. Chem. *273*, 14002–14007.

Prescott, D.M., and Bender, M.A. (1962). Synthesis of RNA and protein during mitosis in mammalian tissue culture cells. Exp. Cell Res. *26*, 260–268.

Pyronnet, S., Pradayrol, L., and Sonenberg, N. (2000). A cell cycle-dependent internal ribosome entry site. Mol. Cell *5*, 607–616.

Pyronnet, S., Dostie, J., and Sonenberg, N. (2001). Suppression of cap-dependent translation in mitosis. Genes Dev. *15*, 2083–2093.

Raczynska, K.D., Simpson, C.G., Ciesiolka, A., Szewc, L., Lewandowska, D., McNicol, J., Szweykowska-Kulinska, Z., Brown, J.W.S., and Jarmolowski, A. (2010). Involvement of the nuclear cap-binding protein complex in alternative splicing in Arabidopsis thaliana. Nucleic Acids Res. *38*, 265–278.

Rahl, P.B., Lin, C.Y., Seila, A.C., Flynn, R.A., McCuine, S., Burge, C.B., Sharp, P.A., and Young, R.A. (2010). c-Myc regulates transcriptional pause release. Cell *141*, 432–445.

Rasmussen, E.B., and Lis, J.T. (1993). In vivo transcriptional pausing and cap formation on three Drosophila heat shock genes. Proc. Natl. Acad. Sci. U. S. A. *90*, 7923–7927.

Reddy, R., Singh, R., and Shimba, S. (1992). Methylated cap structures in eukaryotic RNAs: structure, synthesis and functions. Pharmacol. Ther. *54*, 249–267.

Roberts, S.B., Segil, N., and Heintz, N. (1991). Differential phosphorylation of the transcription factor Oct1 during the cell cycle. Science (80-.). *253*, 1022–1026.

Rojo, F., Najera, L., Lirola, J., Jiménez, J., Guzmán, M., Sabadell, M.D., Baselga, J., and Ramon y Cajal, S. (2007). 4E-binding protein 1, a cell signaling hallmark in breast cancer that correlates with pathologic grade and prognosis. Clin. Cancer Res. *13*, 81–89.

Rousseau, D., Kaspar, R., Rosenwald, I., Gehrke, L., and Sonenberg, N. (1996). Translation initiation of ornithine decarboxylase and nucleocytoplasmic transport of cyclin D1 mRNA are increased in cells overexpressing eukaryotic initiation factor 4E. Proc. Natl. Acad. Sci. U. S. A. *93*, 1065–1070.

Rufener, S.C., and Mühlemann, O. (2013). eIF4E-bound mRNPs are substrates for nonsense-mediated mRNA decay in mammalian cells. Nat. Struct. Mol. Biol. *20*, 710–717.

Ruggero, D., Montanaro, L., Ma, L., Xu, W., Londei, P., Cordon-Cardo, C., and Pandolfi, P.P. (2004). The translation factor eIF-4E promotes tumor formation and cooperates with c-Myc in lymphomagenesis. Nat. Med. *10*, 484–486.

Russo, A.A., Jeffrey, P.D., and Pavletich, N.P. (1996a). Structural basis of cyclin-dependent kinase activation by phosphorylation. Nat. Struct. Biol. *3*, 696–700.

Russo, A.A., Jeffrey, P.D., Patten, A.K., Massagué, J., and Pavletich, N.P. (1996b). Crystal structure of the p27Kip1 cyclin-dependent-kinase inhibitor bound to the cyclin A-Cdk2 complex. Nature *382*, 325–331.

Sabin, L.R., Zhou, R., Gruber, J.J., Lukinova, N., Bambina, S., Berman, A., Lau, C.-K., Thompson, C.B., and Cherry, S. (2009). Ars2 regulates both miRNA- and siRNA-dependent silencing and suppresses RNA virus infection in Drosophila. Cell *138*, 340–351.

Saha, N., Schwer, B., and Shuman, S. (1999). Characterization of human, Schizosaccharomyces pombe, and Candida albicans mRNA cap methyltransferases and complete replacement of the yeast capping apparatus by mammalian enzymes. J. Biol. Chem. *274*, 16553–16562.

Salditt-Georgieff, M., Harpold, M., Chen-Kiang, S., and Darnell, J.E. (1980). The addition of 5' cap structures occurs early in hnRNA synthesis and prematurely terminated molecules are capped. Cell *19*, 69–78.

Sato, H., and Maquat, L.E. (2009). Remodeling of the pioneer translation initiation complex involves translation and the karyopherin importin beta. Genes Dev. *23*, 2537–2550.

Schalm, S.S., and Blenis, J. (2002). Identification of a conserved motif required for mTOR signaling. Curr. Biol. *12*, 632–639.

Schroeder, S.C., Schwer, B., and Shuman, S. (2000). Dynamic association of capping enzymes with transcribing RNA polymerase II. Genes Dev. *14*, 2435–2440.

Schroeder, S.C., Zorio, D. a R., Schwer, B., Shuman, S., and Bentley, D. (2004). A function of yeast mRNA cap methyltransferase, Abd1, in transcription by RNA polymerase II. Mol. Cell *13*, 377–387.

Schwartz, D.C., and Parker, R. (2000). mRNA decapping in yeast requires dissociation of the cap binding protein, eukaryotic translation initiation factor 4E. Mol. Cell. Biol. *20*, 7933–7942.

Schweingruber, C., Rufener, S.C., Zünd, D., Yamashita, A., and Mühlemann, O. (2013). Nonsense-mediated mRNA decay - mechanisms of substrate mRNA recognition and degradation in mammalian cells. Biochim. Biophys. Acta *1829*, 612–623.

Schwer, B., and Shuman, S. (1996). Conditional inactivation of mRNA capping enzyme affects yeast pre-mRNA splicing in vivo. RNA *2*, 574–583.

Schwer, B., Mao, X., and Shuman, S. (1998). Accelerated mRNA decay in conditional mutants of yeast mRNA capping enzyme. Nucleic Acids Res *26*, 2050–2057.

Schwer, B., Saha, N., Mao, X., Chen, H.W., and Shuman, S. (2000). Structure-function analysis of yeast mRNA cap methyltransferase and high-copy suppression of conditional mutants by AdoMet synthase and the ubiquitin conjugating enzyme Cdc34p. Genetics *155*, 1561–1576.

Segil, N., Roberts, S.B., and Heintz, N. (1991). Mitotic phosphorylation of the Oct-1 homeodomain and regulation of Oct-1 DNA binding activity. Science (80-.). *254*, 1814–1816.

Segil, N., Guermah, M., Hoffmann, a, Roeder, R.G., and Heintz, N. (1996). Mitotic regulation of TFIID: inhibition of activator-dependent transcription and changes in subcellular localization. Genes Dev. *10*, 2389–2400.

Shafer, B., Chu, C., and Shatkin, A.J. (2005). Human mRNA cap methyltransferase: alternative nuclear localization signal motifs ensure nuclear localization required for viability. Mol Cell Biol *25*, 2644–2649.

Shah, S., Tugendreich, S., and Forbes, D. (1998). Major binding sites for the nuclear import receptor are the internal nucleoporin Nup153 and the adjacent nuclear filament protein Tpr. J. Cell Biol. *141*, 31–49.

Shatkin, A.J. (1976). Capping of eucaryotic mRNAs. Cell *9*, 645–653.

Shatkin, A.J., and Manley, J.L. (2000). The ends of the affair: capping and polyadenylation. Nat. Struct. Biol. *7*, 838–842.

Shaw, D.J., Eggleton, P., and Young, P.J. (2008). Joining the dots: production, processing and targeting of U snRNP to nuclear bodies. Biochim. Biophys. Acta *1783*, 2137–2144.

Sheth, U., and Parker, R. (2003). Decapping and decay of messenger RNA occur in cytoplasmic processing bodies. Science (80-.). *300*, 805–808.

Shibagaki, Y., Itoh, N., Yamada, H., Nagata, S., and Mizumoto, K. (1992). mRNA capping enzyme. Isolation and characterization of the gene encoding mRNA guanylytransferase subunit from Saccharomyces cerevisiae. J. Biol. Chem. *267*, 9521–9528.

Shimotohno, K., Kodama, Y., Hashimoto, J., and Miura, K.I. (1977). Importance of 5'-terminal blocking structure to stabilize mRNA in eukaryotic protein synthesis. Proc. Natl. Acad. Sci. U. S. A. *74*, 2734–2738.

Shuman, S. (2001). Structure, mechanism, and evolution of the mRNA capping apparatus. Prog. Nucleic Acid Res. Mol. Biol. *66*, 1–40.

Shuman, S., Liu, Y., and Schwer, B. (1994). Covalent catalysis in nucleotidyl transfer reactions: essential motifs in Saccharomyces cerevisiae RNA capping enzyme are conserved in Schizosaccharomyces pombe and viral capping enzymes and among polynucleotide ligases. Proc. Natl. Acad. Sci. U. S. A. *91*, 12046–12050.

Sidorova, J.M., Mikesell, G.E., and Breeden, L.L. (1995). Cell cycle-regulated phosphorylation of Swi6 controls its nuclear localization. Mol. Biol. Cell *6*, 1641–1658.

Sikorski, T.W., and Buratowski, S. (2009). The basal initiation machinery: beyond the general transcription factors. Curr. Opin. Cell Biol. *21*, 344–351.

Sonenberg, N., and Hinnebusch, A.G. (2009). Regulation of translation initiation in eukaryotes: mechanisms and biological targets. Cell *136*, 731–745.

Sonenberg, N., Morgan, M.A., Merrick, W.C., and Shatkin, A.J. (1978). A polypeptide in eukaryotic initiation factors that crosslinks specifically to the 5'-terminal cap in mRNA. Proc. Natl. Acad. Sci. U. S. A. *75*, 4843–4847.

Sonenberg, N., Rupprecht, K.M., Hecht, S.M., and Shatkin, A.J. (1979). Eukaryotic mRNA cap binding protein: purification by affinity chromatography on sepharose-coupled m7GDP. Proc. Natl. Acad. Sci. U. S. A. *76*, 4345–4349.

Sonenberg, N., Trachsel, H., Hecht, S., and Shatkin, A.J. (1980). Differential stimulation of capped mRNA translation in vitro by cap binding protein. Nature *285*, 331–333.

Song, M.-G., Li, Y., and Kiledjian, M. (2010). Multiple mRNA decapping enzymes in mammalian cells. Mol. Cell *40*, 423–432.

Song, M.-G., Bail, S., and Kiledjian, M. (2013). Multiple Nudix family proteins possess mRNA decapping activity. RNA *19*, 390–399.

Songyang, Z., Blechner, S., Hoagland, N., Hoekstra, M.F., Piwnica-Worms, H., and Cantley, L.C. (1994). Use of an oriented peptide library to determine the optimal substrates of protein kinases. Curr. Biol. *4*, 973–982.

De Souza, C.P.C., and Osmani, S.A. (2007). Mitosis, not just open or closed. Eukaryot. Cell *6*, 1521–1527.

Spencer, C.A., Kruhlak, M.J., Jenkins, H.L., Sun, X., and Bazett-Jones, D.P. (2000). Mitotic transcription repression in vivo in the absence of nucleosomal chromatin condensation. J. Cell Biol. *150*, 13–26.

Spriggs, K.A., Bushell, M., and Willis, A.E. (2010). Translational regulation of gene expression during conditions of cell stress. Mol. Cell *40*, 228–237.

St Amour, C. V, Sansó, M., Bösken, C.A., Lee, K.M., Larochelle, S., Zhang, C., Shokat, K.M., Geyer, M., and Fisher, R.P. (2012). Separate domains of fission yeast Cdk9 (P-TEFb) are required for capping enzyme recruitment and primed (Ser7-phosphorylated) Rpb1 carboxyl-terminal domain substrate recognition. Mol. Cell. Biol. *32*, 2372–2383.

Steiger, M., Carr-Schmid, A., Schwartz, D.C., Kiledjian, M., and Parker, R. (2003). Analysis of recombinant yeast decapping enzyme. RNA *9*, 231–238.

Stewart, M. (2007). Molecular mechanism of the nuclear protein import cycle. Nat. Rev. Mol. Cell Biol. *8*, 195–208.

Taylor, J.H. (1960). Nucleic acid synthesis in relation to the cell division cycle. Ann. N. Y. Acad. Sci. *90*, 409–421.

Thermann, R., and Hentze, M.W. (2007). Drosophila miR2 induces pseudo-polysomes and inhibits translation initiation. Nature *447*, 875–878.

Thoreen, C.C., Chantranupong, L., Keys, H.R., Wang, T., Gray, N.S., and Sabatini, D.M. (2012). A unifying model for mTORC1-mediated regulation of mRNA translation. Nature *485*, 109–113.

Topisirovic, I., Svitkin, Y. V., Sonenberg, N., and Shatkin, A.J. (2011). Cap and cap-binding proteins in the control of gene expression. Wiley Interdiscip. Rev. RNA *2*, 277–298.

Trigon, S., Serizawa, H., Conaway, J.W., Conaway, R.C., Jackson, S.P., and Morange, M. (1998). Characterization of the residues phosphorylated in vitro by different C-terminal domain kinases. J. Biol. Chem. *273*, 6769–6775.

Tsukamoto, T., Shibagaki, Y., Imajoh-Ohmi, S., Murakoshi, T., Suzuki, M., Nakamura, A., Gotoh, H., and Mizumoto, K. (1997). Isolation and characterization of the yeast mRNA capping enzyme beta subunit gene encoding RNA 5'-triphosphatase, which is essential for cell viability. Biochem. Biophys. Res. Commun. *239*, 116–122.

Tsukamoto, T., Shibagaki, Y., Niikura, Y., and Mizumoto, K. (1998). Cloning and characterization of three human cDNAs encoding mRNA (guanine-7-)-

methyltransferase, an mRNA cap methylase. Biochem. Biophys. Res. Commun. *251*, 27–34.

Ubersax, J.A., and Ferrell, J.E. (2007). Mechanisms of specificity in protein phosphorylation. Nat. Rev. Mol. Cell Biol. *8*, 530–541.

Uemura, H., and Jigami, Y. (1992). Role of GCR2 in transcriptional activation of yeast glycolytic genes. Mol. Cell. Biol. *12*, 3834–3842.

Vassilev, L.T., Tovar, C., Chen, S., Knezevic, D., Zhao, X., Sun, H., Heimbrook, D.C., and Chen, L. (2006). Selective small-molecule inhibitor reveals critical mitotic functions of human CDK1. Proc. Natl. Acad. Sci. U. S. A. *103*, 10660–10665.

Wada, T., Takagi, T., Yamaguchi, Y., Ferdous, A., Imai, T., Hirose, S., Sugimoto, S., Yano, K., Hartzog, G.A., Winston, F., et al. (1998). DSIF, a novel transcription elongation factor that regulates RNA polymerase II processivity, is composed of human Spt4 and Spt5 homologs. Genes Dev. *12*, 343–356.

Wang, S.P., and Shuman, S. (1997). Structure-Function Analysis of the mRNA Cap Methyltransferase of Saccharomyces cerevisiae. J. Biol. Chem. *272*, 14683–14689.

Wang, Z., and Kiledjian, M. (2001). Functional link between the mammalian exosome and mRNA decapping. Cell *107*, 751–762.

Wang, E.T., Sandberg, R., Luo, S., Khrebtukova, I., Zhang, L., Mayr, C., Kingsmore, S.F., Schroth, G.P., and Burge, C.B. (2008). Alternative isoform regulation in human tissue transcriptomes. Nature *456*, 470–476.

Wang, Z., Jiao, X., Carr-Schmid, A., and Kiledjian, M. (2002). The hDcp2 protein is a mammalian mRNA decapping enzyme. Proc. Natl. Acad. Sci. U. S. A. *99*, 12663–12668.

Waskiewicz, A.J., Flynn, A., Proud, C.G., and Cooper, J.A. (1997). Mitogen-activated protein kinases activate the serine/threonine kinases Mnk1 and Mnk2. EMBO J. *16*, 1909–1920.

Weber, L.A., Feman, E.R., Hickey, E.D., Williams, M.C., and Baglioni, C. (1976). Inhibition of HeLa cell messenger RNA translation by 7-methylguanosine 5'-monophosphate. J. Biol. Chem. *251*, 5657–5662.

Weill, L., Belloc, E., Bava, F.-A., and Méndez, R. (2012). Translational control by changes in poly(A) tail length: recycling mRNAs. Nat. Struct. Mol. Biol. *19*, 577–585.

Wells, S.E., Hillner, P.E., Vale, R.D., and Sachs, A.B. (1998). Circularization of mRNA by eukaryotic translation initiation factors. Mol. Cell *2*, 135–140.

Wen, Y., and Shatkin, A.J. (1999). Transcription elongation factor hSPT5 stimulates mRNA capping. Genes Dev. *13*, 1774–1779.

Wen, Y., and Shatkin, A.J. (2000). Cap methyltransferase selective binding and methylation of GpppG-RNA are stimulated by importin-alpha. Genes Dev *14*, 2944–2949.

Wendel, H.-G., Silva, R.L.A., Malina, A., Mills, J.R., Zhu, H., Ueda, T., Watanabe-Fukunaga, R., Fukunaga, R., Teruya-Feldstein, J., Pelletier, J., et al. (2007). Dissecting eIF4E action in tumorigenesis. Genes Dev. *21*, 3232–3237.

Werner, M., Purta, E., Kaminska, K.H., Cymerman, I. a, Campbell, D. a, Mittra, B., Zamudio, J.R., Sturm, N.R., Jaworski, J., and Bujnicki, J.M. (2011). 2'-O-ribose methylation of cap2 in human: function and evolution in a horizontally mobile family. Nucleic Acids Res. *39*, 4756–4768.

White, R.J., Gottlieb, T.M., Downes, C.S., and Jackson, S.P. (1995). Mitotic regulation of a TATA-binding-protein-containing complex. Mol. Cell. Biol. *15*, 1983–1992.

Whitfield, M.L., Sherlock, G., Saldanha, A.J., Murray, J.I., Ball, C.A., Alexander, K.E., Matese, J.C., Perou, C.M., Hurt, M.M., Brown, P.O., et al. (2002). Identification of Genes Periodically Expressed in the Human Cell Cycle and Their Expression in Tumors. Mol. Biol. Cell *13*, 1977–2000.

Wilker, E.W., van Vugt, M.A.T.M., Artim, S.A., Huang, P.H., Petersen, C.P., Reinhardt, H.C., Feng, Y., Sharp, P.A., Sonenberg, N., White, F.M., et al. (2007). 14-3-3sigma controls mitotic translation to facilitate cytokinesis. Nature *446*, 329–332.

Wilson, K.F., Wu, W.J., and Cerione, R.A. (2000). Cdc42 stimulates RNA splicing via the S6 kinase and a novel S6 kinase target, the nuclear cap-binding complex. J. Biol. Chem. *275*, 37307–37310.

Wong, C.-M., Qiu, H., Hu, C., Dong, J., and Hinnebusch, A.G. (2007). Yeast cap binding complex impedes recruitment of cleavage factor IA to weak termination sites. Mol. Cell. Biol. *27*, 6520–6531.

Wu, H., Lunin, V.V., Zeng, H., Antoshenko, T., MacKenzie, F., Weigelt, J., Arrowsmith, C.H., Edwards, A.M., Bochkarev, A., Min, J., et al. (2007). The crystal structure of human RNA (guanine-7-) methyltransferase in complex with SAH. http://www.thesgc.org/structures/details?pdbid=3BGV

Wu, M., Nilsson, P., Henriksson, N., Niedzwiecka, A., Lim, M.K., Cheng, Z., Kokkoris, K., Virtanen, A., and Song, H. (2009). Structural basis of m(7)GpppG binding to poly(A)-specific ribonuclease. Structure *17*, 276–286.

Xiang, S., Cooper-Morgan, A., Jiao, X., Kiledjian, M., Manley, J.L., and Tong, L. (2009). Structure and function of the 5'-->3' exoribonuclease Rat1 and its activating partner Rai1. Nature *458*, 784–788.

Xu, D., Farmer, A., and Chook, Y.M. (2010). Recognition of nuclear targeting signals by Karyopherin-β proteins. Curr. Opin. Struct. Biol. *20*, 782–790.

Xue, Y., Bai, X., Lee, I., Kallstrom, G., Ho, J., Brown, J., Stevens, A., and Johnson, A.W. (2000). Saccharomyces cerevisiae RAI1 (YGL246c) is homologous to human DOM3Z and encodes a protein that binds the nuclear exoribonuclease Rat1p. Mol. Cell. Biol. *20*, 4006–4015.

Yamada, T., Yamaguchi, Y., Inukai, N., Okamoto, S., Mura, T., and Handa, H. (2006). P-TEFb-mediated phosphorylation of hSpt5 C-terminal repeats is critical for processive transcription elongation. Mol. Cell *21*, 227–237.

Yamada-Okabe, T., Doi, R., Shimmi, O., Arisawa, M., and Yamada-Okabe, H. (1998). Isolation and characterization of a human cDNA for mRNA 5'-capping enzyme. Nucleic Acids Res. *26*, 1700–1706.

Yamaguchi, Y., Takagi, T., Wada, T., Yano, K., Furuya, A., Sugimoto, S., Hasegawa, J., and Handa, H. (1999). NELF, a multisubunit complex containing RD, cooperates with DSIF to repress RNA polymerase II elongation. Cell *97*, 41–51.

Yanagiya, A., Suyama, E., Adachi, H., Svitkin, Y.V., Aza-Blanc, P., Imataka, H., Mikami, S., Martineau, Y., Ronai, Z. a., and Sonenberg, N. (2012). Translational Homeostasis via the mRNA Cap-Binding Protein, eIF4E. Mol. Cell 1–12.

Yankulov, K., Yamashita, K., Richard, R., Egly, J.-M., and Bentley, D.L. (1995). The Transcriptional Elongation Inhibitor 5,6-Dichloro-1-beta-D-ribofuranosylbenzimidazole Inhibits Transcription Factor IIH-associated Protein Kinase. J. Biol. Chem. *270*, 23922–23925.

Young, D.W., Hassan, M.Q., Pratap, J., Galindo, M., Zaidi, S.K., Lee, S., Yang, X., Xie, R., Javed, A., Underwood, J.M., et al. (2007a). Mitotic occupancy and lineage-specific transcriptional control of rRNA genes by Runx2. Nature *445*, 442–446.

Young, D.W., Hassan, M.Q., Yang, X.-Q., Galindo, M., Javed, A., Zaidi, S.K., Furcinitti, P., Lapointe, D., Montecino, M., Lian, J.B., et al. (2007b). Mitotic retention of gene expression patterns by the cell fate-determining transcription factor Runx2. Proc. Natl. Acad. Sci. U. S. A. *104*, 3189–3194.

Yue, Z., Maldonado, E., Pillutla, R., Cho, H., Reinberg, D., and Shatkin, a J. (1997). Mammalian capping enzyme complements mutant Saccharomyces cerevisiae lacking mRNA guanylyltransferase and selectively binds the elongating form of RNA polymerase II. Proc. Natl. Acad. Sci. U. S. A. *94*, 12898–12903.

Zaidi, S.K., Young, D.W., Montecino, M., van Wijnen, A.J., Stein, J.L., Lian, J.B., and Stein, G.S. (2011). Bookmarking the genome: maintenance of epigenetic information. J. Biol. Chem. *286*, 18355–18361.

Zan-Kowalczewska, M., Bretner, M., Sierakowska, H., Szczesna, E., Filipowicz, W., and Shatkin, A.J. (1977). Removal of 5'-terminal m7G from eukaryotic mRNAs by potato nucleotide pyrophosphatase and its effect on translation. Nucleic Acids Res. *4*, 3065–3081.

Zeng, H., Amaya, M.F., Loppnau, P., Bountra, C., Weigelt, J., Arrowsmith, C.H., Edwards, A.M., Botchkarev, A., Min, J., Plotnikov, A.N., et al. (2008). Crystal structure of mRNA cap guanine-N7 methyltransferase (RNMT) in complex with sinefungin. http://www.thesgc.org/structures/details?pdbid=3EPP

Zenklusen, D., Vinciguerra, P., Wyss, J.-C., and Stutz, F. (2002). Stable mRNP formation and export require cotranscriptional recruitment of the mRNA export factors Yra1p and Sub2p by Hpr1p. Mol. Cell. Biol. *22*, 8241–8253.

Zoncu, R., Efeyan, A., and Sabatini, D.M. (2011). mTOR: from growth signal integration to cancer, diabetes and ageing. Nat. Rev. Mol. Cell Biol. *12*, 21–35.